Modeling and Control of a Free-Flying Space Robot Interacting with a Target Satellite

Murad Musa Al-Shibli

A Thesis

in

The Department

of

Mechanical and Industrial Engineering

Presented in Partial Fulfillment of the Requirements

for

the Degree of Doctor of Philosophy at

Concordia University

Montreal, Quebec, Canada

December 2005

Your file Votre référence
ISBN: 978-0-494-16294-1
Our file Notre référence
ISBN: 978-0-494-16294-1

Modeling and Control of a Free-Flying Space Robot Interacting with a Target Satellite

Abstract

Murad Musa Al-Shibli, Ph.D.
Concordia University, 2005

Free-flying space robots have been under intensive consideration to perform diverse important space missions such as: inspection, maintenance, repairing, servicing and rescuing satellites in earth orbit. Recovering the attitude of the satellites, charging the exhausting batteries, and replacing the failed parts like solar panels or antennas are some examples of space missions. To perform contact tasks, the coupling in kinematics and dynamics, constraints and contact forces acting on a free-flying space robot in contact with a target satellite are the subjects addressed in this thesis work.

In the thesis a unified control-oriented modeling approach is proposed to deal with the kinematics, linear and angular momentum, contact constraints and dynamics of a free-flying space robot interacting with a target satellite. This developed approach combines the dynamics of both systems in one structure along with holonomic and nonholonomic constraints in a single framework. Furthermore, this modeling allows considering the generalized contact forces between the space robot end-effecter and the target satellite as internal forces rather than external forces. As a result of this approach, linear and angular momentum will form holonomic and nonholonomic constraints, respectively. Meanwhile, restricting the motion of the space robot end-effector on the surface of the target satellite

will impose geometric constraints. The proposed momentum of the combined system under consideration is a generalization of the momentum model of a free-flying space robot.

A physical interpretation of holonomic/nonholonomic constraints is analyzed based on d'Almberts-Lagrange dynamics and reveals geometric conditions that generate such a behavior. Moreover, a nonholonomy criterion is proposed to verify the integrability of momentum constraints by using a linear transformation via orthogonal projection techniques and singular value decomposition. This criterion can be used to verify the holonomy of a free-flying space robot with or without interaction with a target satellite and to check whether these constraints or their initial conditions are violated.

Based on this unified model, three reduced models are developed. The first reduced dynamics can be considered as a generalization of a free-flying robot without contact with a target satellite. In this reduced model it is found that the Jacobian and inertia matrices can be considered as an extension of those of a free-flying space robot. Since control of the base attitude rather than its translation is preferred in certain cases, a second reduced model is obtained by eliminating the base linear motion dynamics. For the purpose of the controller development, a third reduced-order dynamical model is then obtained by finding a common solution of all constraints using the concept of orthogonal projection matrices.

By exploring the properties of the last reduced dynamic model, an inverse-dynamics control strategy is proposed to meet motion and contact forces desired specifications as well as to cope with the unactuation of the target satellite due to its thrusters' failure or shutdown. In order to overcome the uncertainties in the combined system parameters, an adaptive inverse dynamics controller is further investigated. This controller does not only pose the advantages of the former controller but also adapt with any changes in its parameters.

Finally, simulation results are demonstrated to verify all analytical and theoretical results at the end of the chapters.

Acknowledgment

I would like highly to thank and acknowledge my both co-supervisors: Prof. Chun Yi Su and Prof. Farhad Aghili for their great kindness, support, wise supervision and for their scientific and technical expertise to conduct this research and make it real.

I would like to express my special thanks to the committee examiners for their valuable time, guidance and advice.

I would like to acknowledge our department represented in faculty, staff and School of Graduate studies for providing a good atmosphere for studying and research.

I would like to thank all my friends and dedicate my work to them.

Dedication

To my family:

my mother, my father

my sisters, my brothers and their families:

for their love, care and patience.

Table of Contents

List of Figures xi

List of Tables xiv

Nomenclature xv

Chapter 1: Introduction 1

1.1 Overview 1

1.1.1 Mating and Capturing Mission 4

1.2 Background and Literature Survey 15

1.3 Research Motivation 31

1.4 Contribution 32

1.5 Thesis Organization 35

Chapter 2: Modeling of Kinematics and Momentum of a Free-Flying Space Robot Interacting with a Passive Target Satellite 37

2.1 Introduction 37

2.2 Kinematics Modeling 39

2.3 Linear and Angular Momentum Modeling 42

2.4 Geometric Contact Constraints Modeling 44

2.5 A common solution of holonomic and nonholnomic constraints 45

Chapter 3: Physical Insight of Holonomic/Nonholonomic Constraints of a Space Robot with/without Interaction with a Target Satellite 50

3.1 Introduction 50

3.2 Free-Flying space Robot 53

3.3 Free-flying Space Robot Interacting with a Target Satellite 59

3.4 Simulation Results 62

Chapter 4: Nonholonomy Criterion of a Free-Flying Space Robot with/without Interaction with a Target Satellite 69

4.1 Introduction 69

4.2 Holonomy Criterion 70

4.3 Simulation Results 76

Chapter 5: Modeling of Dynamics of a Free-Flying Space Robot Interacting with a Passive Target Satellite 84

5.1 Introduction 84

5.2 Dynamics Modeling 86

5.3 Constraint Force Decomposition 89

5.4 Dynamics Modeling Reduction 91

5.5 Simulation Results 95

Chapter 6: Inverse Dynamics Control of a Free-Flying Space Robot in Contact with a Target Satellite 100

6.1 Introduction 100

6.2 Inverse Dynamics Controller 102

6.3 Simulation Results 106

Chapter 7: Adaptive Inverse Dynamics Control of a Free-Flying Space Robot in Contact with a Target Satellite: a Hubble Space Telescope Case 113

7.1 Introduction 113

7.2 Inverse Dynamics Controller 115

7.3 Hubble Space Telescope Case 119

7.4 Simulation Results 126

Chapter 8: Discussions, Conclusions and Future Work 135

References 140

Appendix A: Derivation of the linear Velocity of the Target Satellite 153

Appendix B: Derivation of the Dynamics using Lagrangian Multipliers 156

Appendix C: Inertia Matrix $H(\theta)$ for 6-DOF Based-Satellite Space Robot Interacting with a Target Satellite 160

Appendix D: Linear and Angular Jacobian Matrices for a 6-DOF Based Satellite Space Robot Interacting with a Target Satellite 162

Appendix E: Time Derivative of Inertia Matrix $H(\theta)$ for 6-DOF Based-Satellite Space Robot Interacting with a Target Satellite 163

Appendix F: Derivation of the Nonlinear Velocity-Dependent Force Vector $C(\theta,\dot{\theta})$ of 6-DOF Based-Satellite Space Robot Interacting with a Target Satellite 165

Appendix G: Derivation of the Orthogonal Matrix $S(\theta)$ 167

Appendix H: Derivation of the Reduced Dynamics Model of a 6 DOF Based-Satellite Space Robot in Contact with a Target Satellite 169

Appendix K: Derivation of the Regressor Y and the Parameter Vector α of a Based-Satellite 6-DOF Space Robot in Contact with a Target Satellite 175

List of Figures

Figure 1.1	Docking System	6
Figure 1.2	Berthing system	7
Figure 1.3	Volumes of Berthing Box	9
Figure 1.4	Visibility of ground stations, geometrical relation	10
Figure 1.5	Berthing Scenario	13
Figure 1.6	Capture Mechanism	14
Figure 2.1	A Free-flying Space Based Satellite Robotic Manipulator in Contact with a Target Satellite	40
Figure 3.1	Nonholonomic Interpretation of a Free-Flying Space Robot Interacting with a Target Satellite	58
Figure 3.2	Angular Momentum of a Free-Flying Space Robot	64
Figure 3.3	Linear Momentum of a Free-Flying Space Robot	64
Figure 3.4	Angular Momentum of a Free-Floating Space Robot in Contact with a target Satellite	65
Figure 3.5	Linear Momentum of a Free-Floating Space Robot in Contact with a target Satellite	65
Figure 3.6	Angular Momentum of a Free-Flying Space Robot in Contact with a target Satellite (violation of condition 4.30)	66
Figure 3.7	Linear Momentum of a Free-Flying Space Robot in Contact with a target Satellite (violation of condition 4.30)	66

Figure 3.8	Angular Momentum of a Free-Flying Space Robot in Contact with a target Satellite (violation of condition 4.40)	67
Figure 3.9	Linear Momentum of a Free-Flying Space Robot in Contact with a target Satellite (violation of condition 4.40)	67
Figure 4.1	Angular Momentum of a Free-Flying Space Robot	80
Figure 4.2	Linear Momentum of a Free-Flying Space Robot	80
Figure 4.3	Angular Momentum of a Free-Flying Space Robot Subjected to an External Force	81
Figure 4.4	Linear Momentum of a Free-Flying Space Robot Subjected to an External Force	81
Figure 4.5	Angular Momentum of a Free-Floating Space Robot in Contact with a target Satellite	82
Figure 4.6	Linear Momentum of a Free-Floating Space Robot in Contact with a target Satellite	82
Figure 5.1	Angular Velocity of the Base Satellite	97
Figure 5.2	Linear Velocity of the Base Satellite	97
Figure 5.3	Robot Arm Angles	98
Figure 5.4	Angular Velocity of the Target Satellite	98
Figure 5.5	Linear Velocity of the Target Satellite	99
Figure 6.1	Base Satellite Angular Velocity Error	108
Figure 6.2	Base Satellite Linear Velocity Error	109
Figure 6.3	Space Robot Arm Angular Position Error	109
Figure 6.4	Space Robot Arm Angular Velocity Error	110

Figure 6.5	Space Robot Arm Actuation Torque	110
Figure 6.6	Target Satellite Angular Velocity Error	111
Figure 6.7	Target Satellite Linear Velocity Error	111
Figure 6.8	Lagrangian Error	112
Figure 7.1	Hubble Space Telescope Servicing Mission 3A (NASA)	119
Figure 7.2	Hubble Space Telescope Overall Configuration (NASA)	120
Figure 7.3	Hubble Space Telescope Servicing Mission 3A Orbital Replacement Units (NASA)	124
Figure 7.4	Some Astonishing Observation of Hubble Space Telescope for our Solar System and the Universe (NASA)	125
Figure 7.5	A Free-Flying Space Robot Conducting a Maintenance Task on the Surface of the Hubble Space Telescope	128
Figure 7.6	Base Satellite Angular Velocity Error	130
Figure 7.7	Base Satellite Linear Velocity Error	130
Figure 7.8	Space Robot Arm Angular Position Error	131
Figure 7.9	Space Robot Arm Angular Velocity Error	131
Figure 7.10	Space Robot Arm Actuation Torque	132
Figure 7.11	Target Satellite Angular Velocity Error	132
Figure 7.12	Target Satellite Linear Velocity Error	133
Figure 7.13	Lagrangian Multiplier Error	133

List of Tables

Table 5.1	Rank of the Transformation Matrix Y (Sample)	79
Table 7.1	Hubble Space Telescope Specifications (NASA)	121
Table 7.2	Simulated Combined System Parameters	128

Nomenclature

$\sum_I$: the inertial coordinate on the orbit

$\sum_b$: the base coordinate with its origin attached at the base centroid

m_i : the mass of the *i*th body

$I_i \in R^3$: the inertia of the *i*th body

n : number of robot arm joints

$q \in R^n$: the robot joint variable vector $q(q_1, q_2, \cdots, q_n)^T$

$r_b \in R^3$: the position vector pointing the centroid of the base with reference to $\sum_I$

$r_t \in R^3$: the position vector pointing the target satellite with reference to $\sum_I$

$r_i \in R^3$: the position vector pointing the *i*-th body with reference to $\sum_I$

$c_i \in R^3$: the position vector pointing the *i*-th joint with reference to $\sum_I$

EE : the end-effecter

$r_{EE} \in R^3$: the position vector pointing the end-effecter with reference to $\sum_I$

$r_{t_{/b}} \in R^3$: the position vector pointing the target satellite with reference to $\sum_b$

$r_{EE_{/b}} \in R^3$: the position vector pointing the end-effecter with reference to $\sum_b$

$r_{t_{/EE}} \in R^3$: the position vector pointing the target satellite centroid with reference end- effector

$V_i \in R^3$: the linear velocity of the *i*-th body with respect to $\sum_I$

$v_i \in R^3$: the linear velocity of the *i*-th body with respect to $\sum_b$

$V_{EE} \in R^3$: the linear velocity of the end-effecter with respect to $\sum_I$

$V_b \in R^3$: the linear velocity of the base with respect to $\sum_I$

$v_t \in R^3$: the relative velocity between the target satellite and the end-effecter

$\Omega_i \in R^3$: the vector of angular velocity of the *i*-th body in the inertial frame

$\Omega_b \in R^3$: the base angular velocity vector in the inertial frame

$\Omega_t \in R^3$: the vector of angular velocity of the target satellite in the inertial frame

$\omega_t \in R^3$: the vector of angular velocity of the target satellite in its local frame

$\Omega_{EE} \in R^3$: the vector of angular velocity of the end-effecter in the inertial frame

P : the linear momentum

L : the angular momentum

k_i : the unit vector in the direction of z axis of the *i*th link coordinates

$\times$: the outer product of a position vector r

U_3 : the 3×3 unity matrix

O_3 : the 3×3 zero matrix

E_3 : the 3×3 identity matrix

$[r\times]$: the cross matrix function

χ : the pose of the robot end-effecter expressed in the target frame

$\Phi(\chi)$: constraint surface on which the robot end-effector moves

J : the Jacobian matrix

N : number of generalized coordinates of the based-satellite space robot in contact with a target satellite

$\dot{\theta} \in R^N$: the generalized velocity vector

c_0 : the vector of the initial conditions of the momentum

$B(\theta) \in R^{k\times N}$: the matrix of linear and angular momentum

k : the number of momentum constraint equations

m : the number of geometric constraint equations

$N(\cdot)$: the null space of a given matrix

$P_{N(\cdot)}$: the projection matrix on the null space of a given matrix $(\cdot)$

$^+$: the pseudoinverse of a given matrix

r_{c0} : the position vector of the system center of mass

a_i : the i-th body acceleration a_i

f_i : the resultant internal force f_i

F_i : the resultant external force

Z : an arbitrary virtual axis of rotation

δ : the virtual operator

δR_i : the virtual displacement measured in frame fixed at the center of mass

$\delta\phi$: the angular virtual displacement by which the base body rotates about the virtual axis of rotation Z

δW : the virtual work

$\hat{l}$: a unit vector along the virtual axis of rotation Z

L_m : the angular momentum of the manipulator

$L_{t/EE}$: the angular momentum of the target in with respect to the end-effector

P_T : the linear momentum of the target satellite

$\dot{z}(t)$: an arbitrary vector

L^{N-m} : a hypersurface of $(N-m)$ dimension

T : a linear transformation matrix

Y_h : the nonholonomy matrix

$\dot{v}$: an arbitrary vector

U : an orthogonal matrices of size $N \times N$

V^T : an orthogonal matrices of size $N \times N$

Σ : a diagonal matrix with nonnegative diagonal elements in a decreasing order

$\widetilde{A}$: an extended augmented matrix of size $N \times N$

L : the Lagrangian function

λ : the vector of unknown Lagrangian multipliers

J_{L_i} : the Jacobian matrix of the linear velocities of *i*-th body in reference with $\sum_b$

J_{A_i} : the Jacobian matrix of the angular velocities of *i*-th body in reference with $\sum_b$

$J_m \in R^{6\times n}$: the Jacobian matrix of the robot hand

$J_b \in R^{6\times 6}$: the Jacobian matrix of the base satellite

$H(\theta): N\times N$: symmetric and positive definite inertia matrix

$C(\theta,\dot{\theta})\dot{\theta}$: the velocity-dependent nonlinear forces

$\tau \in R^n$: the joint torque vector $(\tau_1,\tau_2,\cdots,\tau_n)^T$

$F_c \in R^6$: the contact forces and moments $(f_h^T,\eta_h^T)^T$ act on the robot end-effecter

$F_b \in R^6$: forces and moments $(f_b^T,\eta_b^T)^T$ act on the centroid of base satellite

F_n : the normal forces

F_t : the tangential forces

$\oplus$: the direct sum of tow vectors

$P_{N,T}$: an idempotent projector

$R(\cdot)$	: the range of a given matrix
$\aleph(\cdot)$	: the null space of a given matrix
$\bar{\tau}$	: the torque input to the combined system
$S(\theta) \in R^{(N)\times(N-k-m)}$	: an orthogonal projector of full rank and belong to the null space
e_p	: the position tracking error
λ_c	: the composite force error
e_F	: the Lagarangian force error
K_P, K_D, K_F, K_I	:diagonal matrices with positive elements
$\hat{C}_1$	: an estimate of vector C_1
$\hat{H}_1$	: an estimates of matrix H_1
$\hat{\alpha}$	: the estimated vector of parameter vector α
Y	:an $N\times(N-m)$ matrix of known functions and known as the regressor
Q	: a positive definite symmetric
V	: Lyaponuv candidate function

Chapter 1

Introduction

1.1 Overview

Free-flying space robots, free-floating space robots, and planetary robots have received special attention to perform many space missions such as: inspection, maintenance, repairing and servicing satellites in earth orbit, as well as exploring planets for life and new resources. Particularly, servicing satellite equipped with robot arms can be employed for recovering the attitude, charging the exhausting batteries, attaching new thrusters, and replacing the failed parts like gyros, solar panels or antennas of another satellite.

The commercial motive for robotic spacecraft and their future central role in space activities is comparatively new, particularly for general earth orbit operations which are presently dominated by manned missions. There is no doubt that robotic and autonomous systems in space will contribute considerably to the future commercialization of space environment. Sending a space robotic servicing mission into the space will not only save design, manufacturing and launching costs but also will protect the environment from floating junk metals and debris. Indeed, it may reduce launch costs, presently approximately $20,000/kg [2]. The production cost per unit mass of a spacecraft/satellite varies from $100,000/kg for commercial spacecraft/satellite to $150,000/kg for interplanetary probes. An average gives $125,000/kg which for 1.5-tonne spacecraft/satellite gives a total production cost of $175million in round figures. The time is indeed ripe to launch a remote space robotic manipulation into space. Modern

spacecrafts/satellites are now being designed to be serviceable in-orbit. Advances in charge-coupled devices sensor technology motivated by remote earth observation satellite and astronomical satellite applications may be utilized for advanced robotic vision. The presently available communications infrastructure, like the European Data relay system telemetry and data relay satellite system, may be flexibly exploited by robotic spacecraft in earth orbit. There is an increasing demand for Earth Observation (EO) satellites for environmental and pollution monitoring, land management, geographical information, global sea state, sea surface winds, Tsunami waves, hurricanes and sea surface temperature. Satellites of this type will become increasingly popular for low-altitude polar orbits. Satellite-based telecommunications, EO, navigation, internet and e-commerce services represent a major market for in-orbit servicing. This demand has the value exceeding some $40 Billions annually with demand doubling every 5 years. New broadband services by satellites are expected to yield around $5 Billion/year.

Between 1962 and 1983 there have been approximately 2500 spacecraft failures of one kind or another. The majority of these failures occur within the first few weeks or months of operational service and in the latter years of operational service due to propellant or battery lifetime limitations. There have been also cases where failures have been recovered. Few examples not to mention all of such failures are: the joint NASA/ESA SOHO mission after two years in a nominal halo orbit, the L1 Lagrangian point, failed in 1998 when ACOS switched into Emergency Sun Re-acquisition (ESR) safe mode and contact was lost. OAO-A2 lost its star tracker due to debris spoofing it; OAO-C lost attitude control causing excess momentum build up and excess spin rates; ATS-6 lost its

star sensor due to debris spoofing and lost momentum wheel actuator; NOAA-6 started tumbling after hydrazine venting. The Hipparcus satellite was launched into the wrong orbit due to a fault in the apogee kick motor, thereby requiring extensive changes to the mission. Galileo which was launched to Jupiter in 1990 had a high-gain antenna which failed to deploy fully and the science mission return had consequently degraded to 30%. Olympus, an EAS excremental telecommunications satellite of 2.6 tones was launched in 1989. In 1991, it went out of control and its fuel froze out but the ground team was able to retrieve it and put it back into operation. Iridium invests in satellite-based worldwide coverage. It has 66 satellites (originally 77) plus six in-orbit spares in low polar earth orbit of 780 km altitude. Those satellites are arranged in six orbital planes of eleven satellites each for global coverage. Although Iridium experienced no launch failures in its fifteen launches, seven 7 satellites failed, of which one expended all its fuel accidentally and 3 had altitude control problems, highlighting the utility of an in-orbit servicing capability.

Most failures occur due to environmental conditions or excess load beyond design tolerance, or through random failures. Design failures account for ~25% of all faults; environmental failures, for ~21%; random failures, for ~30%; software failure, for ~5%. Of all failures, ~19% result from unknown origin. A dedicated robotic interceptor satellite for in-orbit servicing would alleviate these eventualities through maintenance and servicing and effectively increase the overall reliability of all accessible space systems. Consumable replenishment such as fuel, batteries essentially spread fixed cost

overheads over longer operational periods. In fact the cost parameter for a communications satellite for example is given by:

(Launch cost + spacecraft cost)/(number of years of services x number of telephone circuits).

Hence, increasing the lifetime directly reduces the cost parameter in linear fashion. Refueling propellant and replacing worn-out batteries can curtail this limit. Refueling in particular increases the spacecraft net present value by up to 2.44 millions and increases the internal rate of return up to 8.3%. Module replacement like the propulsion subsystem is much cheaper than complete satellite replacement which now have cost ranges of approximately $200-600 millions.

1.1.1 Mating and Capturing Mission

As mentioned before the purpose of a dedicated robotic satellite for in-orbit servicing is to capture malfunctioned spacecrafts and satellites and to perform maintenance and services to effectively increase the overall reliability of all accessible space systems. To gain a clear idea of mating and capturing missions, there are some definitions and techniques that need to be explained before presenting the mathematical formulation. This section will provide a basic understanding of the concepts of mating, docking, berthing and the capturing mechanism [3].

Mating: is a term used to describe the process of achieving contact, capture and connection. It includes two cases: docking and berthing. The responsibility of the mating system is to:

Task 1: Achieve the capture with no escape;

Task 2: Attenuate the residual relative motion between the servicing satellite and target satellite;

Task 3: Bring the interfaces of the structural latches into their operational range;

Task 4: Achieve rigid structural connection;

Task 5: Achieve gas-tight sealing of the connection of a pressurized passage between the chaser and target vehicles;

Task 6: Establish connection of data, power and fluid interfaces.

In docking all tasks are concentrated in one system which is the docking mechanism. In berthing systems tasks 1, 2 and 3 are performed by the manipulator arm while other tasks are performed by a berthing mechanism. The most important mating task is the capture since it is the natural end of the rendezvous process.

Docking: a term is applied to the case where the guidance navigation control (GNC) system of the servicing satellite controls the required vehicle state parameters. That is necessary to ensure that its capture interfaces enter into those of the target satellite, and where the capture location is also the location for structural connection.

For docking, the capture and attachment interfaces are integrated into a single system, the main axis of which is the approach axis.

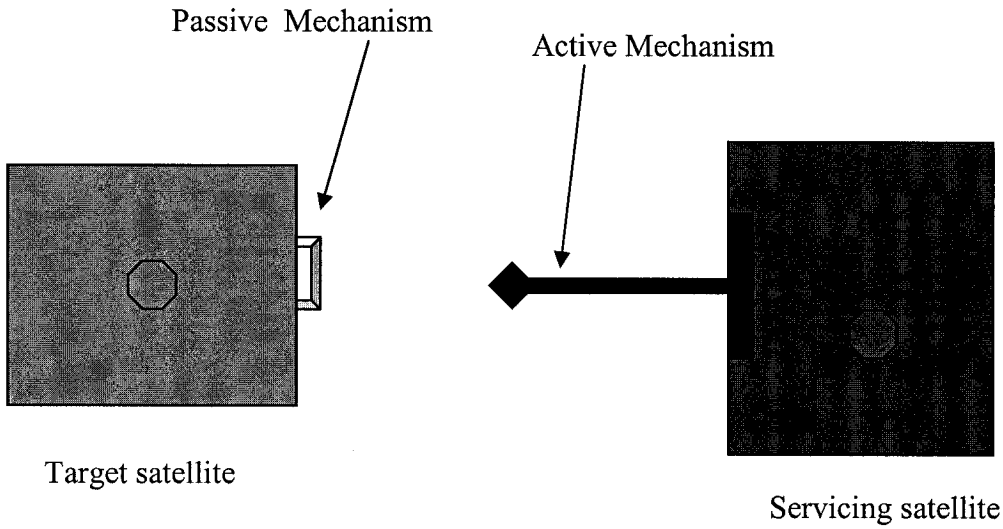

Figure 1.1: Docking System

Berthing: a term used for the case, where

1) The GNC system of the chaser delivers the vehicle to a meeting point with zero nominal relative velocities and angular rates;
2) A manipulator located on either the target or the chaser vehicle to grapple the corresponding capture interface on the other vehicle;
3) The manipulator transfer the captured vehicle with its attachment interface to the final position at the relevant target berthing port and inserts it into the corresponding attachment interfaces of the target vehicle.

For berthing, the approach axis and the axis of attachment, and hence the interfaces for capture and attachment, are fully decoupled. The transfer from the capture position to the attachment position by a manipulator makes it possible to access different berthing ports.

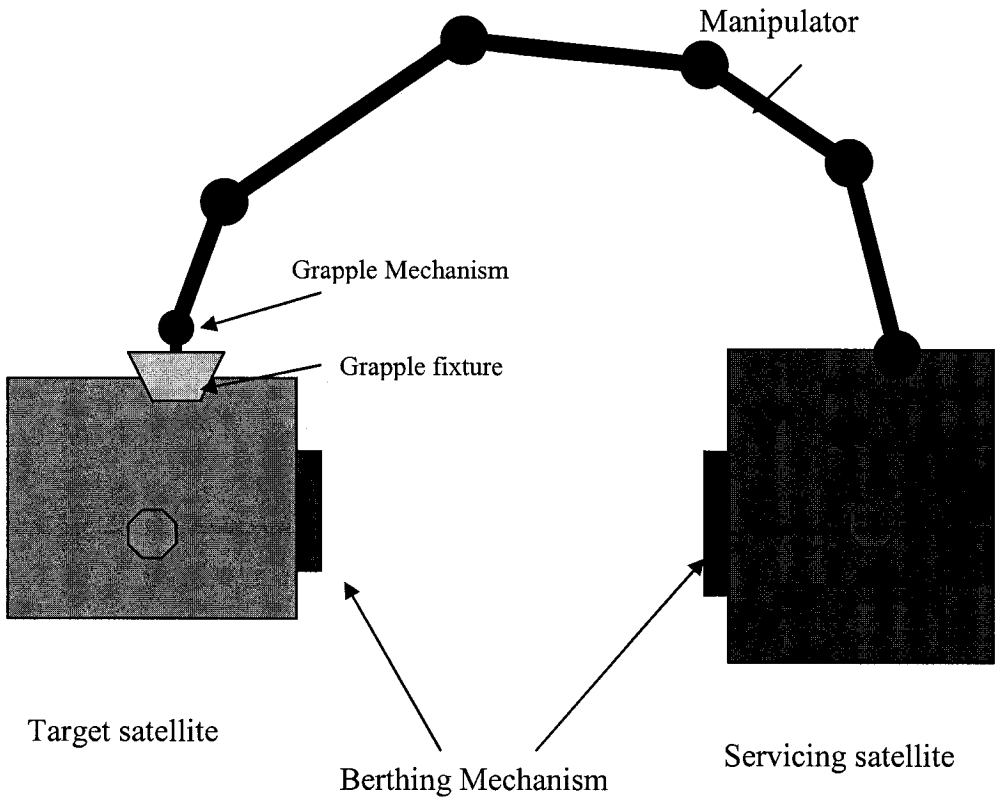

Figure 1.2: Berthing System

The major difference concerning capture between docking and berthing systems is that in the case of docking the body of the approaching vehicle is actively controlled to guide its capture interfaces into the corresponding interfaces on the target vehicle. While in berthing, the manipulator arm plays the active role, guiding its grapple mechanism to capture the passive grapple fixture on the other vehicle. As a matter of fact, the manipulator arm can be located on either the target station or the approaching vehicle, and vice versa for the grapple fixture. Since at contact the two bodies will rebound and separate again, capture must be accomplished in a short time before the interfaces have left the capture volume.

Berthing Box

A berthing box is a volume located very close to the target station into which the chaser has to be placed, to make capture of the grapple interfaces by the manipulator arm possible. Depending on the reachability and articulation capabilities of the manipulator arm used, convenient berthing box can be chosen. From this location the captured vehicle can be transferred to the structural interfaces of the berthing port mechanism. The approach direction to this berthing box depends on the location and reachability of the arm, geometric shape of both vehicles, by the location and nominal attitude of the corresponding capture interfaces and by trajectory safety considerations. Availability and relevant rendezvous sensor interfaces will determine the location and approaching of the berthing box.

Three different regions (volumes) for the berthing box can be identified:

1) Inner berthing box (station keeping volume): which is necessary for the accuracy with which the servicing satellite can position the grapple interfaces with respect to the target coordinates and the controlled motion.
2) Middle berthing box (capture volume): in which the capture has to be achieved as it can be seen from its name. This adds to the inner box the free drift that takes place after thrust is inhibited up to the point in time when the manipulator end effecter has captured the grapple interfaces
3) Outer berthing box (total berthing volume) which adds to the capture volume the distance necessary to stop the manipulator motion.

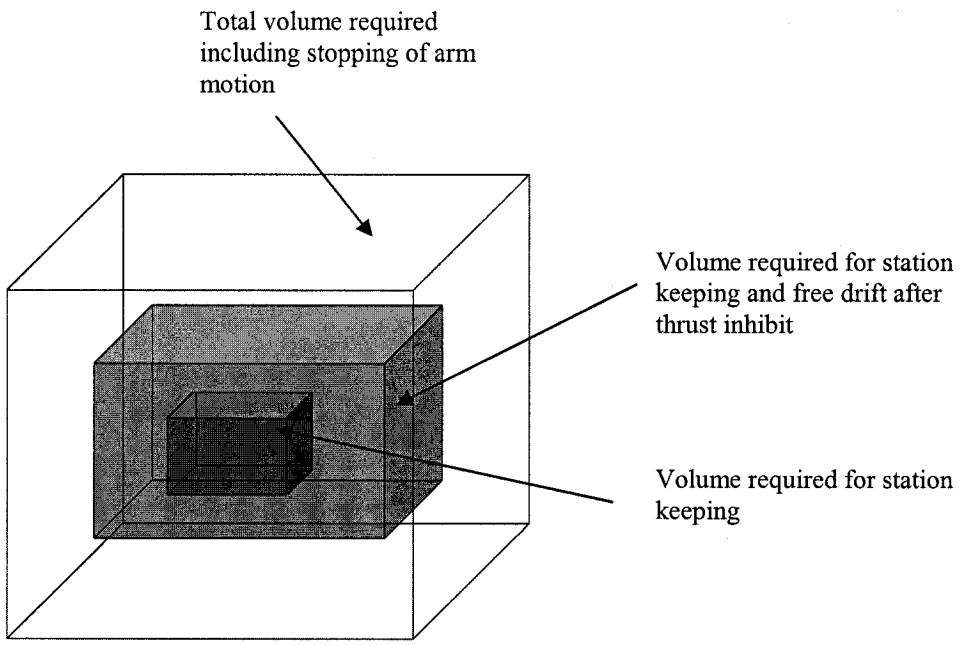

Figure 1.3: Volumes of Berthing Boxes

In order to determine of the allowable position of the berthing box, the maximum outlines of the chaser vehicle must be added to the outer berthing volume, and safety margin around the target vehicle must be added. The manipulator arm must be able to reach the entire berthing box. The berthing box will not be necessary of a cubic shape.

Synchronization Monitoring Needs

For the final rendezvous, there are few concerns must be taken into consideration:

1) **Proper sun illumination conditions:** during the last part of the final approach and during docking/berthing since visual feedback control system will rely for power and measurement reasons on Sun illumination.

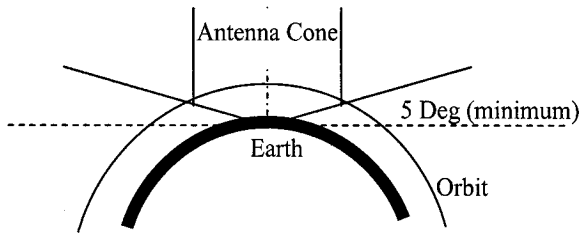

Figure 1.4: Visibility of Ground Stations, Geometrical Relation

2) **Availability of a communication window**: for the transmission of data (video data) to ground either directly to aground station or via relay satellite. Communication from the chaser and the target spacecraft to the ground can be performed either directly between the antennas of the spacecraft and ground or via a relay satellite in geostationary satellite. In the case of direct communication with a ground station, the duration contact is limited by: the altitude of the orbit, the radiation/reception cone angle of the ground antenna and by the part of the cone which will be actually crossed by the orbit as shown in Figure 1.4. The resulting time for possible radio contact is called communication window with the ground station. The useful range starts at elevation angles of 5-7 degrees, i.e. the maximum half cone angle of the antenna's radio/reception cone will be less than 85 deg. In a low earth orbit and under the best conditions (when flying over the center of the cone) the maximum communication duration would be of the order of 10 minutes for a 400 km orbital altitude, and about 7.5 minutes for a 300 km

orbital altitude. For longer communication windows a relay satellite in geostationary orbit should be used. It provides almost half an orbit coverage each.

Berthing Operation

The manipulator arm is mounted on the servicing satellite with a grapple mechanism mounted on the end-effecter. The correspondingly the grapple fixture is mounted on the target satellite. Steps of berthing have to be established for capturing and berthing a target as follows:

1) Acquisition of berthing box by the target: the target vehicle should be located in the station keeping position in the berthing box as explained before.
2) Acquisition of readiness position by manipulator: once the target is in the berthing box, the manipulator with its end-effecter will be moved to a position form where capture operations can start. As a rule and for safety reasons, the manipulator will not be in this position during acquisition of the berthing box by the target.
3) Switch-off of the target thrusters and initiation of capture (free floating): When the front end of the manipulator has acquired the readiness position and when it has been verified that the grapple fixture is within the inner berthing box, the propulsion system of the target will be inhibited and the manipulator will be steered to pursue with its end-effector the grapple fixture on the chaser. After thrust inhibition, the target will start to move away due to the effects of orbital dynamics. As a result, the capture has to be performed in short time to prevent losing the contact.

4) Grappling of capture interfaces by the manipulator: when the correct position of the capture tool (end-effecter) is achieved, the grappling operation is initiated. Grappling has to ensure that the interfaces can no longer escape each other. Consequently, the connection between the manipulator and the captured vehicle is sufficiently rigid to comply with the needs for transfer and insertion. Correct position of the end-effecter (grapple mechanism) with respect to the capture interface on the other vehicle (grapple fixture) requires sensing function like relative attitude angles.
5) Transfer to the berthing port: the front end of the manipulator will be steered so as to perform all necessary translations and rotations to move the berthing mechanism interfaces of the captured vehicle to those of the berthing port on the other vehicle. A path planning will be used so as to ensure no collision between the two satellites occurs.
6) Insertion into the reception interfaces: berthing mechanism has a reception mechanism that must be measured according to the positioning accuracy of the manipulator. After proper positioning has been established, the manipulator will push the berthing interfaces of the captured vehicle gently into those of the berthing port of the other vehicle. The manipulator can provide pushing forces until structural connection commences.

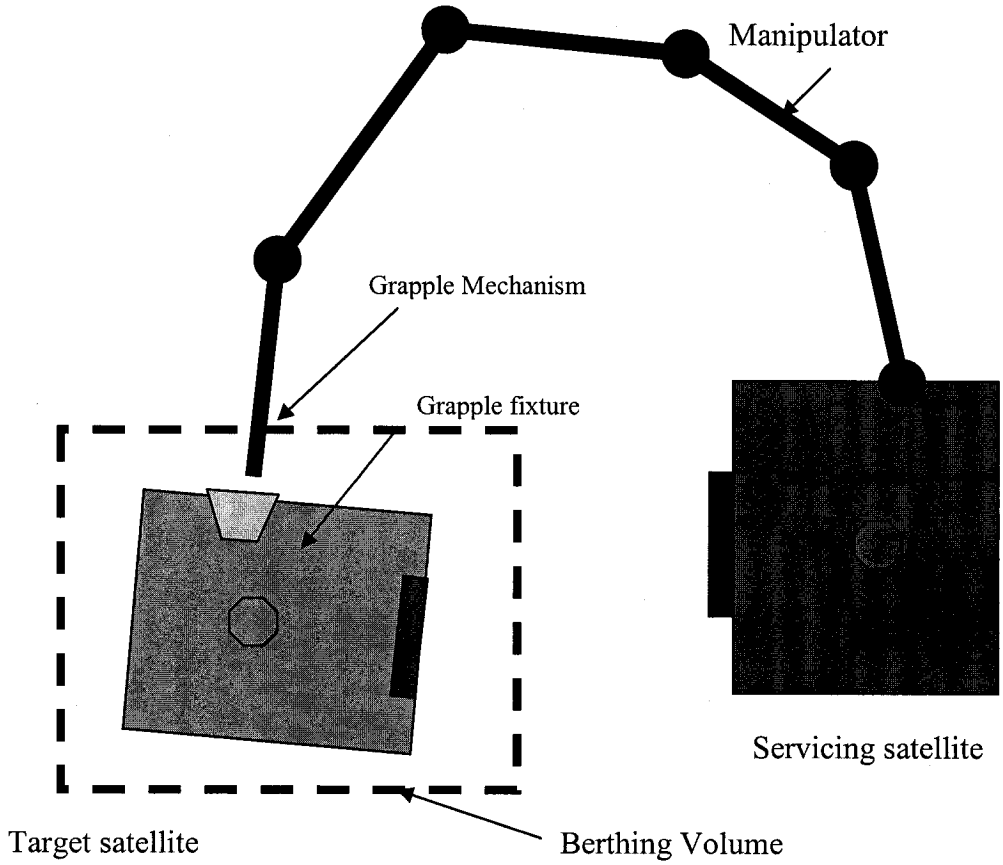

Figure 1.5: Berthing Scenario

7) Structural connection: once they are aligned the structural latches can be engaged to provide rigid connection. More contact task can now be performed on the surface of the target satellite via the manipulator arm.

Grapple Mechanism and Grapple fixture

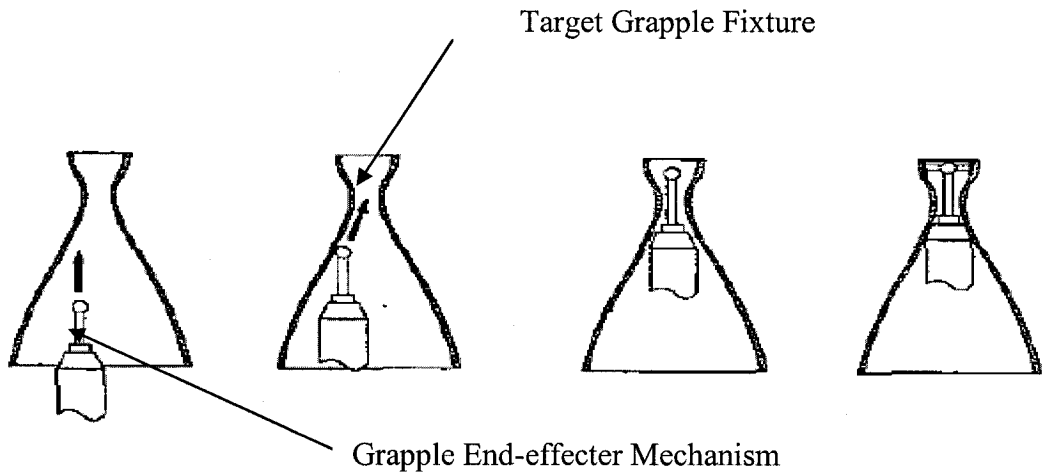

Figure 1.6: Capture Mechanism

The active part of grappling is mounted at the end-effecter of the manipulator. So as to ensure no escape after a contact has been established between the end-effecter and the grapple fixture on the target satellite an elastic grapple mechanism is preferred. The end effecter can be designed as a rod which elastically connected to the last manipulator link. Two main forces will occur at the contact: a longitudinal force along the rod axis and a lateral force which causes a torque about the connection point and its base. Accordingly, a longitudinal motion along the rod axis and an angular motion about the spherical bearing at its base have to be attenuated. Without flexibility in the rod, more specifically in the lateral direction, the tip of the rod would not move to the center of the cone, which is the place where it can be captured. Actually, if the rod were rigid and firmly connected to the chaser body, its tip would behave as the contact point in a non- central impact and would lead to leaving the capture interface.

1.2 Background and Literature Survey

Free-flying space robots, free-floating space robots and telerobotic systems have been under intensive consideration to perform a diverse important space missions such as: retrieving, inspection, maintenance, repairing and servicing satellites in earth orbit. Many satellites have been launched so far; some of them have become uncontrollable and does not work in the orbits. Recovering the attitude of the satellites, charging the exhausting batteries, and replacing the failed parts like solar panels or antennas are some examples of the desired services. Using such servicing robotic system will also benefit the environment by reducing the junk metals floating in the space, and minimize the possibility of sudden crash accidents of orbiting satellites or spacecrafts with these floating junks. The task of capturing satellites is really inevitable for the services. As this task in space is a dangerous task for astronauts, space robots are expected to do it.

There are two major classes of space robots can be classified: 1) free-flying space robots and 2) free-floating space robots. The manipulator system of the first type is a system in which the reaction jets (thrusters) are kept active so as to control the position and attitude of the systems' spacecraft. Such system is clearly highly redundant giving it versatility, and a nearly unlimited workspace. However this kind of space manipulators show some control challenges represented in the disturbance of the spacecraft's motion as a result of the motions of the manipulator. Such disturbances in spacecraft's position and attitude could increase the consumption of the reaction jet attitude control fuel. Since jet fuel is

not renewable, then it will result in limiting the life of the free-flying orbiting servicing system.

In opposition to the free flying robot, a free-floating space robotic system is a system in which the spacecrafts' reaction thrusters are shut down to conserve attitude control fuel. This means that the position and attitude of the spacecraft are not actively controlled during manipulation activity. Then, the spacecraft will react freely in response to the manipulator's motion. As a result, the conservation of the angular momentum will be rise and bring some control challenges such as holonomic and nonholonomic kinematic constraints, which are not found in the terrestrial systems.

Modeling of dynamics and kinematics of space robots is considered a very fundamental part in designing an efficient multi-body system with effective controllers. Many techniques in dynamic modeling of space robots have been reviewed in [2][4][5]. Newton-Euler dynamic approach of multi-body systems is proposed in [6][7]. This approach is characterized the use of a tree topology of open chain multi-body system with the system Center of Mass as the translational DOF. Barycenters are used efficiently to formulate the kinematics and dynamics of free-floating space robots. Another approach is called the direct approach and it uses one body of the system to be the reference frame with a point on it to represent the transitional DOF of the system [8][2][9]. This approach is simpler but results in coupled equations. A virtual manipulator is proposed in [10-14] and used to simplify the system dynamics of space robots. It decouples the system Center of Mass transactional DOF. A solution to the inverse dynamic problem of a space robotic

system in the presence of external generalized forces is proposed in [25]. In [25-29], in order to derive the kinematic model of free-flying space robots, a body is selected first, e.g. the spacecraft in [26] or the whole system as a composite body in [28]. Then, the velocities of the pre-selected body are used to derive the total momenta of the whole system, and finally, the kinematics model is derived. Selecting a body first is not needed to derive the total momenta of the space robot by using the total kinetic energy [29]. This allows to express the total momenta in terms of the velocities of an arbitrary body called the primary body. A modeling for a free-floating multibody planar space robot is derived in [30]. A nonholonomic approach has been conducted for the kinematic modeling and control. A reduced state-space model employed to control multibody space system using nonholonomic techniques for planar space robot is proposed in [31].

To control space robots many schemes has been proposed and can be classified into four categories:

First category: the spacecraft motion attitude and position can be kept fixed by compensating for any dynamics forces exerted on the body of the spacecraft by the manipulator's motion. However, as stated above, this approach has a drawback of consuming large quantities of attitude control fuel which can cause as result of in limiting the life of the active servicing satellite. But to overcome such a significant problem some control techniques have been proposed in [1][15][16][17] by what using what is called Enhanced Disturbance Map.

Second category: only the spacecraft attitude is controlled while the position is not, since the attitude controlled system is more involved than the both parts of the motion. Some researchers have proposed some schemes to calculate the moments needed by the reaction wheels to keep the spacecraft's orientation fixed.

Third category: free-floating space robotic system in which, as briefed previously, the spacecraft reacts freely in response to the motion of the system manipulator. As can be easily concluded, this scheme has the advantage of conserving the jet fuel and avoiding any jet firing effects. It should be mentioned that this approach can only be used in the absence of any external forces or moments. In [18] it has been proved that nearly any control method applied to the terrestrial robotic system can be employed to the space robots given that the right dynamic model is used. But this system behaves some dynamic singularities that depend on the inertia of the system. A Generalized Jacobian Matrix GJM has been derived and proposed in [19] based on what is called resolved rate algorithm. GJM is an extension to the Jacobian matrix of the fixed-base manipulator. The Extensive experiments have been implemented [63] and showed good results. The Virtual Manipulator proposed in [10-14] can also be used to simplify the free-floating system. A transposed Jacobian controller with a Jacobian of the fixed-based system [20] is able to track the end-effecter to the desired trajectory. The rise of conservation of angular momentum in the case of free-floating system makes the path planning of the system because of the nonholonomic constraints is more difficult task. To control the manipulator's joint motion a self-correcting planning scheme is proposed in [12][14]. A Lyapunov functions for nonholonomic behavior of the free-floating space robot are

discussed in [21] to control both the orientation of the spacecraft and manipulator's configuration. In the case of a multi-robotic system, one manipulator can be moved to compensate for the disturbance of the attitude created by the others as investigated in [22].

Holonomic and nonholonomic systems: consider a robotic system whose configuration can be given by a vector of its generalized coordinates $q \in Q$. The configuration space Q of such system is an n-dimensional smooth manifold. For any given trajectory $q(t) \in Q$, the generalized velocity at a configuration q is the vector $\dot{q}$ belonging to the tangent space $T_q(Q)$.

Some robotic systems motion is subject to constraints as a result of its structure or from the way it is actuated and controlled. Such holonomic constraints come as a result of the mechanical interconnections between the various bodies of the system. Many classifications can be devised. One of the classifications is the itegrability of the constraints. If these constraints are integrable, then this system is called a holonomic system. In this case constraints can be expressed in the form

$$h_i(q) = 0, \quad i = 1, \cdots, k < n, \tag{1.1}$$

If the kinematic constraints exist for a holonomic system then Equation (1.1) can be rewritten in the form

$$\frac{\partial h_i(q)}{\partial q}\dot{q} = 0, \quad i = 1, \cdots, k \tag{1.2}$$

Equation (1.2) can be integrated as

$$h_i(q) = c \tag{1.3}$$

which defines a particular surface of h, where c is an integration constant.

On the other hand, if these constraints are not integrable, then the system is called a nonholonomic system. The kinematic constraints can be put in the following mathematical form

$$a_i^T(q)\dot{q} = 0, \quad i = 1, \cdots, k < n, \tag{1.4}$$

$$A^T(q)\dot{q} = 0 \tag{1.5}$$

This will limit admissible motions of the system by restricting the set of generalized velocities that can be achieved by a given configuration. Correspondingly, the number of degrees of freedom is reduced to $n-m$, where m is the number of constraints.

There are different sources of nonholonomy that can be considered such as: rolling without slipping, conservation of angular momentum in multibody systems, and robotics under special control operations.

In the first class, there are many applications: wheeled mobile robots and vehicles, where the rolling contact takes place between the wheels and the ground, multi finger robotic hands, with the constraints arise as a result of the rolling contact between the fingers and the object to grasp.

For the second class the nonholonomic constraints appears when multi body systems are floating freely, i.e. without consisting a fixed frame base. When applying the

conservation of angular momentum then differential constraints are not integrable. Some systems that fall in this category are: space manipulator robotic system fixed on a floating satellite or space structure, and satellites with reaction wheels for attitude stabilization.

For the third class there are many examples such as: underwater robotic system where the forward propulsion is allowed only in the pointing direction, robotic manipulators with more than one passive joint, i.e. underactuated robotic systems.

To solve the challenge of nonintegrability of angular momentum many researchers have proposed different schemes. A nonholonomic path planning of space robots is proposed in [32] via bi-directional approach. The spacecraft orientation can be controlled in addition to the joint variables of the manipulator, by actuating only the joint variables, if the trajectory is carefully planned. This approach is able to converge the spacecraft orientation and joint variables to their desired values, without the need to neglect the linearity of high orders and there is no algorithm limitation about the allowable change.

Nonholonomic motion planning and steering using sinusoids is proposed in [33] to control a hopping robot in flight phase. Stabilization of free-floating manipulators is proposed in [34] based on smooth time-variant dynamic feedback for stabilization of a nonholonomic system. Chained form transformation algorithm for a class of 3-states and 2-inputs attitude control of space robot with zero angular momentum initial conditions is investigated in [35]. In the case of non-zero angular momentum initial conditions, an attitude control of a space robot is proposed in [36]. The proposed controller is based on

the coordinate and input transformation algorithm that converts an affine system with a drift term into the time-state control form and exact linearization.

Fourth category: any desired location or orientation could be reached by activating the spacecraft's jets. As said above, this has an advantage of almost unlimited workspace. To solve the problem of extra consumption of the fuel an economic control scheme is proposed in [23] by switching between the free-flying and free-floating techniques. In other words, in the free-flying mode the system is controlled in a coordinated way so that the manipulator is redundant. In [24] a coordinate control algorithm is proposed by keeping a large workspace and by tracking both the spacecraft and the manipulator in their desired trajectories.

Adaptive control: is very important for the space robot system subject to dynamic uncertainty in space tasks. It has been shown that there are two fundamental challenges in adaptive control of space robots. First, the dynamic equation of the system cannot be linearized in the inertial space. Second, in the case of free-floating space robot the kinematic mapping from the Cartesian space, in which the robot tasks are usually specified, to joint space, where the control executed, becomes non-unique due to non-integrable angular momentum. To overcome these problems [40] has proposed a model allows to categorize the space robot as an under-actuated system and reveals fundamental properties of the system. This scheme is called normal form augmentation approach. It first models the entire system as an extended robot, which is composed, of a pseudo-arm

representing the base motion with respect to the orbit and a real robot. An exact input-output linearization is performed.

In [37-38] an adaptive control of a space robot system with an attitude controlled base on which the robot is attached has been investigated. It has been found that in the joint space the dynamics can be linearized by a set of combined dynamic parameters but it fails in the case of Cartesian space.

An adaptive control of space robot system with an attitude-controlled base is investigated in [41]. Two potential problems in the inertial frame are identified, unavailability of joint trajectory, and nonlinear parameterization of system dynamics. Based on linear momentum conservation law, two adaptive control algorithms with or without acceleration measurement are proposed. Both algorithms guarantee the stability of the closed loop system and zero inertial position tracking error.

A robust adaptive control of space robots is addressed in [39]. In this approach, a globally dynamic model is derived which is applicable whether the momentum wheels are used to control the attitude of the spacecraft or not. It is based on the idea of decomposing the dynamic uncertainties into two parts and combines a robust scheme to handle the system dynamic uncertainties.

In order to eliminate the need of base acceleration, the assumption that the uncertainty bounds must be a priori known, a continuous adaptive robust control scheme is proposed

in [42]. The proposed controller is achieved by using norm-bounded property of uncertainty based on Lyapunov direct method.

Looking at capture and retrieve operation of a floating and tumbling target, such as a malfunctioning satellites, by a servicing robot, we can find three different phases of dynamics and control problems to be investigated [48]:

First phase: Target chasing control phase (before contact with the target): determines the initial conditions. Information about the pre-impact configuration, the mass and inertia properties, and the pre-impact relative velocities between the manipulator hand and the object is required.

Second phase: Impact phase between the target and the robotic hand (at the moment of contact): During the impact phase, contact between the manipulator hand and the object is established, and a force impulse is generated. The magnitude of this force impulse is estimated in a straightforward manner by applying the classical theory of dynamics of systems of rigid bodies.

Third phase: Relieve and suppress control phase of tumbling motion (after contact): the post impact velocities of the hand and the object must also be estimated

Modeling contact and interaction forces between robots and thier environment has received high attention in the last decade. In industrial robots, for example, contact tasks

are intentionally involved between the robot and the manipulating objects as in assembly operations, and between tools and work-piece, like grinding, polishing or cutting. Contact between robot and environment may or may not involve energy exchange. When the environment or the manipulating object imposes only kinematic constraint on the end-effecter of the robot, only static balance forces/torques exist at the point of contact, and thus it implies no energy exchange or power dissipation. This approach is investigated by [52-53] underlying the assumption of kinematic constraints and static balance forces occur. An energy exchange between the robot and the environment is allowed in the study of [54] using a full-dimensional linear impedance model. But it is based on the assumption of small deformation of the environment. A new modeling approach for describing motion of robots in contact with dynamic environment is proposed in [55-58]. The proposed technique allows to model all those cases in which purely kinematic constraints are imposed on the robot end-effecter together with interactive dynamics.

Modeling of contact forces: Contact forces investigation in the operational space of the end-effecter is the main concern of the work done in [87-89]. In [87] a framework for the analysis and control of manipulator systems with respect to the dynamic behavior of their end-effectors is developed. First, issues related to the description of end-effecter tasks that involve constrained motion and active force control are discussed. The fundamentals of the operational space formulation are then presented, and the unified approach for motion and force control is developed. These results are used in the development of a new and systematic approach for dealing with the problems arising at kinematic singularities. At a singular configuration, the manipulator is treated as a mechanism that

is redundant with respect to the motion of the end-effecter in the subspace of operational space orthogonal to the singular direction. In [88] a unified approach for the control of manipulator motions and active forces based on the operational space formulation is presented. The end-effecter dynamic model is used in the development of a control system in which the generalized operational space end-effecter forces are selected as the command vector. This formulation provides a framework for natural and efficient integration of both end-effecter force and motion control. A "generalized position and force specification matrix" is used for the specification of tasks that involve simultaneous motion and force operations. Flexibility in the force sensor, end-effecter, and environment, and problems related to impact are discussed. Meanwhile, in [89] a general first order kinematic model of frictionless rigid-body contact for use in hybrid force/motion control is proposed. It is formulated in an invariant manner by treating motion and force vectors as members of two separate but dual vector spaces. This allows to model tasks that cannot be described using Robert-Craig model; a single Cartesian frame in which directions are either force- or motion-controlled is not sufficient. The model can be integrated with the object and manipulator dynamics in order to model both the kinematics and dynamics of contact. Decoupling between controllers is obtained by applying projection matrices to the controller outputs that depend solely on the kinematic model of contact, not on dynamics.

A unified approach for inverse and direct dynamics of constrained multibody systems that can serve as a basis for analysis, simulation, and control is proposed in [83-84]. The main advantage of the dynamics formulation is that it does not require the constraint

equations to be linearly independent. Thus, a simulation may proceed even in the presence of redundant constraints or singular configurations, and a controller does not need to change its structure whenever the mechanical system changes its topology or number of degrees of freedom. A motion-control scheme is proposed based on a *projected inverse-dynamics* scheme which proves to be stable and minimizes the weighted Euclidean norm of the actuation force. The projection-based control scheme is further developed for constrained systems, e.g., parallel manipulators, which have some joints with no actuators (passive joints). This is complemented by the development of constraint force control. A condition on the inertia matrix resulting in a decoupled mechanical system is analytically derived that simplifies the implementation of the force control. Finally, numerical and experimental results obtained from dynamic simulation and control of constrained mechanical systems, based on the proposed inverse and direct dynamics formulations, are documented

Coordinated space robots: Manipulating a floating payload or articulated structure by a flying space robot is a specially attractive but difficult issue in robotics and dynamics. When a rotating satellite is captured, large forces and moments are exerted at the contact points of the satellites due to inertia force of the capturing satellites [85-86]. The use of two manipulators is highly preferable to reduce these forces and moments as the case of human being two hands. Diverse control schemes are proposed to capture an object using two or more manipulators. In [60] proposed an algorithm of multiple impedance control to enforce the designated impedance of both a manipulated object and all cooperating manipulators of the free-flying-based manipulator system. The stability of such a system

is proved based on Lyaponuv direct method to fulfill a desired force trajectory. The position and force control of coordinated robots mounted on spacecraft, manipulating a satellite with closed kinematic chain constraints is the focus of the study [61]. In this work, the kinematics and dynamics of such coordinated space robotic system is established. Based on these modes, an approach to position and force control of free-flying coordinated space robots is proposed. Moreover, the dynamics of the manipulated object and its interaction with the end-effecter are taken into the account. The stability of the closed-loop free-flying coordinated robotic system is analyzed based on error models of the object and internal forces and it asymptotically converge to zero. Capturing a floating object by flexible two manipulators investigated in [62] [65]. Hybrid position/force control and vibration suppression is proposed. It is established in the way that both hands reach the object simultaneously and grasp the object exerting the desired forces/moments. A nonlinear adaptive control of multi-manipulator of free-flying robots is conducted in [65]. A new task space adaptive control is developed and it uses an inverse-dynamics adaptation algorithm.

Experimental research: Starting in 1999, the International Space Station (ISS) will be launched and assembled in space. Canada's contribution to the ISS is the Mobile Servicing System (MSS) [53]. The MSS is composed of the Mobile Remote Servicer Base System (MBS), the Space Station Remote Manipulator System (SSRMS) and the Special Purpose Dextrous Manipulator (SPDM). The SSRMS is a 15-meter long, seven degrees of freedom flexible manipulator, while the SPDM consists of two 3.4-meter long, seven degrees of freedom arms with an additional degree of freedom through body

rotation. Terminating each of SPDM arms is the Orbital Tool Change-out Mechanism (OTCM) including a gripper, a camera with two lights, a Socket Drive Mechanism and a Force Moment Sensor (FMS). While the SSRMS will be used to assemble the ISS, the SPDM will be required for performing maintenance tasks. The SPDM will be used to replace the so-called Orbital Replacement Units (ORU), the components of the ISS systems replaceable on orbit. The SPDM will operate directly connected to the ISS or to the tip of the SSRMS. Both the SSRMS and the SPDM are teleoperated by an operator located inside the ISS. Due to the important flexibility in the SSRMS/SPDM system, all insertion/extraction tasks involving the SPDM will be done using only one arm with the other arm grasping a stabilization point. Canada is responsible for the verification of all the tasks involving the SPDM. The Canadian Space Agency (CSA) developed the SPDM Task Verification Facility (STVF), a series of simulation and analysis tools to be used for verifying the kinematics (clearance, interface reach, degrees of freedom), dynamics (insertion forces, flexibility), visual accessibility (ability to see the work site) and resource allocations (power, crew time).

In recent years, a number of experiments have been performed on capture of satellites by robot mounted space vehicle. Some of these experiments were implemented on terrestrial robots and others on orbital free-flying space robotic system. The Engineering Test Satellite VII (ETS-VII) developed and launched by National Space Development Agency of Japan (NASDA) has been successfully flown and carried out a lot of remarkable interesting orbital robotics experiments with a 2 meter-long, 6 DOF manipulator arm mounted on this un-manned spacecraft. The experimental results in [63][101] present

post-flight analysis of Reaction Null-Space based reactionless manipulation, or Zero Reaction Maneuver. The ZRM is proven particularly useful to remove the velocity limit of manipulation due to the reaction constraint and the time loss due to the waiting for the attitude recovery.

In [64] an autonomous free-floating robot system is designed to investigate the behavior of free-floating robots that are involved in the capture of satellites in space. The robot is used as a test bed for algorithms that have been developed for efficient and autonomous capture of floating objects in space. The system is running under a real time operating system. It is equipped with 3 DOF arm, a three-axis thruster system and fast communications module. The robot works in conjunction with a host computer. The host computer is used to process the capture algorithm and the robot implements the results in real-time.

Another experiment on a free-flying space robot performing capture and manipulating free-floating objects with unknown inertial properties is carried in [65]. Task space adaptive control framework is developed and able to provide continuously full adaptation capability to complex robot systems in all modes. This scheme consists of generalized inverse-dynamics adaptation algorithm to allow operators to specify a robots task, including payload positions, endpoints positions, and joint configurations.

1.3 Research Motivation and Control Objective

Studies [10-18][20-21][25-30][32-42] describing kinematics and dynamics of a space robot neglect the coupled kinematics and dynamics with a floating target or consider only abstract external forces/moments or impulse forces [46][48-50]. An impedance matching algorithm is proposed to capture the target over a finite time [133]. Since the target has its own inertial and nonlinear forces/moments that significantly influence the ones of the space robot, those forces cannot be ignored. Applying improper forces to the constraint surface may cause severe damage to the target and/or to the space robot and its base satellite or cause the target to escape away. To accomplish a capture in practice is not instantaneous, because the end-effecter needs to keep moving and applying a desired force/moment over a finite time on the surface of the target until the target is totally captured or the contact task is completely accomplished. Not to forget to mention that from trajectory planning point of view, not all trajectories and displacements (velocities) are allowed due to the conservation of momentum and geometric constraints [21]. This shows the significance of modeling motion, dynamics and contact forces of a free-flying space robot interacting with a target satellite and taking into account all constraints impose on the system as a whole. The control objective can then be summarized as follows: given the desired contact forces between the free-flying space robot and the passive target satellite, and given the desired trajectories of space robot arm, design a hybrid control law such that forces and trajectories asymptotically converge to their desired values and adapt with any uncertainty in the system parameters.

1.4 Contribution

A unified control-oriented modeling approach is proposed in this thesis to describe the kinematics, linear and angular momentum, contact constraints and dynamics of a free-flying space robot in contact with a target satellite. This model combines the dynamics of both systems together in one structure and handles all holonomic and nonholnomic constraints in a unified framework. This approach allows considering the generalized contact forces between the space robot end-effecter and the target satellite as internal forces rather than external forces. To have a better understanding of the nonholonomic constraints, a physical insight is explored. It analyzes the geometric conditions behind conservation of linear and angular momentum of a free-flying robot with/without contact with a target satellite.

A criterion of finding out whether the constraints imposed on the system are holonomic or nonholonomic is then proposed. This methodology proposes a linear transformation based on orthogonal projectors and singular value decomposition. The usefulness of this methodology is that it can be used online/offline to verify whether constraints are changed or violated.

Based on this unified model, three reduced models are developed. The first reduced dynamics can be considered as a generalization of a free-flying robot without contact with a target satellite. In this reduced model it is found that the Jacobian and inertia matrices can be considered as an extension of those of a free-flying space robot. Since

control of the base attitude rather than its translation is preferred in certain cases, a second reduced model is obtained by eliminating the base linear motion dynamics. For the purpose of the controller development, a third reduced-order dynamical model is then obtained by finding a common solution of all constraints using the concept of orthogonal projection matrices.

Based on the latter reduced model, an inverse-dynamics and adaptive inverse-dynamics controllers are proposed to handle the overall combined coupled dynamics of the based-satellite servicing robot and the target satellite all together with geometric and momentum constraints imposed on the system. The proposed controllers do not only show the capability to meet motion and contact forces desired specifications and to cope with the under-actuation problem, but also to adapt with uncertainties in the system parameters in the case of the adaptive controller.

This thesis claims the following major contributions in three categories:

A) Modeling:

- Derivation of kinematics, contact constraints and linear momentum of a free-flying space robot in contact with a target satellite as a serial multi-body system [Chapter 2].
- A common solution of contact constraints, linear and angular momentum constraints is proposed using linear algebra techniques [Chapter 2].
- The proposed linear and angular momentum model is a general form of that of a free-flying space robot without interaction with a target [Chapter 2].

- A control-oriented dynamics of a free-flying space robotic system together with the dynamics of the target satellite is formulated in one unified model [Chapter 5].
- A reduced Jacobian matrix and a reduced inertia matrix of a free-flying space robot interacting with a target satellite are, respectively, generalization of the Generalized Jacobain matrix and the inertia matrix of a free-flying space robot. That is, a free-flying space robot is a special case of this proposed model [Chapter 5].
- A second reduced model is obtained by eliminating the base linear motion dynamics which is suitable to control the base attitude rather than its translation in certain cases [Chapter 5].

B) Analysis:

- A physical insight of holonomic/nonholonomic constraints act on a free-flying space robot with/without interaction with a floating target satellite is presented [Chapter 3].
- A new criterion of holonomy/nonholonomy of constraints imposed on a free-flying space robot with or without interaction with a floating object is proposed by utilizing the concept of orthogonal projection matrices and singular value decomposition [Chapter 4].

C) Control:

- An inverse-dynamics-based control approach of a free-flying space robot manipulator interacting with a target satellite is presented. A reduced-order dynamical model is obtained by finding a common solution of all constraints using the concept of

orthogonal projection matrices. The proposed controller does not only show the capability to meet motion and contact forces desired specifications, but also to cope with the under-actuation problem of the target satellite due to its thrusters' failure or shutdown [Chapter 6].

- An adaptive inverse-dynamics-based control approach of a free-flying space robot manipulator interacting with a target satellite is presented. This controller poses the advantages of the inverse-dynamics controller in addition to the ability to overcome the system parameter uncertainty [Chapter 7].

1.5 Thesis Organization

The thesis is composed of eight chapters. In Chapter 2, modeling of kinematics of a free-flying space robot interacting with a target satellite is derived, linear and angular momentum is formulated, then geometric contact constraints are presented, and finally a common solution for all constraints is proposed by using some theorems of linear algebra.

Chapter 3 analyzes the geometric conditions behind holonomic/nonholonomic constraints of a free-flying space robot and reveals the conditions of keeping linear and angular momentum conserved in case of a free-flying space robot interacting with a target satellite. Finally, simulation results are presented to demonstrate the analytical results.

In chapter 4, a nonholonomy criterion is proposed and then simulation results are presented to demonstrate the proposed criteria.

In chapter 5, an overall dynamics modeling is derived, constraint force decomposition is presented, dynamics reduced model is proposed, and at the end simulation results are demonstrated.

In chapter 6, a hybrid inverse-dynamics based controller is proposed to meet the motion desired specifications and track the desired contact forces, and then simulation results are demonstrated to verify the analytical results.

In chapter 7 an adaptive inverse dynamics control law is proposed to meet the specified motion desired values, track the contact forces and adapt with parameters changes, then an introduction to Hubble Space Telescope is given, and finally a simulation of the proposed adaptive algorithm is dedicated to Hubble space Telescope to verify the analytical results.

Finally, in Chapter 8 summary, conclusions, discussions and future work are discussed.

Chapter 2

Modeling of Kinematics and Momentum of a Free-Flying Space Robot Interacting with a Passive Target Satellite

2.1 Introduction

Comprehensive understanding of the kinematics and momentum of space robots and their interaction with a floating object is considered as a very essential part in designing an efficient multi-body system with effective control techniques of contact forces and motion trajectories. Kinematics motion of a space robot system are developed based on the concept of a Virtual Manipulator (VM) [10-14]. Since the VM does not model the angular momentum, then the attitude motion of the base satellite has to be considered by other means. It also assumes imaginary mechanical links. One body of the space robotic system is used as the reference frame with a point on it to represent the transitional DOF of the system [8][2][9]. A tree topology of open chain multi-body system with the system center of mass as the translational DOF is proposed in [6-7]. The velocities of a pre-selected body (such as the spacecraft in [26] or the whole system as a composite body in [28]) are used to derive the total momenta of the whole system. Selecting a body first is not needed to derive the total momenta of the space robot by using the total kinetic energy [29]. However, the latter approach allows to express the total momenta in terms of the velocities of an arbitrary body called the primary body. The kinematics of a free-flying multi-body system is investigated by introducing the conservation of momentum

and deriving a new Jacobian matrix called the Generalized Jacobian [26]. It can be concluded that approaches investigated in [3][13-14][21][25-26][29-30][37-38][46][48-50] [63] either consider the kinematics and momentum of a free-flying space robot separately from the target satellite or assume no interaction.

When a space robot end-effecter interacts with a flying/floating object, it imposes a geometric holonomic (integrable) constraint [6][15][17]. On the other hand, the conservation of momentum exerts kinematic-like constraints on a space robot in the absence of external forces. The linear momentum is considered holonomic but the angular momentum as nonholonomic (non-integrable) [32][26].

This chapter presents kinematics modeling of a free-flying space robot interacting with a target satellite. This approach unifies both systems in one combined serial multi-body system. The advantage of this analysis is to account for all geometric, linear and angular momentum constraints together in a single framework which is significant to develop the system dynamics and control design.

This chapter is organized as follows: in section 2.2, modeling of kinematics of a free-flying space robot interacting with a target satellite is presented, in section 2.3 linear and angular momentum is formulated, then geometric contact constraints are derived in section 2.4, and finally a common solution for all constraints is proposed by using some theorems of linear algebra.

2.2 Kinematics Modeling

The purpose of this part is to model a free-flying space robotic manipulator in contact with a target satellite as a whole. In this model the contact between the space robot and the target satellite is assumed established and not lost. Our combined system can be modeled as a multi-body chain system composed of $n+2$ rigid bodies. While the manipulator links are numbered from 1 to n, the base satellite is denoted by b in particular and the target satellite by t. Moreover, This multi-body system is connected by $n+1$ joints, which are given numbers from 1 to $n+1$. Where the end-effecter is represented as the $(n+1)th$ joint as shown in Figure 2.1.

Referring to Figure 2.1, the position vector of the ith body with respect to the inertial frame can be readily expressed as

$$r_i = r_b + r_{i_{/b}} \tag{2.1}$$

Moreover, the relative vector $r_{i_{/b}}$ is the position of the ith body with respect to the base and can be expressed in the form

$$r_{i_{/b}} = r_i - r_b \tag{2.2}$$

Upon differentiating both sides of (2.1-2.2) with respect to time, the relationship between the ith body velocity is [Please see Appendix A for details]

$$V_i = V_b + \Omega_b \times r_{i_{/b}} + v_i \tag{2.3}$$

where Ω_b is the angular velocity of the base, v_i is the linear velocities of the ith body in base coordinates.

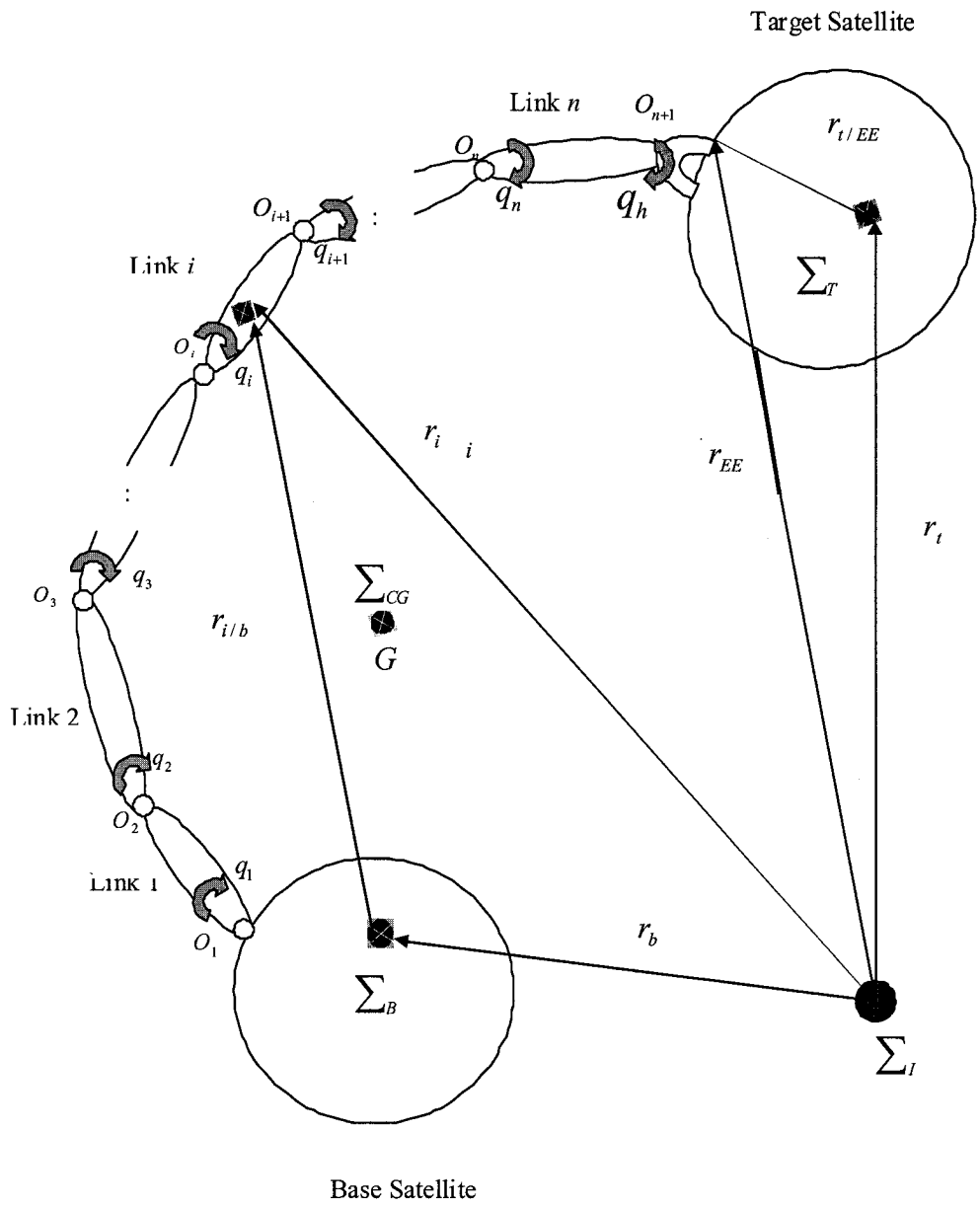

Figure 2.1: A Free-flying Space Based Satellite robotic Manipulator in Contact with a Target Satellite

Now in the case of any *i*th body of the manipulator, the velocity v_i can be expressed in terms of the Jacobian matrix as

$$v_i = J_{L_i}\dot{q} \tag{2.4}$$

Where $\dot{q}$ is the robot joint velocity vector and the linear Jacobina matrix J_{L_i} is defined as

$$J_{L_i} = [k_1 \times (r_i - c_1), k_2 \times (r_i - c_2), \cdots, k_i \times (r_i - c_i), 0, \cdots, 0] \tag{2.5}$$

where $c_i \in R^3$ is the position vector pointing the *i*-th joint with reference to the inertial frame and k_i : a unit vector in the direction of z axis of the *i*th link coordinates

The end-effecter tip velocity is given by

$$V_{EE} = V_b + \Omega_b \times r_{EE/b} + J_{L_{EE}}\dot{q} \tag{2.6}$$

Moreover, the velocity V_T of the target satellite in the reference frame can be obtained from differentiating of (2.2) with respect to time as [please refer to Appendix A for more details]:

$$V_t = V_b + \Omega_b \times r_{t/b} + J_{L_{EE}}\dot{q} + \omega_t \times r_{t/EE} + v_t \tag{2.7}$$

Note that the relative linear velocity v_t and angular velocity ω_t between the end effecter and the target satellite are expressed in the base coordinate system.

Furthermore, the *i*th body angular velocity Ω_i is related to the joint angular velocity ω_i by

$$\Omega_i = \Omega_b + \omega_i \tag{2.8}$$

where ω_i is given by

$$\omega_i = J_{A_i}\dot{q} \tag{2.9}$$

where the angular Jacobain J_{A_i} is defined as $J_{A_i} = [k_1, k_2, \cdots, k_i, 0, \cdots, 0]$.

The absolute angular velocity of the target satellite can then be expressed as

$$\Omega_t = \Omega_b + J_{A_{EE}} \dot{q} + \omega_t \tag{2.10}$$

In the following section, the expressions of linear and angular velocitiues (2.3), (2.7), (2.8) and (2.10) will be used to derive linear and angular momentum of the system as a whole.

2.3 Linear and Angular Momentum Modeling

The linear momentum P and angular momentum L of the whole system is defined by

$$P \overset{def}{=} \sum_{i=0}^{n+1} m_i V_i \tag{2.11}$$

$$L \overset{def}{=} \sum_{i=0}^{n+1} \left({}^{B} I_i \Omega_i + m_i r_i \times V_i \right) \tag{2.12}$$

Substituting Equations (2.1), (2.3), (2.7), (2.8) and (2.10) in (2.11) and (2.12), linear and angular momentum can then be represented in a compact form

$$\begin{bmatrix} P \\ L \end{bmatrix} = \begin{bmatrix} H_{V_b} & H_{V_b \Omega_b} \\ H^T_{V_b \Omega_b} & H_{\Omega_b} \end{bmatrix} \begin{bmatrix} V_b \\ \Omega_b \end{bmatrix} + \begin{bmatrix} H_{V_b q} \\ H_{\Omega_b q} \end{bmatrix} \dot{q} + \begin{bmatrix} H_{V_b \omega_t} & H_{V_b v_t} \\ H_{\Omega_b \omega_t} & H_{\Omega_b v_t} \end{bmatrix} \begin{bmatrix} \omega_t \\ v_t \end{bmatrix} \tag{2.13}$$

where each sub-matrix of the block matrix can be obtained from the following equation

$$H_{V_b} \overset{def}{=} E_3 \sum_{i=0}^{n+1} m_i \in R^{3\times 3} \tag{2.14}$$

$$H_{V_b \Omega_b} \overset{def}{=} - \sum_{i=0, i\neq b}^{n+1} m_i \left[r_{i/b} \times \right] \in R^{3\times 3} \tag{2.15}$$

$$H_{V_b q} \overset{def}{=} \sum_{i=0, i\neq b}^{n+1} m_i J_{L_i} \in R^{3\times n} \tag{2.16}$$

$$H_{\Omega_b} \overset{def}{=} \sum_{i=0, i\neq b}^{n+1} \left\{ I_i + m_i D(r_{i/b}) \right\} + I_b \in R^{3\times 3} \tag{2.17}$$

$$H_{\Omega_b q} \overset{def}{=} \sum_{i=0, i\neq b}^{n+1} \left\{ {}^B I_i J_{A_i} + m_i \left[r_{i/b} \times \right] J_{L_i} \right\} \in R^{3\times n} \tag{2.18}$$

$$H_{V_b \omega_t} \overset{def}{=} -m_{n+1} \left[r_{t/EE} \times \right] \in R^{3\times 3} \tag{2.19}$$

$$H_{\Omega_b \omega_t} \overset{def}{=} m_{n+1} D(r_{t/EE}) + {}^b I_{n+1} \in R^{3\times 3} \tag{2.20}$$

$$H_{V_b v_t} \overset{def}{=} E_3 m_{n+1} \in R^{3\times 3} \tag{2.21}$$

$$H_{\Omega_b v_t} \overset{def}{=} -m_{n+1} \left[r_{n+1} \times \right] \in R^{3\times 3} \tag{2.22}$$

where E_3 is the 3×3 identity matrix, and the matrix function $[r\times]$ for a vector $r = [r_x, r_y, r_z]^T$ is defined as

$$[r\times] \overset{def}{=} \begin{bmatrix} 0 & -r_z & r_y \\ r_z & 0 & -r_x \\ -r_y & r_x & 0 \end{bmatrix} \in R^{3\times 3} \tag{2.23}$$

and

$$D(r) \overset{def}{=} [r\times]^T [r\times] = \begin{bmatrix} r_y^2 + r_z^2 & -r_x r_y & -r_x r_z \\ -r_x r_y & r_x^2 + r_z^2 & -r_y r_z \\ -r_x r_z & -r_y r_z & r_x^2 + r_y^2 \end{bmatrix} \in R^{3\times 3} \tag{2.24}$$

Note that (2.13) is just the momentum equations and assuming zero initial conditions $(P=0, L=0)$ will result in holonomic and nonholonomic constraints because of the conservation of linear and angular momentum, respectively, and these constraints are given by

$$\begin{bmatrix} 0 \\ 0 \end{bmatrix} = \begin{bmatrix} H_{V_b} & H_{V_b\Omega_b} \\ H^T_{V_b\Omega_b} & H_{\Omega_b} \end{bmatrix} \begin{bmatrix} V_b \\ \Omega_b \end{bmatrix} + \begin{bmatrix} H_{V_bq} \\ H_{\Omega_bq} \end{bmatrix} \dot{q} + \begin{bmatrix} H_{V_b\omega_t} & H_{V_bv_t} \\ H_{\Omega_b\omega_t} & H_{\Omega_bv_t} \end{bmatrix} \begin{bmatrix} \omega_t \\ v_t \end{bmatrix} \tag{2.25}$$

Then it is possible that the relative linear and angular velocities of the target satellite can be calculated without measurement as

$$\begin{bmatrix} \omega_t \\ v_t \end{bmatrix} = -\begin{bmatrix} H_{V_b\omega_t} & H_{V_bv_t} \\ H_{\Omega_b\omega_t} & H_{\Omega_bv_t} \end{bmatrix}^{-1} \begin{bmatrix} H_{V_b} & H_{V_b\Omega_b} \\ H^T_{V_b\Omega_b} & H_{\Omega_b} \end{bmatrix} \begin{bmatrix} V_b \\ \Omega_b \end{bmatrix} - \begin{bmatrix} H_{V_b\omega_t} & H_{V_bv_t} \\ H_{\Omega_b\omega_t} & H_{\Omega_bv_t} \end{bmatrix}^{-1} \begin{bmatrix} H_{V_bq} \\ H_{\Omega_bq} \end{bmatrix} \dot{q} \tag{2.26}$$

Last equation shows the dependence of target velocities on both base and manipulator velocities since the base satellite, the robot arm, and the target satellite all are modeled as one serial multibody system.

2.4 Geometric Contact Constraints Modeling

As discussed earlier in this thesis, the holonomic constraints arise as a result of restricting the motion of the robot end-effecter on the surface of the target satellite. These holonomic constraints are usually given in a set of nonlinear equations.

Now assuming the contact between the end-effecter and the target is established, then the constraint forces will act on both bodies. We assume that the end-effecter moves on a the surface of the target satellite S and the profile of this surface is known. Let χ present

the pose of the robot end-effecter expressed in the target frame. Then the motion of end-effecter is subjected to the following kinematic constraints as

$$\Phi(\chi) = 0 \tag{2.27}$$

where $\Phi(\cdot): R^n \rightarrow R^m$ is assumed to be twice differentiable. The robot joint and target coordinates are related through the forward kinematic function

$$\chi = f(\theta) \tag{2.28}$$

Now differentiating (2.27) and (2.28) with respect to time and applying the chain rule yields

$$J\dot{\theta} = 0 \tag{2.29}$$

where the matrix $J = \frac{\partial \Phi(\chi)}{\partial \chi} \frac{\partial f(\theta)}{\partial \theta}$ is the Jacobian matrix.

2.5 A Common Solution of both Holonomic and Nonholnomic Constraints

As it can be seen from the previous analysis there are three types of constraints act on the system

1) Linear momentum constraint: which is a hololonmic. Integrating this constraint will yield that the center of mass is stationary or moving in a constant linear velocity.

2) Angular momentum constraint: which is nonholonomic. The nature of this constraint is not pure kinematics due to the inertia properties involved. This type of constraint appears as a result of flying in the space that not subjected to external forces.

3) Kinematic constraints: and this obvious from (2.29).

In the present section, a space robot in contact with a target satellite as one combined system is considered. This entire system is subjected to holonomic and nonholonomic constraints at the same time as explained before. Now, let $\dot{\theta} = \begin{bmatrix} V_b^T & \Omega_b^T & \dot{q}^T & \omega_T^T & v_T^T \end{bmatrix}$, then as expressed in (2.29), the kinematic constraints are given by

$$J(\theta)\dot{\theta} = 0 \tag{2.30}$$

On the other hand, holonomic/nonholonomic constraints come into play as a result of the conservation of the linear and angular momentum, respectively. These momenta constraints are not given in algebraic form but there are given in kinematical-like form as

$$B(\theta)\dot{\theta} = c_0 \tag{2.31}$$

where $B(\theta) \in R^{k \times N}$ is defined as

$$B(\theta) = \begin{bmatrix} H_{V_b} & H_{V_b\Omega_b} & H_{V_bq} & H_{V_b\omega_t} & H_{V_bv_t} \\ H^T_{V_b\Omega_b} & H_{\Omega_b} & H_{\Omega_bq} & H_{\Omega_b\omega_t} & H_{\Omega_bv_t} \end{bmatrix} \tag{2.32}$$

and c_0 represents the vector of the initial conditions of the momentum and is given by

$$c_0 = \begin{bmatrix} P_0 \\ L_0 \end{bmatrix} \tag{2.33}$$

Note that (2.31) has k momentum constraint equations with $k \leq N$.

The purpose of representing holonomic constraints in the form (2.30) is to treat both holonomic and nonholonmic constraints at the velocity level. But a difference exists in the matter of initial conditions. Holonomic constraints are restricted to position initial conditions, but nonholonomic are restricted to their momentum conditions.

Now, holnomic and nonholonomic constraints can be combined together as

$$\begin{bmatrix} J(\theta) \\ B(\theta) \end{bmatrix} \dot{\theta} = \begin{bmatrix} 0 \\ c_0 \end{bmatrix} \tag{2.34}$$

where the new combined matrix $\begin{bmatrix} J(\theta) \\ B(\theta) \end{bmatrix}$ is of dimension $(k+m)\times N$. This implies a set of $(k+m)$ linear equations with $\dot{\theta}$ as vector of the unknown variables. Since matrices $J(\theta)$ and $B(\theta)$ have the same number of columns, we now seek for their common solutions, if exist, expressing them in terms of the solutions of (2.30) and (2.31).

The common solutions of Equations (2.30) and (2.31) are the solutions of the combined Equations (2.34). From the theory of linear algebra, the solutions of Equations (2.30) and (2.31) constitute the intersection manifold

$$\{N(J)\} \cap \{B^{+}c_0 + N(B)\} \tag{2.35}$$

where $N(J)$ and $N(B)$ are the null space of J and B, respectively, and the upper right script $^{+}$ represents the Pseudoinverse. Equation (2.35) is the set of solutions of (2.30) and (2.31) is consistent if (2.35) is nonempty. Then the common solution (corollary proposed in reference [116]) is any of the equivalent manifolds

$$P_{N(J)}\left(P_{N(J)} + P_{N(B)}\right)^{+} B^{+}c_0 + N(J) + N(B) \tag{2.36}$$

$$B^{+}c_0 - P_{N(B)}\left(P_{N(J)} + P_{N(B)}\right)^{+} B^{+}c_0 + N(J) + N(B) \tag{2.37}$$

$$\left(J^{+}J + B^{+}B\right)^{+} B^{+}c_0 + N(J) \cap N(B) \tag{2.38}$$

where $P_{N(\cdot)}$ is the projection matrix on the null space of a given matrix $(\cdot)$ and any solution of (2.36), or (2.37) or (2.38) can be used to find manifold of the combined system.

Since each of the manifolds given in Equations (2.36)-(2.38) gives a solution of the combined system (2.34), these expressions can also be used to obtain the generalized (pseudo-inverse) of the combined matrices. Each of the following expressions (Theorem proposed reference [116]) is the inverse of the combined matrix $\begin{bmatrix} J(\theta) \\ B(\theta) \end{bmatrix}$:

$$\begin{bmatrix} J(\theta) \\ B(\theta) \end{bmatrix}^{-1} = \begin{bmatrix} J^+ & 0 \end{bmatrix} + P_{N(J)} \left(P_{N(J)} + P_{N(B)} \right)^+ \begin{bmatrix} -J^+ & B^+ \end{bmatrix} \tag{2.39}$$

$$\begin{bmatrix} J(\theta) \\ B(\theta) \end{bmatrix}^{-1} = \begin{bmatrix} 0 & B^+ \end{bmatrix} - P_{N(B)} \left(P_{N(J)} + P_{N(B)} \right)^+ \begin{bmatrix} -J^+ & B^+ \end{bmatrix} \tag{2.40}$$

$$\begin{bmatrix} A(\theta) \\ B(\theta) \end{bmatrix}^{-1} = \left(J^+ J + B^+ B \right)^+ \begin{bmatrix} J^+ & B^+ \end{bmatrix} \tag{2.41}$$

Moreover, if

$$R(J^+) \cap R(B^+) = \{0\} \tag{2.42}$$

then each expressions of (2.39)-(2.41) is the Moore-Penrose inverse of $\begin{bmatrix} J(\theta) \\ B(\theta) \end{bmatrix}$.

The proposed model in the present chapter considers all holonomic and nonholnomic constraints in a single framework. Linear and angular momentum impose holonomic and nonholonomic constraints, respectively, while restricting the motion of the end-effector leads to holonomic constraints. The equations that describe the momentum of a totally single free-flying (or free-floating) space robot without interaction with a floating target

are a special case of the proposed model in the present chapter. The next chapter will focus Physical Insight of Nonholonomic Constraints of a Space Robot with/without Intercation with a Target Satellite.

Chapter 3

Physical Insight of Nonholonomic Constraints of a Space Robot with/without Interaction with a Target Satellite

3.1 Introduction

In the previous chapter kinematics, geometric and momentum constraints of a free-flying space robot interacting with a target satellite are obtained. Since it is concluded that the conservation of momentum exerts kinematic-like constraints on a space robotic system in the absence of external forces, one may raise the question: what is the physical interpretation of such a behavior? Some researchers have looked at this problem from trajectory planning point of view, since they restrict the kinematically possible displacements (possible values of the velocities) of the individual parts of the system [32-36]. The physical characteristics of the nonholonomic constraints are exhibited by the fact that even if the manipulator joints return to their initial configuration after a sequence of motion, the vehicle orientation may not be the same as the initial value [32]. A major characteristic of a space robot is clearly the distinction from ground-based robot is the lack of a fixed base in space environment [26]. If a space robot is operated in a certain task, position and attitude of the base satellite are disturbed by reaction forces and moments due to the robot motion, so it cannot accomplish a task without provision for this disturbance. No space manipulator can avoid the reaction disturbance. Physical interpretation of such behavior will give us more idea about the nature of holonomic and nonholonomic constraints and geometric conditions that generate those constraints.

The present chapter presents a physical interpretation of nonholonomic constraints act on a free-flying space robot with or without interaction with a floating object. The analysis in this chapter uncovers the physical meaning and geometric conditions behind such constraints and gives a new light on the nonholonomic behavior of a free-flying space robot. Physical interpretation will provide us with a better understanding of a space robot especially in contact task planning and control, which are more difficult than conventional holonomic systems.

The chapter is organized as follows: in section 3.2 the geometric conditions behind nonholonomic constraints of a totally free-flying space robot are analyzed, section 3.3 reveals the conditions of keeping linear and angular momentum conserved in case of a free-flying space robot interacting with a target satellite, Finally, simulation results are presented in section 3.4 to demonstrate the analytical results.

Conservation Theorem for the Linear Momentum of a Space Robot: if the total external forces, F_{ext}, are zero then the time derivative of the linear momentum is $\dot{P} = 0$, and the linear momentum P is conserved.

Conservation Theorem for the Angular Momentum of a Space Robot: if the total torque (moment of external forces), N, is zero then the time derivative of the angular momentum is $\dot{L} = 0$, and the angular momentum L is conserved.

Assume that initially external forces are all zeros. The law of conservation of linear momentum is written, in general as,

$$\sum_{i=0}^{n} m_i v_i = \sum_{i=0}^{n} m_i \dot{r}_i = 0 \tag{3.1}$$

which can be readily integrated to

$$\sum_{i=0}^{n} m_i r_i = m_t r_{c0} = const \tag{3.2}$$

where $m_t = \sum_{i=1}^{n} m_i$ is the total mass of the system, r_{c0} is the position vector of the system center of mass and c is a constant vector. As a consequence, the conservation of linear momentum gives rise to three holonomic constraints (in the x, y, z coordinates), indicating that the system center of mass does not move or moves in a constant velocity. The conservation of angular momentum is expressed as

$$L = \sum_{i=0}^{n} \left({}^{B} I_i \Omega_i + m_i (r_i \times V_i) \right) \tag{3.3}$$

Equation (3.3) represents a three differential constraints which are, in general, nonholonomic in the three dimensional case (x, y, z coordinates).

It is known that the equation of motion can be extended to include a system of particles or multibody system isolated within an enclosed region in space. There is no restriction in the way the particles are connected. So it is applicable to the motion of a solid, liquid or gas system. The equation of motion can be expressed as

$$\sum_{i=1}^{n} (m_i a_i - f_i - F_i) = 0 \tag{3.4}$$

where m_i is the mass of i-th body with an acceleration a_i subjected to a resultant internal force f_i and a resultant external force F_i. Here the external forces F_i represent, for example, the effect of centrifugal forces, Coriolos forces, or contact forces between i-th body and adjacent bodies are not included within the system.

Assume that in our case the space robot admits an arbitrary virtual rotation about some axis Z. This axis is a fixed straight line or straight line of fixed direction passing through the center of mass of the system. Since the center of mass is generally in motion, the defind virtual axis Z passing through the center of mass is also in motion. If external forces do not exert any moment about this axis, then the law of conservation of angular momentum about this axis holds.

3.2 Free-Flying Space Robot

In this section a physical explanation of the nonholonomic constraint imposed on a free-flying space robot is discussed. When no external forces are applied, and in the absence of gravity and dissipation forces, the linear and angular momentum of the multibody system are conserved.

Then by virtue of the principle of virtual work by d'Almberts-Lagrange equation [119]:

$$\sum_{i=0}^{n}(m_i a_i - f_i - F_i)\delta r_i = 0 \tag{3.5}$$

which implies no work as a result of the virtual displacement δR_i measured in frame fixed at the center of mass as shown in Figure (2.1). The position vector of the i-th body can be given as

$$r_i = r_b + r_{i/b} \tag{3.6}$$

where r_i is the position vector from the fixed center C to the i-th body, r_b is the position vector form the center of mass to the base satellite, and $r_{i/b}$ is the vector from the base to i-th body.

Now taking the displacement of vector r_i, we obtain

$$dr_i = dr_b + d\phi \times r_{i/b} + J_{Li} dq_i \tag{3.7}$$

Similarly, the virtual displacement can be stated as

$$\delta r_i = \delta r_b + \delta\phi \times r_{i/b} + J_{Li} \delta q_i \tag{3.8}$$

where $\delta\phi$ is the angular virtual displacement by which the base body rotates about the virtual axis of rotation Z, δq_i is the virtual angular displacement of robot i-th body, and J_{Li} is the linear Jacobian defined as $\sum_{i=o}^{n} k_i \times (r_i - c_i)$.

Substituting $\sum_{i=o}^{n} k_i \times (r_i - c_i)$ for J_{Li} in Equation (3.8) leads

$$\delta r_i = \delta r_b + \delta\phi \times r_{i/b} + \sum_{i=o}^{n} k_i \times (r_i - c_i)\delta q_i \tag{3.9}$$

Now substitute the virtual displacement (3.9) into d'Almberts-Lagrange Equations (3.5) to have

$$m_i\ddot{r}_i \cdot \delta r_b + m_i\ddot{r}_i \cdot \delta\phi \times r_{i/b} + m_i\ddot{r}_i \cdot \sum_{i=o}^{n} k_i \times (r_i - c_i)\delta q_i =$$

$$f_i \cdot \delta R_b + f_i \cdot \delta\phi \times r_{i/b} + f_i \cdot \sum_{i=o}^{n} k_i \times (r_i - c_i)\delta q_i +$$

$$F_i \cdot \delta r_b + F_i \cdot \delta\phi \times r_{i/b} + F_i \cdot \sum_{i=o}^{n} k_i \times (r_i - c_i)\delta q_i \tag{3.10}$$

In equation (3.10) the expression on the right hand side represent the virtual work of the internal forces f_i and the external forces F_i which can be rewritten as

$$(f_i + F_i)\delta r_b + (M_f + M_F)\delta\phi + M_m\delta q_i =$$

$$(f_i + F_i)\delta r_b + (R_{i/b} \times f_i + r_{i/b} \times F_i)\delta\phi +$$

$$\sum_{i=o}^{n}(r_i - c_i) \times f_i k_i \delta q_i + \sum_{i=o}^{n}(r_i - c_i) \times F_i k_i \delta q_i \tag{3.11}$$

By taking the work effect of all bodies, the total virtual work δW can be then given as

$$\delta W_f + \delta W_F + \delta W_m = (f_i + F_i)\delta r_b + (M_f + M_F)\delta\phi + M_m\delta q_i \tag{3.12}$$

Recalling that the linear momentum $P_i = m_i\dot{R}_i = m_i V_i$, then the first term in the left hand side of Equations (3.10) can be expressed in term of linear momentum as

$$m_i\ddot{r}_i\delta r_b = \frac{dP_i}{dt}\delta r_b \tag{3.13}$$

Introducing the angular momentum of the i-th body about the base

$$L_{i/b} = r_{i/b} \times m_i V_i \tag{3.14}$$

Using (3.14) and (3.6), the middle and the last terms in the left hand side of Equations (3.10) can be rewritten respectively, as

$$m_i\ddot{r}_i \cdot \delta\phi \times r_{i/b} = \delta\phi \cdot r_{i/b} \times m_i\ddot{r}_i = \left(\frac{dL_{i/b}}{dt} - \dot{r}_b \times P\right)\delta\phi \tag{3.15}$$

$$m_i\ddot{r}_i \cdot \sum_{i=o}^{n} k_i \times (r_i - c_i)\delta q_i = \sum_{i=o}^{n} k_i \cdot (r_i - c_i) \times m_i\ddot{r}_i \cdot \delta q_i = \left(\frac{dL_m}{dt} - (\dot{r}_i - \dot{c}_i) \times P\right)\delta q_i \tag{3.16}$$

where $L_m = (r_i - c_i) \times m_i V_i$.

After all, the virtual work of the whole system is presented as follows

$$\frac{dP}{dt}\delta r_b + \left(\frac{dL_{i/b}}{dt} - \dot{r}_b \times P\right)\delta\phi + \left(\frac{dL_m}{dt} - (\dot{r}_i - \dot{c}_i) \times P\right)\delta q = (f + F)\delta R_b + (M_f + M_F)\delta\phi + M_m\delta q \tag{3.17}$$

Since the virtual variations δr_b, $\delta\phi$ and δq are independent we can reach the well known variation of linear and angular momentum equations, respectively, as

$$\frac{dP}{dt} = f + F \tag{3.18}$$

$$\left(\frac{dL_{i/b}}{dt} - \dot{r}_b \times P\right) + \left(\frac{dL_m}{dt} - (\dot{r}_i - \dot{c}_i) \times P\right) = M_f + M_F + M_m \tag{3.19}$$

According to Equations (3.18) and (3.19), there are three conditions that the moments of forces about the virtual axis of rotation to vanish, that is

$$\frac{dP}{dt} = 0 \tag{3.20}$$

$$\frac{dL_{i/b}}{dt} - V_b \times P = 0 \tag{3.21}$$

$$\frac{dL_m}{dt} - (\dot{r}_i - \dot{c}_i) \times P = 0 \tag{3.22}$$

Note that Equation (3.20) is guaranteed automatically by the law of conservation of linear momentum. To ensure the validity of (3.21) there are two requirements must be met, first

$$V_{i/b} \times P\delta\phi = V_{i/b} \times V_c \cdot m_t\delta\phi = 0 \tag{3.23}$$

$$(\dot{r}_i - \dot{c}_i) \times P\delta q = (\dot{r}_i - \dot{c}_i) \times V_c \cdot m_t\delta q = 0 \tag{3.24}$$

which requires that $V_{i/b}$ and V_c are parallel, $(\dot{r}_i - \dot{c}_i)$ and V_c are parallel, where V_c is the velocity of center of mass of the robotic system. The second requirement is that $M_F \delta\phi = 0$, that is the projection of $dL_{i/b}$ onto the direction $\delta\phi$ is conserved, then

$$\frac{dL_{i/b}}{dt}\delta\phi = \frac{d}{dt}\left(L_{i/b}\hat{i}\right)\delta\phi = 0 \tag{3.25}$$

where $\hat{i}$ is a unit vector along the virtual axis of rotation Z. From (3.25) it follows that

$$L_{i/b}\hat{i} = const \tag{3.26}$$

While the third condition can be guaranteed by $M_m \delta q$, that is the projection

$$\frac{dL_m}{dt}\delta q = \frac{d}{dt}\left(L_m \hat{i}\right)\delta q = 0 \tag{3.27}$$

Similarly, it follows from (3.27) that

$$L_m \hat{i} = const \tag{3.28}$$

It is possible now to describe the previous analysis in the following theorem:

Theorem 3.1: A totally free-flying space robot defined by d'Almberts-Lagrange dynamics (3.5) is said to be nonholonmic system if conditions (3.23), (3.24), (3.26) and (3.28) are satisfied.

Physical interpretation of Theorem 3.1 shown in Figure 3.1 as follows: according to the previous analysis, when external forces exert no moment around the axis of rotation, the conservation of momentum holds. From geometrical view point, if the ith-body's relative linear velocity with respect to the base satellite is parallel to the linear velocity of the

system center of mass, and if the relative linear velocity between the ith-body's centroid and its joint are

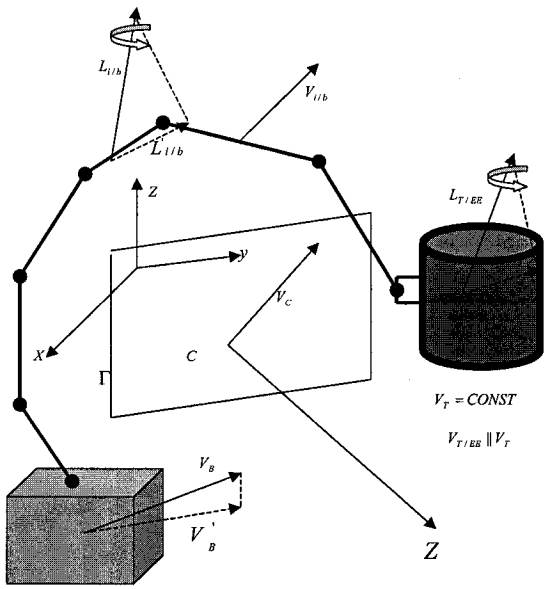

Figure 3.1: Nonholonomic Interpretation of a Free-Flying Space Robot Interacting with a Target Satellite

parallel to the linear velocity of the system center of mass, and if the projections of angular momentum along their corresponding angular displacements is constant, then the system poses a nonholonomic constraints. In other words, any motion in base satellite or the manipulator or both will cause the system to adjust its motion to keep the direction of base linear velocity and the projections of the angular momentum parallel to the virtual axis of rotation. It also embodies that the momentum is transferred from/to the manipulator to/from the base to maintain the momentum constant.

3.3 Free-Flying Space Robot Interacting with a Target Satellite

We assume now that the space robot established a contact with a target satellite. It is desired to find out the conditions to keep the momentum conserved. A similar analysis to section 4.2 above is followed. Applying the principle of virtual work by d'Almberts-Lagrange equation

$$\sum_{i=0}^{n+1}(m_i\ddot{r}_i - f_i - F_i)\delta r_i = 0 \tag{3.29}$$

and from (3.26) the virtual dispalcemnt of the target is given as

$$\delta r_i = \delta r_b + \delta\phi \times r_{i/b} + \sum_{i=o}^{n} k_i \times (r_i - c_i)\delta q_i + \delta\phi_T \times R_{t/EE} + \delta r_{t'} \tag{3.30}$$

Substituting (3.30) and (3.9) into (3.29) yields to

$$\begin{aligned} m_i\ddot{r}_i \cdot \delta R_b + m_i\ddot{r}_i \cdot \delta\phi \times r_{i/b} + m_i\ddot{r}_i \cdot \sum_{i=o}^{n} k_i \times (r_i - c_i)\delta q_i + \\ m_t\ddot{r}_t \cdot \delta\phi_t \times r_{t/EE} + m_t\ddot{r}_t \cdot \delta r_{t'} = \\ f_i \cdot \delta r_b + f_i \cdot \delta\phi \times r_{i/b} + f_i \cdot \sum_{i=o}^{n} k_i \times (r_i - c_i)\delta q_i + \\ F_i \cdot \delta r_b + F_i \cdot \delta\phi \times r_{i/b} + F_i \cdot \sum_{i=o}^{n} k_i \times (r_i - c_i)\delta q_i + \\ f_t \cdot \delta r_{t'} + f_i \cdot \delta\phi_t \times r_{t/EE} + F_t \cdot \delta r_{t'} + F_t \cdot \delta\phi_t \times R_{t/EE} \end{aligned} \tag{3.31}$$

The last line in (3.31) can be expressed in terms of virtual work as

$$\delta W_{ft} + \delta W_{Ft} + \delta W_{tr} = f_t \cdot \delta r_t + f_t \cdot \delta\phi \times r_{t/EE} + F_T \cdot \delta r_{t'} + F_t \cdot \delta\phi \times r_{t/EE} \tag{3.32}$$

Rewriting the terms $m_t\ddot{r}_t \cdot \delta\phi_t \times r_{t/EE}$ and $m_t\ddot{r}_t \cdot \delta\phi_t$ in (3.31), respectively, as

$$m_t \ddot{r}_t \delta r_{t'} = \frac{dP_t}{dt} \delta r_{t'} \tag{3.33}$$

$$m_t \ddot{r}_t \cdot \delta\phi_t \times r_{t/EE} = \delta\phi_t \cdot r_{t/EE} \times m_t \ddot{r}_t = \left(\frac{dL_{t/EE}}{dt} - \dot{r}_{t/EE} \times P_t \right) \delta\phi_t \tag{3.34}$$

where $L_{t/EE} = r_{t/EE} \times m_t V_t$.

After all, the virtual work of the whole system is presented as follows

$$\begin{aligned} &\frac{dP}{dt} \delta r_b + \left(\frac{dL_{i/b}}{dt} - \dot{r}_{i/b} \times P \right) \delta\phi + \\ &\left(\frac{dL_m}{dt} + (\dot{r}_i - \dot{c}_i) \times P \right) \delta q + \\ &\frac{dP_t}{dt} \delta r_t + \left(\frac{dL_{t/EE}}{dt} - \dot{r}_{t/EE} \times P_t \right) \delta\phi_t = \\ &(f + F) \delta R_b + (M_f + M_F) \delta\phi + \\ &M_m \delta q + (f_t + F_t) \cdot \delta r_{t'} + (M_{ft} + M_{Ft}) \delta\phi \end{aligned} \tag{3.35}$$

According to Equation (3.35), there are five conditions that the moments of forces about the virtual axis of rotation to vanish. Three of these conditions are similar to the conditions (3.20)-(3.22), in addition to

$$\frac{dP_t}{dt} = 0 \tag{3.36}$$

$$\left(\frac{dL_{t/EE}}{dt} - \dot{r}_{t/EE} \times P_t \right) = 0 \tag{3.37}$$

where P_t : is the linear momentum of the target satellite. Condition (3.36) implies that

$P_t = const$, that is

$$V_t = const \tag{3.38}$$

Meanwhile, conditions (3.37) implies

$$L_{T/EE} \hat{I} = const \tag{3.39}$$

and

$$\dot{r}_{t/EE} \times P_t = v_{t/EE} \times m_t V_t \tag{3.40}$$

For the moment of forces to vanish, condition (3.39) implies that: 1) the projection of $L_{t/EE}$ is constant along Z, 2) and condition (3.40) requires that $v_{t/EE}$ is parallel to V_t.

Now we conclude the previous analysis in the following theorem:

Theorem 3.2: A combined free-flying space robot interacting with a target satellite defined by d'Almberts-Lagrange dynamics (3.29) is said to nonholonmic system if conditions (3.23), (3.24), (3.26), (3.28) and (3.38)-(3.40) are satisfied.

Based on theorem 2 the physical interpretation can then be summarized as follows: in addition to the conditions concluded in the case of free-flying space robot, it is concluded also that to hold a constant momentum (holonomic and nonholonomic behavior): (1) the target linear velocity should not change, (2) The linear relative velocity between the target and the end-effector should be in the same direction of that of the target satellite, (3) and the projection of relative angular momentum is kept constant along the axis of rotation.

3.4 Simulation Results

The purpose of the simulation in the present section is to verify the holonomic and nonholonomic conditions in Theorem 3.1 and Theorem 3.2.

A 6 DOF free-flying space robot is tested to verify its nonholonomic and holonomic behavior. The first five links are assumed to be revolute and the last one is prismatic. The first link is mounted on the base satellite by a revolute joint. The mass of the base satellite is assumed 300 kg. The mass of the target is assumed 1500 kg, The masses of the robot link are assumed $[10 \quad 10 \quad 10 \quad 10 \quad 10 \quad 10]^T$ kg. The length of each link is assumed as 1m.

The inertia matrix of the base satellite is assumed as

$$\begin{bmatrix} 100 & 0 & 0 \\ 0 & 100 & 0 \\ 0 & 0 & 100 \end{bmatrix} kg.m^2$$

The inertia matrix of the target satellite is considered as

$$\begin{bmatrix} 300 & 0 & 0 \\ 0 & 300 & 0 \\ 0 & 0 & 300 \end{bmatrix} kg.m^2$$

The inertia of each link of the space robot arm is assumed as

$$\begin{bmatrix} 3 & 0 & 0 \\ 0 & 3 & 0 \\ 0 & 0 & 3 \end{bmatrix} kg.m^2$$

All initial values for the position and angular velocity and acceleration of the robot joints is assumed to be zero. All initial values for the orientation, angular velocity and angular acceleration of the base satellite are assumed to be zero. All initial values for the

orientation, angular velocity and angular acceleration of the target satellite are also assumed to be zero.

The Simulation is run to record the system momentum response assuming zeros external forces and initial conditions. Figures 3.2 and 3.3 show that linear and angular momentum of a free-flying space robot is conserved and kept zero (range of 10e-8). These results comply with the concept that for a free-flying space robot its momentum is conserved in the absence of any external forces.

Another simulation is also implemented to check the conservation of momentum of a free-flying space robot interacting with a target satellite as a combined system with nonzero initial linear velocity. Figures 3.4 and 3.5 show that linear and angular momentum of a free-flying space together with its target is conserved. But since the initial conditions are assumed 10 m/sec the momentum is hold at values different than zero. Figures 3.6 and 3.7 show non-conservation of momentum in case the target satellite linear velocity is changing and chosen for simulation as $(1-\cos t)$ in the x-direction and this violates condition (3.38). While Figures 3.8 and 3.9 demonstrate the momentum for the cases when the end-effector moves in a direction not parallel to that of the target chosen 20 m/esc in x and y-direction, and 20 m/sec for the base satellite in x-direction only. The latter case violates condition (3.40).

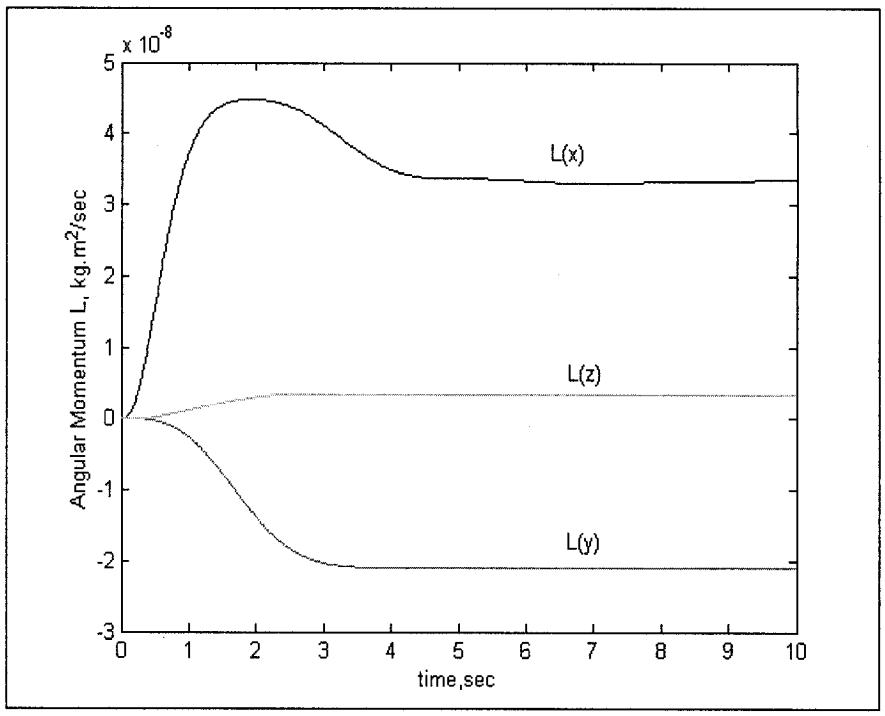

Figure 3.2: Angular Momentum of a Free-Flying Space Robot

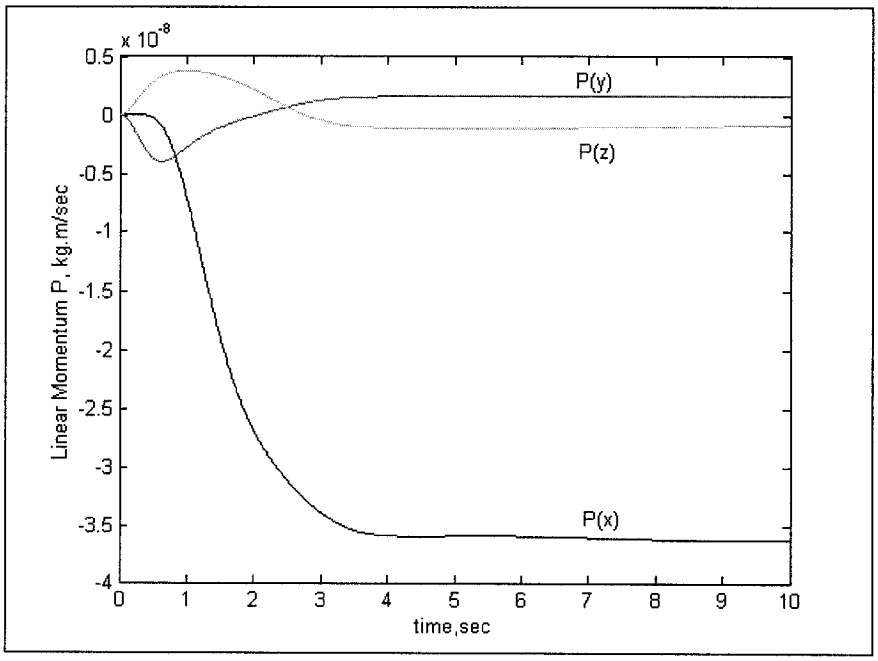

Figure 3.3: Linear Momentum of a Free-Flying Space Robot

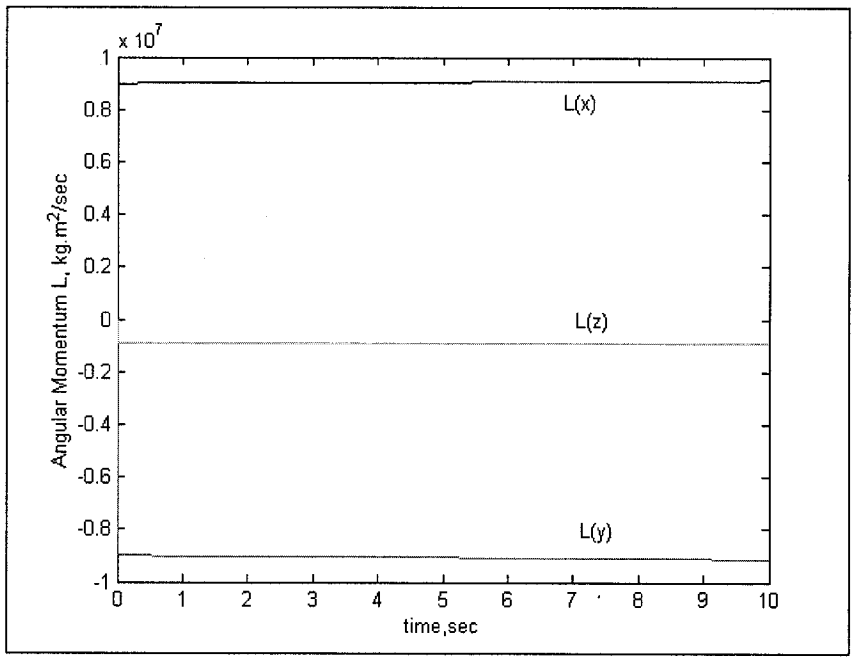

Figure 3.4: Angular Momentum of a Free-Flying Space Robot in Contact with a Target Satellite

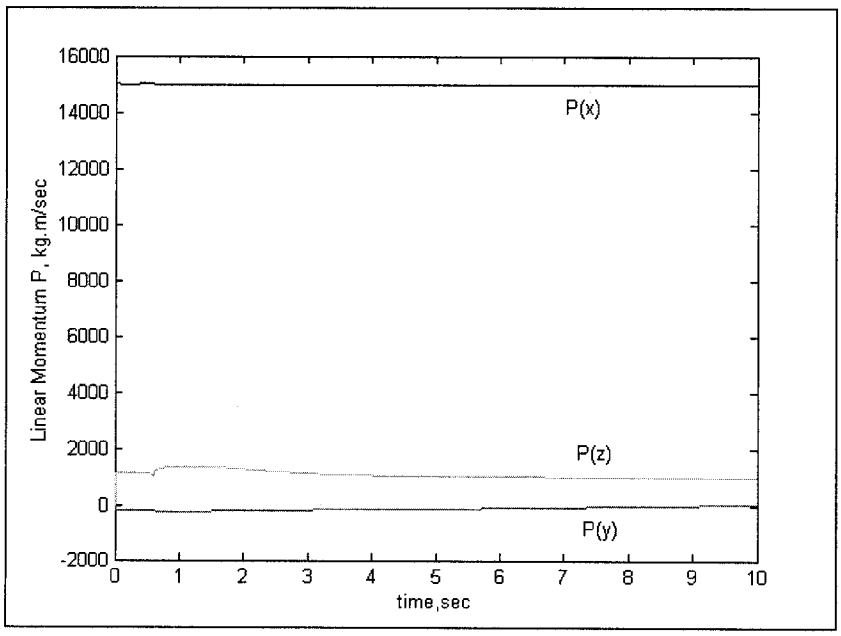

Figure 3.5: Linear Momentum of a Free-Flying Space Robot in Contact with a Target Satellite

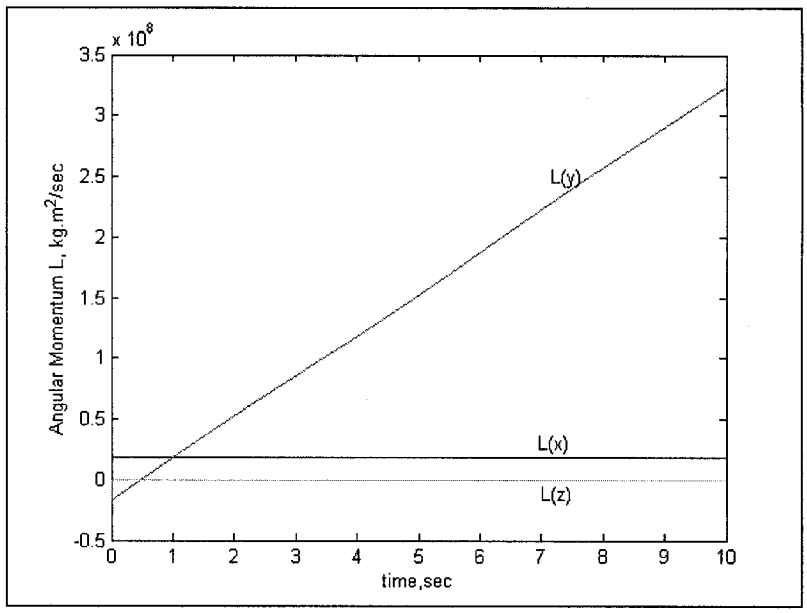

Figure 3.6: Angular Momentum of a Free-Flying Space Robot in Contact with a Target Satellite (violation of condition 3.30)

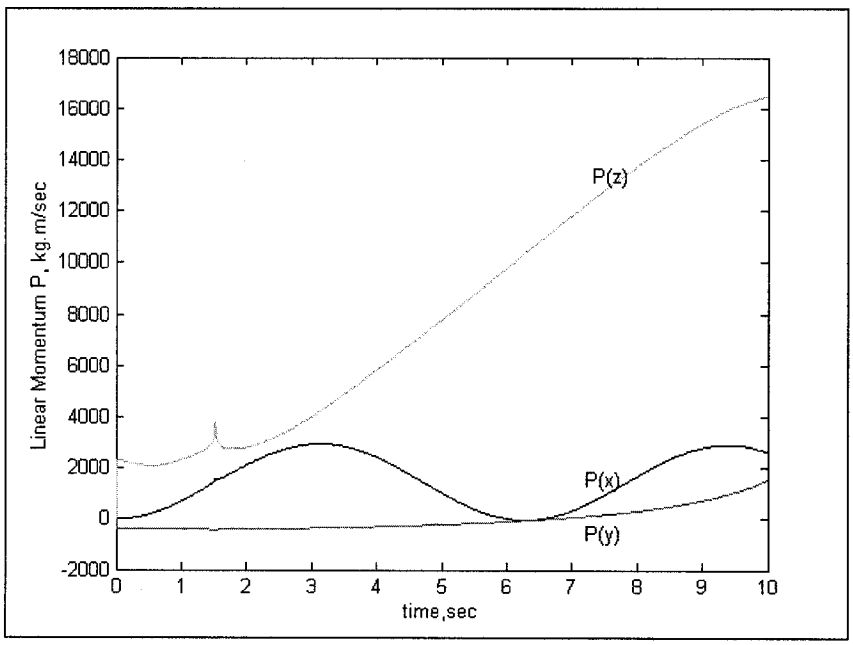

Figure 3.7: Linear Momentum of a Free-Flying Space Robot in Contact with a Target Satellite (violation of condition 3.30)

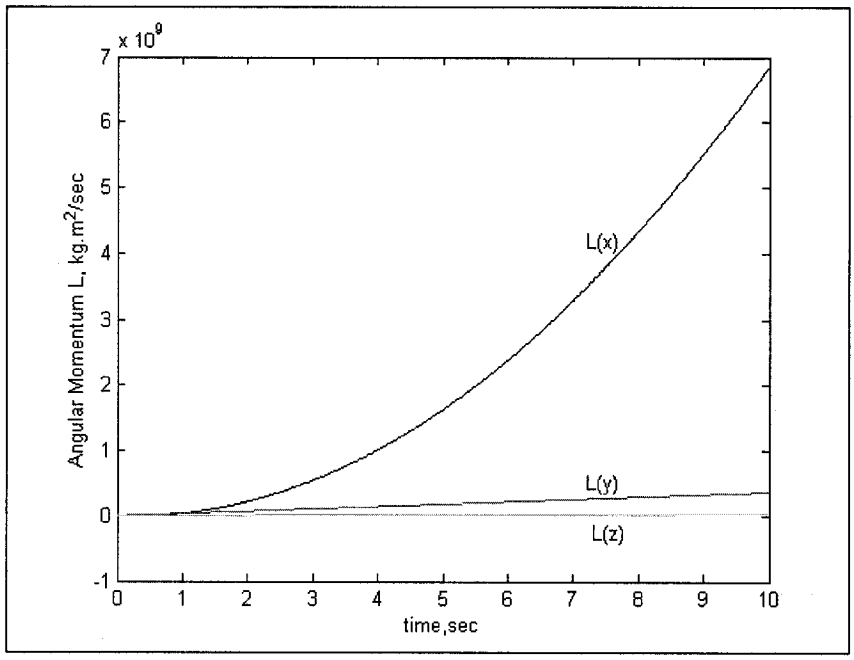

Figure 3.8: Angular Momentum of a Free-Flying Space Robot in Contact with a Target Satellite (violation of condition 3.40)

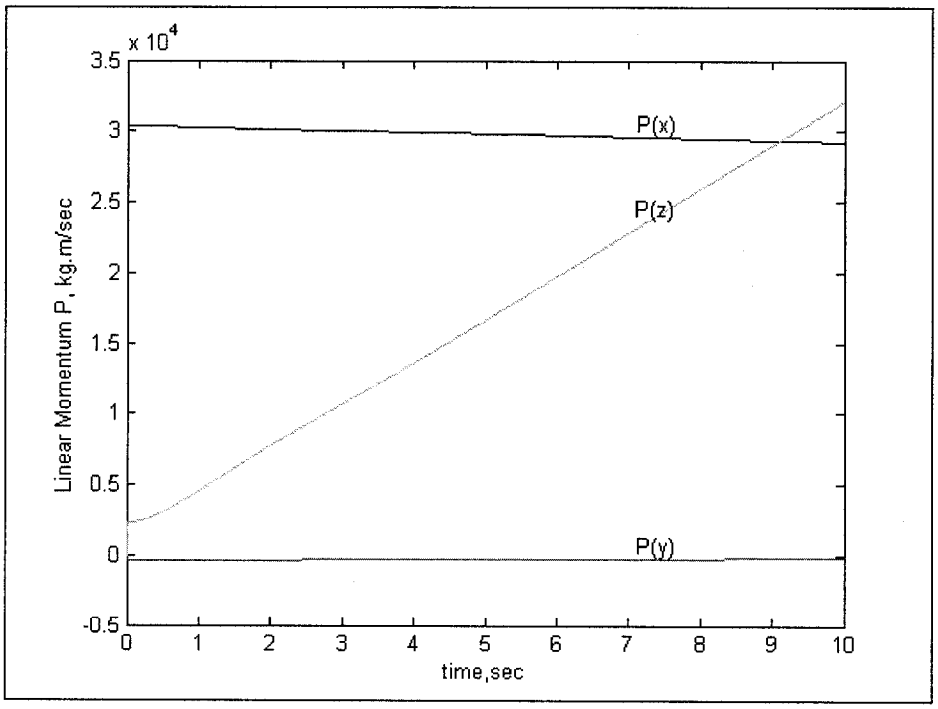

Figure 3.9: Linear Momentum of a Free-Flying Space Robot in Contact with a Target Satellite (violation of condition 3.40)

The obtained simulation results show that if a free-flying space robot with or without interaction with a target satellite is not exposed to external forces, then its momentum is conserved. There are few geometric conditions that generate holonomic and nonholonomic behavior, if these conditions are violated then the momentum is not conserved any more.

From geometrical view point and in case of a totally free-flying space robot, if the linear velocity of the base satellite is parallel to the linear velocity of the system center of mass then it poses a holonomic constraint. If the ith-body's relative linear velocity with respect to the base satellite is parallel to the linear velocity of the system center of mass, and if the relative linear velocity between the ith-body's centroid and its joint are parallel to the linear velocity of the system center of mass, and if the projection of angular momentum is along their corresponding angular displacements, then the system poses nonholonomic constraints. In the case of interacting with a un-actuated floating target satellite, another three conditions should be held to keep the momentum constant. These conditions are the following: the target linear velocity is constant, the relative linear velocity between the robot end-effector and the satellite should be parallel to that of the target satellite, and finally the angular momentum projection along the axis of rotation is hold constant as well. In the next chapter, a holonomy criterion will be presented to verify whether the constraints impose on a free-flying space robot with or without contact with a target satellite are holonomic or nonholonomic constraints.

Chapter 4

Nonholonomy Criterion of a Free-Flying Space Robot with/without Interaction with a Target Satellite

4.1 Introduction

The physical interpretation of holonomic and nonholonomic constraints of a free-flying space robot interacting with a target satellite has been analyzed in the previous chapter. As a continuation to this analysis, a criterion to check the integrability of such constraints is proposed later in the present chapter. Verifying the intergrability of holonomic and nonholnomic constrained systems has attracted the attention of several studies [32][119-121]. Frobenius theorem is a well-known approach to answer the question of integrability of such systems under concern. Conditions of the integrability of nonholonomic systems are reported in [32] using Lie algebra techniques. A necessary and sufficient condition is reported by using what is called bilinear covariants in [119-120]. Nonholomic behavior of a free-flying space robot is investigated in the absence of external forces by Lie algebra techniques [32]. Differential-form-based integrability conditions for dynamic constraints using the Frobenius theorem are proposed in [142]. In the latter, the conditions can be used for the classification of holonomic and nonholonomic constraints. Unfortunately, using Lie algebra and bilinear covariants is cumbersome and time consuming in the case of complicated space robotic systems.

This chapter presents a new methodology of finding holonomy/nonholonomy of constraints impose on a free-flying space robot with or without interaction with a floating object. The holonomy criterion is proposed by utilizing the concept of orthogonal projection matrices and singular value decomposition (SVD). This criteria can easily be used to verify the holonomy of a space robot exposed to different types of constraints. Using this methodology will also enable us to verify online whether the constraints or their initial conditions are violated in case of real-time applications and to take a corrective action or switch the controllers if needed.

This chapter is organized as follows: in section 4.2 a simple and effecient nonholonomy criteria is proposed, and then simulation results are presented to demonstrate the proposed criteria in section 4.3.

4.2 Holonomy Criteria

Establishing criteria that determine whether a mechanical system is holonomic or nonholonomic is so crucial. In case of a mechanical system with kinematic or kinematic-like constraints, a necessary and sufficient condition is needed. That is because analysis and control of nonholonomic systems are treated in away different from that of holonomic systems.

In this work, a transformation matrix is proposed to construct a linear transformation by using the concept of orthogonal projection techniques. This matrix is sufficient and

necessary to verify the integrability of holonomic and nonholonomic system. Let us first define a system subjected to linear kinematic (or kienmatic-like) constraints given in the form

$$A\dot{\theta} = 0 \tag{4.1}$$

where the constraint matrix $A \in R^{m \times N}$ represents linear or angular momentum constraint matrix, and the generalized velocities $\dot{\theta} \in R^N$ are represented as $\dot{\theta} = \begin{bmatrix} V_b^T & \Omega_b^T & \dot{q}^T & \omega_T^T & v_T^T \end{bmatrix}$. Assuming zero initial conditions, the constraint matrix in case of linear momentum is defined as

$$A = \begin{bmatrix} M_{V_b} & M_{V_b\Omega_b} & M_{V_b q} & M_{V_b \omega_T} & M_{V_b v_T} \end{bmatrix}$$

While in case of the angular momentum is given as

$$A = \begin{bmatrix} M^T_{V_b\Omega_b} & M_{\Omega_b} & M_{\Omega_b q} & M_{\Omega_b \omega_T} & M_{\Omega_b v_T} \end{bmatrix}$$

In case of a free-flying space robot or losing contact with the target, the constraint matrix is, then, reduced to

$A = \begin{bmatrix} M_{V_b} & M_{V_b\Omega_b} & M_{V_b q} \end{bmatrix}$ for linear momentum, and $A = \begin{bmatrix} M^T_{V_b\Omega_b} & M_{\Omega_b} & M_{\Omega_b q} \end{bmatrix}$ for angular momentum where all terms related to the target satellite are set to zero (see [156] [63] for more details).

From linear algebra point of view, Equation (4.1) represents a system of m linear equations with $\dot{\theta}$ being the vector of unknowns. Since the number of equations is less than that of unknowns, it has infinitely many solutions given by

$$\dot{\theta} = P_{\perp}\dot{z}(t) \tag{4.2}$$

for an arbitrary $\dot{z}(t)$,and the orthogonal projector $P_{\perp}$ is an $N \times (N-m)$ dimensional full

rank matrix whose column space is in the null space of , i.e.,

$$AP_{\perp} = 0 \tag{4.3}$$

For a system to be holonomic, a complete integrability of all m equations has to be fulfilled. But it might not be possible to determine whether a system of linear constraints is integrable because of unavailability of integrablity techniques or time consuming.

Geometrically, the constraints (4.1) mean that a point of an N-dimensional space $R(\theta_1, \theta_2, \cdots, \theta_N)$ cannot be displaced arbitrarily, but it must move a long a curve that touches at each of its points a hyperplane L^{N-m} of dimension $N-m$, which contains all displacement vectors $d\theta_1, d\theta_2, \cdots, d\theta_N$ satisfying the constraint equation (4.1) [119-120]. A system of Pfaffian equations is completely integrable if all admissible curves emanating from any point in the space lie on a surface of dimension $N-m$ passing through that point. However, if the system is not integrable, any point in the configuration space can be reached, although its possible displacement is restricted.

To construct a linear transformation by using the concept of orthogonal projection techniques, a linear transformation matrix T is defined at each point of the space $R(\theta_1, \theta_2, \cdots, \theta_N)$, which should map all vectors lying in T^{N-m} to zero and map all vectors orthogonal to the hypersurface L^{N-m} onto themselves.

For this purpose, the transformation T is decomposed in such away that,

$$T = \mathrm{Y}_h A \tag{4.4}$$

where the matrix $\mathrm{Y}_h \in R^{m \times m}$ is of full rank and will be determined later. To obtain such a

transformation, it is required that the m rows A_i are mapped by the transformation T onto themselves as

$$\mathrm{Y}_h A A_i = \mathrm{Y}_h A_i = A_i \tag{4.5}$$

The condition (4.5) admits a unique solution of Y_h and its elements should not vanish for a system to be holonomic. To find the elements of the matrix Y_h, we augment the matrix A into a square matrix $\widetilde{A} \in R^{N\times N}$ in such a way that its determinant does not vanish. The elements y_{ij} of Y_h are the elements of first m rows and first m columns of the inverse augmented matrix.

From the theory of linear algebra, the constrained system defined in (4.1) is equivalent to the following unconstrained but larger linear system [116]:

$$\begin{bmatrix} A \\ P_\perp \end{bmatrix} \dot{\theta} = \begin{bmatrix} 0 \\ 0 \end{bmatrix} \tag{4.6}$$

where the augmented matrix $\widetilde{A}$ is defined as

$$\widetilde{A} = \begin{bmatrix} A \\ P_\perp \end{bmatrix} \tag{4.7}$$

and $P_\perp$ is defined in (4.2). In order to obtain $P_\perp$, treating $\dot{\theta}$ as the vector of unknowns, (4.1) can be solved using the Moore–Penrose inverse as

$$\dot{\theta} = (I - A^{+}A)\dot{\nu} \tag{4.8}$$

where $I \in R^{N\times N}$ is the identity matrix, the vector $\dot{\nu}$ is an arbitrary vector, and A^{+} is the Moore-Penrose inverse defined as

$$A^{+} = A^{T}(AA^{T})^{-1} \tag{4.9}$$

Equation (4.8) is similar to (4.2), but not exactly the same, as seen below.

Let $D = (I - A^{+}A)$. Matrix D in (4.8) is not yet $P_{\perp}$ in (4.2) since they are of different dimensions. The projector $P_{\perp}$ is $N \times (N-m)$, whereas D is an $N \times N$ square matrix. $P_{\perp}$ is of full rank but D is not. Notice that we used $\dot{z}(t)$ in (4.2) instead of $\dot{v}(t)$ in (4.8). The rank of D is $(N-m)$. All the columns of the matrix D are in the null space of A, that is, $AD = 0$. Then any $N-m$ linearly independent columns of D can be chosen to form $P_{\perp}$. But it may create discontinuity in $\dot{v}(t)$ if different set of linearly independent columns is chosen. To remedy this problem, we compute the singular value decomposition of D to select the proper columns of $P_{\perp}$ such that

$$D = U\Sigma V^{T} \tag{4.10}$$

where U and V^{T} are orthogonal matrices of size $N \times N$, and the diagonal matrix Σ with nonnegative diagonal elements in a decreasing order as

$$\Sigma = diag\{\kappa_1, \kappa_2, \cdots, \kappa_{N-m}, 0, \cdots, 0\} \tag{4.11}$$

Let $u_1, u_2, \cdots, u_N$ denote the column vectors of U

$$U = [u_1 \quad u_2 \quad \cdots \quad u_N] \tag{4.12}$$

Since $AD = A(U\Sigma V^{T}) = 0$ and the matrix V^{T} is orthogonal, then by simulation it can be verified that $AU\Sigma = 0$. Because the structure of Σ, it follows that the first $N-m$ columns of U are in the null space of A, i.e.,

$$Au_i = 0, i = 1,2,\cdots,N \tag{4.13}$$

Then the first $N-m$ columns of U may be chosen form the orthogonal projector $P_{\perp}$ as

$$P_{\perp} = \begin{bmatrix} u_1 & u_2 & \cdots & u_{N-m} \end{bmatrix} \tag{4.14}$$

It is obvious that $P_{\perp}$ is of full rank because U is orthogonal.

Back to he extended augmented matrix $\widetilde{A}$ defined in (4.7). By finding its inverse, then the unique matrix Y_h is composed of the elements of the first m rows and first m columns of the inverse augmented matrix $\widetilde{A}$ as:

$$\widetilde{A}^{-1} = \begin{bmatrix} \widetilde{A}^{-1}{}_{11} & \widetilde{A}^{-1}{}_{12} \\ \widetilde{A}^{-1}{}_{21} & \widetilde{A}^{-1}{}_{22} \end{bmatrix} \tag{4.15}$$

$$\mathrm{Y}_h = \widetilde{A}^{-1}{}_{11} \in R^{m \times m} \tag{4.16}$$

By then, the transformation matrix T can be constructed as $T = \mathrm{Y}_h A$. By this end, a necessary and sufficient condition is obtained to verify the integrability of constrained system. If the transformation matrix Y_h is not rank deficient, then the system is integrable.

The above can be summarized as follows.

Theorem 4.1: For a system subjected to linear kinematic (kinematic-like) constraint defined in (4.1), these constraints are said to be holonomic constraint if we can construct a linear transformation matrix T that maps all vectors lying in T^{N-m} to zero and maps all vectors orthogonal to the hypersurface L^{N-m} onto themselves. If the transformation matrix Y_h is full rank, then the system is integrable, otherwise it is nonintegrable.

4.3 Simulation Results

The objective in the present section is to simulate the nonholonomy matrix given in (4.16). A 6 DOF free-flying space robot is tested to verify its nonholonomy behavior with zero initial linear velocity. The first five links are assumed to be revolute and the last one is prismatic. The first link is mounted on the base satellite by a revolute joint. The mass of the base satellite is assumed 300 kg. The mass of the target is assumed 1500 kg, The masses of the robot link are assumed $[10 \quad 10 \quad 10 \quad 10 \quad 10 \quad 10]$ kg. The length of each link is assumed as 1m.

The inertia matrix of the base satellite is assumed as

$$\begin{bmatrix} 100 & 0 & 0 \\ 0 & 100 & 0 \\ 0 & 0 & 100 \end{bmatrix} kg.m^2$$

The inertia matrix of the target satellite is considered as

$$\begin{bmatrix} 300 & 0 & 0 \\ 0 & 300 & 0 \\ 0 & 0 & 300 \end{bmatrix} kg.m^2$$

The inertia of each link of the space robot arm assumed as

$$\begin{bmatrix} 3 & 0 & 0 \\ 0 & 3 & 0 \\ 0 & 0 & 3 \end{bmatrix} kg.m^2$$

All initial values for the position and angular velocity and acceleration of the robot joints is assumed to be zero. All initial values for the orientation, angular velocity and angular acceleration of the base satellite are assumed to be zero. All initial values for the

orientation, angular velocity and angular acceleration of the target satellite are also assumed to be zero.

The simulation results shows that by using this algorithm the rank of the transformation matrix Y_h is full (rank=3) in the case of linear momentum while in the case of angular momentum the rank of the transformation matrix Y_h is not full rank (rank=2) as shown in Table 4.1. These results comply with the theoretical and physical results. Another simulation was run assuming external forces exposed to the space robot hand. It shows that the transformation matrix Y_h is of full rank (rank=3) in both cases of linear and angular momentum.

This approach is also implemented to check the nonholonomy of a space robot interacting with a target satellite (of 1400 kg mass) as a combined system with nonzero initial linear velocity 20 m/sec for both the base satellite and the target satellite. The simulation shows that the holonomy matrix has full rank in case of the linear momentum, but it is rank-deficient in case of angular momentum. Which agrees with the theoretical approach considered in this work that both linear and angular momentum are conserved but the linear momentum is holonomic and the angular momentum is nonholonomic.

The momentum response of a free-flying space robot is also recorded in Figure 4.1-4.6. For a free-flying space robot not exposed to external forces, the momentum holds at constant values (zero) for zero initial value conditions as shown in Figures 4.1 and 4.2. On the contrary, if there are external forces act on the system then the momentum is not

conserved as in Figures 4.6 and 4.4. The simulation in Figure 4.5 and 4.6 show also that the linear and angular momentum of a free-flying space robot interacting with a target satellite also hold at constant values.

Table 4.1: Simulation Results of Rank of the Transformation Matrix Y_h (a sample)

Case	Y_h matrix	Rank
Angular momentum of a free-flying space robot with no external forces	[0.0000 0.0000 0.0000 0.0000 0.0011 0.0005 0.0000 - 0.0025 -.0011]	2 Nonholonomic
Angular momentum of a free-flying space robot with external forces (10 N)	[-0.0001 0.0008 0.0003 -0.0002 0.0027 0.0012 0.0004 -0.0062 -0.0026]	3 Angular momentum not conserved
Linear momentum of a free-flying space robot with no external forces	[0.0018 0.0000 0.0000 0.0000 0.0018 0.0000 0.0000 0.0000 0.0018]	3 Holonomic
Linear momentum of a free-flying space robot with external forces (10 N)	[0.0018 0.0000 0.0000 0.0000 0.0018 0.0000 0.0000 0.0000 0.0018]	3 Linaer momentum not conserved
Angular momentum of a free-flying space robot interacting with a target satellite	1.0e-004 * [0.0002 0.0002 0.0000 -0.0002 -0.0002 0.0000 0.3262 0.3268 0.0000]	2 Nonholonomic
linear momentum of a free-flying space robot interacting with a target satellite	1.0e-005 * [0.2350 0.1770 -0.0032 0.1770 0.1407 -0.0023 -0.0032 -0.0023 0.0049]	3 Holonomic

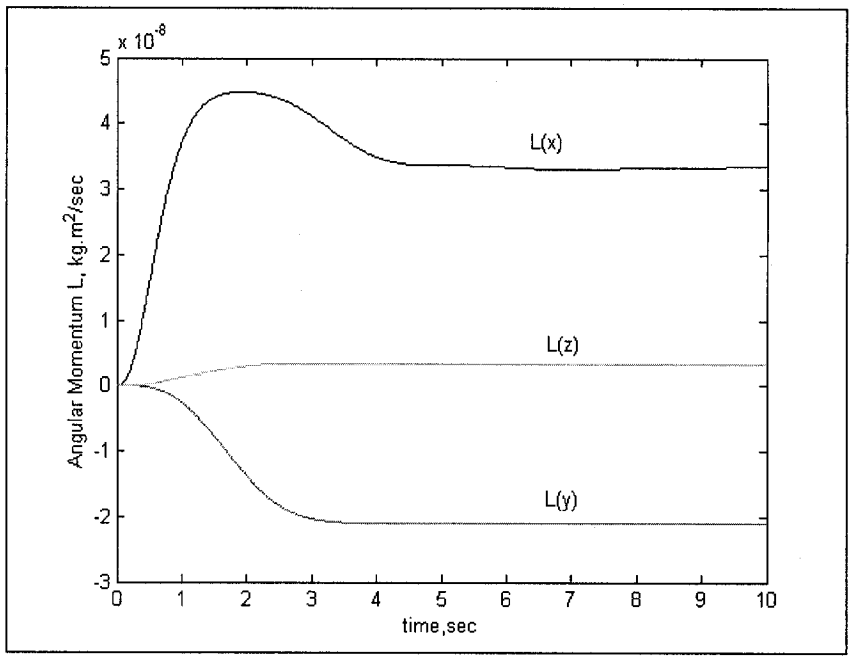

Figure 4.1: Angular Momentum of a Free-Flying Space Robot

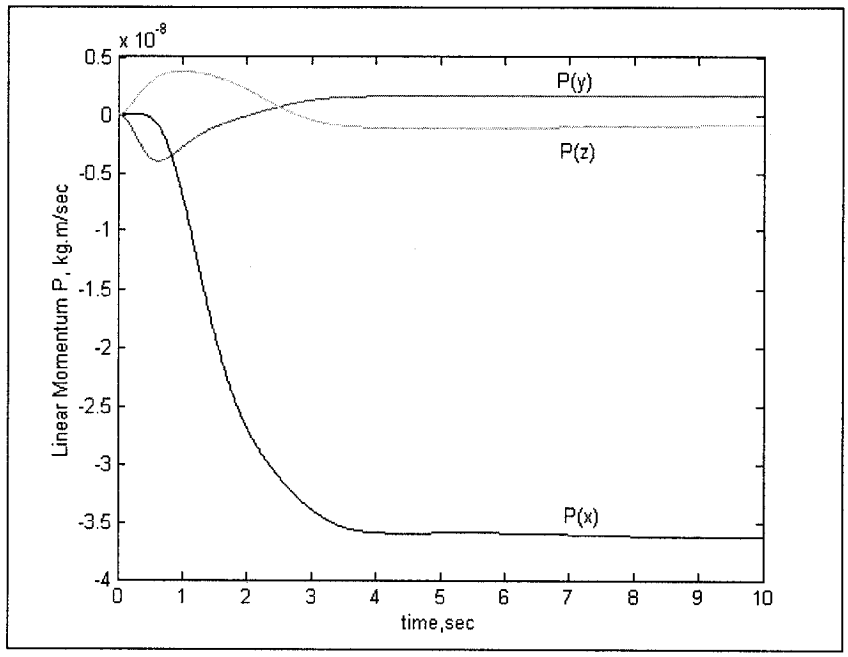

Figure 4.2: Linear Momentum of a Free-Flying Space Robot

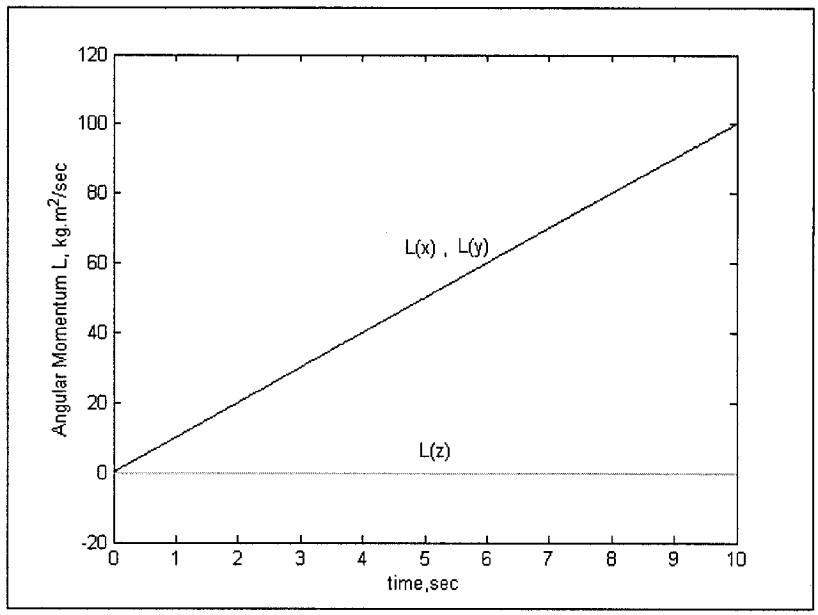

Figure 4.3: Angular Momentum of a Free-Flying Space Robot Subjected to an External Force

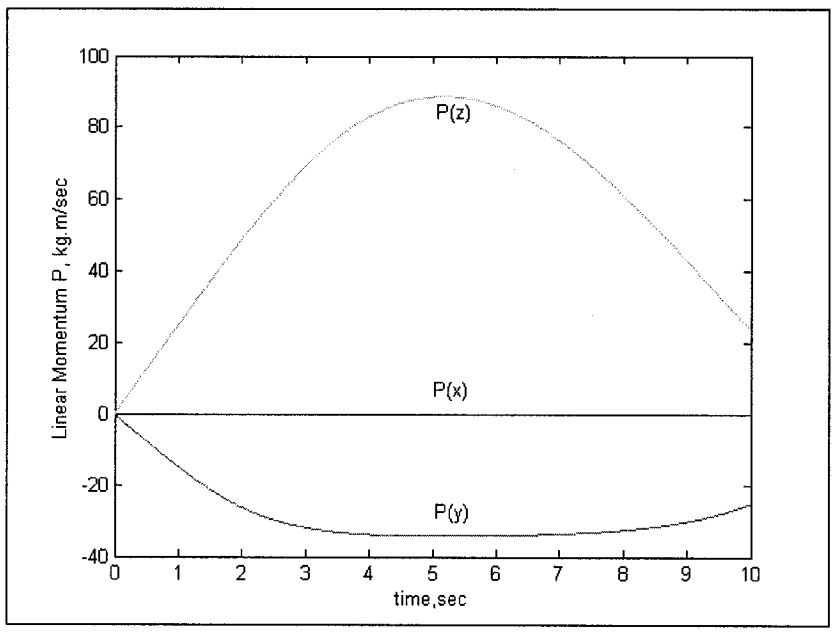

Figure 4.4: Linear Momentum of a Free-Flying Space Robot Subjected to an External Force

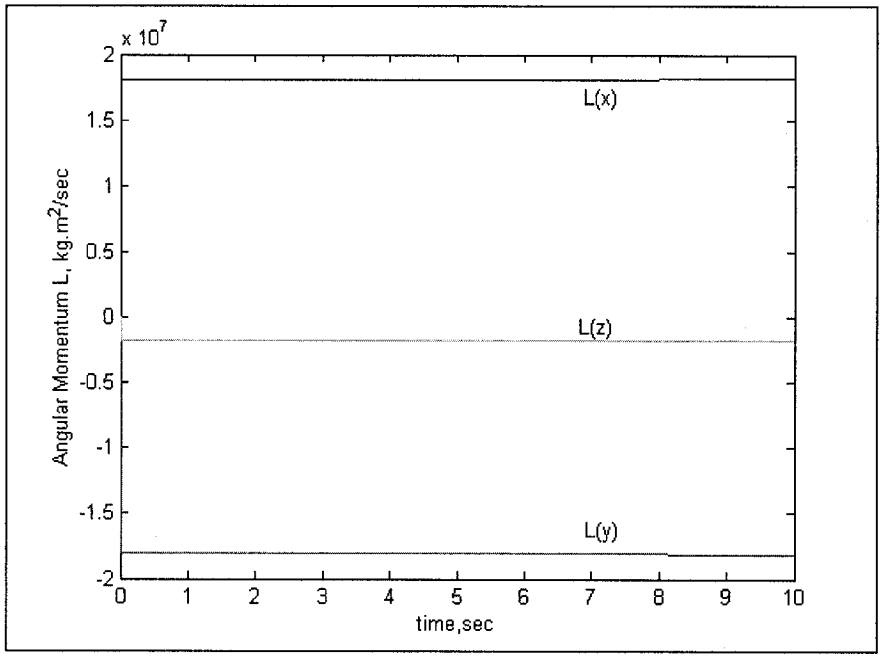

Figure 4.5: Angular Momentum of a Free-Flying Space Robot in Contact with a Target Satellite

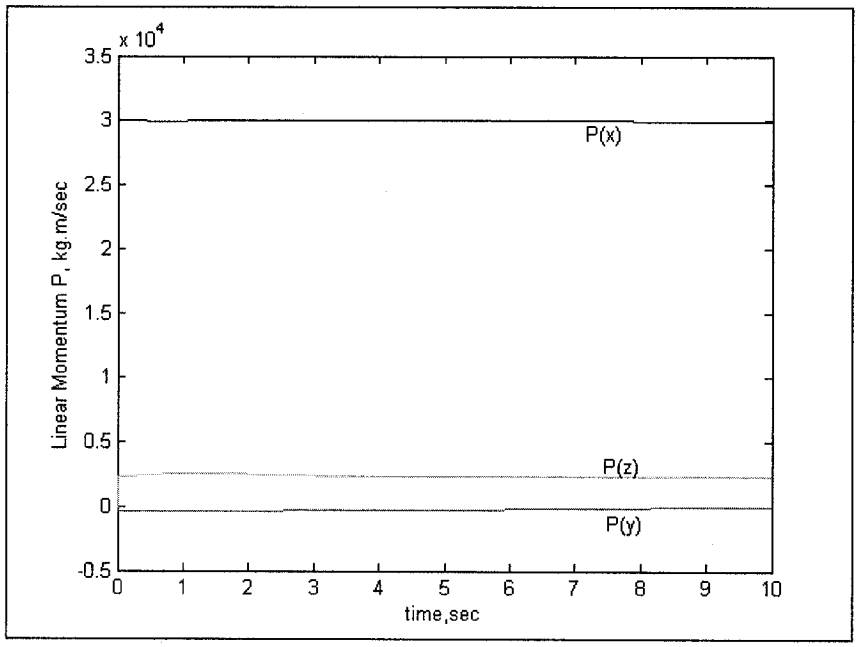

Figure 4.6: Linear Momentum of a Free-Flying Space Robot in Contact with a Target Satellite

The proposed criterion and the simulations results in the present chapter show that for a system subjected to linear kinematic (kinematic-like) constraints, these constraint are said to be holonomic constraint if the rank of the proposed linear transformation matrix is full, otherwise, they are said to be nonholonomic. This approach is useful to verify the non-violation of constraints and their initial conditions in real-time application and to switch controllers or correct the situation. The following chapter will focus on modeling the dynamics of the whole system subjected to holonomic and nonholonmic constraints as step towards designing an efficient controller.

Chapter 5

Modeling of Dynamics of a Free-Flying Space Robot Interacting with a Passive Target Satellite

5.1 Introduction

Free-flying space robots dedicated for maintenance or rescue operations are involved in contact tasks. Many studies on space-based robotic systems have assumed zero external applied forces. Dynamics of space robots by using what is so-called the virtual manipulator (VM) is proposed in [10-14]. Multi-body systems approach based on Newton-Euler dynamic is proposed in [6][7]. Both have used Barycenters to efficiently formulate the dynamics of free-floating space robots. A free-floating multi-body planar space robot dynamics is derived in [30]. A reduced state-space model employed to control multibody space system using nonholonomic techniques for planar space robot is presented in [31]. Study of contact forces between free-flying space robots, and minimization of the impulse at contact is the main concern of work done in [43] [48-50]. A generalized formulation of the dynamic equations for a space-based robot in both open and closed chain kinematic configurations is presented in [95]. The dynamic equation of a space-based manipulator with impact external forces and moving base are considered in [43]. This study takes into account both relative translational and rotational motions between contacting bodies. A joint space planning strategy that achieves both trajectory

tracking and impact minimization is proposed in the later. Contact forces, impact phenomenon dynamics and impulse minimization for free-floating multi-body space robots have been also studied in [48-50]. In [48] a framework includes some means to conveniently express force impulse characteristics, such as the impulse index and the impulse ellipsoid is developed and applied to Ex-IIT experiment. Moreover, in [49], the study presents the joint and the base reactions in terms of finite velocity changes and clarifies their role for the post impact motion behavior of the robot. This analysis makes use of a joint space orthogonal decomposition and involves reaction null space. It has been shown that it is possible to transfer the whole angular momentum from the base toward the manipulator. Contact dynamic emulation for hardware-in-loop simulation of robots interacting with environment is the concern of the research [51]. In the latter, a hardware-in-loop simulation technique is developed, where a simulation of the space robot dynamics is combined with emulation of the contact dynamics by using a rigid robot prototype performing contact task and implemented on a single axis arm. An impedance matching algorithm is proposed to capture the target over a finite time in [133]. Studies [10-18][20-21][25-30][32-42] describing the dynamics of a space robot neglect the coupled dynamics with a floating target or consider only abstract external forces/moments or impulse forces [46][48-50].

In this chapter a unified control-oriented dynamics model is developed by unifying dynamics of the space-robot and the target satellite together along with all holonomic and nonholonomic constraints. Many space missions can benefit from such a control system,

for example, autonomous docking of satellites, rescuing satellites, and satellite servicing, where it is vital to limit the contact force during the robotic operation. It worthy to monition that the advantage of this approach is considering the contact forces between the space robot end-effector and the target as internal forces rather than external forces. This chapter is organized as follows: in section 5.2 the overall dynamics modeling is derived, constraint force decomposition is proposed in section 5.3, section 5.4 presents dynamics reduced model, at the end in section 5.5 simulation results are demonstrated.

5.2 Dynamics Modeling

To derive the dynamic equation of a space robot, consider the total system kinetic energy as the total summation of the transitional and rotational energy of each body in the system which can be expressed as

$$T \overset{def}{=} \frac{1}{2}\sum_{i=0}^{n}\left(m_i V_i^T V_i + \Omega_i^{T\,b} I_i \Omega_i\right) \tag{5.1}$$

where V_i and Ω_i is the transitional and rotational velocities of i-th body as derived in (2.3), (2.7), (2.8) and (2.10), respectively, or

$$\begin{aligned} T = \frac{1}{2}\Big(& V_b^T H_{V_b} V_b + V_b^T H_{V_b\Omega_b}\Omega_b + V_b^T H_{V_b q}\dot{q} + V_b^T H_{V_b\omega_t}\omega_t + V_b^T H_{V_b V_R} v_t + \\ & \Omega_b^T H_{V_b\Omega_b}^T V_b + \Omega_b^T H_{\Omega_b}\Omega_b + \Omega_b^T H_{\Omega_b q}\dot{q} + \Omega_b^T H_{\Omega_b\omega_t}\omega_t + \Omega_b^T H_{\Omega_b V_R} v_t + \\ & \dot{q}^T H_{V_b q}^T V_b + \dot{q}^T H_{\Omega_b q}^T \Omega_b + \dot{q}^T H_q \dot{q} + \dot{q}^T H_{q\omega_t}\omega_t + \dot{q}^T H_{qv_t} v_t + \\ & \omega_t^T H_{V_b\omega_t}^T V_b + \omega_T^T H_{\Omega_b\omega_t}^T \Omega_b + \omega_t^T H_{q\omega_t}^T \dot{q} + \omega_t^T H_{\omega_t}\omega_t + \omega_t^T H_{v_t\omega_t} v_t + \\ & v_t^T H_{V_b v_t}^T V_b + v_t^T H_{v_t\Omega_b}^T \Omega_b + v_t^T H_{v_t q}^T \dot{q} + v_t^T H_{v_t\omega_t}^T \omega_t + v_t^T H_{v_t} v_t \Big) \end{aligned} \tag{5.2}$$

Now as defined before let $\dot{\theta} = \begin{bmatrix} V_b^T & \Omega_b^T & \dot{q}^T & \omega_t^T & v_t^T \end{bmatrix}$, then the total kinetic energy can be expressed in a compact form by rearranging the terms in (5.2) as

$$T = \frac{1}{2}\dot{\theta}^T H(\theta)\dot{\theta} \tag{5.3}$$

where the inertia matrix $H(\theta)$ is given in the block matrix

$$H(\theta) = \begin{bmatrix} H_{V_b} & H_{V_b\Omega_b} & H_{V_bq} & H_{V_b\omega_t} & H_{V_bv_t} \\ H^T_{V_b\Omega_b} & H_{\Omega_b} & H_{\Omega_bq} & H_{\Omega_b\omega_t} & H_{\Omega_bv_t} \\ H^T_{V_bq} & H^T_{\Omega_bq} & H_q & H_{q\omega_t} & H_{qv_t} \\ H^T_{V_b\omega_t} & H^T_{\Omega_b\omega_t} & H^T_{q\omega_t} & H_{\omega_t} & H_{\omega_Tv_t} \\ H^T_{V_bv_t} & H^T_{\Omega_bv_t} & H^T_{qv_t} & H^T_{\omega_tv_t} & H_{v_t} \end{bmatrix} \tag{5.4}$$

Some of the sub-matrices are defined previously in (2.14)-(2.22), while the remaining matrices are defined as

$$H_q \overset{def}{=} \sum_{i=0, i\neq b}^{n+1} \left\{ m_i J_{L_i}^T \cdot J_{L_i} + {}^B I_i J_{A_i}^T J_{A_i} \right\} \in R^{n\times n} \tag{5.5}$$

$$H_{\omega_t} \overset{def}{=} I_{n+1} + m_{n+1} D(r_{t/EE}) \in R^{3\times 3} \tag{5.6}$$

$$H_{q\omega_t} \overset{def}{=} I_{n+1} J_{A_{n+1}}{}^T + m_{n+1} J_{L_{n+1}}{}^T \left[r^T_{t/EE} \times \right] \in R^{3\times n} \tag{5.7}$$

$$H_{qv_t} \overset{def}{=} m_{n+1} J_{L_{n+1}}{}^T E_3 \in R^{3\times n} \tag{5.8}$$

$$H_{\omega_tv_t} \overset{def}{=} -m_{n+1} \left[r_{t/EE} \times \right] \in R^{3\times 3} \tag{5.9}$$

$$H_{v_t} \overset{def}{=} E_3 \cdot m_{n+1} \in R^{3\times 3} \tag{5.10}$$

From the kinetic energy formulation, the dynamics equations can be derived by using the Lagrangian approach. Since there is no potential energy accounted in our system, the Lagrange function L is equal to the kinetic energy T, i.e.,

$$L = \frac{1}{2}\dot{\theta}^T H(\theta)\dot{\theta} = T \tag{5.11}$$

Recalling Equations (2.30), geometric contact constraints at the velocity level can be put in the form assuming zero initial condition as follows:

$$\sum_{k=1}^{n} j_{lk} d\theta_k = 0, \text{ for } l = 1, \cdots, m \tag{5.12}$$

The dynamics equations can be derived by using the Lagrangian approach [117] (see Appendix B for details).

$$\frac{d}{dt}\frac{\partial T}{\partial \dot{\theta}} - \frac{\partial T}{\partial \theta} = \bar{\tau} + J^T \lambda \tag{5.13}$$

or

$$H(\theta)\ddot{\theta} + C(\theta, \dot{\theta})\dot{\theta} = \bar{\tau} + J^T \lambda \tag{5.14}$$

Where $H(\theta)$ is the inertia matrix defined in (5.4) and the velocity-dependent nonlinear forces $C(\theta, \dot{\theta})\dot{\theta}$ are given as

$$C(\theta, \dot{\theta})\dot{\theta} = \dot{H}\dot{\theta} - \frac{\partial}{\partial \theta}\left(\frac{1}{2}\dot{\theta}^T H \dot{\theta}\right) \tag{5.15}$$

the input to the system $\bar{\tau}$ is defined as $\bar{\tau} = \begin{bmatrix} F_{b_L} \\ F_{b_A} \\ \tau \\ 0 \\ 0 \end{bmatrix}$ where F_{b_L}, F_{b_A} are the linear and angular forces at the base satellite and τ is the torque input at robot the joints, and the

zeros to represent that there is no actuation at the target satellite, and λ is the vector of unknown Lagrangian multipliers.

The combined system dynamics model can be represented as (assuming the target satellite is unactauted due to jet failure or shutdown)

$$\begin{bmatrix} H_{V_b} & H_{V_b\Omega_b} & H_{V_bq} & H_{V_b\omega_t} & H_{V_bv_t} \\ H^T_{V_b\Omega_b} & H_{\Omega_b} & H_{\Omega_bq} & H_{\Omega_b\omega_t} & H_{\Omega_bv_t} \\ H^T_{V_bq} & H^T_{\Omega_bq} & H_q & H_{q\omega_t} & H_{qv_t} \\ H^T_{V_b\omega_t} & H^T_{\Omega_b\omega_t} & H^T_{q\omega_t} & H_{\omega_t} & H_{\omega_Tv_t} \\ H^T_{V_bv_t} & H^T_{\Omega_bv_t} & H^T_{qv_t} & H^T_{\omega_tv_t} & H_{v_t} \end{bmatrix} \begin{bmatrix} \dot{V}_b \\ \dot{\Omega}_b \\ \ddot{q} \\ \dot{\omega}_t \\ \dot{v}_t \end{bmatrix} + \begin{bmatrix} C_{V_0}(\theta,\dot{\theta}) \\ C_{\Omega_b}(\theta,\dot{\theta}) \\ C_q(\theta,\dot{\theta}) \\ C_{w_t}(\theta,\dot{\theta}) \\ C_{v_t}(\theta,\dot{\theta}) \end{bmatrix} = \begin{bmatrix} F_{bL} \\ F_{bA} \\ \tau \\ 0 \\ 0 \end{bmatrix} + \begin{bmatrix} J^T_{bL} \\ J^T_{bA} \\ J^T_q \\ J^T_{Tw_t} \\ J^T_{Tv_t} \end{bmatrix} \lambda \qquad (5.16)$$

where J_{bL}, J_{bA} are the linear and angular Jacobians of the base, J_q is the Jacobian of the robot arm, and J_{Tw_t}, J_{Tv_t} are the linear and angular Jacobians of the target.

The dynamic developed in (5.16) along with the combined constraints in (2.34) completes the overall modeling of a space robot interacting with a target satellite. The dynamical model (5.16) results in an undercatauted system. That is the number of inputs (actuators) is less than the number of degrees of freedom. A solution to solve this drawback is proposed in Chapters 6 and 7.

5.3 Constraint Force Decomposition

Only forces which are tangential to the admissible velocities can produce work and contribute to the target motion. But on the contrast, forces which are perpendicular to the motion plane do not contribute to the motion and do no work. This complies with the concept of the virtual work (inner product) $f^T \cdot v = 0$, thereby leading to the idea of

decomposing the constraint forces into two types: normal forces F_n and tangential forces F_t. Let us define two subspaces: the normal subspace N and the tangential subspace T of C^6. Subspaces N and T are complementary to each other by the definition of the direct sum as

$$N \oplus T = C^6 = \{F_n + F_t : F_n \in N, F_t \in T\} \tag{5.17}$$

The manipulation $\oplus$ is called the direct sum since $N \cap \mathrm{T} = \{O\}$. Every $F \in C^6$ can be expressed uniquely as a sum of

$$F = F_n + F_t \quad (F_n \in N, F_t \in T) \tag{5.18}$$

F_n is the projection of F on N along T, and F_t is the projection of F on T along N. From theory of linear algebra, since N and T are complementary subspaces, there is a unique idempotent projector $P_{N,T}$ such that $R(P_{N,T}) = N$ and $\aleph(P_{N,\mathrm{T}}) = \mathrm{T}$ where $R(\cdot)$ is the range of a given matrix and $\aleph(\cdot)$ is the null space.

On the other hand, let $\{F_{n1}, F_{n2}, \cdots, F_{n6}\}$ and $\{F_{t1}, F_{t2}, \cdots, F_{t6}\}$ be any two bases for N and T, respectively, for linear and angular forces/moments. Then the projector $P_{N,\mathrm{T}}$, if it exists, is uniquely determined by

$$\begin{cases} P_{N,T} F_{ti} = F_{ti}, & i = 1, \cdots, 6 \\ P_{N,T} F_{ni} = 0, & i = 1, \cdots, 6 \end{cases} \tag{5.19}$$

Let $F_n = [F_{n1} \quad F_{n2} \quad \cdots \quad F_{n6}]$ denote the matrix whose columns are the vectors F_{ni}. Similarly, let $F_t = [F_{t1} \quad F_{t2} \quad \cdots \quad F_{t6}]$. Then, (5.19) is equivalent to

$$P_{N,T}[F_t \quad F_n] = [F_t \quad O] \tag{5.20}$$

Since $[F_n \quad F_t]$ are nonsingular, the unique solution of (5.20), and therefore (5.19), is

$$P_{N,T} = [F_t \quad O]\,[F_t \quad F_n]^{-1} \tag{5.21}$$

Since (3.30) implies

$$P_{N,T}[F_t \quad O] = [F_t \quad O] \tag{5.22}$$

Therefore for every $F \in C^6$, the unique decomposition is given by (**Corollary in reference [116]**)

$$P_{N,T}F = F_t \tag{5.23}$$

and

$$(I - P_{N,T})F = F_n \tag{5.24}$$

This analysis can give a light on forces which contribute to the motion and which do not. Forces which are tangent to the admissible velocities will perform work while forces which are perpendicular to admissible will perform no work.

5.4 Dynamics Model Reduction

It is possible that we can make a benefit from canceling out the generalized variables belong to the target satellite in the dynamics model obtained before. An advantage of conservation of angular momentum is ability to calculate the target velocities in terms of the base and manipulator's velocities as shown in Equation (2.26). Furthermore, since the

target satellite is assumed to be a floating body without any actuation, then a reduction in the dynamic model (5.16) can be obtained as shown in the following analysis.

The last two rows in the Equation (5.16) represent the dynamics of the target satellite. It is possible that we can take out the linear and angular accelerations of the target as follows

$$\begin{bmatrix}\dot{\omega}_T\\ \dot{v}_T\end{bmatrix}=\begin{bmatrix}H_{\omega_T} & H_{\omega_T v_T}\\ H^T_{\omega_T v_T} & H_{v_T}\end{bmatrix}^{-1}\left(\begin{bmatrix}J^T_{Tw_T}\\ J^T_{Tv_T}\end{bmatrix}\lambda-\begin{bmatrix}H^T_{V_b\omega_T} & H^T_{\Omega_b\omega_T} & H^T_{q\omega_T}\\ H^T_{V_b v_T} & H^T_{\Omega_b v_T} & H^T_{qv_T}\end{bmatrix}\begin{bmatrix}\dot{V}_b\\ \dot{\Omega}_b\\ \ddot{q}\end{bmatrix}-\begin{bmatrix}C_{w_T}\\ C_{v_T}\end{bmatrix}\right) \tag{5.25}$$

or

$$\begin{bmatrix}\dot{\omega}_T\\ \dot{v}_T\end{bmatrix}=\begin{bmatrix}H_{\omega_t} & H_{\omega_t v_t}\\ H^T_{\omega v_t} & H_{v_t}\end{bmatrix}^{-1}\begin{bmatrix}J^T_{Tw_t}\\ J^T_{Tv_t}\end{bmatrix}\lambda-\begin{bmatrix}H_{\omega_t} & H_{\omega_t v_t}\\ H^T_{\omega_t v t} & H_{v_t}\end{bmatrix}^{-1}\begin{bmatrix}H^T_{V_b\omega_t} & H^T_{\Omega_b\omega_t} & H^T_{q\omega_t}\\ H^T_{V_b v_t} & H^T_{\Omega_b v_t} & H^T_{qv_t}\end{bmatrix}\begin{bmatrix}\dot{V}_b\\ \dot{\Omega}_b\\ \ddot{q}\end{bmatrix}$$
$$-\begin{bmatrix}H_{\omega_t} & H_{\omega_t v_t}\\ H^T_{\omega_t v_t} & H_{v_t}\end{bmatrix}^{-1}\begin{bmatrix}C_{w_t}\\ C_{v_t}\end{bmatrix} \tag{5.26}$$

Now substituting for $\dot{\omega}_T$ and $\dot{v}_T$ from Equation (5.26) and for ω_T and v_T from Equation (2.26) in the dynamic equation (5.16) one will have the following reduced dynamical model

$$\begin{bmatrix}\widetilde{H}_{V_b} & \widetilde{H}_{V_b\Omega_b} & \widetilde{H}_{V_b q}\\ \widetilde{H}^T_{V_b\Omega_b} & \widetilde{H}_{\Omega_b} & \widetilde{H}_{\Omega_b q}\\ \widetilde{H}^T_{V_b q} & \widetilde{H}^T_{\Omega_b q} & \widetilde{H}_q\end{bmatrix}\begin{bmatrix}\dot{V}_b\\ \dot{\Omega}_b\\ \ddot{q}\end{bmatrix}+\begin{bmatrix}\widetilde{C}_{V_0}\\ \widetilde{C}_{\Omega_b}\\ \widetilde{C}_q\end{bmatrix}=\begin{bmatrix}F_{bL}\\ F_{bA}\\ \tau\end{bmatrix}+\begin{bmatrix}\widetilde{J}^T_{bL}\\ \widetilde{J}^T_{bA}\\ \widetilde{J}^T_q\end{bmatrix}\lambda \tag{5.27}$$

where

$$\begin{bmatrix} \widetilde{H}_{V_b} & \widetilde{H}_{V_b\Omega_b} & \widetilde{H}_{V_bq} \\ \widetilde{H}^T_{V_b\Omega_b} & \widetilde{H}_{\Omega_b} & \widetilde{H}_{\Omega_bq} \\ \widetilde{H}^T_{V_bq} & \widetilde{H}^T_{\Omega_bq} & \widetilde{H}_q \end{bmatrix} =$$

$$\begin{bmatrix} H_{V_b} & H_{V_b\Omega_b} & H_{V_bq} \\ H^T_{V_b\Omega_b} & H_{\Omega_b} & H_{\Omega_bq} \\ H^T_{V_bq} & H^T_{\Omega_bq} & H_q \end{bmatrix} - \begin{bmatrix} H_{V_b\omega_t} & H_{V_bv_t} \\ H_{\Omega_b\omega_t} & H_{\Omega_bv_t} \\ H_{q\omega_t} & H_{qv_t} \end{bmatrix} \begin{bmatrix} H_{\omega_t} & H_{\omega_tv_t} \\ H^T_{\omega_tv_t} & H_{v_t} \end{bmatrix}^{-1} \begin{bmatrix} H^T_{V_b\omega_t} & H^T_{\Omega_b\omega_t} & H^T_{q\omega_t} \\ H^T_{V_bv_t} & H^T_{\Omega_bv_t} & H^T_{qv_t} \end{bmatrix} \tag{5.28}$$

$$\begin{bmatrix} \widetilde{C}_{V_0} \\ \widetilde{C}_{\Omega_b} \\ \widetilde{C}_q \end{bmatrix} = - \begin{bmatrix} H_{V_b\omega_t} & H_{V_bv_t} \\ H_{\Omega_b\omega_t} & H_{\Omega_bv_t} \\ H_{q\omega_t} & H_{qv_t} \end{bmatrix} \begin{bmatrix} H_{\omega_t} & H_{\omega_tv_t} \\ H^T_{\omega_tv_t} & H_{v_t} \end{bmatrix}^{-1} \begin{bmatrix} C_{w_t} \\ C_{v_t} \end{bmatrix} + \begin{bmatrix} C_{V_0} \\ C_{\Omega_b} \\ C_q \end{bmatrix} \tag{5.29}$$

and finally,

$$\begin{bmatrix} \widetilde{J}^T_{bL} \\ \widetilde{J}^T_{bA} \\ \widetilde{J}^T_q \end{bmatrix} = \begin{bmatrix} J^T_{bL} \\ J^T_{bA} \\ J^T_q \end{bmatrix} - \begin{bmatrix} H_{V_b\omega_t} & H_{V_bv_t} \\ H_{\Omega_b\omega_t} & H_{\Omega_bv_t} \\ H_{q\omega_t} & H_{qv_t} \end{bmatrix} \begin{bmatrix} H_{\omega_t} & H_{\omega_tv_t} \\ H^T_{\omega_tv_t} & H_{v_t} \end{bmatrix}^{-1} \begin{bmatrix} J^T_{Tw_t} \\ J^T_{Tv_t} \end{bmatrix} \tag{5.30}$$

As it can be seen easily, the target satellite linear and angular motions are implicitly accounted in the reduced dynamics obtained in Equations (5.27). The dynamics (5.27) is a generalized model for a space robot without a contact with a floating body. A totally free-flying space robot can be considered to be a special case of this model. Moreover, the inertia matrix in dynamics (5.28) is a generalization of the inertia matrix of a free-flying space robot without a contact with a target. The Jacobian matrix (5.30) can be considered as an extension of the Generalized Jacobian [26] of a free-flying space robot.

Since we are interested in controlling the base attitude rather than its translation, another reduction can be achieved by eliminating out the base linear motion in the dynamics (5.27) as follows:

From the first row of the dynamics (5.27) the linear acceleration of the base is

$$\dot{V}_b = -\widetilde{H}_{V_b}^{-1}\widetilde{H}_{V_b\Omega_b}\dot{\Omega}_b - \widetilde{H}_{V_b}^{-1}\widetilde{H}_{V_bq}\ddot{q} - \widetilde{H}_{V_b}^{-1}\widetilde{C}_{V_0} + \widetilde{H}_{V_b}^{-1}F_{bL} + \widetilde{H}_{V_b}^{-1}\widetilde{J}_{bL}^{T}\lambda \tag{5.31}$$

Substituting now (5.31) for $\dot{V}_b$ in the second and third rows of Equations (5.27) will result in

$$\begin{bmatrix} \hat{H}_{\Omega_b} & \hat{H}_{\Omega_bq} \\ \hat{H}^{T}_{\Omega_bq} & \hat{H}_q \end{bmatrix}\begin{bmatrix} \dot{\Omega}_b \\ \ddot{q} \end{bmatrix} + \begin{bmatrix} \hat{C}_{\Omega_b}(\theta,\dot{\theta}) \\ \hat{C}_q(\theta,\dot{\theta}) \end{bmatrix} = \begin{bmatrix} \hat{F}_b \\ \hat{\tau} \end{bmatrix} + \begin{bmatrix} \hat{J}_b^T \\ \hat{J}_q^T \end{bmatrix}\lambda \tag{5.32}$$

where the inertia matrix and other vectors are defined as

$$\hat{H}_{\Omega_b} = \widetilde{H}_{\Omega_b} - \widetilde{H}^{T}_{V_b\Omega_b}\widetilde{H}_{V_b}^{-1}\widetilde{H}_{V_b\Omega_b},\ \hat{H}_{\Omega_bq} = \widetilde{H}_{\Omega_bq} - \widetilde{H}^{T}_{V_b\Omega_b}\widetilde{H}_{V_b}^{-1}\widetilde{H}_{V_bq},\ \hat{H}_q = \widetilde{H}_q - \widetilde{H}^{T}_{V_bq}\widetilde{H}_{V_b}^{-1}\widetilde{H}_{V_bq}$$

$$\hat{C}_{\Omega_b} = \widetilde{C}_{\Omega_b} - \widetilde{H}^{T}_{V_b\Omega_b}\widetilde{H}_{V_b}^{-1}\widetilde{C}_{V_0},\ \hat{C}_q = \widetilde{C}_q - \widetilde{H}^{T}_{V_bq}\widetilde{H}_{V_b}^{-1}\widetilde{C}_{V_0},\ \hat{F}_b = F_{bA} - \widetilde{H}^{T}_{V_b\Omega_b}\widetilde{H}_{V_b}^{-1}F_{bL}$$

$$\hat{\tau} = \tau - \widetilde{H}^{T}_{V_bq}\widetilde{H}_{V_b}^{-1}F_{bL},\ \hat{J}_b^T = \widetilde{J}_{bA}^T - \widetilde{H}^{T}_{V_b\Omega_b}\widetilde{H}_{V_b}^{-1}\widetilde{J}_{bL}^T \text{ and } \hat{J}_q^T = \widetilde{J}_q^T - \widetilde{H}^{T}_{V_bq}\widetilde{H}_{V_b}^{-1}\widetilde{J}_{bL}^T.$$

5.5 Simulation Results

A 6-DOF space robot arm mounted on base satellite is used to demonstrate the analytical results obtained in the dynamical model (5.16). We assume that the end-effecter established a contact with a target satellite. This target satellite is assumed to be totally floating and unactuated due to the thrusters' failure.

The first five links are assumed to be revolute and the last one is prismatic. The first link is mounted on the base satellite by a revolute joint. The mass of the base satellite is assumed 300 kg. The mass of the target is assumed 1500 kg, The masses of the robot link are assumed $[10 \quad 10 \quad 10 \quad 10 \quad 10 \quad 10]^{'}$ kg. The length of each link is assumed as 1m.

The inertia matrix of the base satellite is considered as

$$\begin{bmatrix} 100 & 0 & 0 \\ 0 & 100 & 0 \\ 0 & 0 & 100 \end{bmatrix} kg.m^2$$

The inertia matrix of the target satellite is considered as

$$\begin{bmatrix} 300 & 0 & 0 \\ 0 & 300 & 0 \\ 0 & 0 & 300 \end{bmatrix} kg.m^2$$

The inertia of each link of the space robot arm assumed as

$$\begin{bmatrix} 3 & 0 & 0 \\ 0 & 3 & 0 \\ 0 & 0 & 3 \end{bmatrix} kg.m^2$$

All initial values for the position and angular velocity and acceleration of the robot joints is assumed to be zero. All initial values for the orientation, angular velocity and angular acceleration of the base satellite and the target satellite are assumed to be zero. All initial

values for the orientation, angular velocity and angular acceleration of the target satellite are also assumed to be zero. The desired values of the base satellite Euler angles are assumed zero. The initial linear velocities of both the base and the target are assumed to be 10 m/sec to keep a constant linear relative velocity while conducting the task and to avoid any damage.

Two different PD controllers are used, to control the base satellite reaction wheels and robot arm as: $\tau_{rw} = k_p(A_b - A_{b,des}) + k_D\Omega_b$, $\tau_{robot} = k_1(q_{des} - q) + k_2\dot{q}$, respectively, where $k_p = [10 \quad 10 \quad 10]$, $k_D = [10 \quad 10 \quad 10]$, $k_1 = 10, k_2 = 10$.

The simulation is used to test the dynamics of the whole system and to verify the analytical results. The simulation results are shown in Figures 5.1-5.5. Figures 5.1 and 5.2 show a very slight variation in the base satellite attitude and small increase in its linear velocity over 3 minutes. On the contrast, Figures 5.4 and 5.5 show that the target drifts away, but a slight rise in its linear velocity. Figure 5.3 shows that most robot arm links approach their desired values. Several simulations are run and show that linear forces are preferable on angular forces and as long as the forces are relatively small comparing to the target mass/inertia, its linear velocities slightly change. The PD controllers implemented in this simulation are not sufficient to control the angular motion of the target satellite, hence another approaches should be investigated as it will be shown in the following two chapters.

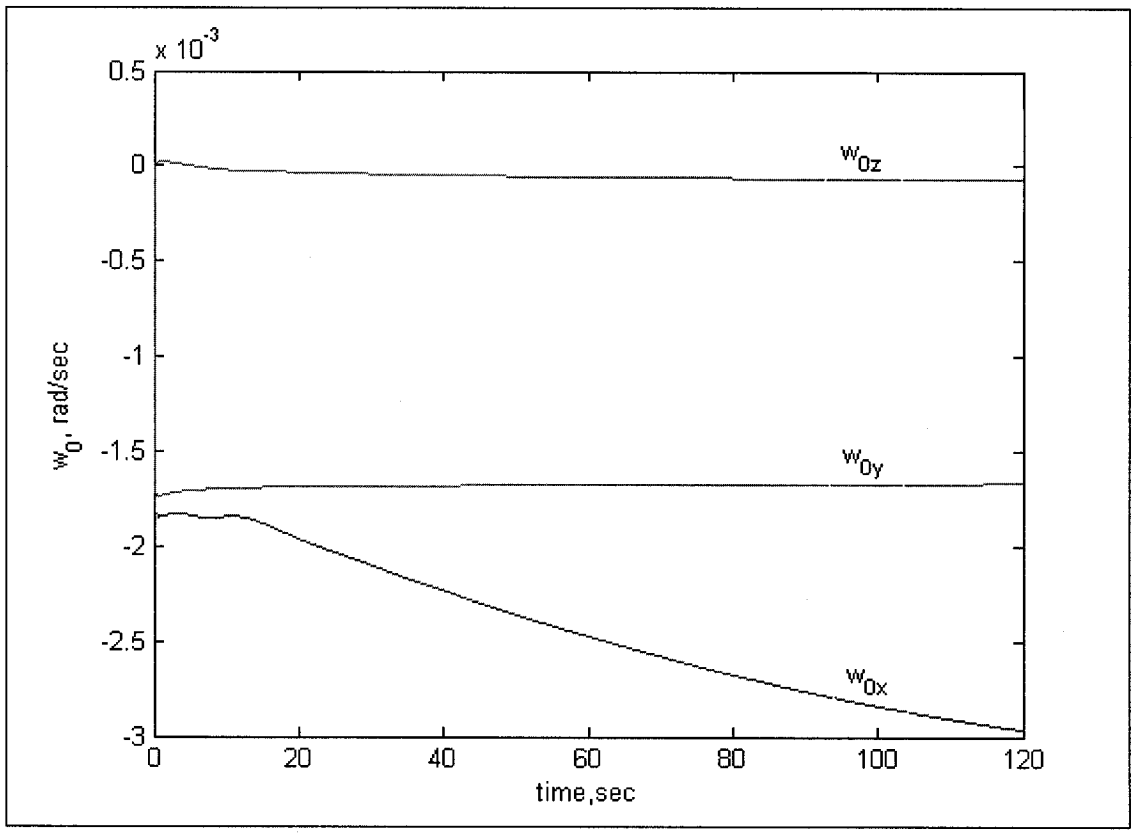

Fig 5.1: Angular Velocity of the Base Satellite

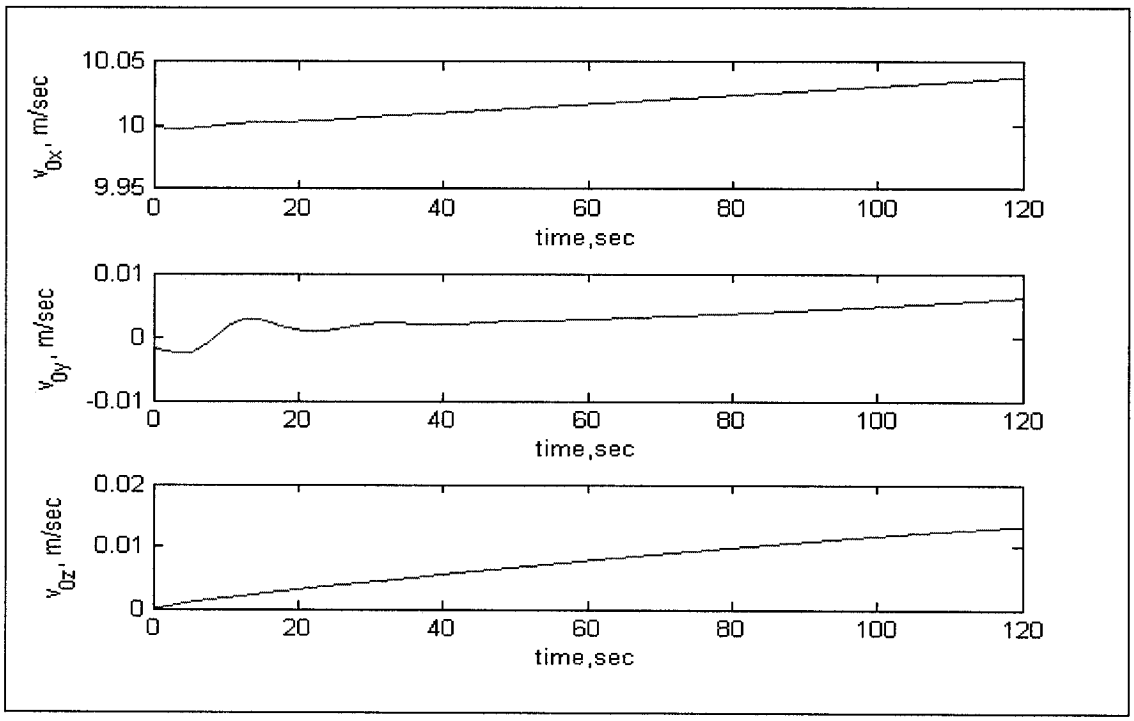

Fig 5.2: Linear Velocity of the Base Satellite

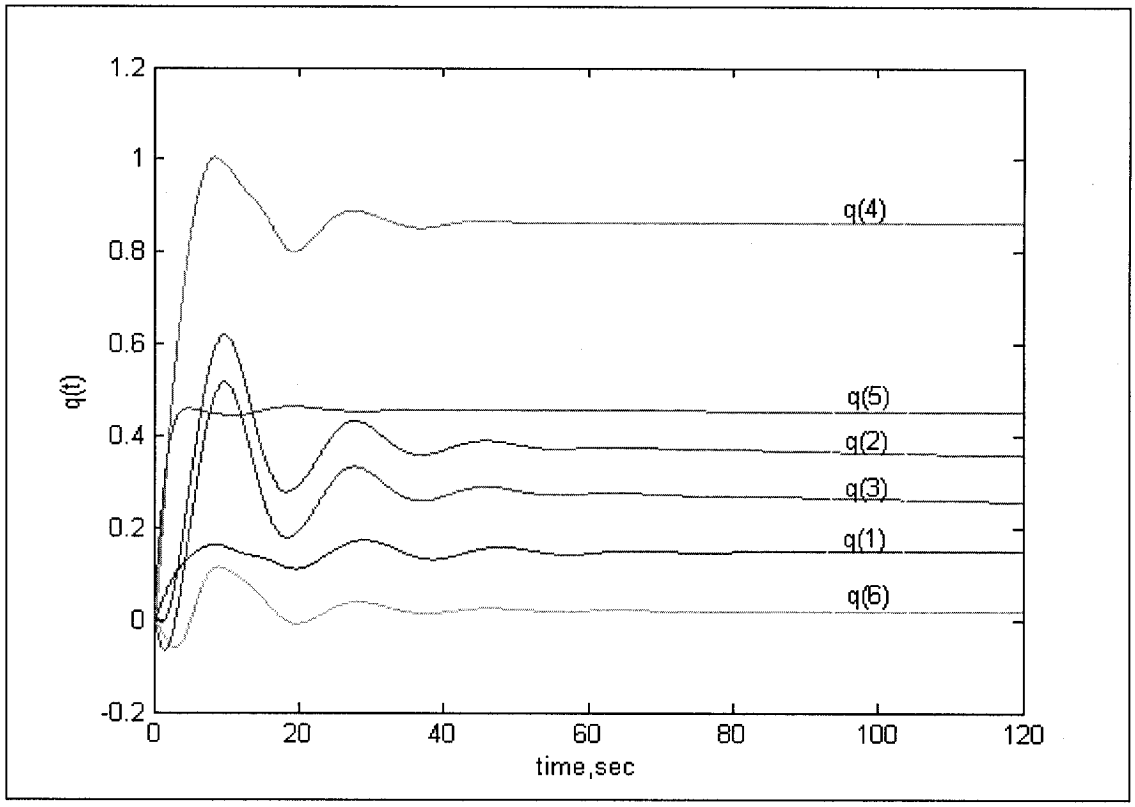

Fig 5.3: Robot Arm Angles

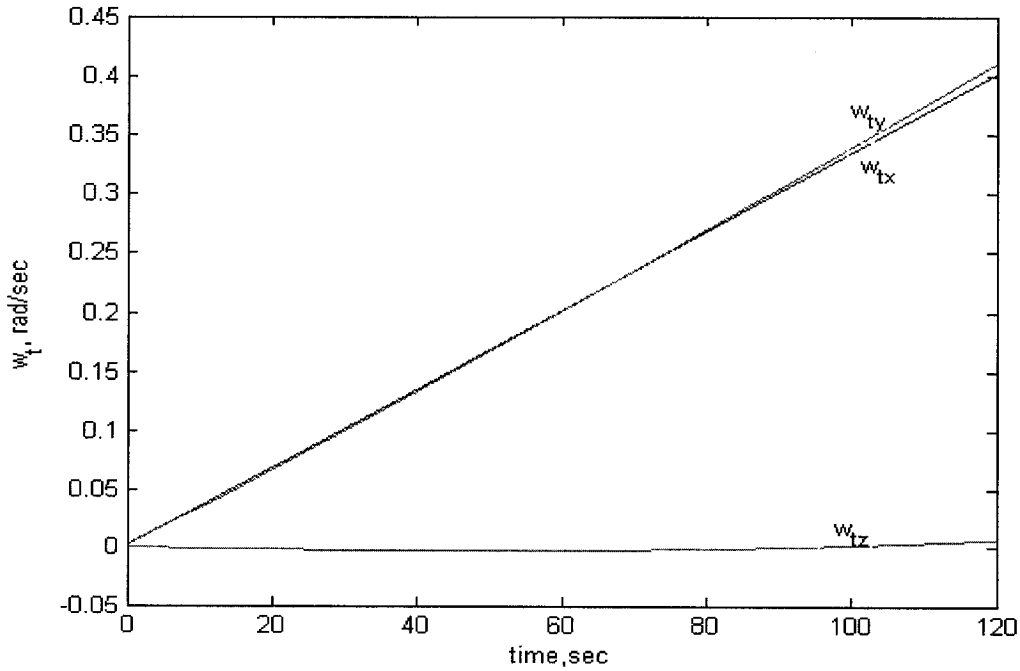

Fig 5.4: Angular Velocity of the Target Satellite

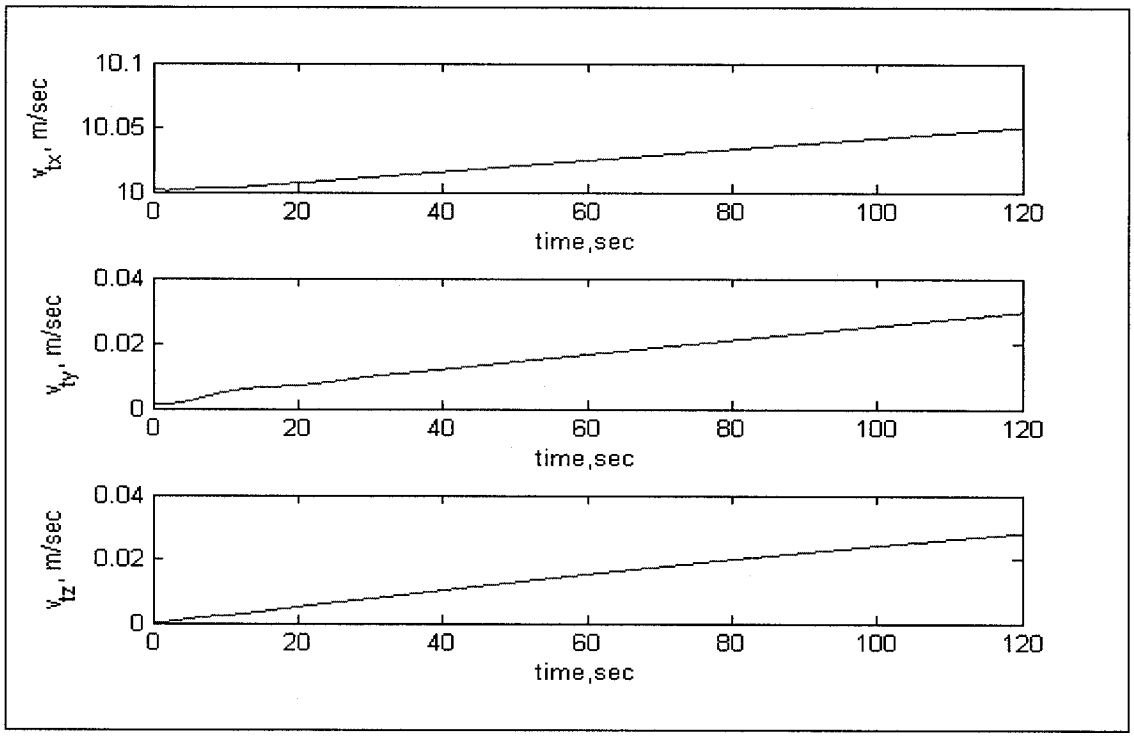

Fig 5.5: Linear Velocity of the Target Satellite

An overall control-oriented modeling approach is developed in the present chapter to deal with the kinematics, constraints and dynamics of a free-flying space robot interacting with a target satellite. Based on the Lagrangian approach, a generalized dynamical model suitable for control algorithms is proposed.

In the next chapter a hybrid inverse-based-dynamics controller will be investigated. The purpose of designing this controller is to control simultaneously force and motion of a free-flying space robot in contact with a target satellite subjected to holonomic and nonholonomic constraints.

Chapter 6

Inverse Dynamics Control of a Free-Flying Space Robot in Contact with a Target Satellite

6.1 Introduction

A unified approach for inverse and direct dynamics of constrained multibody systems that can serve as a basis for analysis, simulation, and control is proposed in [83-84]. An inverse dynamics type controller which ensures tracking of the end-effector position along the unconstrained directions and ensures tracking of contact force along the constrained direction is presented in [156]. An impedance matching algorithm is outlined to capture the target satellite over a finite time in [133]. An efficient algorithm of the inverse dynamics computation of space manipulators is proposed in [25]. This algorithm is based on differentiating the momentum with respect to time at the acceleration level assuming non-zero initial conditions. Using free-flying space robots to perform contact tasks on the surface of target satellites has not yet received enough attention. Orbital exchange-unit and refueling missions have been verified by ETS-VII [63]. More service operations such as handling a wire and plugging a connector wire have been also tested by teleoperation. It is clear that a more skillful dexterous manipulation study is needed. The big challenge in this task is the coupling between the space robot and its base satellite on one hand, and between the servicing satellite and the target satellite on the other hand. Any motion or external forces exert on each system will affect the motion of the other. Another challenge will rise is the consumption of the control fuel which is

considered as a limited source in the space operations. To mention some of contact tasks but not all, they may include repairing failed parts such as solar panels, removing old thrusters, attaching new thrusters, replacing charging batteries, refueling jet control fuel, upgrading some control components, grab space objects or spacecrafts or telescopes and bring it into the atmosphere in a controlled manner, guiding it to harmlessly splash into a remote part of an ocean (like Hubble Space Telescope scenario).

As it is assumed in this thesis that space robot end-effector has established a contact with the targets satellite, then it necessary to design a hybrid force/motion algorithm to control simultaneously motion trajectories and contact tasks on the surface of the target satellite over a finite time. This is very essential due to the fact that the most critical stage in this process is to maintain a contact with the targets satellite until it is totally captured or the contact task is completely accomplished. To the best of author's knowledge, an inverse-based-dynamics controller has not been yet designed for the application of a free-flying space robot interacting with a target satellite. It can be verified that by reviewing studies [10-18][20-21][25-30][32-42], the coupled dynamics or contact interaction of a space robot with a target satellite is ignored or only abstract external forces/moments or impulse forces are considered as in [46][48-50].

This chapter presents an inverse-dynamics-based control approach of a free-flying space robot manipulator interacting with a target satellite. The proposed controller handles the overall combined coupled dynamics of the based-satellite servicing robot and the passive target satellite all together along with geometric and momentum constraints imposed on the system. A reduced-order dynamical model is obtained by finding a common solution

of all constraints using the concept of orthogonal projection matrices. The proposed controller does not only show the capability to meet motion and contact forces desired specifications, but also to cope with the under-actuation problem of the target satellite due to its thrusters' failure.

This chapter is organized as follows, in section 6.2 a hybrid inverse-dynamics based controller is proposed, and finally in section 6.3 simulation results are demonstrated to verify the analytical results.

6.2 Inverse Dynamics Controller

The basic idea of inverse dynamics control is to seek a nonlinear dynamics control law that cancels exactly all nonlinear terms in the system dynamics (5.16) so that the closed loop dynamics is linear and decoupled [83-85][129].

Now assuming zero initial constraint conditions, the overall dynamics subjected to the holonomic and nonholonomic constraints can be expressed in a compact form as

$$H\ddot{\theta} + C\dot{\theta} = \bar{\tau} + F_c \tag{6.1}$$

$$A(\theta)\dot{\theta} = 0 \tag{6.2}$$

where $\dot{\theta}$ is the vector of generalized variables defined as $\dot{\theta} = \begin{bmatrix} V_b^T & \Omega_b^T & \dot{q}^T & \omega_t^T & v_t^T \end{bmatrix}$, the inertia matrix H is defined in (5.4), the nonlinear vector $C(\theta, \dot{\theta})$ is the centrifugal/Coriolos forces as defined in (5.15), the generalized constraint forces are

$F_c = J^T\lambda$, $\lambda \in R^m$ is the vector of unknown Lagrangian multipliers, J^T and $\bar{\tau}$ are defined, respectively, as

$$J^T = \begin{bmatrix} J_{bL}^T \\ J_{bA}^T \\ J_q^T \\ J_{Tw_t}^T \\ J_{Tv_t}^T \end{bmatrix}, \bar{\tau} = \begin{bmatrix} F_{b_L} \\ F_{b_A} \\ \tau \\ 0 \\ 0 \end{bmatrix}$$ as in (5.16), and finally the constraint matrix $A(\theta) = \begin{bmatrix} J(\theta) \\ B(\theta) \end{bmatrix}$ as given in (2.34).

In the constraint equation (6.2) there are $(k+m)$ linear equations and N of the generalized velocities $\dot{\theta}$. It is clear that there are fewer equations than unknowns, this implies the existence of infinite solutions. From the theory of linear algebra, the solution of (6.2) can be given by

$$\dot{\theta} = S(\theta)\dot{\nu} \tag{6.3}$$

where $S(\theta) \in R^{(N)\times(N-k-m)}$ is an orthogonal projector of full rank and belong to the null space of $A(\theta)$ (it implies that $S^T A^T = 0$) and the vector $\dot{\nu} \in R^{(N-k-m)}$ can be chosen arbitrary. For example the Euler angles of the base and target satellites and the joint angles for the robot arm are good candidates for ν.

Now differentiating (6.3) at the acceleration level with respect to time yields

$$\ddot{\theta} = S\ddot{\nu} + \dot{S}\dot{\nu} \tag{6.4}$$

Upon substituting the velocities (6.3) and the acceleration (6.4) into the dynamics (6.1) we obtain

$$HS\ddot{\nu} + \left(H\dot{S} + CS\right)\dot{\nu} = \bar{\tau} + J^T\lambda \tag{6.5}$$

Let us define the controller as $\bar{\tau}$

$$\bar{\tau} = \left(H\dot{S} + CS\right)\dot{v} + HS(\ddot{v}_d + K_D\dot{e}_p + K_P e_p) - J^T\lambda_c \tag{6.6}$$

where the position tracking error is defined as $e_p = v_d - v$ and composite force error λ_c is defined as

$$\lambda_c = \lambda_d - K_F e_F - K_I \int e_F dt \tag{6.7}$$

where $e_F = \lambda - \lambda_d$ and the gain matrices K_P, K_D, K_F and K_I are chosen as diagonal with positive elements. Note that the input to the proposed controller (6.6) consists of the joint angles and velocities, angular velocity of the base, relative velocities of both satellites, contact forces. The output of the controller is the robot arm joint torques. Note also that $s^T\bar{\tau} \in R^{N-k-m}$ has the advantage of overcoming the underactuation of the system as a result of target satellite jet shutdown or failure, and the inputs provided by the robot and the base is enough to control the whole system. This is because the number of constraints $k+m \geq$ the number of passive inputs of the target satellite.

Now let us substitute the control law (6.6)-(6.7) into the dynamics (6.5) and by multiplying both sides with S^T, then, the closed loop dynamics is given by

$$S^T MS(\ddot{e}_p + K_D\dot{e}_p + K_P e_p) = -S^T J^T\left(K_F e_F + K_I \int e_F dt\right) = 0 \tag{6.8}$$

Since J belongs to the null space of S, that is, $S^T J^T = 0$, then the right hand side of (6.8) is zero. Since by the virtue of (6.3), the projection matrix $S(q)$ and its transpose are of full rank, and the inertia matrix is symmetric positive definite, then $S^T MS$ is also a positive definite. Now we need to verify the terms inside the brackets in (6.8) are zero. This condition can be guaranteed by choosing the proper positive gains K_D and K_P such that $v \to v_d$ as $t \to \infty$. If the gain matrices K_D and K_P are chosen as diagonal with

positive diagonal elements, then the resulted closed loop dynamics is linear, decoupled and exponentially stable and stability can then be guaranteed. The closed loop dynamics natural frequency and damping ration can be chosen to meet specific requirements. Since $v \to v_d$ as $t \to \infty$, then $e_p = v_d - v$ is bounded, and $\dot{e}_p, \ddot{e}_p \to 0$ as $t \to \infty$, i.e. signals $\dot{e}_p$ and $\ddot{e}_p$ are bounded. By substituting the control law (6.6) and (6.7) into the reduced model (6.5) yields

$$HS(\ddot{e}_p + K_D \dot{e}_p + K_P e_p) = J^T \left[(I + K_F) e_F + K_I \int e_F dt \right] \tag{6.9}$$

Also by inspecting the right hand side of (6.7) it can be seen that the time derivative of the term inside the bracket as $(I + K_F)\dot{e}_F + K_I e_F = 0$ can be guaranteed to be stable by choosing the suitable gain matrices K_F and K_I.

Now we can readily summarize the hybrid inverse-dynamics controller in the following theorem:

Theorem 6.1: For the dynamic system given in (6.1) and subjected to constraints (6.2), the inverse dynamics control law defined by (6.6) and (6.7) is globally stable and guarantees zero steady state and force tracking errors.

6.3 Simulation Results

The goal of the simulation in the current section is to verify the effectiveness of the inverse dynamics controller (6.6) and (6.7) in controlling the dynamics (6.1) subjected to the constraints (6.2).

For simulation we assume that the end-effecter of the servicing space robot manipulator has established a contact with a target satellite. The robot arm is composed of 6-DOF and mounted on base satellite is used to demonstrate the analytical results. This target satellite is assumed to be totally floating and unactuated due to the thrusters' failure. The first five links are assumed to be revolute and the last one is prismatic. The first link is mounted on the base satellite by a revolute joint. The mass of the base satellite is assumed 300 kg. The mass of the target is assumed 1500 kg, The masses of the robot link are assumed $[10 \quad 10 \quad 10 \quad 10 \quad 10 \quad 10]$ kg. The length of each link is assumed as 1m.

The inertia matrix of the base satellite is assumed as

$$\begin{bmatrix} 100 & 0 & 0 \\ 0 & 100 & 0 \\ 0 & 0 & 100 \end{bmatrix} kg.m^2$$

The inertia matrix of the target satellite is considered as

$$\begin{bmatrix} 300 & 0 & 0 \\ 0 & 300 & 0 \\ 0 & 0 & 300 \end{bmatrix} kg.m^2$$

The inertia of each link of the space robot arm assumed as

$$\begin{bmatrix} 3 & 0 & 0 \\ 0 & 3 & 0 \\ 0 & 0 & 3 \end{bmatrix} kg.m^2$$

All initial values for the position and angular velocity and acceleration of the robot joints is assumed to be zero. All initial values for the orientation, angular velocity and angular acceleration of the base satellite are assumed to be zero. All initial values for the orientation, angular velocity and angular acceleration of the target satellite are also assumed to be zero. The desired values of the space robot joints are assumed to as $[0.3 \quad 0.2 \quad 0.4 \quad 0.45 \quad 0.5 \quad 0.0]^T$ rad. The desired values of the base satellite Euler angles are assumed zero. The initial linear velocities of both the base and the target are assumed to be 20 m/sec to keep a constant linear relative velocity while conducting the task and to avoid any damage. All other initial conditions are assumed to be zero. The contact forces are assumed to be linear and only in the x-direction as $\lambda_{des} = 10$. The motion and force gain diagonal matrices K_P, K_D, K_F, K_I are chosen as:

$K_P = diag(30,30,30,30,30,30,30,30,30,30)$,

$K_D = diag(25,25,25,25,25,25,25,25,25,25)$,

$K_F = diag(10,10,10,10,10,10)$,

$K_I = diag(50,50,50,50,50,50)$.

The simulation is used to verify the effectiveness of the proposed controller (6.6)-(6.7) and if it can track the desired motion and the specified contact forces and, moreover, overcome the under-actuation (passivity) in the target satellite. The simulation results are shown in Figures 6.1-6.8. Figures 6.1 and 6.2 show, respectively, a fast response for both linear and angular velocities of the base. Figure 6.3 and 6.4 represent, respectively, the error response of robot arm angular position and velocities. The controller is able to bring

the links to the steady state position at around 25 sec. Figure 6.5 shows the joints actuators response which approaches zero after 25 sec. In Figure 6.6 and 6.7, the linear and angular velocities error response of the target satellite present a noticeable fast response. Finally, Figure 6.8 shows the error in the Lagrangian force multiplier. The error gets close to zero at time 25 sec. It can be seen that the simulation results ensure that the proposed controller is effective in controlling the force/motion of the of a free-flying space robot in contact with a target satellite.

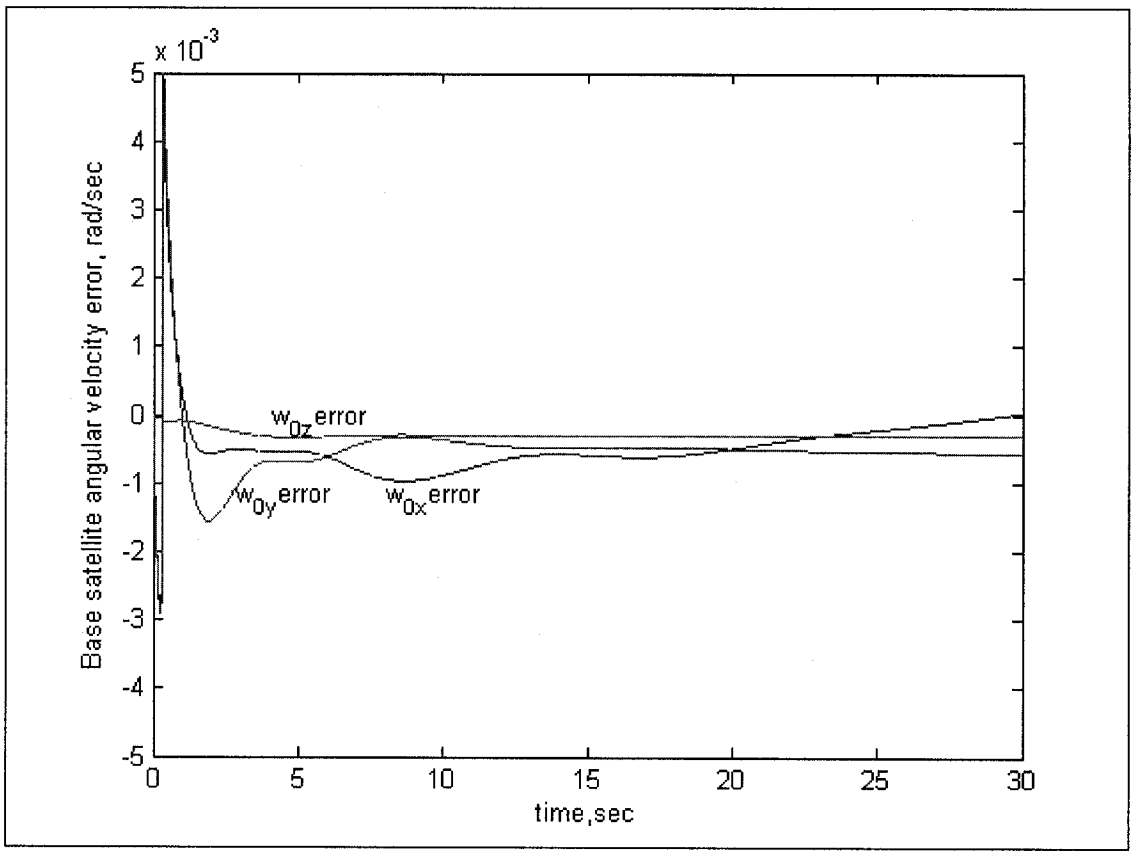

Figure 6.1: Base Satellite Angular Velocity Error

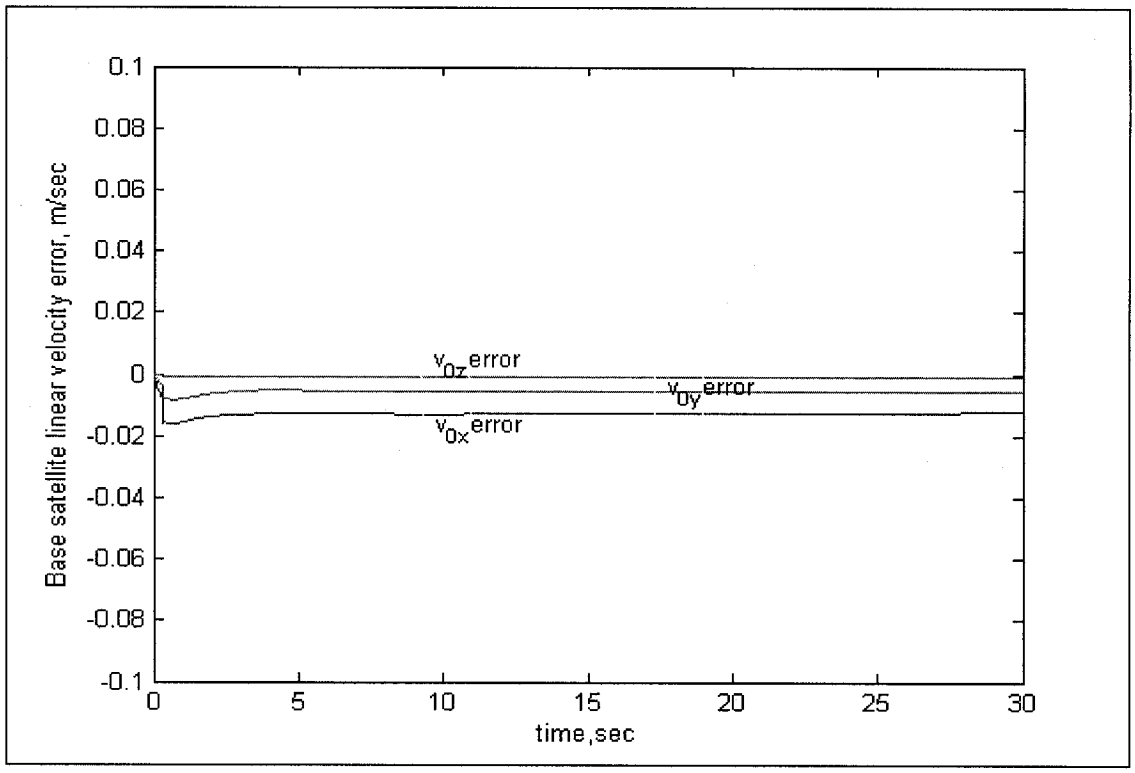

Figure 6.2: Base Satellite Linear Velocity Error

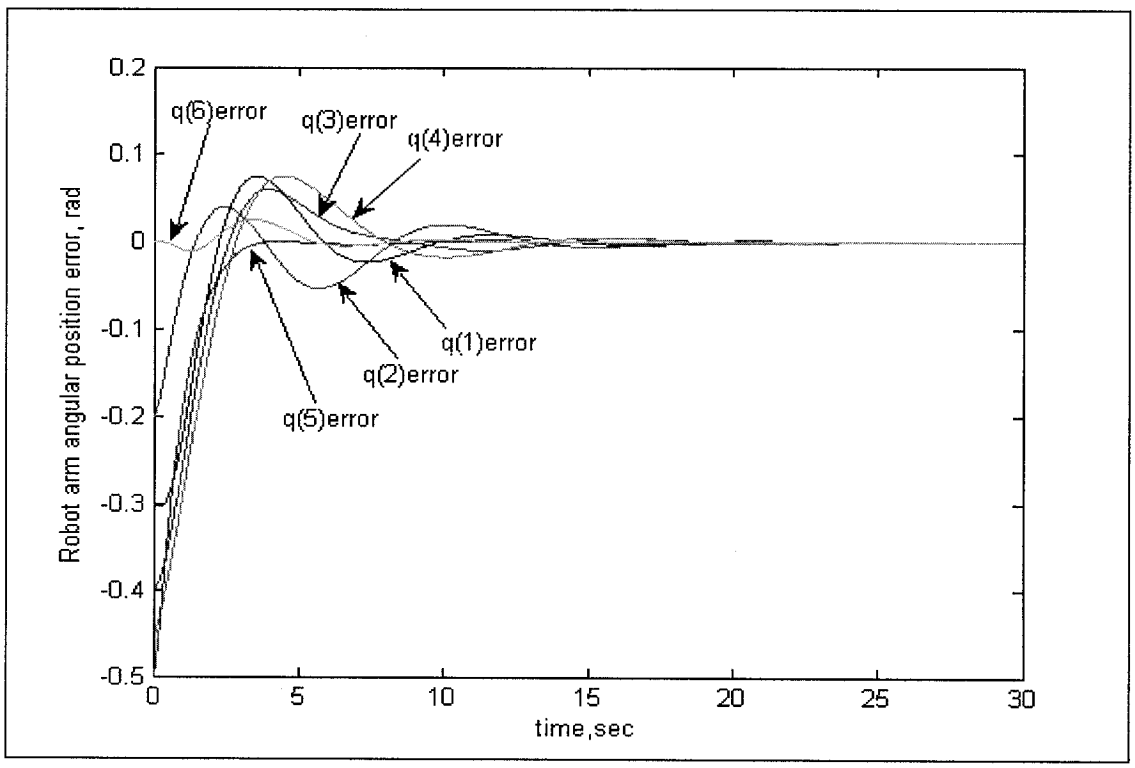

Figure 6.3: Space Robot Arm Angular Position Error

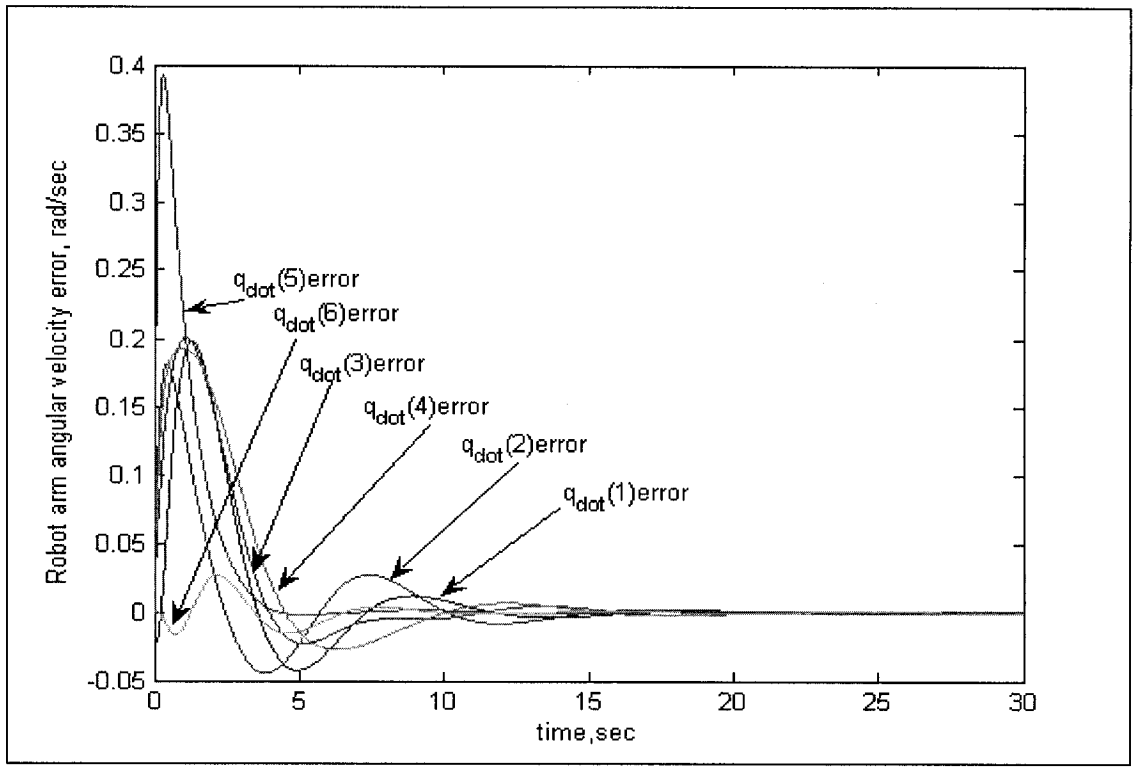

Figure 6.4: Space Robot Arm Angular Velocity Error

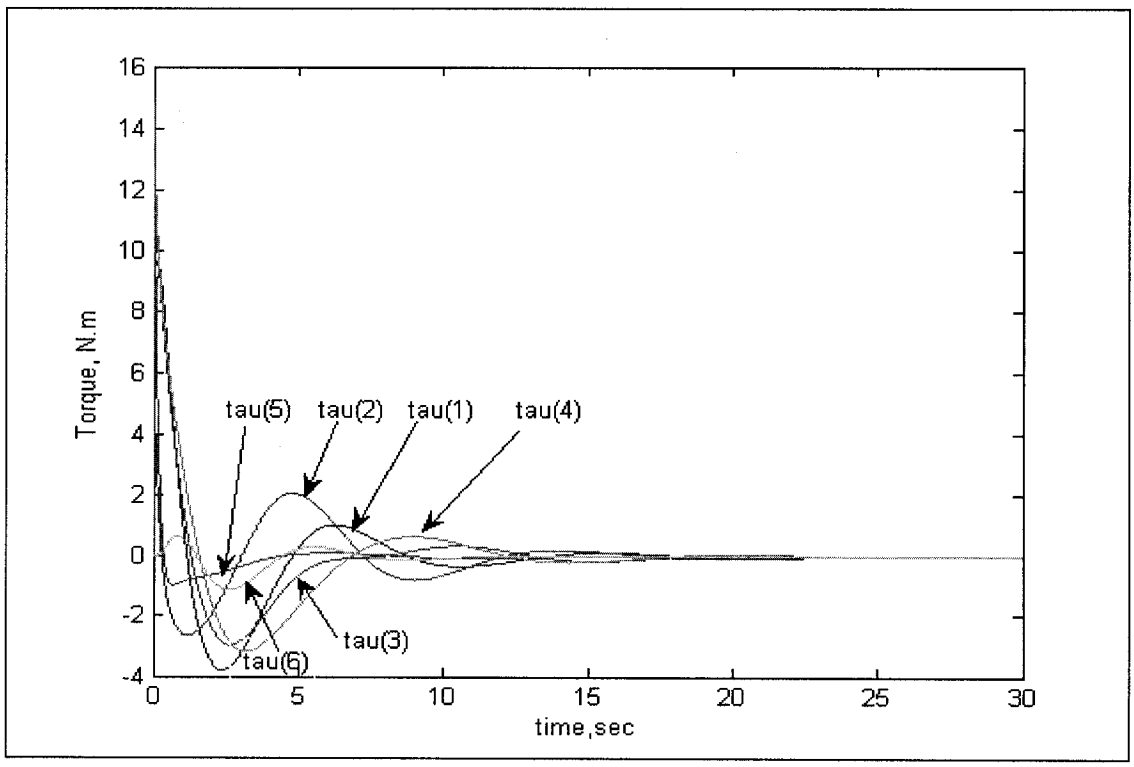

Figure 6.5: Space Robot Arm Actuation Torque

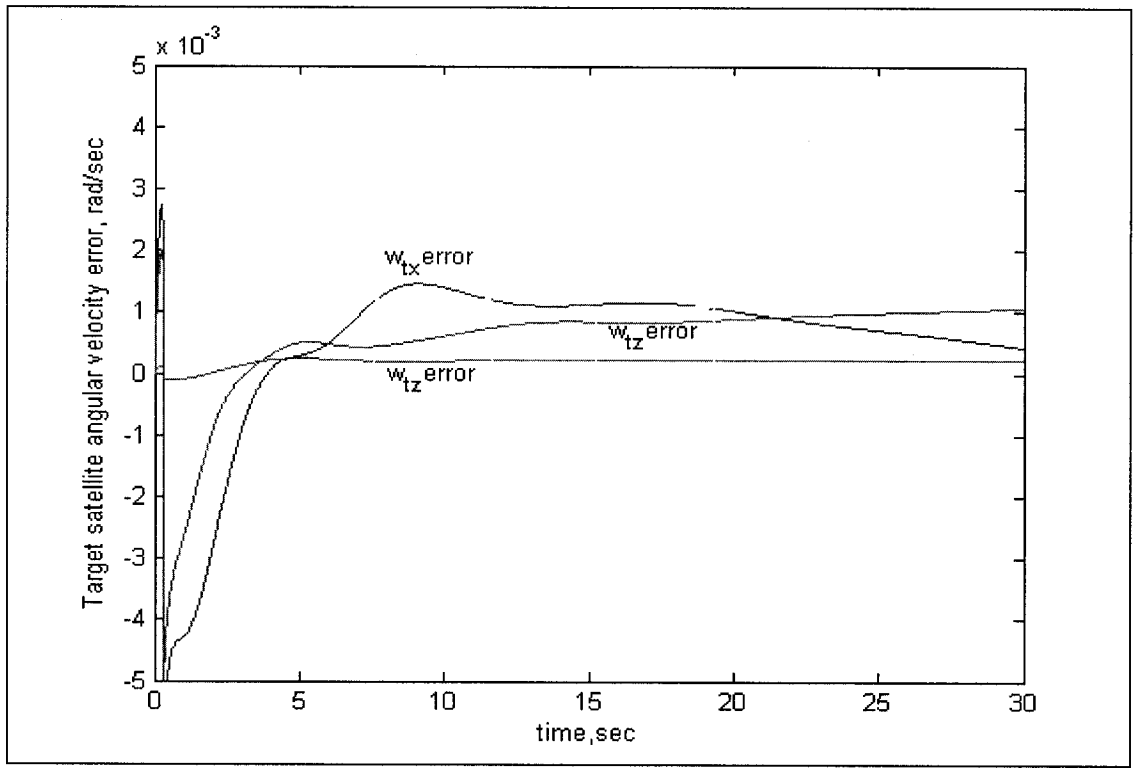

Figure 6.6: Target Satellite Angular Velocity Error

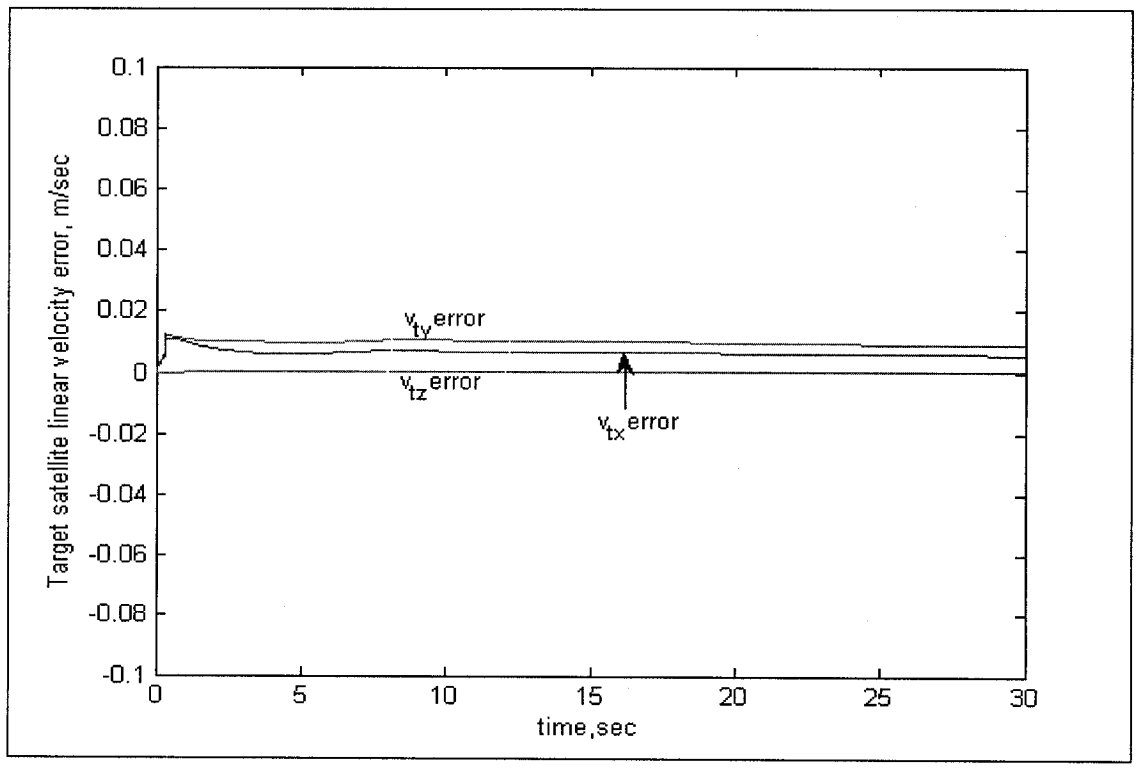

Figure 6.7: Target Satellite Linear Velocity Error

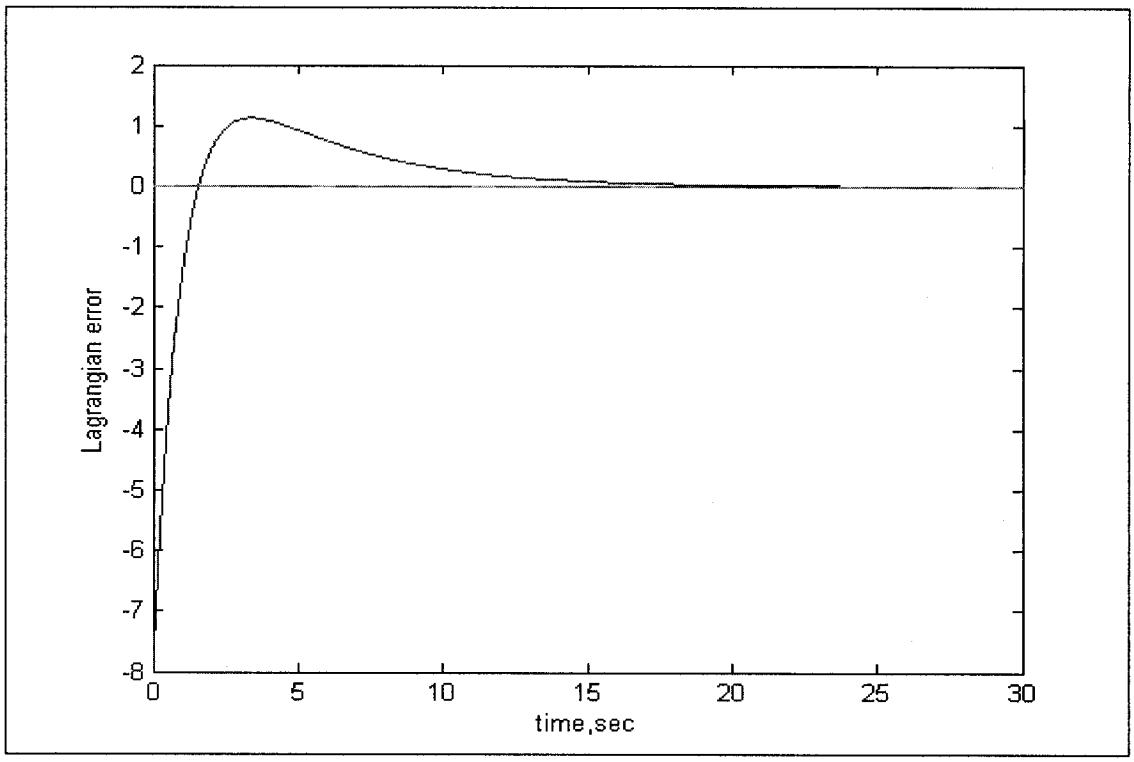

Figure 6.8: Lagrangian Error

The hybrid inverse-dynamics based controller proposed in this paper is capable of tracking the desired motion values and contact force specifications. The reduced-order dynamics obtained by using the orthogonal projector techniques does not suffer of passivity or under-actuation. This controller deals with all geometric constraints and momentum constraints.

The following chapter will focus on designing a controller using adaptive-inverse-dynamics control approach to solve the problem of system parameters uncertainty as well as controlling force/motion of a free-flying space robot interaction with a target satellite.

Chapter 7

Adaptive Inverse Dynamics Control of a Free-Flying Space Robot in Contact with a Target Satellite: a Hubble Space Telescope Case

7.1 Introduction

Robust motion tracking control of partially nonholonomic mechanical systems is investigated in [126]. Robust adaptive motion/force tracking control of uncertain nonholonomic mechanical systems is presented in [131]. Robust motion/force control of uncertain holonomic/nonholonomic mechanical systems is concerned in [132]. A robust impedance matching scheme for emulation of robots is proposed in [107]. In which control of emulating robot is investigated, by matching contact force frequency-rsponse of the emulating robot and that of the space robot. Adaptive impedance control of mechanical systems with classical nonholonomic constraints with unknown parameters is investigated in [113]. Adaptive force-motion control of coordinated robots interacting with geometrically unknown environments is proposed in [114]. The latter proposed adaptive hybrid force/motion controller guarantees asymptotic tracking of desired motion and force trajectories while ensuring exact identification of constraint Jacobian matrix without persistency of excitation condition. Adaptive inverse dynamics control of rigid robots is presented in [129].

An articulated-body model for a free-flying robot and its use for adaptive motion control with no external forces or moments is proposed in [98]. The inertia parameters for the robot end-effector and load are assumed to be *a priori* unknown. A novel feature of this approach is that the parameter estimates are obtained using momentum integrals only. In another study, truss assembly by space robot and task error recovery via reinforcement learning are investigated in [99]. In the latter, the experimental system consists of a space robot model, a frictionless table system, a computer system, and a vision sensor system. The robot model composed of two manipulators and a satellite vehicle can move freely on a two-dimensional planar table without friction by using air-bearings. The robot model has successfully performed the automatic truss structure construction including many jobs, e.g., manipulator berthing, component manipulation, arm trajectory control avoiding collision, assembly considering contact with the environment. Moreover, even if the robot fails in a task planned in advance, the robot accomplishes it by task re-planning through reinforcement learning. Adaptive and robust composite control of coordinated motion of space robot system with prismatic joint is studied in [106]. Digital adaptive control of space robot manipulators using transpose of generalized Jacobian matrix is the concern of study [108].

Adaptive control algorithms [37-42] which reviewed in chapter one, and studies [98-99][108] ignored the presence of external forces acting on a space robot. They also have not accounted for constraints acting on the space robotic system (by linear momentum, angular momentum, and contact constraints) all together simultaneously. For this reason,

this chapter is devoted to treat the uncertainty of the combined system as a whole along with all holonomic and nonholonmic constraints.

This chapter is organized as follows: in the next section 7.2 an adaptive inverse dynamics control law is proposed to meet the specifications of motion desired values, to track the contact forces and to adapt with parameters changes, then in section 7.3 an introduction to Hubble Space Telescope is given, and finally a simulation of the proposed adaptive algorithm is dedicated to Hubble space Telescope to verify the analytical results.

7.2 Adaptive Inverse Dynamics Control

Similar to the analysis followed in the previous chapter and as in (6.1)-(6.5)

$$HS\dot{\nu} + \left(H\dot{S} + CS\right)\nu = \bar{\tau} + J^T\lambda \tag{7.1}$$

Now we assume that there are some uncertainties in the system parameters such as masses and inertias and for this reason an adaptive control approach will be investigated. The dynamics (7.1) can be represented by benefiting from the property of linearity in parameters as

$$H_1\dot{\nu} + C_1\nu = \mathrm{Y}\alpha \tag{7.2}$$

where $H_1 = HS$, $C_1 = \left(H\dot{S} + CS\right)$, Y is an $N \times (N-m)$ matrix of known functions and known as the regressor, and α is an $(N-m)$-dimensional vector of the system parameters. After examining the structure of dynamics (7.2), three properties are obtained (For more details see [75-80][109-112]):

Property 1: The modified inertia matrix $H_2 = S(\theta)^T H(\theta) S(\theta)$ is symmetric positive definite. *Property 2*: If Property 1 is verified, then $\left(H_2 - 2\dot{C}_2\right)$ is skew-symmetric matrix where $C_2 = S^T C_1$. *Property 3*: The dynamics (7.2) is linear in its parameters.

The nonlinear control law is proposed to have the form

$$\bar{\tau} = \hat{H}_1(\ddot{v}_d + K_D\dot{e} + K_P e) + \hat{C}_1\dot{v} - J^T\lambda_c \tag{7.3}$$

where e, v, and v_d are as defined in the previous chapter, $\lambda_c = \lambda_d - K_F e_F$ and K_F is a positive definite diagonal matrix for the force control feedback gain, $e_F = \lambda - \lambda_d$, and $\hat{H}_1$ and $\hat{C}_1$ are the estimates of H_1 and C_1, respectively. Note that the geometric of the Jacobian in (7.3) is assumed to be determined. Using the estimates $\hat{H}_1$ and $\hat{C}_1$ in the dynamics (7.2), one can obtain

$$\hat{H}_1\ddot{v} + \hat{C}_1\dot{v} = Y\hat{\alpha} \tag{7.4}$$

where $\hat{\alpha}$ is the estimated vector of parameters α.

Upon substituting (7.3) into (7.1), and by adding and subtracting at the same time the term $\hat{H}_1\ddot{v}$ on the left hand side of (7.2) we get

$$\hat{H}_1\ddot{v} - \hat{H}_1\ddot{v} + H_1\ddot{v} + C_1\dot{v} = \hat{H}_1(\ddot{v}_d + K_D\dot{e} + K_P e) + \hat{C}_1\dot{v} - J^T(1 + K_F)e_F \tag{7.5}$$

Canceling out the similar terms in (7.5), yields

$$H_1\ddot{v} - \hat{H}_1\ddot{v} + C_1\dot{v} - \hat{C}_1\dot{v} = \hat{H}_1(\ddot{v}_d - \ddot{v} + K_D\dot{e}_P + K_P e_P) - J^T(1 + K_F)e_F \tag{7.6}$$

or,

$$\tilde{H}_1\ddot{v} + \tilde{C}_1\dot{v} = \hat{H}_1(\ddot{e}_P + K_D\dot{e}_P + K_P e_P) - J^T(1 + K_F)e_F \tag{7.7}$$

where $\ddot{e}_P = \ddot{v}_d - \ddot{v}$, $(\tilde{\cdot}) = (\cdot) - (\hat{\cdot})$, by multiplying (7.7) by S^T, and by using Equations (7.2) and (7.4), then the closed loop dynamics error (7.7) becomes

$$(\ddot{e}_P + K_D \dot{e}_P + K_P e_P) = Y_1 \tilde{\alpha} \tag{7.8}$$

where $\left(S^T \hat{H}_1\right)^{-1} Y = Y_1$.

It is possible now to express the error dynamics (7.8) in a state space form as

$$\dot{x} = Ax + B\tilde{\alpha} \tag{7.9}$$

$$\text{where } x = \begin{bmatrix} e_p \\ \dot{e}_p \end{bmatrix},\ A = \begin{bmatrix} O & I \\ -K_P & -K_D \end{bmatrix},\ B = \begin{bmatrix} O \\ Y_1 \end{bmatrix} \tag{7.10}$$

where A is a Hurwitz matrix, that is, the real parts of its eigenvalues are negative, which guarantees globally exponentially stability. Based on the state space formulation and Lyapunov techniques an adaptive control law can be chosen as

$$\dot{\tilde{\alpha}} = -\Gamma^{-1} Y_1^T B^T P x \tag{7.11}$$

where $\Gamma > 0$ and symmetric , and P is a unique positive definite solution to the Lyapunov equation $A^T P + PA = -Q$, where Q is a positive definite symmetric.

Let the Lyaponuv candidate function chosen as

$$V = x^T P x + \tilde{\alpha}^T \Gamma \tilde{\alpha} \tag{7.12}$$

Now if we take the time derivative of V along the trajectories of (7.9) and by using the adaptation law (7.11), one gets

$$\begin{aligned} \dot{V} &= \dot{x}^T P x + x^T P \dot{x} + \dot{\tilde{\alpha}}^T \Gamma \tilde{\alpha} + \tilde{\alpha}^T \Gamma \dot{\tilde{\alpha}} \\ &= \left(Ax + BY_1\tilde{\alpha}\right)^T P x + x^T P\left(Ax + BY_1\tilde{\alpha}\right) - \left(\Gamma^{-1} Y_1^T B^T P x\right)^T \Gamma \tilde{\alpha} - \tilde{\alpha}^T \Gamma\ \Gamma^{-1} Y_1^T B^T P x \\ &= x^T A^T P x + \tilde{\alpha}^T Y_1^T B^T P x + x^T P A x + x^T P B Y_1 \tilde{\alpha} - x^T P^T B Y_1\ \Gamma^{-T} \Gamma \tilde{\alpha} - \tilde{\alpha}^T \Gamma\ \Gamma^{-1} Y_1^T B^T P x \\ &= x^T \left(A^T P + PA\right) x + \tilde{\alpha}^T Y_1^T B^T P x + x^T P^T B Y_1 \tilde{\alpha} - x^T P^T B Y_1 \tilde{\alpha} - \tilde{\alpha}^T Y_1^T B^T P x \end{aligned} \tag{7.13}$$

By canceling out equivalent terms, this reduces to

$$\dot{V} = -x^T Q x \leq 0 \tag{7.14}$$

Since $\dot{V}$ is negative semidefinite with regard to x and the parameter error, and V is lower bounded by zero, V remains bounded in the time interval $[0,\infty)$. This fact can be stated as

$$\int_0^\infty -\dot{V}dt < \infty \tag{7.15}$$

Now if we assume that $\dot{x}$ is bounded then from (7.12) $\ddot{V}$ is bonded. If $\ddot{V}$ is bounded then $\dot{V}$ is uniformly continuous. If $\dot{V}$ is uniformly continous and has a finite intrgral as given in (7.13) then by Barbalat's lemma $\dot{V} \to 0$ as $t \to \infty$ which implies $x \to 0$ as $t \to \infty$.

Based on Equation (7.7), implies

$$J^T(1+K_F)e_F = -Y\tilde{\alpha} = \sigma \tag{7.16}$$

where σ is a bounded function. Thus

$$J^T e_F = (K_F + I)^{-1}\sigma \tag{7.17}$$

and the force tracking error $(F - F_d)$ is bounded and can be adjusted by changing the feedback gain K_F, where F is defined as $F = J^T\lambda$ and F_d is its desired value defined as $F = J^T\lambda_d$. Thus, the previous adaptive algorithm can be concluded in the following theorem:

Theorem 7.1: For the dynamic system given in (6.1) and subjected to constraints (6.2), the adaptive control law defined by (7.3) and (7.11) is globally stable and guarantees zero position tracking and bounded force tracking errors.

7.3 Hubble Space Telescope Case Study

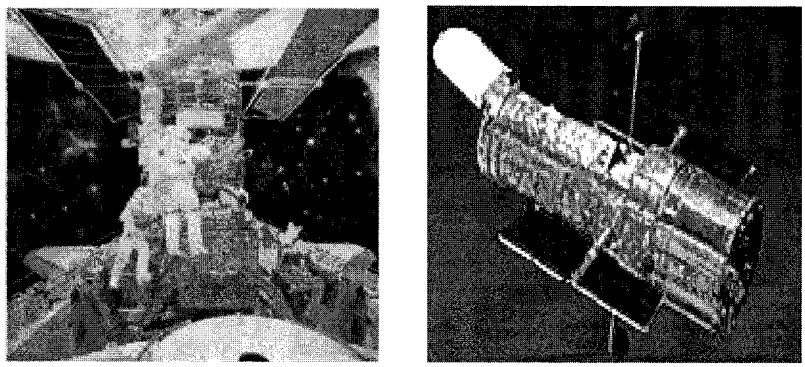

Figure 7.1: Hubble Space Telescope Servicing Mission 3A (NASA [141])

Humankind has sought to expand its knowledge of the universe by studying the stars. Throughout history, great scientists such as Nicholaus Copernicus, Galileo Galilei, Johannes Kepler, Issac Newton, Edwin Hubble, and Albert Einstein have each contributed significantly to our understanding of the universe. The launch of the Hubble Space Telescope in 1990 signified another great step toward unraveling the mysteries of space. Spectacular discoveries such as massive black holes at the center of galaxies, the common existence of precursor planetary systems like our own, and the quantity and distribution of cold dark matter, are just a few examples of the Telescope's findings. Now, with NASA's Servicing Mission 3A, we are equipped to carry the quest for knowledge into the 21st century [141].

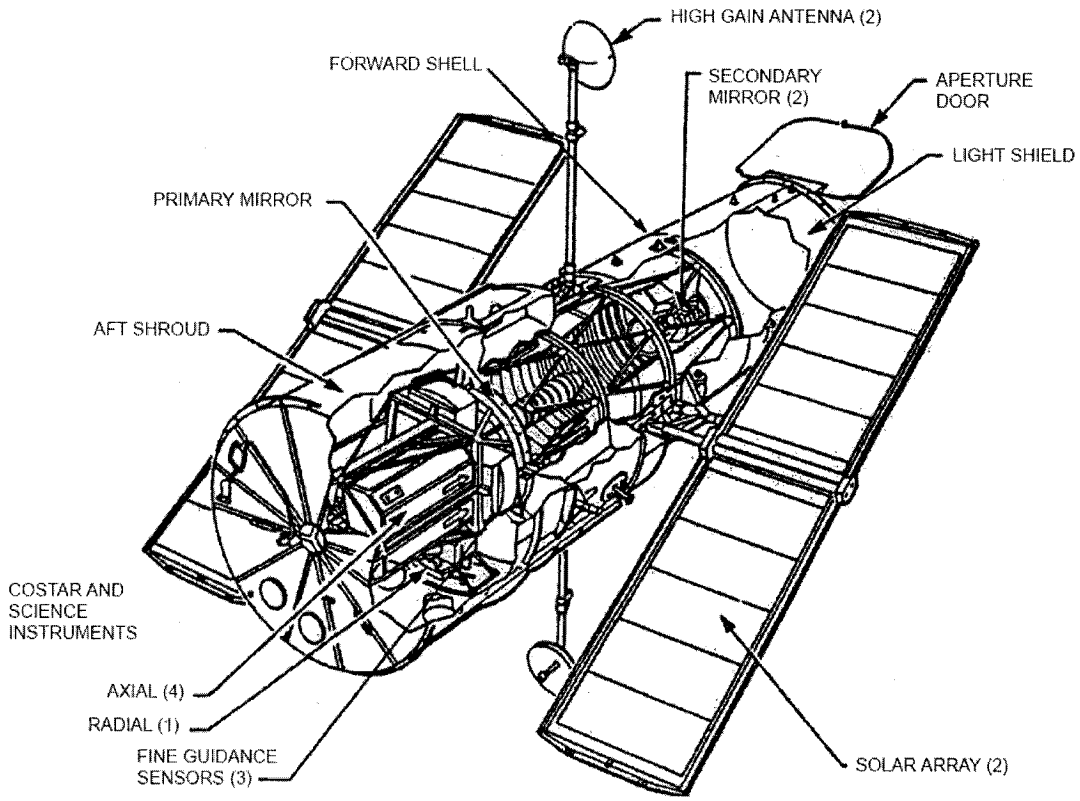

Figure 7.2: Hubble Space Telescope Overall Configuration (NASA [141])

Figures 7.2 shows the overall Telescope configuration. Table 7.1 lists specifications for the Telescope. The major elements are:

1) Optical Telescope Assembly (OTA) – two mirrors and associated structures that collect light from celestial objects.

2) Science instruments – devices used to analyze the images produced by the OTA.

3) Support Systems Module (SSM) – spacecraft structure that encloses the OTA and science instruments.

4) Solar Arrays (SA).

Table 7.1: Hubble Space Telescope Specifications (NASA [141])

Weight	24,500 lb (11,110 kg)
Length	43.5 ft (15.9 m)
	10 ft (3.1 m) Light Shield and Forward Shell
	14 ft (4.2 m) Equipment Section and Aft Shroud
Diameter	Ritchey-Chretien design Cassegrain telescope
Optical system	189 ft (56.7 m) folded to 21 ft (6.3 m)
Focal length	94.5 in. (2.4 m) in diameter
Primary mirror	12.2 in. (0.3 m) in diameter
Secondary mirror	See instruments/sensors
Field of view	0.007 arcsec for 24 hours
Pointing accuracy	5 mv to 29 mv (visual magnitude)
Magnitude range	1100 to 11,000 Å
Wavelength range	0.1 arcsec at 6328 Å
Angular resolution	320 nmi (593 km), inclined 28.5 degrees from equator
Orbit	97 minutes per orbit
Orbit time	20 years
Mission	

Component Degradation: Servicing plans take into account the need for routine replacement of some items, for example, restoring HST system redundancy and limited-life items such as tape recorders and gyroscopes.

Equipment Failure: Given the enormous scientific potential of the Telescope – and the investment in designing, developing, building, and putting it into orbit – NASA must be able to correct unforeseen problems that arise from random equipment failures or malfunctions. The Space Shuttle program provides a proven system for transporting astronauts to the Telescope fully trained for its on-orbit servicing. Originally, planners considered using the Shuttle to return the Telescope to Earth approximately every five years for maintenance. However, the idea was rejected for both technical and economic reasons. Returning Hubble to Earth would entail a significantly higher risk of

contaminating or damaging delicate components. Ground servicing would require an expensive clean room and support facilities, including a large engineering staff, and the Telescope would be out of action for a year or more – a long time to suspend scientific observations. Shuttle astronauts can accomplish most maintenance and refurbishment within a 10-day on-orbit mission – with only a brief interruption to scientific operations and without the additional facilities and staff needed for ground servicing.

Orbital Replacement Units: Advantages of ORUs include modularity, standardization, and accessibility.

Modularity: Engineers studied various technical and human factors criteria to simplify Telescope maintenance. Due to the limited time available for repairs and the astronauts' limited visibility, mobility, and dexterity in the EVA environment, designers simplified the maintenance tasks by planning entire components for replacement. The modular ORU concept is key to successfully servicing the Telescope on orbit. ORUs are self-contained boxes installed and removed using fasteners and connectors. They range from small fuses to phone-booth-sized science instruments weighing more than 700 lb (318 kg). Figure 7.3 shows the ORUs for SM3A.

Standardization: Standardized bolts and connectors also simplify on-orbit repairs. Captive bolts with 7/16-in., double-height hex heads hold many ORU components in place. To remove or install the bolts, astronauts need only a 7/16-in. socket fitted to a power tool or manual wrench. Standardization limits the number of crew aids and tools.

Some ORUs do not contain these fasteners. When the maintenance philosophy changed from Earth-return to on-orbit-only servicing, other components were selected as replaceable units after their design had matured. This added a greater variety of fasteners to the servicing requirements, including non-captive 5/16-in.-head bolts and connectors without wing tabs. Despite these exceptions, the high level of standardization among units reduces the number of tools needed for the servicing mission and simplifies astronaut training.

Accessibility: To be serviced in space, Telescope components must be seen and reached by an astronaut in a bulky pressure suit, or they must be within range of the appropriate tool. Therefore, most ORUs are mounted in equipment bays around the perimeter of the spacecraft. To access these units, astronauts simply open a large door that covers the appropriate bay. Handrails, foot restraint sockets, tether attachments, and other crew aids are essential to efficient, safe on-orbit servicing. In anticipation of servicing missions, 31 foot restraint sockets and 225 ft of handrails were designed into the Telescope. The foot restraint sockets and handrails greatly increase the mobility and stability of EVA astronauts, giving them safe worksites conveniently located near ORUs. Crew aids such as portable lights, special tools, installation guiderails, handholds, and portable foot restraints (PFR) also ease servicing of the telescope components. In addition, foot restraints, translation aids and handrails are built into various equipment and instrument carriers specific to each servicing mission.

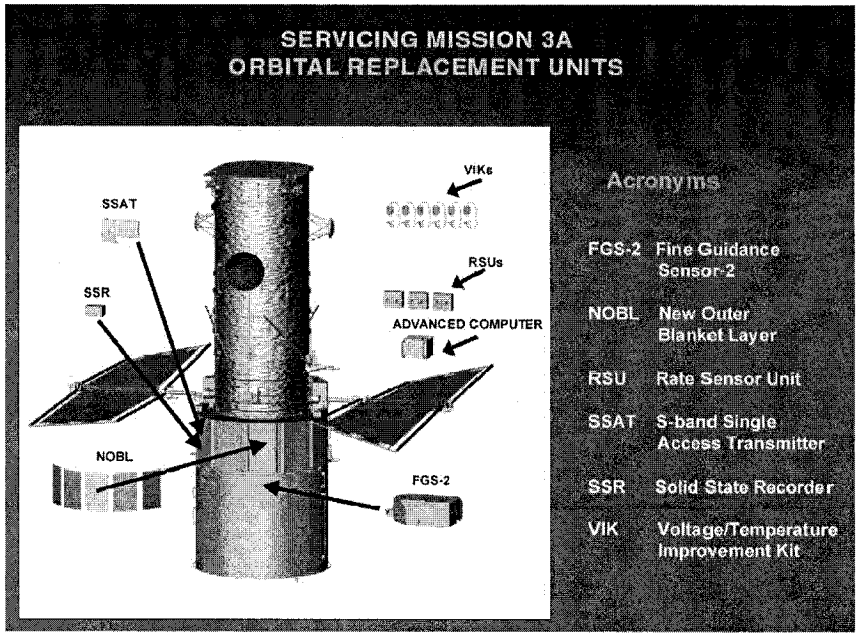

Figure 7.3: Hubble Space Telescope Servicing Mission 3A Orbital Replacement Units (NASA [141])

Shuttle Support Equipment: To assist the astronauts in servicing the Telescope, *Discovery* will carry into orbit several thousand pounds of hardware and Space Support Equipment (SSE), including the Remote Manipulator System (RMS), FSS, and ORU Carrier (ORUC).

Remote Manipulator System: The *Discovery* RMS, also known as the robotic arm, will be used extensively during SM3A. The astronaut operating this device from inside the cabin is designated intravehicular activity (IVA) crew member. The RMS will be used to:

- Capture, berth, and release the Telescope
- Transport new components, instruments, and EVA astronauts between worksites
- Provide a temporary work platform for one or both EVA astronauts.

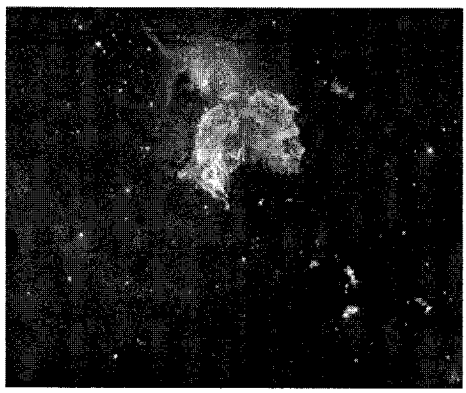

(a) Supernova Remnant N 63A Menagerie

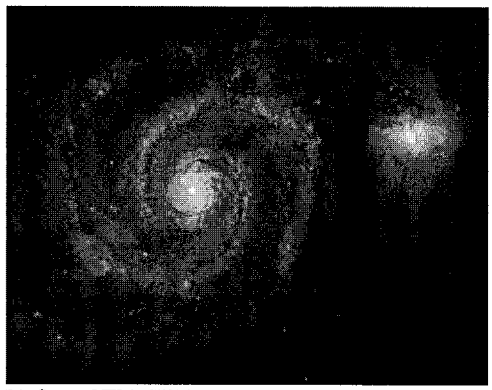

(b) Out of This Whirl: the Whirlpool Galaxy (M51) and Companion Galaxy

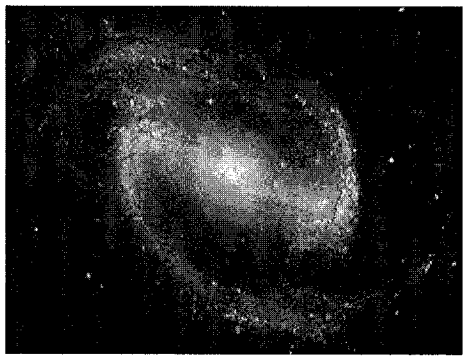

(c) Barred Spiral Galaxy NGC 1300

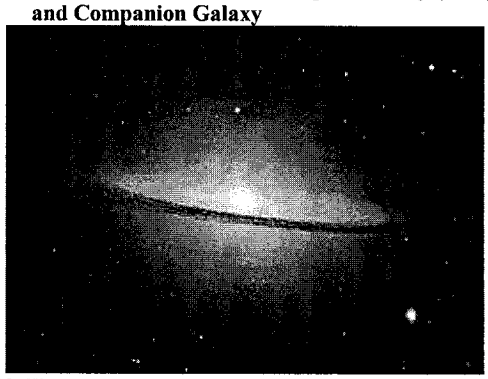

(d) Hubble Mosaic of the Majestic Sombrero Galaxy

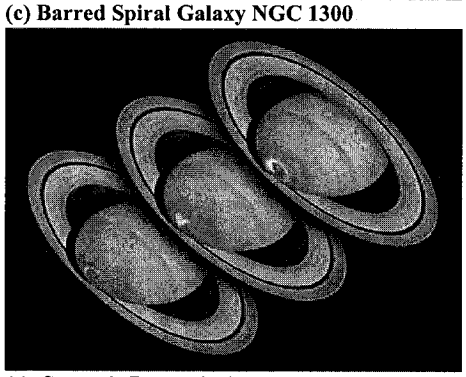

(e) Saturn's Dynamic Auroras

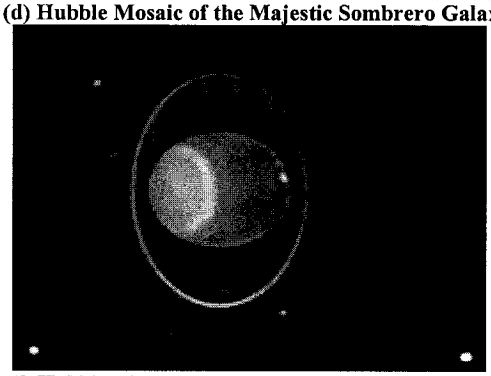

(f) Hubble Finds Many Bright Clouds on Uranus

(g) Space Phenomenon Imitates Art in Universe's Monocerotis Version of van Gogh Painting

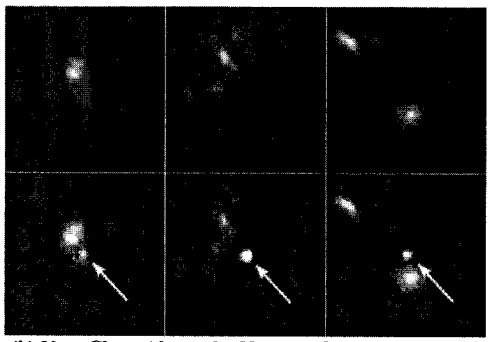

(k) New Clues About the Nature of Dark Energy: Einstein May Have Been Right After All

Figure 7.4: Some Astonishing Observation of Hubble Space Telescope for our Solar System and the Universe (NASA [141])

7.4 Simulation Results

The purpose of the simulation in the present section to verify the effectiveness of the adaptive controller (7.3) and the adaptation law (7.3) to control the entire system under consideration and described by the dynamics (6.1) subjected to the constraints (6.2). For simulation we assume that the end-effecter of the servicing space robot manipulator has established a contact with the Hubble Telescope.

The robot arm is composed of 6-DOF and mounted on base satellite is used to demonstrate the analytical results. The Hubble Telescope satellite is assumed to be totally floating and unactuated due to the thrusters' shutdown for maintenance. All six space robot links are assumed to be revolute. The first link is mounted on the base satellite by a revolute joint. The mass of the base satellite is assumed 3000 kg. The mass of the target is assumed 11000 kg, The masses of the robot link are assumed $[100 \quad 100 \quad 50 \quad 50 \quad 10 \quad 10]^T$. The length of each link is assumed as 1m.

The inertia matrix of the base satellite is considered as $[10 \quad 10 \quad 10 \quad 10 \quad 10 \quad 10]^T$

$$\begin{bmatrix} 1000 & 0 & 0 \\ 0 & 500 & 0 \\ 0 & 0 & 300 \end{bmatrix}$$

The inertia matrix of the target satellite is considered as

$$\begin{bmatrix} 3000 & 0 & 0 \\ 0 & 1000 & 0 \\ 0 & 0 & 1000 \end{bmatrix}$$

The inertia of first two links of the space robot arm assumed as

$$\begin{bmatrix} 30 & 0 & 0 \\ 0 & 30 & 0 \\ 0 & 0 & 30 \end{bmatrix}$$

The inertia of the third and the fourth links of the space robot arm considered as

$$\begin{bmatrix} 15 & 0 & 0 \\ 0 & 15 & 0 \\ 0 & 0 & 15 \end{bmatrix}$$

The inertia of the fifth and sixth of the space robot arm assumed as

$$\begin{bmatrix} 10 & 0 & 0 \\ 0 & 10 & 0 \\ 0 & 0 & 10 \end{bmatrix}$$

All initial values for the position and angular velocity and acceleration of the robot joints is assumed to be zero. All initial values for the orientation, angular velocity and angular acceleration of the base satellite are assumed to be zero. All initial values for the orientation, angular velocity and angular acceleration of the target satellite are also assumed to be zero. The desired values for the robot angular position are chosen as $[0.3 \quad 0.2 \quad 0.4 \quad 0.45 \quad 0.5 \quad 0.0]^T$. The desired values of the base satellite Euler angles are assumed zero. The initial relative linear velocities of both the base and the target are assumed to be zero m/sec to keep a constant linear relative velocity while conducting the task and to avoid any damage. All other initial conditions are assumed to be zero. The contact forces are assumed to be linear and only in the y-direction and with desired value as $\lambda_{des} = 100$. The motion and force gain diagonal matrices K_P, K_D, K_F are chosen as $K_P = diag(20,20,50,50,50,50,50,50,30,30)$, $K_D = diag(20,20,50,50,50,50,50,50,40,40)$, $K_F = diag(80,80,80,80,80,80)$.

Please see Appendix K for more details on the regressor Y and the parameter vector α .

Table 7.2: Simulated Combined system parameters

Link i	Mass (kg)	I_{xx} (kg.m2)	I_{yy} (kg.m2)	I_{zz} (kg.m2)
Base Satellite	3000	1000	1000	1000
Target Satellite	11000	3000	3000	3000
Link 1	100	30	30	30
Link 2	100	30	30	30
Link 3	50	15	15	15
Link 4	50	15	15	15
Link 5	20	7	7	7
Link 6	10	3	3	3

We assumed that the space robot end-effector move on the surface of a Hubble telescope in the z-direction as shown in Figure 7.5. The constraints on the end-effector can be described by the hypersurfaces S_1

$$S_1 : F(x, y, z) = x^2 + y^2 - a^2 = 0, -h \le z \le h$$

Then $\frac{\partial \Phi(\chi)}{\partial \chi} = [2x \quad 2y \quad 0 \quad 0 \quad 0 \quad 0]$

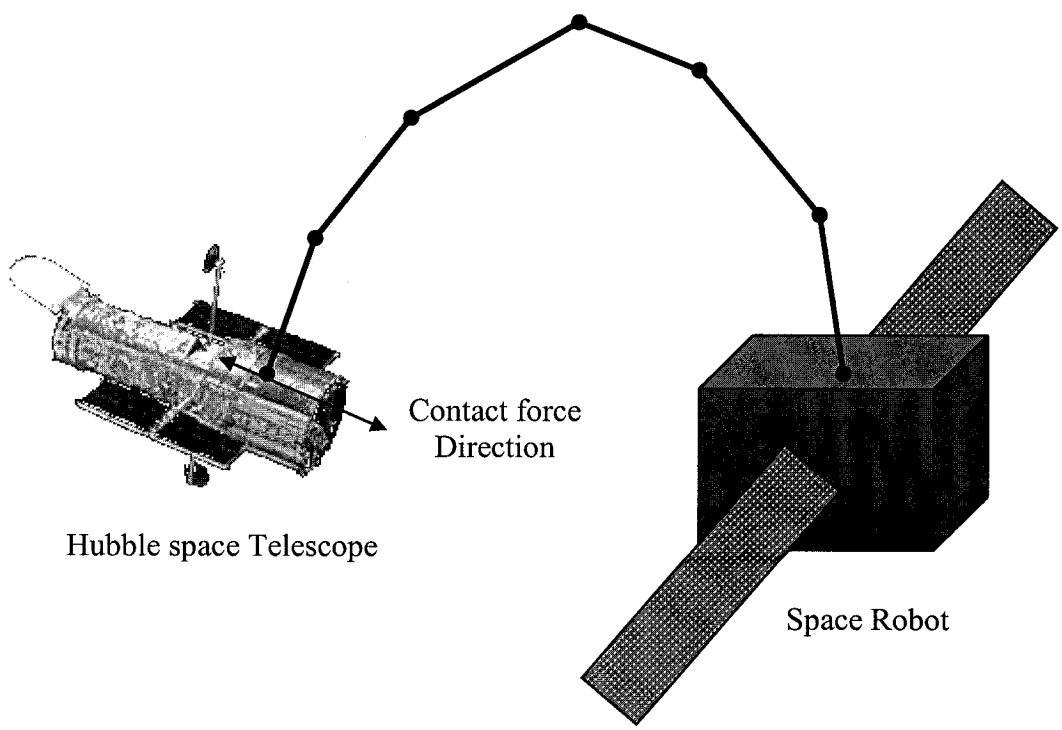

Figure 7.5: A Free-Flying Space Robot Conducting a Maintenance Task on the Surface of the Hubble Space Telescope

The simulation is used to verify that the proposed adaptive inverse-dynamics controller (7.3) and (7.11) can track the desired motion and the specified contact forces and, moreover, overcome the uncertainty in the system parameters.

The simulation results are shown in Figures 7.6-7.13. Figures 7.6 and 7.7 show, respectively, a fast response for both linear and angular velocities of the servicing base satellite. Figure 7.8 and 7.9 show, respectively, that robot arm angular position and velocities converge to their desired values. The controller is able to bring the links to the steady state position at around 40 sec. Figure 7.10 shows the joints actuators response which approaches zero after 40 sec. In Figure 7.11 and 7.12, the linear and angular velocities error response of the Hubble Telescope present a noticeable and fast response after 40 sec.. Finally, Figure 7.13 shows the Lagrangian multiplier error converges close to zero at time 40 sec. The simulation results show that the adaptive inverse-dynamics controller is effective to meet the specifications.

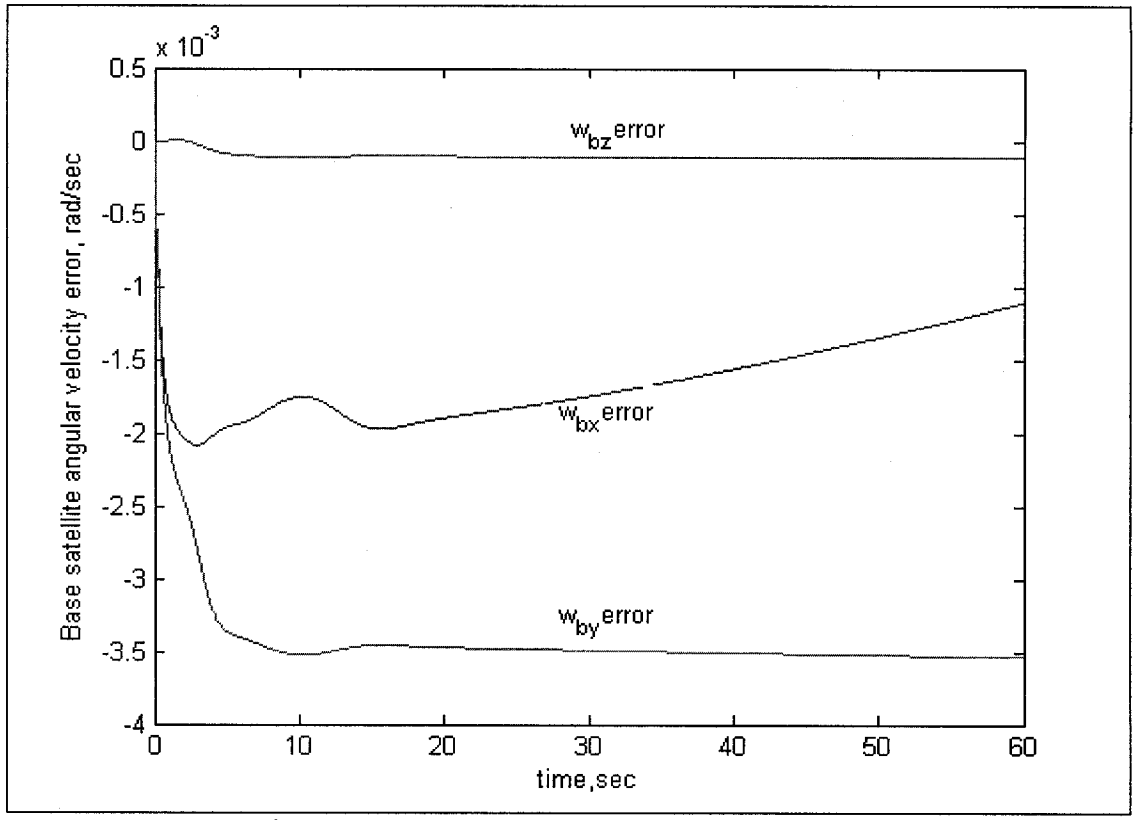

Figure 7.6: Base Satellite Angular Velocity Error

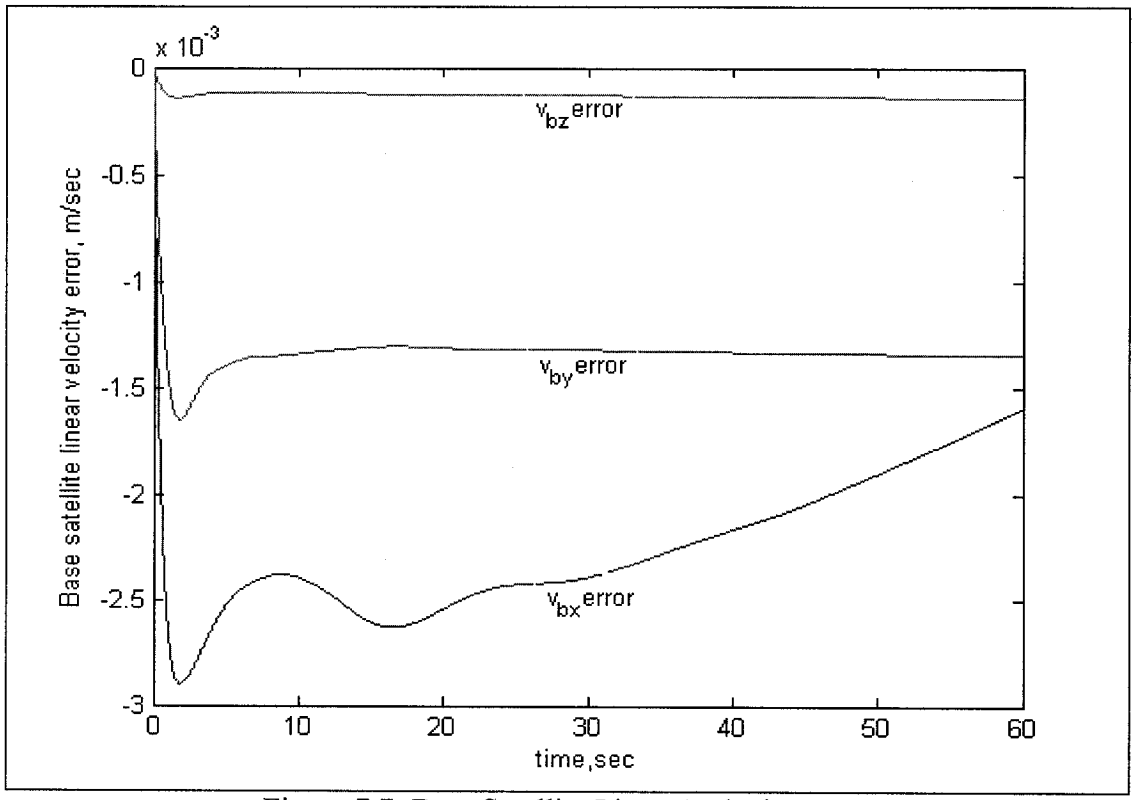

Figure 7.7: Base Satellite Linear Velocity Error

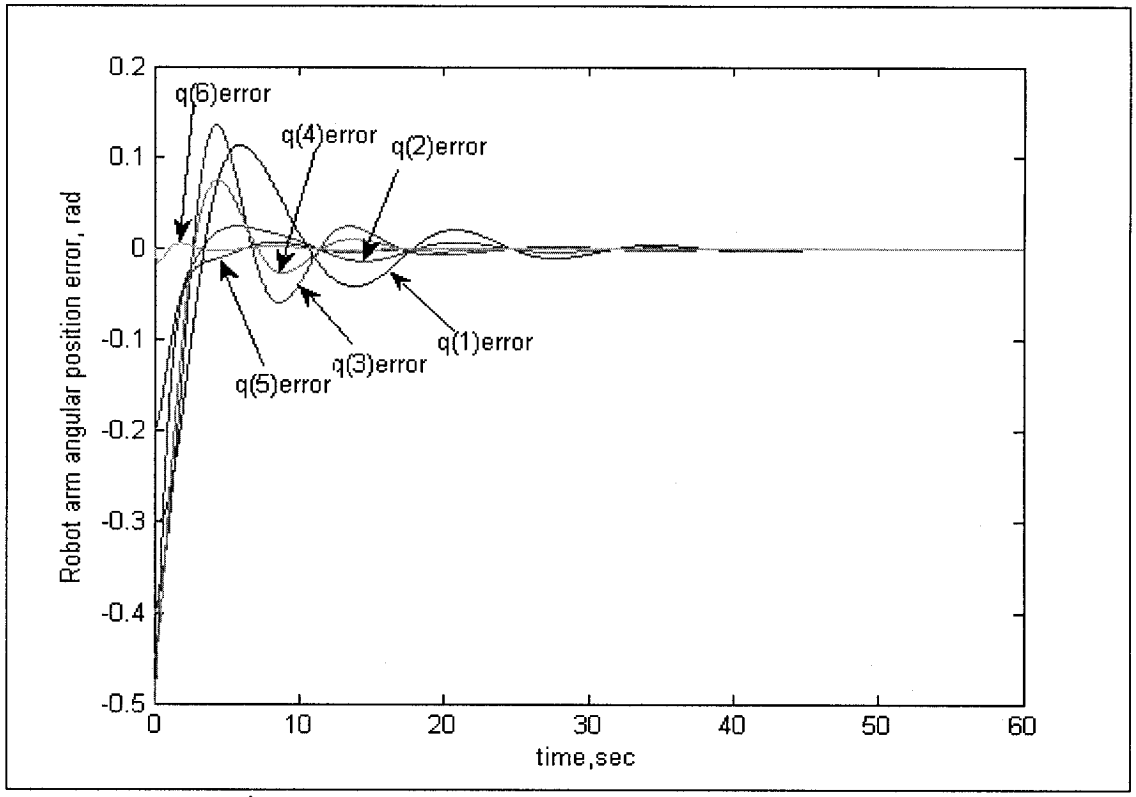

Figure 7.8: Space Robot Arm Angular Position Error

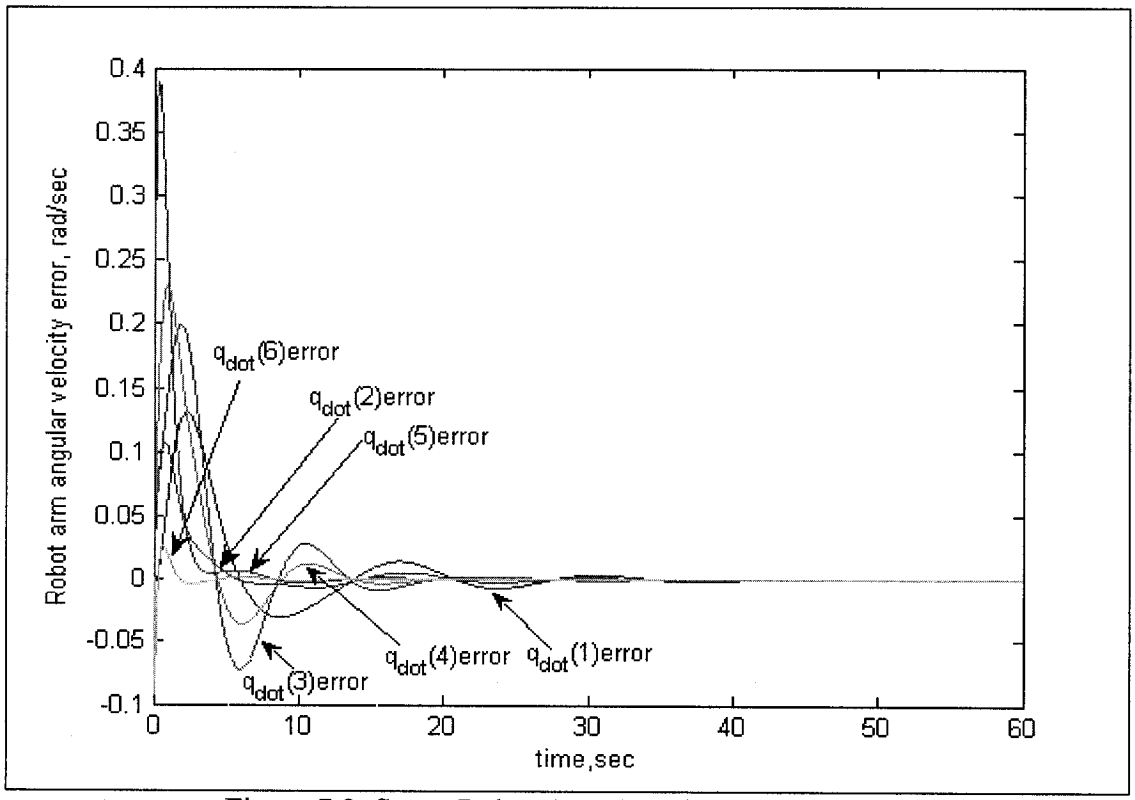

Figure 7.9: Space Robot Arm Angular Velocity Error

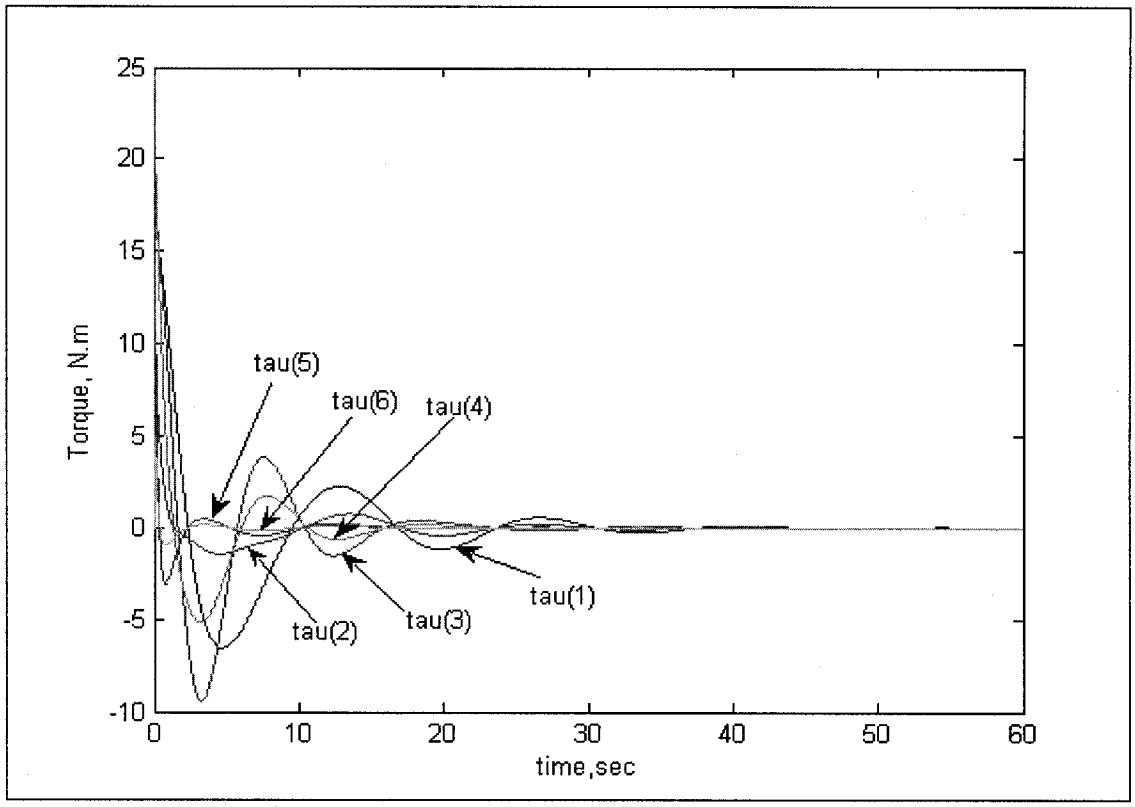

Figure 7.10: Space Robot Arm Actuation Torque

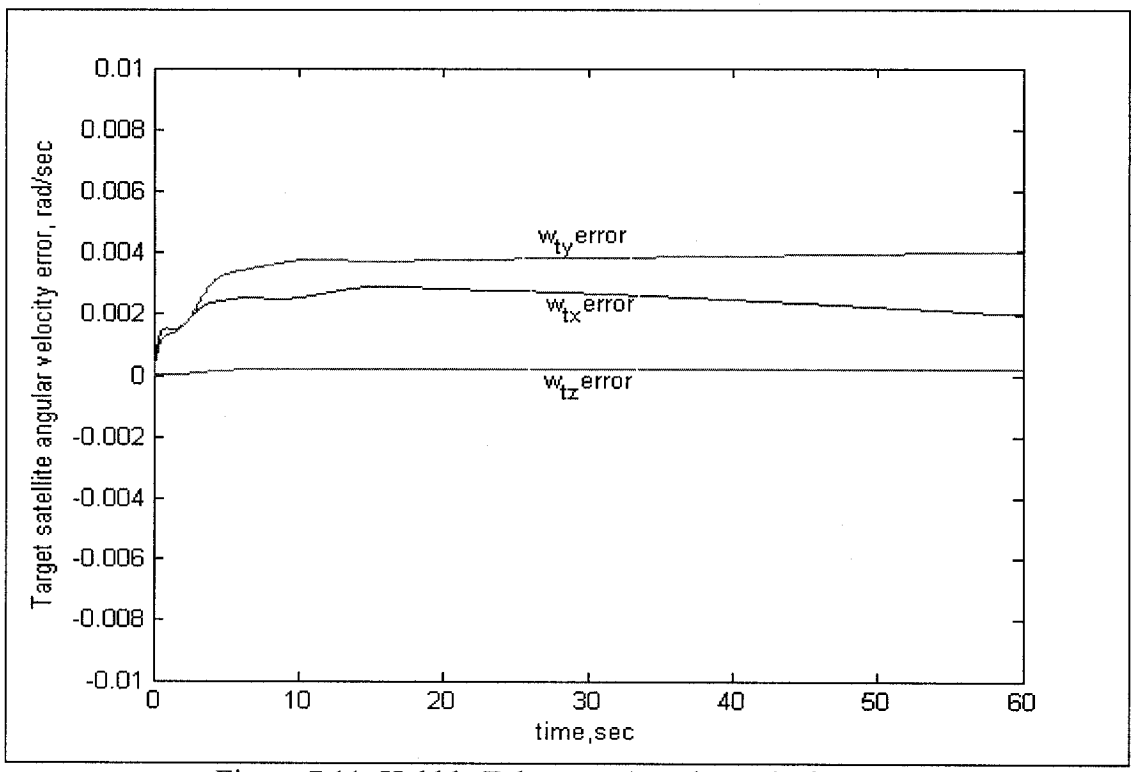

Figure 7.11: Hubble Telescope Angular Velocity Error

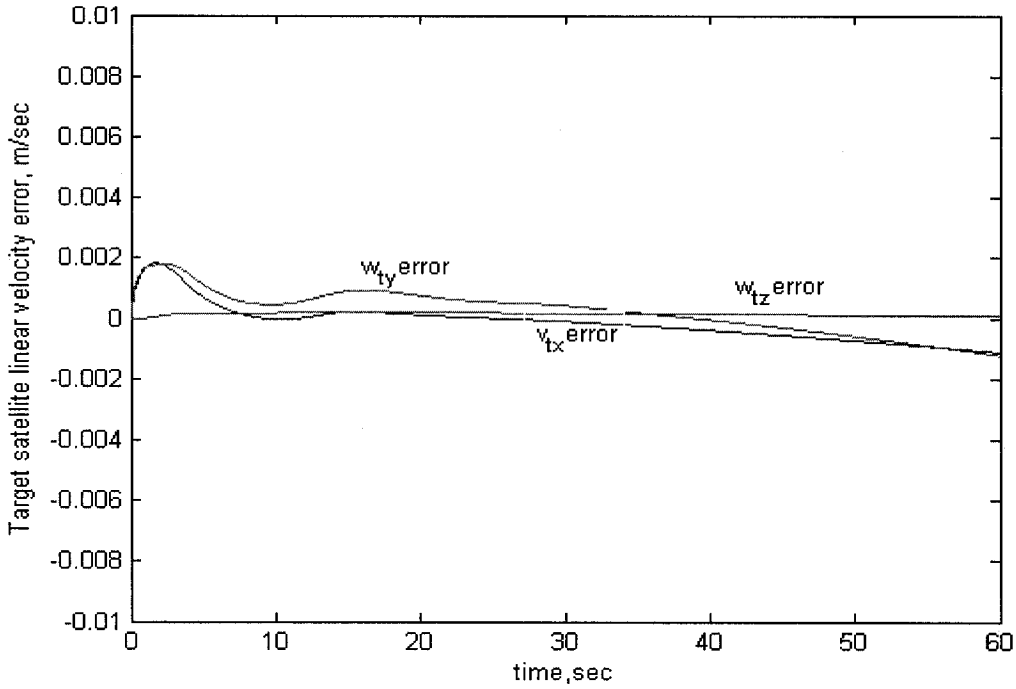

Figure 7.12: Hubble Telescope Linear Velocity Error

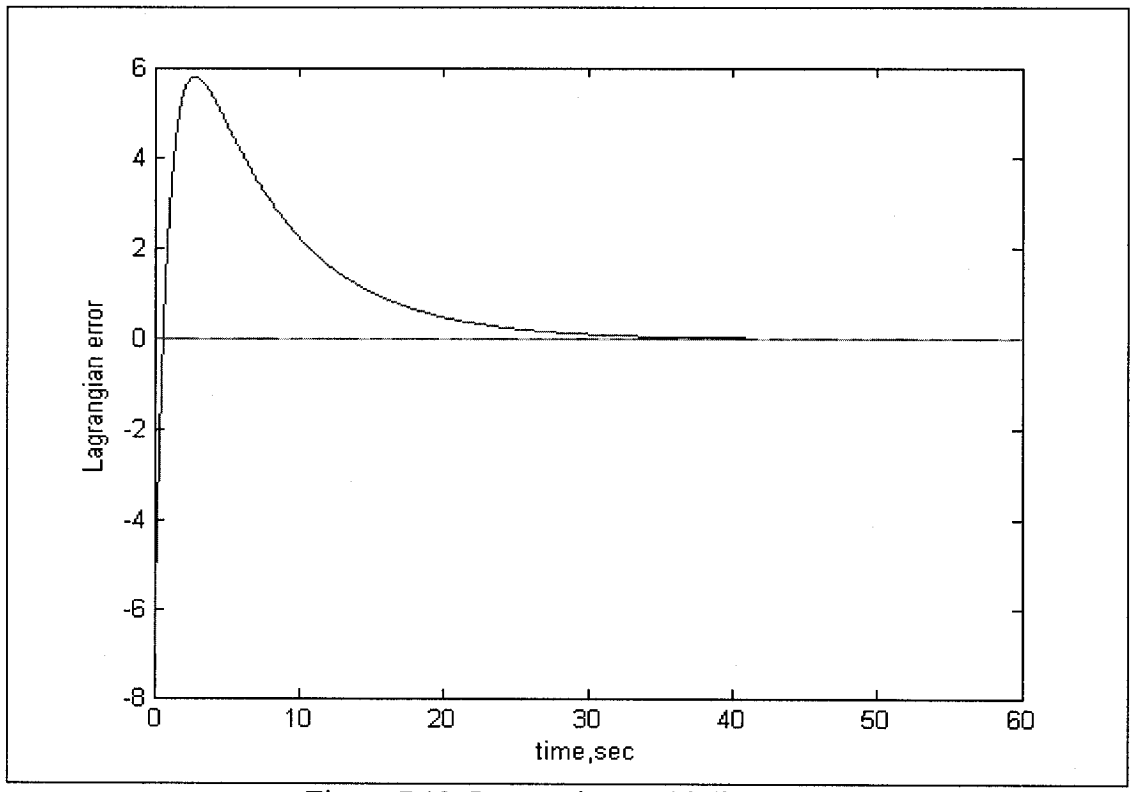

Figure 7.13: Lagrangian Multiplier Error

An adaptive inverse-dynamics based controller proposed in this paper is capable to track the desired motion values and contact force specifications and moreover, to overcome the combined system parameters uncertainty. Moreover, the reduced-order dynamics established by using the orthogonal projector techniques does not suffer of passivity or under-actuation. In the following chapter conclusions, discussions and future work will be presented.

Chapter 8

Discussion, Conclusion and Future Work

An overall control-oriented frame work for describing kinematics, linear and angular momentum, geometric contact constraints, and dynamics of a free-flying space robot in contact with a target satellite has been presented. The basic idea is to model the base satellite, the robot arm manipulator and the target satellite in one serial multi-body system. The advantage of this approach is that it allows considering the generalized constraint forces between the space robot end-effecter and the target satellite as internal forces rather than external forces. Assuming that the robot end-effctor has established a contact with the target satellite and this interaction is not lost, basic consideration have led to the following results.

The entire system combined of the based-satellite servicing robot and the target satellite is modeled in one kinematics form. This unified modeling is the basic block in building the linear and angular momentum and dynamics modeling in Chapter 2.

The linear and angular momentum of the combined system is found to be conserved in absence of existence of external forces. The momentum model can be considered as a generalization of the momentum of a totally free-flying robot. From this proposed formulation the relative linear and angular velocities of the target satellite can be

calculated without the need of measurement. The unified momentum modeling will also serve to establish a holonomy criteria.

The constraints impose on the end-effector as a result of restriction its motion on the surface of the target satellite have been also formulated by describing the hypersurfaces in the end-effector coordination system as formulated in chapter 2. The Jacobian matrix has been derived from this hypersurface and end-effector forward kinematics. A common solution of all constraints: linear momentum, angular momentum, and geometric constraints is proposed based on linear algebra theorems. It found that both linear and geometric constraints are holonomic but the angular momentum is nonholonomic.

Based on the Lagrangian approach, a generalized dynamical model suitable for control algorithms is developed in chapter 5. This model describes the coupled dynamics of both the target satellite and the servicing based satellite free-flying robot. The reduced Jacobian Matrix and Inertia matrix of a free-flying space robot interacting with a target satellite can be considered, respectively, as a generalization of the Generalized Jacobain Matrix and The Inertia Matrix of a free-flying space robot. That is, a totally free-flying space robot is recovered as a special case of this canonical model. A decomposition of generalized constraint contact forces is discussed to which forces contribute to the motion and which do not.

A physical interpretation of nonholonomic behavior is discussed in Chapter 3. It reveals the geometric conditions behind the nonholonomic behavior of two cases, the case when

a free-flying space robot does not make any contact with a target and the case with interaction with a target. This analysis is useful in designing a feasible contact tasks. It is found out that some surface tasks exhibit nonholonomic behavior and some other do not.

A methodology of a holonomy (integrability) of linear and angular momentum constraints is presented in Chapter 4 based on orthogonal projection and singular value decomposition techniques. For a system subjected to linear kinematic (kinematic-like) constraints, these constraint are said to be holonomic constraint, if the rank of the proposed linear transformation matrix is full, otherwise, it is said to be nonholonomic. This criteria can be used both off-line and on-line. The advantage of this criteria is that it can be used easily and efficiently to check whether the constraints had been changed or the initial condition on the momentum are violated or the contact is lost.

An approach to designing controllers for dynamic motion/force hybrid control of the interaction of a space robot with a target satellite has been presented in Chapter 6. This design method based on the hybrid-inverse-based-dynamics concept consists of three steps. The first step is to find a solution of the combined constraints. The second step is to substitute the obtained solution into the generalized dynamics to lead to a reduced dynamical model. Finally, an inverse dynamics controller is proposed. This controller results in a linear, decoupled model, but it guarantees a global stability of the system states and force tracking. It should not be forgetten that it does not suffer of the under-actuation comes from the assumption that the target satellite is passive.

To overcome the uncertainty in the system parameters like mass and inertia, an adaptive inverse dynamics controllers is proposed in Chapter 7 which carried the same features of former controller to track the desired motion values and contact force specifications and moreover, the ability to adapt any changes or uncertainties in the system parameters.

Simulation results verified all proposed theorems and analytical results in this dissertation.

Future work: will focus on implementing all obtained theoretical results in a hardware-in-the-loop experiment in the labs of the Canadian Space Agency. It would be also a great opportunity to implement real-time experiment of the proposed modeling, analysis and control in this thesis on the ETS-VII free-flying space robot by ANSDA.

Since the modeling and control in this thesis is based on the assumption that the space robot links are rigid, flexibility in the system structure would be also another field for investigation. A new modeling approach should be investigated because the flexibility will increase the number of degrees of freedom, and hence this will lead to underactauted robotic system.

In section related to geometric constraints, it is assumed that the geometry of the contact constraint surface is known. But in some cases the geometry of the constraint surface may not be known, this is another issue to be investigated to obtain the Jacobian matrix.

In Chapters 3, 4, 5, 6 and 7, the initial values for the linear and angular momentum are assumed to be zero. In some applications, there is a drift in the momentum, that is the initial value are not zero, future work will also investigate extending the nonholonomy criterion, dynamics and control to the case when the initial conditions of the momentum are nonzero (drifted systems).

References

[1] S. Dubowsky, E. E. Vance, and M.A. Torres, "The control of space manipulators subject to spacecraft attitude control saturation limits," in *Proc. NASA Conf. Space Telerobotics*, vol. IV, pp. 409-418, JPL, Pasadena, CA, Jan. 31-Feb. 2, 1989.

[2] A. Ellery, *An Introduction to Space Robotics*, Springer, New York, 2000.

[3] W. Fehse, *Automated Rendezvous and Docking of Spacecraft*, Cambridge University Press, Cambridge, 2003.

[4] P. C. Hughes, *Spacecraft attitude dynamics*, New York: Wiley, 1986.

[5] P. W. Likins, "Analytical dynamics and nonrigid spacecraft simulation," JPL Tech. Rep. 32-1593, July 1974.

[6] W. W. Hooker and G. Margulies, "The dynamical attitude equations for an n-body satellite," *J. Astronaunt Sciences*, vol. XII, no. 4, pp. 123-128, winter 1965.

[7] R. E. Roberson and J. Wittenburg, "A dynamical formalism for an arbitrary number of rigid bodies, with reference to the problem of satellite attitude control," in *Proc. IFAC Congress,* London, 1966, Butterworth, London, 1968.

[8] J. Y. L. Ho, "Direct path method for flexible multibody spacecraft dynamics," *J. Spacecraft and Rockects*, vol. 14, pp. 102-110, 1997.

[9] W. W. Hooker, "Equations of motion for interconnected rigid and elastic bodies: A derivation independent of angular momentum," *Celestial Mechanics*, vol. 11, pp. 337-359, 1975.

[10] Z. Vafa and S. Dubbowsky, "Minimization of spacecraft disturbances in space robotic systems," in *Proc. 11th AAS Guidance and Control* 1988; A*dvances in the Astronautical Sciences*, vol. 66., 91-108., R. D. Culp and P. L. Shattuk, Eds. San Diego: Univelt, Inc., 1988.

[11] Z. Vafa and S. Dubbowsky, "On the dynamics of manipulators in space using the virtual manipulator approach," in *IEEE Proc. on Int. Conf. Robotics Automat.*, Reliegh, NC, Mar. 1987.

[12] Z. Vafa and S. Dubbowsky, "On the dynamics of manipulators in space using the virtual manipulator, with applications to path palnning," *J. Astronaut. Sci.*, Special Issue on Space Robotics, vol. 38, no. 4, pp. 441-472, Oct-Dec. 1990.

[13] Z. Vafa and S. Dubbowsky, "The kinematics and dynamics of space manipulators: The virtual manipulator approach," *Int. J. Robotics Res.*, vol. 9, no. 4, pp. 3-21, Aug. 1990.

[14] Z. Vafa, "The kinematics, dynamics and control of space manipultors," Ph.D. Thesis, Department of Mechanical Engineering, MIT, Cambridge, MA, Nov., 1987.

[15] S. Dubowsky and M.A. Torres, "Minimizing attitude control fuel in space manipulator systems," *Porc. I.-SAIRAS'90*, kobe, Japan, 1990.

[16] S. Dubowsky and M.A. Torres, "Path planning for space manipulators to minimize spacecraft attitude disturbance," *Poc. 1991 IEEE Int. Conf.. Robotics Automation*, Sacramento, CA, April 1991.

[17] M. Torres and Dubowsky, "Minimizing spacecraft attitude disturbances space manipulator systems," accepted for publication in the *AIAA J. Giudance, Contr., 1990.*

[18] E. Papadopolous and S. Dubowsky, "On the nature of control algorithms for free-floating space manipulators," *IEEE Trans. Robotics Automat.*, vol. 7, 750-758, Dec. 1991.

[19] Y. Umetani and K. Yoshida, "Experimental study of a two dimensional free-flying robot satellite model," in *Proc. NASA Conf. Space Telerobotics*, Pasadena, CA, JAN. 1989.

[20] Y. Mastuni, F. Miyazaki, and S. Arimoto, "sensory feedback control for space manipulators," in *Proc. IEEE Int. Conf. Robotics Automation*, Scottsdale, AZ, May 1989.

[136] Y. Nakamura, W. Chung; O.J. Sordalen, "Design and control of the nonholonomic manipulator," *IEEE Transactions on Robotics and Automation*, Volume 17, Issue 1, Page(s):48 – 59, Feb 2001.

[22] K. Yoshida, R. Kurazume, and Y. Umetani, "Dual arm coordination in space free-flying robot," in *Proc. IEEE Int. Conf. Robotics Automation*, Sacamento, CA, Apr. 1991.

[23] J. R. Spofford and D. L. Akin, "Redundancy control of a free-flying telrobot," in *Proc. AIAA Guidance, Navigation and Control Conf.*, Minneapolis, MN, Aug. 1988.

[24] E. Papadopolous and S. Dubowsky, " Coordinated manipulator/spacecraft motion control for space robotics systems," in *Proc. IEEE Int. Conf. Robotics Automat.*, Sacramento, CA, pp. 1696-1701, Apr. 1991.

[25] R. Mukherjee and Y. Nakamura, "Formulation and efficient computation of inverse dynamics of space robots," *IEEE Trans. Robot. Automat.*, Vol. 8, no 3, pp. 400-406, 1992.

[26] Y. Umetani and K. Yoshida, "Resolved motion rate control of space manipulators with Generlized Jacobian Matrix," *IEEE Trans. Robot. Automat.*, Vol. 5, NO. 3,PP. 303-314,1989.

[27] k. Yamada and K. Tsuchiya, "Efficient computation algorithms for manipulator control of space robot," *Soc. Instrument Cntrl. Eng. Trans.*, vol. 26,no.7, pp. 765-772,1990 (in Japanese).

[28] Y. Yokokohji, T. Toyoshima and T. Yoshikawa, "Efficient computation algorithms for trajectory control of free-flying space robots with multiple arms," *IEEE Trans. Robot. Automat.*, vol. 9, no. 5, pp. 571-580, 1993.

[29] S. k. Saha, "A unified approach to space robot kinematics," *IEEE Trans. on Robot. and Autmat.*, vol. 12, no. 3, June 1996.

[30] A. De Luca, G. Oriolo, "Modeling and Control of Nonholonomic Mechanical Systems," in Kinematics and Dynamics of Multi-Body Systems, J. Angeles, A. Kecskemethy Eds., CISM Courses and Lectures no. 360, pp. 277-342, Springer-Verlag, Wien, 1995.

[31] A. M. Bloch, M. Reyhanoglu, and N. H. McClamroch, "Control and stabilization of nonholonomic dynamic systems," *IEEE Trans. on Automat. Cntrl*,vol. 37, no. 11, Nov. 1992.

[32]Y. Nakmura and R. Mukherjee, "Nonholonmic path planning of space robots via bi-directional approach," I*EEE Trans. Robotics Automat.*, vol. 7,pp. 500-514, August 1991.

[33] R. Murray and S. Sastry, "Nonholonomic motion planning: steering using sinusoids," *IEEE Transactions on Automatic Control*, Volume 38, Issue 5, Page(s): 700–716, May 1993.

[34] A. Kapitanovsky,A. Goldenberg, and J. Mills, "An approach to classification, analysis and feedback control of kinematic drift in free-floating manipulators," *IEEE Int. Conference on Robotics and Automation*, vol. 1 Page(s):83 - 88 , 8-13 May 1994.

[35] F. Matsuno and J. Tsurusaki, "Chained form transformation algorithm for a class of 3-states and 2-inputs nonholonomic systems and attitude control of space robot," *Proceedings of the 38th IEEE Conference on Decision and Control*, Volume 3, Page(s): 2126 – 2131, 7-10 Dec. 1999.

[36] F. Matsuno and K. Saito, "Attitude control of a space robot with initial angular momentum," *IEEE International Conference on Robotics and Automation (ICRA)*, Volume 2, Page(s):1400-140, 2001.

[37] Y. Xu, H.-Y. Shum, J.-J. Lee, T. Kanade, "Adaptive control of space robot system with an attitude controlled base," *IEEE Int. Conf. on Robot. And Automat.*, nice, France, May 1992.

[38] Y. Xu, H.-Y. Shum, T. Kanade , J.-J. Lee, "Parameterization and adaptive controlofspace robot systems," *IEEE Trans. on Aerospace and Electronic Sys.*, vol. 30, no.2, April 1994.

[39] J.-H. Jean, L.-C. Fu, "On the adaptive control of space robots," *IEEE 31st Conf. On decision and Control*, Arizona, Dec. 1992.

[40] Y.-L. Gu, Y. Xu, "A normal form augmentation approach to adaptive control of space robot systems," *IEEE International Conference Robotics and Automation Proceedings*, vol.2 Page(s):731 - 737, 2-6 May 1993.

[41] B. Ma, W. Huo, "Adaptive control of space robot system with an attitude controlled base," *IEEE International Conference Robotics and Automation Proceedings*, Volume 2, Page(s):1265 – 127, 21-27 May1995.

[42] J.-H. Shin, I.-K. Jeong, J.-J. Lee, W. Ham, "Adaptive robust control for free-flying space robots using norm-bounded property of uncertainty," *IEEE/RSJ International Conference on Intelligent Robots and Systems 'Human Robot Interaction and Cooperative Robots'*, Volume 2, Page(s):59 – 64, 5-9 Aug. 1995.

[43] L.B. Wee, M. Walker, "On the Dynamics of Contact between Space Robots and Configuration Control for Impact Minimization", *IEEE trans. on Robotics and Automation*, Vol. 9, No. 5, Oct. 1993.

[44] D. T. Greewood, *Principles of Dynamics*. Englewood Cliffs, NJ: Prentice-Hall Inc., 1988.

[45] Y.F. Zheng, "Collision Effects on Two Coordinating Robots in Assembly and Effect Minimization," *IEEE Trans Sys.*, Man, Cybern., Vol. SMC-17, no. 1, 1987.

[46] I. Walker, "The Use of Kinematic Redundancy in Reducing Impact and Contact Effects in Manipulation," in *Proc. IEEE Int. Conf. Robotics Automat.*, Cininnati, OH, 1990.

[47] A. Liegeois, "Automatic Supervisory Control of the Configuration and Behavior of Multibody Mechanisms," *IEEE Trans. syst.*, Man, Cybern., vol. SMC-7, PP.868-871, 1977.

[48] k. Yoshida, N. Sashida, "Modeling of Impact Dynamics and Impulse Minimization for Space Robots," *Procc. Of the 2993 IEEE/RSJ Int. Conf. on Intelligent Robots and Systems*, Yokohama, Japan, July 26-30, 1993.

[49] D. Nenchev, K. Yoshida, "Impact Analysis and Post-Impact Motion Control Issues of a Free-Floating Space Robot Subject to a Force Impulse", *IEEE Transactions on Robotics and Automatic, Vol. 15, N0. 3*, June 1999.

[50] K. Yoshida, et al, " Modeling of Collision Dynamics for Space Free-Floating Links with Extended Generalized Inertia Tensor," *in Proc. 1992 IEEE Int. Conf. Robot. Automat.*, pp.899-904, Nice, France, May 12-14, 1992.

[51] F Agili, J.-C. Piedboeuf, "Contact Dynamics emulation for hardware-in-loop simulation of robots interacting with environment," *IEEE Int. Conf. on Robot. And Automat.*, Volume 1,Page(s):523 – 529, Washington DC., 11-15 May 2002.

[52] Aghili, F.; Piedboeuf, J.-C., "Hardware-in-loop simulation of robots interacting with environment via algebraic differential equation," *IEEE/RSJ International Conference on Intelligent Robots and Systems, (IROS 2000)*, Vol.3, Pages: 1590 – 1596, 2000.

[53] Piedboeuf, J.-C.; de Carufel, J.; Aghili, F.; Dupuis, E., "Task verification facility for the Canadian special purpose dextrous manipulator," *IEEE International Conference on Robotics and Automation*, Volume 2, Page(s):1077–1083, 10-15 May 1999.

[54] Kazerooni H., Sheridan T. B., Houpt P. K., "Robust compliant motion for manipulators, Part I: The fundamental concepts of compliant motion," *IEEE J. of Robotitcs and Automation*, vol. RA-2, no. 2, pp. 83-92, 1986.

[55] A. De Luca, C. Manes, "On the modeling of robots in contact with a dynamic environment," *Advanced Robotics, 1991. ICAR Fifth International Conference on 'Robots in Unstructured Environments'*, vol.1, pages 568 - 574, 19-22 June 1991.

[56] De Luca, A., Mattone, R., "Modeling and control alternatives for robots in dynamic cooperation," *IEEE International Conference on Robotics and Automation*, vol.1, pp.:138-145. 21-27 May 1995.

[57]De Luca, A., Manes, C., "Modeling of robots in contact with a dynamic environment," *IEEE Transactions on Robotics and Automation*, Volume: 10, Issue: 4, Pages: 542 – 548, Aug. 1994.

[58] C. Manes, "Recovering model consistence for force and velocity measures in robot hybrid control," *IEEE International Conference Robotics and Automation*, vol.2, Pages:1276–1281,12-14May1992.

[59] M. Vukobratovic, A. Tuneski, "Mathematical model of multiple manipulators: cooperative compliant manipulation on dynamical environment," *Mechanism and Machine Theory*, issue 33, pp. 1211-1239, 1998.

[60] S. Ali and R. Rastegari, "Force tracking in multiple impedance control of space free-flyers," *IEEE/RSJ Intl. Conf. on Intel. Robots and Sys.*, Volume 3, Page(s):1646 –1651, 31 Oct.-5 Nov. 2000.

[61] Y.-R. Hu and G. Vukovich, "Dynamic control of free-flying coordinated space robots," *Proc. Of 34th Conf. on Dec. and Cntrl*, New Orleans, LA, Dec. 1995.

[62] M. Yamano, A. Konno, and M. Uchiyama, "Experiments on capturing a floating object by two flexible manipulators," *IEEE Int. Conf. on Robot. and Automat.*, San Francisco, CA, April 2000.

[63] K. Yoshida, "Engineering Test Satellite VII Flight Experiment For Space Robot Dynamics and Control: Theories on Laboratory Test Beds Ten Years Ago, Now in Orbit", *The Int. Journal of Robotic Research*, vol. 22, no. 5, 2003.

[64] M. Annapragada, S. Agrawal, "Design and experiments on free-floating planar robot for optimal chase and capture operations in space," *Robotics and Autonomous Systems*, Vol. 26, pp. 281-297, 1999.

[65] V. W. Chen, R. H. Cannon, "Experiments in nonlinear adaptive control of multi-manipulator free-flying robots," *IEEE International Conference on Robotics and Automatio*n, vol.3, Page(s):2213–2220, 8-13 May 1994.

[66] I. Watanabe et al., "A Testbed to Evaluate the Task be Executed by Autonomous Space Robots: An Experiment on Satellite Berthing', *J. of the Robotics Society of Japan*, Vol. 16, No. 7, pp. 974-994, 1998 (in Japanese).

[67] M. Yamano, A. Konno, M. Uchiyama, "Experiments on Capturing a Floating Object by Two Flexible Manipulators', *Int. Conf. on Robotics & Automation*, San Francisco, CA, April 2002.

[68] S. Dubowsky, E. Papadopoulos, "The Kinematic, Dynamics, and Control of Free-Flying and Free-Flaoting Space Robotic Systems," *IEEE Trans. on Robotics and Automation*, Vol. 9, No. 5, Oct. 1993.

[69] M. Annaprgada, S. Agrawal, "Design and Experiments on a Free-Floating Planar Robot for Optimal Chase and Capture Operations in Space," *Robotics and Autonomous Systems* Vol. 26, pp. 281-297, 1999.

[70] Y. Watanabe, K. Araki, Y. Nakamura, " Microgravity Experiments for a Visual Feedback Control of a space robot Capturing a Target," *in Proc. 1998 IEEE/RSJ, Int. Conf. on Intelligent Robots and Systems*, Victoria, B.C., Canada, Oct. 1998.

[71] T. Yoshikawa, A. Sudou, "Dynamic hybrid position/force control of robot manipulators-on-line estimation of unknown constraint," *IEEE Transactions on Robotics and Automation*, Volume 9, Issue 2, Pages:220-225, April 1993.

[72] N. Hogan, "Impedance Control: An Approach to Manipulation," *ASME Journal of Dynamics Systems, Measurement & Control*, vol. 107, pp 1-24, 1985.

[73] S. Moosavian, R. Rastegari, "Disturbance rejection analysis of multiple impedance control for space free-flying robots," *IEEE/RSJ Intl. Conf. on Intel. Robots and Sys.*, Volume 3, Page(s): 2250 - 2255, 31 30 Sept.-5 Oct. 2002.

[74] M. Zribi, S. Ahmad, "Adaptive control for multiple cooperative robot arms" *Proceedings of the 31st IEEE Conference on Decision and Control*, Pages: 1392 – 1398, vol. 2, 16-18 Dec 1992.

[75] C.-Y. Su, Y. Stepanenko, and A. A. Goldenberg, "Reduced order model and robust control architecture for mechanical systems with nonholonomic Phaffian constraints," *IEEE Transactions on Systems, Man, and Cybernetics - Part A: Systems and Human*, vol. 29, no. 3, pp. 307-313, 1999.

[76] C.-Y. Su and Y. Stepanenko, " Robust motion/force control of mechanical systems with classical nonholonomic constraints," *IEEE Transactions on Automatic Control*, vol. 39, no. 3, 609-614, 1994.

[77] Su, C.-Y., and Stepanenko, Y., "Adaptive variable structure set-point control of underactuated robots," *IEEE Transactions on Automatic Control*, vol. 44, no. 11, 1999.

[78] C.-Y. Su, and T.-P. Leung, "A sliding mode controller with bound-estimation for robot manipulator," *IEEE Transactions on Robotics and Automation*, vol. 9, no.2, 208-214, 1993.

[79] C.-Y. Su and Y. Stepanenko, "Redesign of hybrid adaptive/robust motion control of rigid-link electrically-driven robot manipulators," *IEEE Transactions on Robotics and Automation*, vol.14, no. 4, pp. 651-655, 1998

[80] C.-Y. Su and Y. Stepanenko, "Hybrid adaptive/robust motion control of rigid-link electrically-driven robot manipulators," *IEEE Transactions on Robotics and Automation*, vol. 11, no. 3, pp. 426-432, 1995.

[81] Aghili, F.; Dupuis, E.; Martin, E.; Piedbceuf, J.-C., "Force/moment accommodation control for tele-operated manipulators performing contact tasks in stiff environment,' *IEEE/RSJ International Conference on Intelligent Robots and Systems*, Volume 4, Page(s):2227-2233, Oct. 29-Nov. 3, 2001.

[82] Y. Xu and T. Kanade, *Space Robotics: Dynamics and Contro*l, Kluwer Academic Publisher, Boston, 1993.

[83] F. Aghili, "A Unified Approach for Inverse and Direct Dynamics of Constrained Multibody Systems Based on Linear Projection Operator: Applications to Control and Simulation," *IEEE Transactions on Robotics*, Volume 21, Issue 5, Page(s): 834-849, Oct. 2005.

[84] F. Aghili, "Inverse and direct dynamics of constrained multibody systems based on orthogonal decomposition of generalized force," *ICRA '03. IEEE Inter. Conf. on Robot. and Automat.*, Volume: 3, Pages: 4035-4041, 14-19 Sept. 2003.

[85] F. Aghili, "Control of Constrained Mechanical Systems with Passive Joints," *RSJ '04, IEEE Inter. Conf. on Intelligent Robots and Systems*, Pages 3288-3294, Sendai, Japan, Sep 28-Oct. 2, 2004.

[86] M. Namvar, F. Aghili, "Adaptive Force-Motion Control of Coordinated Robots Interacting With Geometrically Unknown Environments," *IEEE Transactions on Robotics*, Volume 21, Issue 4, Page(s):678 – 694, 2005.

[87] O. Khatib, "A unified approach for motion and force control of robot manipulators: The operational space formulation," *IEEE Journal of Robotics and Automation*, pages:43-53, Volume: 3, Issue: 1, Feb 1987.

[88] O. Khatib, J. Burdick, "Motion and force control of robot manipulators," *Proceedings IEEE International Conference on Robotics and Automation*, Pages:1381-1386, Volume: 3, April 1986.

[89] R. Featherstone, S.S. Thiebaut, O. Khatib, "A general contact model for dynamically-decoupled force/motion control," *Proceedings IEEE International Conference on Robotics and Automation*, Pages:3281 - 3286 vol.4, 10-15 May 1999.

[90] H. West, H. Asada, "A method for the design of hybrid position/Force controllers for manipulators constrained by contact with the environment," *IEEE International Conf. on Robotics and Automation,* vol. 2, March 1985.

[91] M. T. Freeman, "Spacecraft on-orbit deployment anomalies: What can be done?," *IEEE Aerospace and Electronic Systems Magazine*, Volume:8, Issue: 4, April. 1, 1993.

[92] M. Oya, C.-Y Su, R. Katoh, "Robust adaptive motion/force tracking control of uncertain nonholonomic mechanical systems,"*IEEE Transactions on Robotics and Automation*, Volume: 19, Issue: 1, Pages:175–181, Feb.2003.

[94] Aghili, F.; Dupuis, E.; Martin, E.; Piedbceuf, J.-C., "Force/moment accommodation control for tele-operated manipulators performing contact tasks in stiff environment," *IEEE/RSJ International Conference on Intelligent Robots and Systems*, Volume 4, Page(s):2227-2233, Oct. 29-Nov. 3, 2001.

[94] F. Aghili , "On-orbit calibration of the SPDM force-moment sensor," *IEEE Int. Conf. Conference on Robotics and Automation (ICRA '00),* Volume 4, Page(s):3603–3608, 24-28 April 2000.

[95] C.S. Bonaventura, K.W. Lilly, "A constrained motion algorithm for the Shuttle Remote Manipulator System," *IEEE Control Systems Magazine*, Volume 15, Issue 5, Page(s):6 – 16, Oct. 1995.

[96] G. Hirzinger, B. Brunner, J. Dietrich, J. Heindl, "Sensor-based space robotics-ROTEX and its telerobotic features," *IEEE Transactions on Robotics and Automation*, Volume 9, Issue 5, Page(s):649 – 663, Oct. 1993.

[97] K. Yoshida, D. N. Nenchev, N. Inaba, M. Oda, "Extended ETS-VII experiments for space robot dynamics and attitude disturbance control," *22nd International Symposium on Space Technology and Science*, Morioka, Japan, 25-29 May, 2000.

[98] L.-B. Wee; M.W. Walker, N.H. McClamroch, "An articulated-body model for a free-flying robot and its use for adaptive motion control," *IEEE Transactions on Robotics and Automation*, Volume 13, Issue 2, Page(s):264 – 277, April 1997.

[99] K. Senda, T. Matsumoto, "Truss assembly by space robot and task error recovery via reinforcement learning," *IEEE/RSJ International Conference on Intelligent Robots and Systems (IROS 2000)*, Volume 1, Page(s):410 - 415 , 31 Oct.-5 Nov. 2000.

[100] W. Haoying, W. Hongxin, L. Bin, "Adaptive control for capture object of Space robot,' *Proceedings of the 3rd World Congress on Intelligent Control and Automatio*n, Volume 2, Page(s):1275 – 1279, 28 June-2 July, 2000.

[101] M. Oda, "Space robot experiments on NASDA's ETS-VII satellite-preliminary overview of the experiment results," *IEEE International Conference on Robotics and Automation*, Volume 2, Page(s):1390 - 1395, 10-15 May, 1999.

[102] G. Hirzinger, B. Brunner, R. Lampariello, K. Landzettel, J. Schott, B.-M Steinmetz, "Advances in orbital robotics," *IEEE International Conference on Robotics and Automation (ICRA '00),* Volume 1, Page(s):898 – 907, 24-28 April, 2000.

[103] K. Hasegawa, Y. Ohkami, S. Narita, T. Shirai, K. Hoshide, K. Ozawa, M. Oda, "Development of powerful robotic hand using linear actuator for space robot operations," *First IEEE Technical Exhibition Based Conference on Robotics and Automation*, TExCRA '04, Page(s):43 - 44, 18-19 Nov., 2004.

[104] M. Nohmi, "Attitude control of a tethered space robot by link motion under microgravity," *IEEE Proceedings of International Conference on Control Applications*, Volume 1, Page(s):424 – 429, 2-4 Sept., 2004.

[105] M. Marchesi, F. Angrilli, R. Venezia, "Coordinated control for free-flyer space robots,' *IEEE International Conference on Systems, Man, and Cybernetics*, Volume 5, Page(s):3550 - 3555 8-11 Oct., 2000.

[106] C. Li, "Adaptive and robust composite control of coordinated motion of space robot system with prismatic joint," *Proceedings of the 4th World Congress on Intelligent Control and Automation*, Volume 2, Page(s):1255 – 1259, 10-14 June, 2002.

[107] F. Aghili, M. Namvar, "A robust impedance matching scheme for emulation of robots,' *IEEE/RSJ International Conference on Intelligent Robots and Systems (IROS 2004)*. Volume 3, Page(s):2142 – 2148, 28 Sept.-2 Oct., 2004.

[108] Y. Taira, S. Sagara, R. Katoh, "Digital adaptive control of space robot manipulators using transpose of generalized Jacobian matrix," *IEEE/RSJ International Conference on Intelligent Robots and Systems (IROS 2000)*, Volume 2, Page(s):1553 – 1558, 31 Oct.-5 Nov., 2000.

[109] C.-Y Su; Y. Stepanenko, "Adaptive control of mechanical systems with classical nonholonomic constraints," *IEEE International Conference on Systems, Man and Cybernetics, 'Intelligent Systems for the 21st Century'*, Volume 5, Page(s):4143 – 4148, 22-25 Oct., 1995.

[110] C.-Y Su; M. Oya, R. Katoh, "Robust adaptive motion/force control of uncertain nonholonomic mechanical systems," *Proceedings of the 2001American Control Conference*, Volume 4, Page(s):3268 – 3273, 25-27 June, 2001.

[111] C.-Y Su; Y. Stepanenko, "Robust motion/force control of mechanical systems with classical nonholonomic constraints," *IEEE Transactions on Automatic Control*, Volume 39, Issue 3, Page(s):609 – 614, March 1994.

[112] C.-Y Su; Y. Stepanenko, "Motion/force control of uncertain acatastatic nonholonomic mechanical systems via sliding modes," *Proceedings of the American Control Conference*, Volume 5, Page(s):3510 – 351, 2-4 June, 1999.

[113] S.S. Ge, T.H. Lee, T.H., J. Wang, "Adaptive impedance control of mechanical systems with classical nonholonomic constraints," *IEEE International Conference on Control Applications (CCA '01)*, Page(s):960 – 965, 2001 5-7 Sept., 2001.

[114] E.G. Papadopoulos, "Path Planning For Space Manipulators Exhibiting Nonholonomic Behavior," *IEEE/RSJ International Conference on Intelligent Robots and Systems*, Volume 1, Page(s):669 – 675, July 7-10, 1992.

[115] M. Namvar, F. Aghili, "Adaptive Force-Motion Control of Coordinated Robots Interacting With Geometrically Unknown Environments," *IEEE International Conference on Robotics and Automation (ICAR '04)*, Volume 3, Page(s): 3061–3068, Apr. 26-May 1, 2004

[116] A. Ben-Israel, N.E.T Greville, *Generalized Inverses: Theory and Application*, 2nd Edition, Springer, New York, 2003.

[117] H. Goldstien, *Classical Mechanics*, 2nd ed., Addison-Wesley, 1980.

[118] K. Yoshida, and S. Abiko, "Inertia parameter identification of a space free-flying robot," Int. AIAA Guidance, Navigation and Control Conference, August, 2002.

[119] Ju. I. Neimark, N. A. Fufaef, *Dynamics of Nonholonomic Systems*, Vol. 33, Translations of Mathematical Monographs, American Mathe-matical Society, Providence, Rhode Island, 1972.

[120] A. M. Lopsec, Nichthholomome Systeme in Mehrdimensionalen Euklidischen Raumen, *Trudy Sem. Vektor. Tenzor Anal.* 4, 302-317; *Russian transl.*, ibid, 318-332, (1937).

[121] C. Lanczos , *The Variational Principle of Mechanics*, University of Toronto Press, Toronto, 1966.

[122] K. Yoshida, K. Hashizume, D. N. Nenchev, N. Inaba, and M. Oda, "Control of a space manipulator for autonomous target capture—ETS-VII flight experiments and analysis," *Int. AIAA Guidance, Navigation, and Control Conference*, Denver, CO, 14-17 August, 2000.

[123] H. Nijmeijer and A. van der Schaft, *Nonlinear Dynamical Control Systems*, Springer-Verlag, Berlin 1990.

[124] R. C. Hibbeller, *Dynamics*, Prentice Hall, New Jersey 2001.

[125] H. Goldstien, *Classical Mechanics*, 2nd ed., Addison-Wesley, 1980.

[126] J. Wang, C.-Y. Su, M. Oya, "Robust motion tracking control of partially nonholonomic mechanical systems," *ICRA '04. 2004 IEEE International Conference on Robotics and Automation*, Vol.5, Page(s): 4608 – 4613, 26 April-1 May, 2004.

[127] I.D. Walker, R.A. Freeman, S.I. Marcus, "Internal object loading for multiple cooperating robot manipulators," *Proceedings. IEEE International Conference on Robotics and Automation*, pp. 606-611, 14-19 May, 1989.

[128] D. M. Dawson, F. L. Lewis, M W. Spong, R. Ortega, "Comments on 'On adaptive inverse dynamics control of rigid robots' [with reply]," *IEEE Transactions on Automatic Control*, Volume 36, Issue 10, Pages:1215 – 1216, Oct. 1991.

[129] M. W. Spong, R. Ortega, "On adaptive inverse dynamics control of rigid robots," *IEEE Transactions on Automatic Control*, Volume 35, Issue 1, Page(s):92 – 95, Jan. 1990.

[130] Gautier, M., and Khalil, W., "On the identification of the inertial parameters of robots," *Proceedings of 27th IEEE CDC*, pages 2264-2269, 1988.

[131] M. Oya, C.-Y. Su, R. Katoh, "Robust adaptive motion/force tracking control of uncertain nonholonomic mechanical systems," *IEEE Trans. on Robotics and Automation*, Vol. 19, Issue 1, Page(s):175 – 181, Feb. 2003.

[132] Z.P. Wang, S.S. Ge, T.H. Lee, "Robust motion/force control of uncertain holonomic/nonholonomic mechanical systems," *IEEE/ASME Transactions on Mechatronics*, Volume 9, Issue 1, Page(s):118 – 123, March, 2004.

[133] K. Yoshida, H. Nakanishi, "Impedance matching in capturing a satellite by a space robot," *IEEE/RSJ International Conference on Intelligent Robots and Systems*, Volume 4, Page(s):3059 – 3064, 27-31 Oct. 2003.

[134] Z. H. Lou, Y. Sakawa, "Control of a space manipulator for capturing a tumbling object," *Proceedings of the 29th IEEE Conference on Decision and Control*, vol.1, Page(s):103 - 108, 5-7 Dec. 1990.

[135] D.N Dimitrov, K. Yoshida, "Utilization of the bias momentum approach for capturing a tumbling satellite," *IEEE/RSJ International Conference on Intelligent Robots and Systems*, Volume 4, Page(s): 3333 - 3338 vol.4, 28 Sept.-2 Oct., 2004.

[136] Y. Nakamura, W. Chung; O.J. Sordalen, "Design and control of the nonholonomic manipulator," *IEEE Transactions on Robotics and Automation*, Volume 17, Issue 1, Page(s):48 – 59, Feb 2001.

[137] D.N Dimitrov, K. Yoshida, "Momentum distribution in a space manipulator for facilitating the post-impact control," IEEE/RSJ International Conference on Intelligent Robots and Systems, Volume 4, Page(s):3345 - 3350 vol.4, 28 Sept.-2 Oct., 2004.

[138] E. Papadopoulos, S. Dubowsky, "On the nature of control algorithms for free-floating space manipulators," *IEEE Transactions on Robotics and Automation*, Volume 7, Issue 6, Page(s):750 - 758, Dec. 1991.

[139] H.P. Frisch, "A vector-dyadic development of the equations of motion for n coupled rigid bodies and point masses," NASA TN D-7767, Washington, dc, 1974.

[140] W. Jerkovsky, "The structure of multibody dynamics equations," *J. Guidance Contr.*, vol. 1, no. 3, PP. 3-21, 1983.

[141] Lockheed Martin, *Hubble Space Telescope: Servicing Mission 3A Media Reference Guide*, 1999.

[142] T.-J Tarn, M. Zhang and A. Serrani, " New Integrability Conditions for Differential Constraints," *Systems & Control Letters,* Volume 49, Issue 5, Pages 335-345 , 15 August 2003.

[143] V. L. Pisacane and R. C. Moore, *Fundamentals of space systems*, Oxford University Press, New York, 1994.

[144] T. R. Kane, P. W. Likins, David A. Levinson, *Spacecraft dynamics,* McGraw-Hill Book Co., New York, 1983.

[145] B. N. Datta, *Numerical linear algebra and applications,* Brooks/Cole Pub., Pacific Grove, 1995.

[146] P. E. Gill, W. M., Margaret H. Wright, *Numerical linear algebra and optimization*, Addison-Wesley Pub. Co., Advanced Book Program, Redwood City, California, 1991.

[147] B. Siciliano and L. Villani, *Robot force control*, Kluwer Academic, Boston, 1999.

[148] D. M. Gorinevsky, A. M. Formalsky, A. Yu. Schneider, *Force control of robotics systems*, Nauka Publishers, Moscow, Boca Raton, CRC press, Florida, 1997.

[149] T. Yoshikawa, "Dynamic hybrid position/force control of robot manipulators--Description of hand constraints and calculation of joint driving force," *IEEE Journal of Robotics and Automation*, Volume 3, Issue 5, Page(s):386–392, Oct 1987.

[150] J. J. Slotine, W. Li, *Applied Nonlinear Control*, Prentice Hall, 1995.

[151] H. Khalil, *Nonlinear Systems*, Third Edition, Prentice Hall, N.Y., 2002.

[152] M.W. Spong, and M. Vidyasagar, *Robot Dynamics and Control*, John Wiley & Sons, Inc., New York, 1989.

[153] S. Chiaverini, B. Siciliano, L. Villani, " Force and position tracking: parallel control with stiffness adaptation," *IEEE Control Systems Magazine*, Volume: 18, Issue: 1, page(s): 27 – 33, Feb. 1998.

[154] M. Shibli, F. Aghili, C.-Y. Su, "Hybrid Inverse Dynamics Control of a Free-Flying Space Robot in Contact with a Target Satellite," *IEEE 1st International Symposium Systems and Control in Aerospace and Astronautics (ISSCAA 2006)*, Harbin, China, Jan. 19-21, 2006.

[155] M. Shibli, F. Aghili, C.-Y. Su, "Modeling of a Free-Flying Space Robot in Contact with a Target Satellite," *IEEE CCA05 Conference on Control Applications*, Toronto, Canada, 28-31 August, 2005. (Best Student Paper Award Finalist)

[156] M. Shibli, C.-Y. Su, F. Aghili "Online Nonholonomy Criterion of a Free-Flying Space Robot with/without Interaction with a Target Satellite," *36th International Symposium on Robotics (ISR 2005), Co-sponsored by IEEE Robotics and Automation*, Tokyo, Japan, Nov. 28-Dec. 1, 2005.

[157] M. Shibli, C.-Y. Su,, F. Aghili, "Physical Insight of Holonomic Nonholonomic Constraints of a Free-Flying Space Robot with/without Contact with a Target Satellite," *36th International Symposium on Robotics (ISR 2005), Co-sponsored by IEEE Robotics and Automation*, Tokyo, Japan, Nov. 28-Dec. 1, 2005.

Appendix A

Derivation of the linear Velocity of the Target Satellite

Referring to Figure 2.1, the position vector of the *i*th body with respect to the inertial frame can be readily expressed as

$$r_i = r_b + r_{i/b} \tag{A1}$$

Moreover, the relative vector $R_{i/b}$ can be expressed in the form

$$r_{i/b} = r_i - r_b \tag{A2}$$

Now the purpose is to derive the equation of that describes the linear velocity of the target satellite. From the principles of dynamics and because the target satellite is linked to the base satellite space servicing robot by the robot end-effector there is a relative linear and angular motion between the target satellite and the space robot.

The position of the contact point on the target satellite with respct to the base can be described based on (A1) as follows

$$r_t = r_b + r_{t/b} \tag{A3}$$

Then the velocity of the contact point is determined by taking the time derivative of (A3), which yields

$$V_t = V_b + \frac{dr_{t/b}}{dt} \tag{A4}$$

The last term in (4) is evaluated as follows:

$$\begin{aligned}\frac{dr_{t/b}}{dt} &= \frac{d}{dt}(x_t\hat{i} + y_t\hat{j}) \\ &= \frac{dx_t}{dt}\hat{i} + x_t\frac{d\hat{i}}{dt} + \frac{dy_t}{dt}\hat{j} + y_t\frac{d\hat{j}}{dt} \\ &= \left(\frac{dx_t}{dt}\hat{i} + \frac{dy_t}{dt}\hat{j}\right) + \left(x_t\frac{d\hat{i}}{dt} + y_t\frac{d\hat{j}}{dt}\right)\end{aligned} \tag{A5}$$

The first three terms in the first parenthesis represent the components of velocity of the contact point as measured by an observer attached to the moving base coordinate system. This term will be denoted by v_t. The other three terms in the second parenthesis represent the instanenous time rate of change of the unit vector $\hat{i}, \hat{j}$ and $\hat{k}$ and measured in the inertial frame and given as [124]:

$$\frac{d\hat{i}}{dt} = \frac{d\theta}{dt}(\hat{j}) = \Omega_b\hat{j} \tag{A6}$$

$$\frac{d\hat{j}}{dt} = \frac{d\theta}{dt}(-\hat{i}) = -\Omega_b\hat{i} \tag{A7}$$

Viweing the axes in three dimension, and noting that $\Omega_b = \Omega_b\hat{k}$, we can express the derivative (A6) and (A7) in terms of the cross product as

$$\frac{d\hat{i}}{dt} == \Omega_b : \hat{i} \tag{A8}$$

$$\frac{d\hat{j}}{dt} == \Omega_b : \hat{j} \tag{A9}$$

Substituting these results into (A5) and using the distributive property of the vector cross product, one obtains

$$\frac{dr_{t/b}}{dt} = v_t + \Omega_b : (x_t\hat{i} + y_t\hat{j}) = v_t + \Omega : r_{t/b} \tag{A10}$$

Since the target satellite is linked with the space robot via the end-effector joint and using the Jacobian transformation, hence equation (A4) becomes

$$V_t = V_b + \Omega_b \times r_{t/b} + J_{L_{EE}} \dot{q} + \omega_t \times r_{t/EE} + v_t \tag{A11}$$

Appendix B

Derivation of the Dynamics using Lagrangian Multipliers

Recalling Equations (2.30) of kinematic contact constraints at the velocity level which can be put in the form assuming zero initial condition

$$\sum_{k=1}^{n} j_{lk} d\theta_k = 0, \text{ for } l = 1, \cdots, m \tag{B1}$$

The last Equations represent a relation connecting the differential of $\theta's$. Now, the variation process involved in Hamilton's principle is one in which time, for each point on the path, is held constant. Hence the virtual displacements occurring in the variation must satisfy equations of constraint of the form

$$\sum_{k=1}^{n} a_{lk} \delta\theta_k = 0 \tag{B2}$$

Now we use Equations (B2) to reduce the number of virtual displacements to independent ones.

Obviously, the holonomic geometric constraints are behind the generalized constraint forces as a result of the contact between the manipulator end-effecter and the surface of the target satellite. On the other hand, nonholonomic constraints do not contribute to constraint forces. Remember that a dynamical system subjected to m constraints can be solved using the method of undetermined Lagrangian multipliers as follows.

The Lagrange multiplier method can be used for holonomic constraints when it is not convenient to reduce all the generalized coordinates to independent coordinates. This is possible, as in our case, when the system is subjected to different types of constraints holonomic constraints and nonholonomic constraints. The procedure for eliminating these extra virtual displacement is called the method of Lagrange undetermined multipliers. If Equation (B2) hold then it also true that

$$\lambda_l \sum_{k=1}^{N} a_{lk} \delta\theta_k = 0 \tag{B3}$$

where λ_l with $l = 1,2,\cdots,m$ are some undetermined constants, functions of time in general. Let us now combine these m equations with the equation corresponding to a conservative system

$$\int_a^b \sum_k^N \left(\frac{\partial T}{\partial \theta_k} - \frac{d}{dt}\frac{\partial T}{\partial \dot{\theta}_k} \right) \delta\theta_k dt = 0 \tag{B4}$$

To do this first sum the Equations (B3) over l, and then integrate the resulting equation from point a to point b:

$$\int_a^b \sum_{l=1}^{m} \sum_{k=1}^{N} \lambda_l a_{lk} \delta\theta_k = 0 \tag{B5}$$

This may combined with Equations (B4), yielding the relation

$$\int_a^b \sum_{k=1}^{N} \left(\frac{\partial T}{\partial \theta_k} - \frac{d}{dt}\frac{\partial T}{\partial \dot{\theta}_k} + \sum_{l=1}^{m} \lambda_l a_{lk} \right) \delta\theta_k dt = 0 \tag{B6}$$

The $\delta\theta_k$'s are still independent, of course; they are connected by the m relations (B2). That is, while the first $N-m$ of these may be chosen independently, the last m are then

fixed by Equations (B2). However, the values of $\lambda_l's$ are still at our disposal. Suppose we now choose the $\lambda_l's$ to be such that

$$\frac{\partial T}{\partial \theta_k} - \frac{d}{dt}\frac{\partial T}{\partial \dot{\theta}_k} + \sum_{l=1}^{m} \lambda_l a_{lk} = 0, k = N - m + 1, \cdots, N \tag{B7}$$

which are in the nature of equations of motion for the last m of the θ_k variables. With the $\lambda_l's$ determined by (B7), we can write (B6) as

$$\int_a^b \sum_{k=1}^{N-m} \left(\frac{\partial T}{\partial \theta_k} - \frac{d}{dt}\frac{\partial T}{\partial \dot{\theta}_k} + \sum_{l}^{m} \lambda_l a_{lk} \right) \delta\theta_k dt = 0 \tag{B8}$$

Here the only $\delta\theta_k's$ involved are independent ones. Hence it follows that

$$\frac{\partial T}{\partial \theta_k} - \frac{d}{dt}\frac{\partial T}{\partial \dot{\theta}_k} + \sum_{l=1}^{m} \lambda_l a_{lk} = 0, k = 1,2,\cdots, n - m \tag{B9}$$

Combining (B7) and (B9), we finally have the complete set of Lagrange's equations for holnomic system

$$\frac{\partial T}{\partial \theta_k} - \frac{d}{dt}\frac{\partial T}{\partial \dot{\theta}_k} = \sum_{l=1}^{m} \lambda_l a_{lk}, k = 1,2,\cdots, N \tag{B10}$$

Now we have N unknowns, namely the N coordinates θ_k and the m $\lambda_l's$, while Equations (B10) gives us a total of only N equations. The additional equations needed, of course, are exactly the equations of constraints linking up the $\theta_k's$, given in (B2), except that now to be considered in a differential form

$$\sum_{k=1}^{N} a_{lk}\dot{\theta}_k = 0, \text{ for } l = 1,2,\cdots, m \tag{B11}$$

Equations (B10) and (B11) together constitute $N+m$ equations for $N+m$ unknowns. What are the physical meaning behind the Lagrangian undetermined multipliers? They

are the forces of constraints. Such forces applied to the system are needed so as to maintain the kinematical constraints which are called the generalized forces of constraints.

Appendix C

Inertia Matrix $H(\theta)$ for 6-DOF Based-Satellite Space Robot Interacting with a Target Satellite

$$H(\theta)=\begin{bmatrix} H_{V_b} & H_{V_b\Omega_b} & H_{V_bq} & H_{V_b\omega_t} & H_{V_bv_t} \\ H^T_{V_b\Omega_b} & H_{\Omega_b} & H_{\Omega_bq} & H_{\Omega_b\omega_t} & H_{\Omega_bv_t} \\ H^T_{V_bq} & H^T_{\Omega_bq} & H_q & H_{q\omega_t} & H_{qv_t} \\ H^T_{V_b\omega_t} & H^T_{\Omega_b\omega_t} & H^T_{q\omega_t} & H_{\omega_t} & H_{\omega_Tv_t} \\ H^T_{V_bv_t} & H^T_{\Omega_bv_t} & H^T_{qv_t} & H^T_{\omega_tv_t} & H_{v_t} \end{bmatrix}$$, where each sub-matrix is given as:

$$H_{V_b}=E_3(m_b+m_1+m_2+m_3+m_4+m_5+m_6+m_t)=E_3m_{total}$$

$$H_{V_b\Omega_b}=-\left(m_1\left[r_{1/b}\times\right]+m_2\left[r_{2/b}\times\right]+m_3\left[r_{3/b}\times\right]+m_4\left[r_{4/b}\times\right]+m_5\left[r_{5/b}\times\right]+m_6\left[r_{6/b}\times\right]+m_t\left[r_{t/b}\times\right]\right)$$

$$H_{V_bq}=\left(m_1J_{L_1}+m_2J_{L_2}+m_3J_{L_3}+m_4J_{L_4}+m_5J_{L_5}+m_6J_{L_6}+m_tJ_{L_t}\right)$$

$$H_{V_b\omega_t}=-m_t\left[r_{t/EE}\times\right]$$

$$H_{V_bv_t}=E_3m_t$$

$$H_{\Omega_b}=I_b+I_1+I_2+I_3+I_4+I_5+I_6+I_7+$$
$$m_1D(r_{1/b})+m_2D(r_{2/b})+m_3D(r_{3/b})+m_4D(r_{4/b})+m_5D(r_{5/b})+m_6D(r_{6/b})+m_tD(r_{t/b})$$

$$H_{\Omega_bq}={}^BI_1J_{A_1}+{}^BI_2J_{A_2}+{}^BI_3J_{A_3}+{}^BI_4J_{A_4}+{}^BI_5J_{A_5}+{}^BI_6J_{A_6}+{}^BI_tJ_{A_t}+m_1\left[r_{1/b}\times\right]J_{L_1}+$$
$$m_2\left[r_{2/b}\times\right]J_{L_2}+m_3\left[r_{3/b}\times\right]J_{L_3}+m_4\left[r_{4/b}\times\right]J_{L_4}+m_5\left[r_{5/b}\times\right]J_{L_5}+m_6\left[r_{6/b}\times\right]J_{L_6}+m_7\left[r_{7/b}\times\right]J_{L_7}$$

$$H_{\Omega_b\omega_t}=m_tD(r_{t/EE})+{}^bI_t$$

$$H_{\Omega_bv_t}=-m_t\left[r_t\times\right]$$

$$H_q=\left(m_1J^T_{L_1}\cdot J_{L_1}+m_2J^T_{L_2}\cdot J_{L_2}+m_3J^T_{L_3}\cdot J_{L_3}+m_4J^T_{L_4}\cdot J_{L_4}+m_5J^T_{L_5}\cdot J_{L_5}+m_6J^T_{L_6}\cdot J_{L_6}+m_tJ^T_{L_t}\cdot J_{L_t}\right)$$
$$+\left({}^BI_1J^T_{A_1}J_{A_1}+{}^BI_2J^T_{A_2}J_{A_2}+{}^BI_3J^T_{A_3}J_{A_3}+{}^BI_4J^T_{A_4}J_{A_4}+{}^BI_5J^T_{A_5}J_{A_5}+{}^BI_6J^T_{A_6}J_{A_6}+{}^BI_7J^T_{A_7}J_{A_7}\right)$$

$$H_{q\omega_t} = I_t J_{A_t}{}^T + m_t J_{L_t}{}^T \left[r^T_{t/EE} \times \right]$$

$$H_{qv_t} = m_t J_{L_t}{}^T$$

$$H_{\omega_t} = I_t + m_t D(r_{t/EE})$$

$$H_{\omega_t v_t} = -m_t \left[r_{t/EE} \times \right]$$

$$H_{v_t} = E_3 \cdot m_t$$

Appendix D

Linear and Angular Jacobian Matrices for a 6-DOF Based Satellite Space Robot Interacting with a Target Satellite

$$J_{L_1} = [k_1 \times (r_1 - c_1), 0,0,0,0,0,0]$$

$$J_{L_2} = [k_1 \times (r_2 - c_1), k_2 \times (r_2 - c_2), 0,0,0,0,0]$$

$$J_{L_3} = [k_1 \times (r_3 - c_1), k_2 \times (r_3 - c_2), k_3 \times (r_3 - c_3), 0,0,0,0]$$

$$J_{L_4} = [k_1 \times (r_4 - c_1), k_2 \times (r_4 - c_2), k_3 \times (r_4 - c_3), k_4 \times (r_4 - c_4), 0,0,0]$$

$$J_{L_5} = [k_1 \times (r_5 - c_1), k_2 \times (r_5 - c_2), k_3 \times (r_5 - c_3), k_4 \times (r_5 - c_4), k_5 \times (r_5 - c_5), 0,0]$$

$$J_{L_6} = [k_1 \times (r_6 - c_1), k_2 \times (r_6 - c_2), k_3 \times (r_6 - c_3), k_4 \times (r_6 - c_4), k_5 \times (r_6 - c_5), k_6 \times (r_6 - c_6), 0]$$

$$J_{L_t} = [k_1 \times (r_t - c_1), k_2 \times (r_t - c_2), k_3 \times (r_t - c_3), k_t \times (r_t - c_4), k_5 \times (r_t - c_5), k_6 \times (r_t - c_6), k_t \times (r_t - c_t)]$$

$$J_{A_1} = [k_1, 0,0,0,0,0,0]$$

$$J_{A_2} = [k_1, k_2, 0,0,0,0,0]$$

$$J_{A_3} = [k_1, k_2, k_3, 0,0,0,0]$$

$$J_{A_4} = [k_1, k_2, k_3, k_4, 0,0,0]$$

$$J_{A_5} = [k_1, k_2, k_3, k_4, k_5, 0,0]$$

$$J_{A_6} = [k_1, k_2, k_3, k_4, k_5, k_6, 0]$$

$$J_{A_t} = [k_1, k_2, k_3, k_4, k_5, k_6, k_t]$$

Appendix E

Time Derivative of Inertia Matrix $H(\theta)$ for 6-DOF Based-Satellite Space Robot Interacting with a Target Satellite

$$\dot{H}(\theta)=\begin{bmatrix} \dot{H}_{V_b} & \dot{H}_{V_b\Omega_b} & \dot{H}_{V_bq} & \dot{H}_{V_b\omega_t} & \dot{H}_{V_bv_t} \\ \dot{H}^T_{V_b\Omega_b} & \dot{H}_{\Omega_b} & \dot{H}_{\Omega_bq} & \dot{H}_{\Omega_b\omega_t} & \dot{H}_{\Omega_bv_t} \\ \dot{H}^T_{V_bq} & \dot{H}^T_{\Omega_bq} & \dot{H}_{q} & \dot{H}_{q\omega_t} & \dot{H}_{qv_t} \\ \dot{H}^T_{V_b\omega_t} & \dot{H}^T_{\Omega_b\omega_t} & \dot{H}^T_{q\omega_t} & \dot{H}_{\omega_t} & \dot{H}_{\omega_Tv_t} \\ \dot{H}^T_{V_bv_t} & \dot{H}^T_{\Omega_bv_t} & \dot{H}^T_{qv_t} & \dot{H}^T_{\omega_tv_t} & \dot{H}_{v_t} \end{bmatrix}$$

$$\dot{H}_{V_b}=O_{3\times3}$$

$$\dot{H}_{V_b\Omega_b}=-\left(m_1\left[\dot{r}_{1/b}\times\right]+m_2\left[\dot{r}_{2/b}\times\right]+m_3\left[\dot{r}_{3/b}\times\right]+m_4\left[\dot{r}_{4/b}\times\right]+m_5\left[\dot{r}_{5/b}\times\right]+m_6\left[\dot{r}_{6/b}\times\right]+m_t\left[\dot{r}_{t/b}\times\right]\right)$$

$$\dot{H}_{V_bq}=\left(m_1\dot{J}_{L_1}+m_2\dot{J}_{L_2}+m_3\dot{J}_{L_3}+m_4\dot{J}_{L_4}+m_5\dot{J}_{L_5}+m_6\dot{J}_{L_6}+m_t\dot{J}_{L_t}\right)$$

$$\dot{H}_{V_b\omega_t}=-m_t\left[\dot{r}_{t/EE}\times\right]$$

$$\dot{H}_{V_bv_t}=O_{3\times3}$$

$$\dot{H}_{\Omega_b}=m_1\dot{D}(r_{1/b})+m_2\dot{D}(r_{2/b})+m_3\dot{D}(r_{3/b})+m_4\dot{D}(r_{4/b})+m_5\dot{D}(r_{5/b})+m_6\dot{D}(r_{6/b})+m_t\dot{D}(r_{t/b})$$

$$\begin{aligned}\dot{H}_{\Omega_bq}=&{}^BI_1\dot{J}_{A_1}+{}^BI_2\dot{J}_{A_2}+{}^BI_3\dot{J}_{A_3}+{}^BI_4\dot{J}_{A_4}+{}^BI_5\dot{J}_{A_5}+{}^BI_6\dot{J}_{A_6}+{}^BI_t\dot{J}_{A_t}+m_1\left[\dot{r}_{1/b}\times\right]J_{L_1}+m_1\left[\dot{r}_{1/b}\times\right]\dot{J}_{L_1}+\\ &m_2\left[\dot{r}_{2/b}\times\right]J_{L_2}+m_2\left[r_{2/b}\times\right]\dot{J}_{L_2}+m_3\left[\dot{r}_{3/b}\times\right]J_{L_3}+m_3\left[r_{3/b}\times\right]\dot{J}_{L_3}+m_4\left[\dot{r}_{4/b}\times\right]J_{L_4}+m_4\left[r_{4/b}\times\right]\dot{J}_{L_4}\\ &+m_5\left[\dot{r}_{5/b}\times\right]J_{L_5}+m_5\left[r_{5/b}\times\right]\dot{J}_{L_5}+m_6\left[\dot{r}_{6/b}\times\right]J_{L_6}+m_6\left[r_{6/b}\times\right]\dot{J}_{L_6}+m_7\left[\dot{r}_{7/b}\times\right]J_{L_7}+m_7\left[r_{7/b}\times\right]\dot{J}_{L_7}\end{aligned}$$

$$\dot{H}_{\Omega_b\omega_t}=m_t\dot{D}(r_{t/EE})$$

$$\dot{H}_{\Omega_bv_t}=-m_t\left[\dot{r}_t\times\right]$$

$$\dot{H}_q = 2\cdot\left(m_1 J_{L_1}^T\cdot\dot{J}_{L_1} + m_2 J_{L_2}^T\cdot\dot{J}_{L_2} + m_3 J_{L_3}^T\cdot\dot{J}_{L_3} + m_4 J_{L_4}^T\cdot\dot{J}_{L_4} + m_5 J_{L_5}^T\cdot\dot{J}_{L_5} + m_6 J_{L_6}^T\cdot\dot{J}_{L_6} + m_t J_{L_t}^T\cdot\dot{J}_{L_t}\right)$$
$$+2\cdot\left({}^B I_1 J_{A_1}^T\dot{J}_{A_1} + {}^B I_2 J_{A_2}^T\dot{J}_{A_2} + {}^B I_3 J_{A_3}^T\dot{J}_{A_3} + {}^B I_4 J_{A_4}^T\dot{J}_{A_4} + {}^B I_5 J_{A_5}^T\dot{J}_{A_5} + {}^B I_6 J_{A_6}^T\dot{J}_{A_6} + {}^B I_7 J_{A_7}^T\dot{J}_{A_7}\right)$$

$$\dot{H}_{q\omega_t} = I_t\dot{J}_{A_t}^T + m_t\dot{J}_{L_t}^T\left[r_{t/EE}^T\times\right] + m_t J_{L_t}^T\left[\dot{r}_{t/EE}^T\times\right]$$

$$\dot{H}_{qv_t} = m_t\dot{J}_{L_t}^T$$

$$\dot{H}_{\omega_t} = m_t\dot{D}(r_{t/EE})$$

$$\dot{H}_{\omega_t v_t} = -m_t\left[\dot{r}_{t/EE}\times\right]$$

$$H_{v_t} = O_{3\times 3}$$

Appendix F

Derivation of the Nonlinear Velocity-Dependent Force Vector $C(\theta,\dot{\theta})$ of 6-DOF Based-Satellite Space Robot Interacting with a Target Satellite

$$\dot{H}_{V_b}\cdot V_b = O_{3\times 3}$$

$$\dot{H}_{V_b\Omega_b}\cdot\Omega_b = -m_1\left[\dot{r}_{1/b}\times\right]\Omega_b - m_2\left[\dot{r}_{2/b}\times\right]\Omega_b - m_3\left[\dot{r}_{3/b}\times\right]\Omega_b - m_4\left[\dot{r}_{4/b}\times\right]\Omega_b - \\ - m_5\left[\dot{r}_{5/b}\times\right]\Omega_b - m_6\left[\dot{r}_{6/b}\times\right]\Omega_b - m_t\left[\dot{r}_{t/b}\times\right]\Omega_b$$

$$\dot{H}_{V_bq}\cdot\dot{q} = \left(m_1\dot{J}_{L_1}\dot{q}_1 + m_2\dot{J}_{L_2}\dot{q}_2 + m_3\dot{J}_{L_3}\dot{q}_3 + m_4\dot{J}_{L_4}\dot{q}_4 + m_5\dot{J}_{L_5}\dot{q}_5 + m_6\dot{J}_{L_6}\dot{q}_6\right)$$

$$\dot{H}_{V_b\omega_t}\cdot w_t = -m_t\left[\dot{r}_{t/EE}\times\right]w_t$$

$$\dot{H}_{V_bv_t}\cdot v_t = O_{3\times 3}$$

$$\dot{H}_{\Omega_b}\cdot\Omega_b = m_1\dot{D}(r_{1/b})\Omega_b + m_2\dot{D}(r_{2/b})\Omega_b + m_3\dot{D}(r_{3/b})\Omega_b + m_4\dot{D}(r_{4/b})\Omega_b \\ + m_5\dot{D}(r_{5/b})\Omega_b + m_6\dot{D}(r_{6/b})\Omega_b + m_t\dot{D}(r_{t/b})\Omega_b$$

$$\dot{H}_{\Omega_bq}\cdot\dot{q} = {}^BI_1\dot{J}_{A_1}\dot{q}_1 + {}^BI_2\dot{J}_{A_2}\dot{q}_2 + {}^BI_3\dot{J}_{A_3}\dot{q}_3 + {}^BI_4\dot{J}_{A_4}\dot{q}_4 + {}^BI_5\dot{J}_{A_5}\dot{q}_5 + {}^BI_6\dot{J}_{A_6}\dot{q}_6 + \\ m_1\left[\dot{r}_{1/b}\times\right]J_{L_1}\dot{q}_1 + m_1\left[\dot{r}_{1/b}\times\right]\dot{J}_{L_1}\dot{q}_1 + m_2\left[\dot{r}_{2/b}\times\right]J_{L_2}\dot{q}_2 + m_2\left[r_{2/b}\times\right]\dot{J}_{L_2}\dot{q}_2 \\ + m_3\left[\dot{r}_{3/b}\times\right]J_{L_3}\dot{q}_3 + m_3\left[r_{3/b}\times\right]\dot{J}_{L_3}\dot{q}_3 + m_4\left[\dot{r}_{4/b}\times\right]J_{L_4}\dot{q}_4 + m_4\left[r_{4/b}\times\right]\dot{J}_{L_4}\dot{q}_4 \\ + m_5\left[\dot{r}_{5/b}\times\right]J_{L_5}\dot{q}_5 + m_5\left[r_{5/b}\times\right]\dot{J}_{L_5}\dot{q}_5 + m_6\left[\dot{r}_{6/b}\times\right]J_{L_6}\dot{q}_6 + m_6\left[r_{6/b}\times\right]\dot{J}_{L_6}\dot{q}_6$$

$$\dot{H}_{\Omega_b\omega_t}\cdot\omega_t = m_t\dot{D}(r_{t/EE})\omega_t$$

$$\dot{H}_{\Omega_bv_t}\cdot v_t = -m_t\left[\dot{r}_t\times\right]v_t$$

$$\dot{H}_q\cdot\dot{q} = 2\cdot\left(m_1J_{L_1}^T\cdot\dot{J}_{L_1}\dot{q}_1 + m_2J_{L_2}^T\cdot\dot{J}_{L_2}\dot{q}_2 + m_3J_{L_3}^T\cdot\dot{J}_{L_3}\dot{q}_3 + m_4J_{L_4}^T\cdot\dot{J}_{L_4}\dot{q}_4 + m_5J_{L_5}^T\cdot\dot{J}_{L_5}\dot{q}_5 + m_6J_{L_6}^T\cdot\dot{J}_{L_6}\dot{q}_6\right) \\ + 2\cdot\left({}^BI_1J_{A_1}^T\dot{J}_{A_1}\dot{q}_1 + {}^BI_2J_{A_2}^T\dot{J}_{A_2}\dot{q}_2 + {}^BI_3J_{A_3}^T\dot{J}_{A_3}\dot{q}_3 + {}^BI_4J_{A_4}^T\dot{J}_{A_4}\dot{q}_4 + {}^BI_5J_{A_5}^T\dot{J}_{A_5}\dot{q}_5 + {}^BI_6J_{A_6}^T\dot{J}_{A_6}\dot{q}_6\right)$$

$$\dot{H}_{q\omega_t}\cdot\omega_t = I_t\dot{J}_{A_t}{}^T\omega_t + m_t\dot{J}_{L_t}{}^T\left[r_{t/EE}^T\times\right]\omega_t + m_tJ_{L_t}{}^T\left[\dot{r}_{t/EE}^T\times\right]\omega_t$$

$$\dot{H}_{qv_t} \cdot v_t = m_t \dot{J}_{L_t}{}^T v_t$$

$$\dot{H}_{\omega_t} \cdot \omega_t = m_t \dot{D}(r_{t/EE})\omega_t$$

$$\dot{H}_{\omega_t v_t} = -m_t \left[\dot{r}_{t/EE} \times\right] v_t$$

$$H_{v_t} = O_{3\times 3}$$

$$\begin{aligned}\frac{\partial T}{\partial \theta} = \frac{1}{2}\Big(& V_b^T \frac{\partial H_{V_b}}{\partial \theta} V_b + V_b^T \frac{\partial H_{V_b\Omega_b}}{\partial \theta}\Omega_b + V_b^T \frac{\partial H_{V_b q}}{\partial \theta}\dot{q} + V_b^T \frac{\partial H_{V_b\omega_t}}{\partial \theta}\omega_t + V_b^T \frac{\partial H_{V_b V_R}}{\partial \theta} v_t + \\ & \Omega_b^T \frac{\partial H^T_{V_b\Omega_b}}{\partial \theta} V_b + \Omega_b^T \frac{\partial H_{\Omega_b}}{\partial \theta}\Omega_b + \Omega_b^T \frac{\partial H_{\Omega_b q}}{\partial \theta}\dot{q} + \Omega_b^T \frac{\partial H_{\Omega_b\omega_t}}{\partial \theta}\omega_t + \Omega_b^T \frac{\partial H_{\Omega_b V_R}}{\partial \theta} v_t + \\ & \dot{q}^T \frac{\partial H^T_{V_b q}}{\partial \theta} V_b + \dot{q}^T \frac{\partial H^T_{\Omega_b q}}{\partial \theta}\Omega_b + \dot{q}^T \frac{\partial H_q}{\partial \theta}\dot{q} + \dot{q}^T \frac{\partial H_{q\omega_t}}{\partial \theta}\omega_t + \dot{q}^T \frac{\partial H_{qv_t}}{\partial \theta} v_t + \\ & \omega_t^T \frac{\partial H^T_{V_b\omega_t}}{\partial \theta} V_b + \omega_T^T \frac{\partial H^T_{\Omega_b\omega_t}}{\partial \theta}\Omega_b + \omega_t^T \frac{\partial H^T_{q\omega_t}}{\partial \theta}\dot{q} + \omega_t^T \frac{\partial H_{\omega_t}}{\partial \theta}\omega_t + \omega_t^T \frac{\partial H_{v_t\omega_t}}{\partial \theta} v_t + \\ & v_t^T \frac{\partial H^T_{V_b v_t}}{\partial \theta} V_b + v_t^T \frac{\partial H^T_{v_t\Omega_b}}{\partial \theta}\Omega_b + v_t^T \frac{\partial H^T_{v_t q}}{\partial \theta}\dot{q} + v_t^T \frac{\partial H^T_{v_t\omega_t}}{\partial \theta}\omega_t + v_t^T \frac{\partial H_{v_t}}{\partial \theta} v_t \Big)\end{aligned}$$

$$C(\theta,\dot{\theta}) = \dot{H}\dot{\theta} - \frac{\partial}{\partial \theta}\left(\frac{1}{2}\dot{\theta}^T H \dot{\theta}\right) = \begin{bmatrix} \dot{H}_{V_b} V_b + \dot{H}_{V_b\Omega_b}\Omega_b + \dot{H}_{V_b q}\dot{q} + \dot{H}_{V_b\omega_t}\omega_t + \dot{H}_{V_b v_t} v_t \\ \dot{H}^T_{V_b\Omega_b} V_b + \dot{H}_{\Omega_b}\Omega_b + \dot{H}_{\Omega_b q}\dot{q} + \dot{H}_{\Omega_b\omega_t}\omega_t + \dot{H}_{\Omega_b v_t} v_t \\ \dot{H}^T_{V_b q} V_b + \dot{H}^T_{\Omega_b q}\Omega_b + \dot{H}_q\dot{q} + \dot{H}_{q\omega_t}\omega_t + \dot{H}_{qv_t} v_t \\ \dot{H}^T_{V_b\omega_t} V_b + \dot{H}^T_{\Omega_b\omega_t}\Omega_b + \dot{H}^T_{q\omega_t}\dot{q} + \dot{H}_{\omega_t}\omega_t + \dot{H}_{\omega_T v_t} v_t \\ \dot{H}^T_{V_b v_t} V_b + \dot{H}^T_{\Omega_b v_t}\Omega_b + \dot{H}^T_{qv_t}\dot{q} + \dot{H}^T_{\omega_t v_t}\omega_t + \dot{H}_{v_t} v_t \end{bmatrix} -$$

$$\frac{1}{2}\begin{bmatrix} V_b^T \frac{\partial H_{V_b}}{\partial \theta} V_b + V_b^T \frac{\partial H_{V_b\Omega_b}}{\partial \theta}\Omega_b + V_b^T \frac{\partial H_{V_b q}}{\partial \theta}\dot{q} + V_b^T \frac{\partial H_{V_b\omega_t}}{\partial \theta}\omega_t + V_b^T \frac{\partial H_{V_b V_R}}{\partial \theta} v_t \\ \Omega_b^T \frac{\partial H^T_{V_b\Omega_b}}{\partial \theta} V_b + \Omega_b^T \frac{\partial H_{\Omega_b}}{\partial \theta}\Omega_b + \Omega_b^T \frac{\partial H_{\Omega_b q}}{\partial \theta}\dot{q} + \Omega_b^T \frac{\partial H_{\Omega_b\omega_t}}{\partial \theta}\omega_t + \Omega_b^T \frac{\partial H_{\Omega_b V_R}}{\partial \theta} v_t \\ \dot{q}^T \frac{\partial H^T_{V_b q}}{\partial \theta} V_b + \dot{q}^T \frac{\partial H^T_{\Omega_b q}}{\partial \theta}\Omega_b + \dot{q}^T \frac{\partial H_q}{\partial \theta}\dot{q} + \dot{q}^T \frac{\partial H_{q\omega_t}}{\partial \theta}\omega_t + \dot{q}^T \frac{\partial H_{qv_t}}{\partial \theta} v_t \\ \omega_t^T \frac{\partial H^T_{V_b\omega_t}}{\partial \theta} V_b + \omega_T^T \frac{\partial H^T_{\Omega_b\omega_t}}{\partial \theta}\Omega_b + \omega_t^T \frac{\partial H^T_{q\omega_t}}{\partial \theta}\dot{q} + \omega_t^T \frac{\partial H_{\omega_t}}{\partial \theta}\omega_t + \omega_t^T \frac{\partial H_{v_t\omega_t}}{\partial \theta} v_t \\ v_t^T \frac{\partial H^T_{V_b v_t}}{\partial \theta} V_b + v_t^T \frac{\partial H^T_{v_t\Omega_b}}{\partial \theta}\Omega_b + v_t^T \frac{\partial H^T_{v_t q}}{\partial \theta}\dot{q} + v_t^T \frac{\partial H^T_{v_t\omega_t}}{\partial \theta}\omega_t + v_t^T \frac{\partial H_{v_t}}{\partial \theta} v_t \end{bmatrix}$$

Appendix G

Derivation of the Orthogonal Matrix $S(\theta)$

$$A(\theta)\dot{\theta} = \begin{bmatrix} H_{V_b} & H_{V_b\Omega_b} & H_{V_bq} & H_{V_b\omega_T} & H_{V_bv_T} \\ H^T_{V_b\Omega_b} & H_{\Omega_b} & H_{\Omega_bq} & H_{\Omega_b\omega_T} & M_{\Omega_bv_T} \\ J_1 & J_2 & J_3 & J_4 & J_5 \end{bmatrix} \begin{bmatrix} \dot{V}_b \\ \dot{\Omega}_b \\ \ddot{q} \\ \dot{\omega}_t \\ \dot{v}_t \end{bmatrix} \tag{G1}$$

where

$$A^T = \begin{bmatrix} H_{V_b} & H^T_{V_b\Omega_b} & J_1 \\ H_{V_b\Omega_b} & H_{\Omega_b} & J_2 \\ H_{V_bq} & H_{\Omega_bq} & J_3 \\ H_{V_b\omega_T} & H_{\Omega_b\omega_T} & J_4 \\ H_{V_bv_T} & M_{\Omega_bv_T} & J_5 \end{bmatrix} \tag{G2}$$

$$S(\theta) = \begin{bmatrix} S_{11} & S_{12} & S_{13} \\ S_{21} & S_{22} & S_{23} \\ S_{31} & S_{32} & S_{33} \\ S_{41} & S_{42} & S_{43} \\ S_{51} & S_{52} & S_{53} \end{bmatrix} \tag{G3}$$

The constraints should satisfy

$$S^T(\theta)A^T(\theta) = \begin{bmatrix} S_{11} & S_{21} & S_{31} & S_{41} & S_{51} \\ S_{12} & S_{22} & S_{32} & S_{42} & S_{52} \\ S_{13} & S_{23} & S_{33} & S_{43} & S_{53} \end{bmatrix} \begin{bmatrix} H_{V_b} & H^T_{V_b\Omega_b} & J_1 \\ H_{V_b\Omega_b} & H_{\Omega_b} & J_2 \\ H_{V_bq} & H_{\Omega_bq} & J_3 \\ H_{V_b\omega_T} & H_{\Omega_b\omega_T} & J_4 \\ H_{V_bv_T} & H_{\Omega_bv_T} & J_5 \end{bmatrix} = O \tag{G4}$$

Solving of (4) leads to a proper selction of the elements of S as

$$S_{31} = E \tag{G5}$$

$$S_{41} = -\left(H_{\Omega_bq} - H_{V_bq}H_{V_b\Omega_b}{}^{-1}H_{\Omega_b}\right)\left(H_{\Omega_b\omega_T} - H_{V_b\omega_T}H_{V_b\Omega_b}{}^{-1}H_{\Omega_b}\right)^{-1} \tag{G6}$$

$$S_{21} = -S_{31} H_{V_b q} H_{V_b \Omega_b}^{-1} + \left(H_{\Omega_b q} - H_{V_b q} H_{V_b \Omega_b}^{-1} H_{\Omega_b}\right)\left(H_{\Omega_b \omega_T} - H_{V_b \omega_T} H_{V_b \Omega_b}^{-1} H_{\Omega_b}\right)^{-1} H_{V_b \omega_T} H_{V_b \Omega_b}^{-1} \quad \text{(G7)}$$

$$S_{32} = E \quad \text{(G8)}$$

$$S_{52} = -\left(J_3 - H_{V_b q} H_{V_b}^{-1} J_1\right)\left(J_5 - H_{V_b v_T} H_{V_b}^{-1} J_1\right)^{-1} \quad \text{(G9)}$$

$$S_{12} = -H_{V_b q} H_{V_b}^{-1} - \left(J_3 - H_{V_b q} H_{V_b}^{-1} J_1\right)\left(J_5 - H_{V_b v_T} H_{V_b}^{-1} J_1\right)^{-1} H_{V_b v_T} H_{V_b}^{-1} \quad \text{(G10)}$$

$$S_{23} = E \quad \text{(G11)}$$

$$S_{43} = -\left(J_2 - H_{V_b \Omega_b} H_{V_b}^{-1} J_1\right)\left(J_4 - H_{V_b \omega_T} H_{V_b}^{-1} J_1\right)^{-1} \quad \text{(G12)}$$

$$S_{13} = -H_{V_b \Omega_b} H_{V_b}^{-1} + \left(J_2 - H_{V_b \Omega_b} H_{V_b}^{-1} J_1\right)\left(J_4 - H_{V_b \omega_T} H_{V_b}^{-1} J_1\right)^{-1} H_{V_b \omega_T} H_{V_b}^{-1} \quad \text{(G13)}$$

Where the other elements are chosen as $S_{11} = S_{22} = S_{33} = S_{42} = S_{53} = O$. The results then can summarized as follows

$$S = \begin{bmatrix} 0 & S_{12} & S_{13} \\ S_{21} & 0 & E \\ E & E & 0 \\ S_{41} & 0 & S_{43} \\ 0 & S_{52} & 0 \end{bmatrix} \quad \text{(G15)}$$

The time derivative of matrix S is given as (G16)

$$\dot{S} = \begin{bmatrix} 0 & \dot{S}_{12} & \dot{S}_{13} \\ \dot{S}_{21} & 0 & 0 \\ 0 & 0 & 0 \\ \dot{S}_{41} & 0 & \dot{S}_{43} \\ 0 & \dot{S}_{52} & 0 \end{bmatrix} \quad \text{(G17)}$$

Appendix H

Derivation of the Reduced Dynamics Model of a 6 DOF Based-Satellite Space Robot in Contact with a Target Satellite

$$HS = \begin{bmatrix} H_{V_b\Omega_b}S_{21} + H_{V_bq}E + H_{V_b\omega_t}S_{41} & H_{V_b}S_{12} + H_{V_bq}E + H_{V_bv_t}S_{52} & H_{V_b}S_{13} + H_{V_b\Omega_b}E + H_{V_b\omega_t}S_{43} \\ H_{\Omega_b}S_{21} + H_{\Omega_bq}E + H_{\Omega_b\omega_t}S_{41} & H^T_{V_b\Omega_b}S_{12} + H_{\Omega_bq}E + H_{\Omega_bv_t}S_{52} & H^T_{V_b\Omega_b}S_{13} + H_{\Omega_b}E + H_{\Omega_bv_t}S_{43} \\ H^T_{\Omega_bq}S_{21} + H_qE + H_{q\omega_t}S_{41} & H^T_{V_bq}S_{12} + H_qE + H_{qv_t}S_{52} & H^T_{V_bq}S_{13} + H^T_{\Omega_bq}E + H_{qv_t}S_{43} \\ H^T_{\Omega_b\omega_t}S_{21} + H^T_{q\omega_t}E + H_{\omega_t}S_{41} & H^T_{V_b\omega_t}S_{12} + H^T_{q\omega_t}E + H_{\omega_Tv_t}S_{52} & H^T_{V_b\omega_t}S_{13} + H^T_{\Omega_b\omega_t}E + H_{\omega_Tv_t}S_{43} \\ H^T_{\Omega_bv_t}S_{21} + H^T_{qv_t}E + H^T_{\omega_tv_t}S_{41} & H^T_{V_bv_t}S_{12} + H^T_{qv_t}E + H_{v_t}S_{52} & H^T_{V_bv_t}S_{13} + H^T_{\Omega_bv_t}E + H_{v_t}S_{43} \end{bmatrix}$$

$$H\dot{S} = \begin{bmatrix} H_{V_b\Omega_b}\dot{S}_{21} + H_{V_b\omega_t}\dot{S}_{41} & H_{V_b}\dot{S}_{12} + H_{V_bv_t}\dot{S}_{52} & H_{V_b}\dot{S}_{13} + H_{V_b\omega_t}\dot{S}_{43} \\ H_{\Omega_b}\dot{S}_{21} + H_{\Omega_b\omega_t}\dot{S}_{41} & H^T_{V_b\Omega_b}\dot{S}_{12} + H_{\Omega_bv_t}\dot{S}_{52} & H^T_{V_b\Omega_b}\dot{S}_{13} + H_{\Omega_bv_t}\dot{S}_{43} \\ H^T_{\Omega_bq}\dot{S}_{21} + H_{q\omega_t}\dot{S}_{41} & H^T_{V_bq}\dot{S}_{12} + H_{qv_t}\dot{S}_{52} & H^T_{V_bq}\dot{S}_{13} + H_{qv_t}\dot{S}_{43} \\ H^T_{\Omega_b\omega_t}\dot{S}_{21} + H_{\omega_t}\dot{S}_{41} & H^T_{V_b\omega_t}\dot{S}_{12} + H_{\omega_Tv_t}\dot{S}_{52} & H^T_{V_b\omega_t}\dot{S}_{13} + H_{\omega_Tv_t}\dot{S}_{43} \\ H^T_{\Omega_bv_t}\dot{S}_{21} + H^T_{\omega_tv_t}\dot{S}_{41} & H^T_{V_bv_t}\dot{S}_{12} + H_{v_t}\dot{S}_{52} & H^T_{V_bv_t}\dot{S}_{13} + H_{v_t}\dot{S}_{43} \end{bmatrix}$$

$$\overline{C} = CS =$$

$$\overline{C}_1 = \dot{H}_{V_b\Omega_b}\Omega_bS_{21} + \dot{H}_{V_bq}\dot{q}E + \dot{H}_{V_b\omega_t}\omega_tS_{41} + \frac{1}{2}\left(V_b^T\frac{\partial H_{V_b\Omega_b}}{\partial\theta}\Omega_bS_{21} + V_b^T\frac{\partial H_{V_bq}}{\partial\theta}\dot{q}E + V_b^T\frac{\partial H_{V_b\omega_t}}{\partial\theta}\omega_tS_{41}\right)$$

$$+ \dot{H}_{V_b}V_bS_{12} + \dot{H}_{V_bq}\dot{q}E + \dot{H}_{V_bv_t}v_tS_{52} + \frac{1}{2}\left(V_b^T\frac{\partial H_{V_b}}{\partial\theta}V_bS_{12} + V_b^T\frac{\partial H_{V_bq}}{\partial\theta}\dot{q}E + V_b^T\frac{\partial H_{V_bV_R}}{\partial\theta}v_tS_{52}\right)$$

$$+ \dot{H}_{V_b}V_bS_{13} + \dot{H}_{V_b\Omega_b}\Omega_bE + \dot{H}_{V_b\omega_t}\omega_tS_{43} + \frac{1}{2}\left(V_b^T\frac{\partial H_{V_b}}{\partial\theta}V_bS_{13} + V_b^T\frac{\partial H_{V_b\Omega_b}}{\partial\theta}\Omega_b + V_b^T\frac{\partial H_{V_b\omega_t}}{\partial\theta}\omega_tS_{43}\right)$$

$$\overline{C}_2 = \dot{H}_{\Omega_b}\Omega_b S_{21} + \dot{H}_{\Omega_b q}\dot{q}E + \dot{H}_{\Omega_b\omega_t}\omega_t S_{41} + \frac{1}{2}\left(\Omega_b^T \frac{\partial H_{\Omega_b}}{\partial\theta}\Omega_b S_{21} + \Omega_b^T \frac{\partial H_{\Omega_b q}}{\partial\theta}\dot{q}E + \Omega_b^T \frac{\partial H_{\Omega_b\omega_t}}{\partial\theta}\omega_t S_{41}\right)$$
$$+ \dot{H}^T_{V_b\Omega_b} V_b S_{12} + \dot{H}_{\Omega_b q}\dot{q}E + \dot{H}_{\Omega_b v_t} v_t S_{52} + \frac{1}{2}\left(\Omega_b^T \frac{\partial H^T_{V_b\Omega_b}}{\partial\theta} V_b S_{12} + \Omega_b^T \frac{\partial H_{\Omega_b q}}{\partial\theta}\dot{q}E + \Omega_b^T \frac{\partial H_{\Omega_b V_R}}{\partial\theta} v_t S_{52}\right)$$
$$+ \dot{H}^T_{V_b\Omega_b} V_b S_{13} + \dot{H}_{\Omega_b}\Omega_b E + \dot{H}_{\Omega_b\omega_t}\omega_t S_{43} + \frac{1}{2}\left(\Omega_b^T \frac{\partial H^T_{V_b\Omega_b}}{\partial\theta} V_b S_{13} + \Omega_b^T \frac{\partial H_{\Omega_b}}{\partial\theta}\Omega_b E + \Omega_b^T \frac{\partial H_{\Omega_b\omega_t}}{\partial\theta}\omega_t S_{43}\right)$$

$$\overline{C}_3 = \dot{H}^T_{\Omega_b q}\Omega_b S_{21} + \dot{H}_q\dot{q}E + \dot{H}_{q\omega_t}\omega_t S_{41} + \frac{1}{2}\left(\dot{q}^T \frac{\partial H^T_{\Omega_b q}}{\partial\theta}\Omega_b S_{21} + \dot{q}^T \frac{\partial H_q}{\partial\theta}\dot{q}E + \dot{q}^T \frac{\partial H_{q\omega_t}}{\partial\theta}\omega_t S_{41}\right)$$
$$+ \dot{H}^T_{V_b q} V_b S_{12} + \dot{H}_q\dot{q}E + \dot{H}_{qv_t} v_t S_{52} + \frac{1}{2}\left(\dot{q}^T \frac{\partial H^T_{V_b q}}{\partial\theta} V_b S_{12} + \dot{q}^T \frac{\partial H_q}{\partial\theta}\dot{q}E + \dot{q}^T \frac{\partial H_{qv_t}}{\partial\theta} v_t S_{52}\right)$$
$$+ \dot{H}^T_{V_b q} V_b S_{13} + \dot{H}^T_{\Omega_b q}\Omega_b E + \dot{H}_{\omega_t}\omega_t S_{43} + \frac{1}{2}\left(\dot{q}^T \frac{\partial H^T_{V_b q}}{\partial\theta} V_b S_{13} + \dot{q}^T \frac{\partial H^T_{\Omega_b q}}{\partial\theta}\Omega E + \dot{q}^T \frac{\partial H_{q\omega_t}}{\partial\theta}\omega_t S_{43}\right)$$

$$\overline{C}_4 = \dot{H}^T_{\Omega_b\omega_t}\Omega_b S_{21} + \dot{H}^T_{q\omega_t}\dot{q}E + \dot{H}_{\omega_t}\omega_t S_{41} + + \frac{1}{2}\left(\omega_T^T \frac{\partial H^T_{\Omega_b\omega_t}}{\partial\theta}\Omega_b S_{21} + \omega_t^T \frac{\partial H^T_{q\omega_t}}{\partial\theta}\dot{q}E + \omega_t^T \frac{\partial H_{\omega_t}}{\partial\theta}\omega_t S_{41}\right)$$
$$+ \dot{H}^T_{V_b\omega_t} V S_{12} + \dot{H}^T_{q\omega_t}\dot{q}E + \dot{H}_{\omega_T v_t} v_t S_{52} + \frac{1}{2}\left(\omega_t^T \frac{\partial H^T_{V_b\omega_t}}{\partial\theta} V_b S_{12} + \omega_t^T \frac{\partial H^T_{q\omega_t}}{\partial\theta}\dot{q}E + \omega_t^T \frac{\partial H_{v_t\omega_t}}{\partial\theta} v_t S_{52}\right)$$
$$+ \dot{H}^T_{V_b v_t} V_b S_{13} + \dot{H}^T_{\Omega_b\omega_t}\Omega_b E + \dot{H}_{\omega_t}\omega_t S_{43} + \frac{1}{2}\left(\omega_T^T \frac{\partial H^T_{V_b\omega_t}}{\partial\theta} V_b S_{13} + \omega_T^T \frac{\partial H^T_{\Omega_b\omega_t}}{\partial\theta}\Omega_b E + \omega_t^T \frac{\partial H_{\omega_t}}{\partial\theta}\omega_t S_{43}\right)$$

$$\overline{C}_5 = \dot{H}^T_{\Omega_b v_t}\Omega_b S_{21} + \dot{H}^T_{qv_t}\dot{q}E + \dot{H}^T_{\omega_t v_t}\omega_t S_{41} + +\frac{1}{2}\left(v_t^T\frac{\partial H^T_{v_t\Omega_b}}{\partial\theta}\Omega_b S_{21} + v_t^T\frac{\partial H^T_{v_t q}}{\partial\theta}\dot{q}E + v_t^T\frac{\partial H^T_{v_t\omega_t}}{\partial\theta}\omega_t S_{41}\right)$$

$$+\dot{H}^T_{V_b v_t}V_b S_{12} + \dot{H}^T_{qv_t}\dot{q}E + \dot{H}_{v_t}v_t S_{52} + \frac{1}{2}\left(v_t^T\frac{\partial H^T_{V_b v_t}}{\partial\theta}V_b S_{12} + v_t^T\frac{\partial H^T_{v_t q}}{\partial\theta}\dot{q}E + v_t^T\frac{\partial H_{v_t}}{\partial\theta}v_t S_{52}\right)$$

$$+\dot{H}^T_{V_b v_t}V_b S_{13} + \dot{H}^T_{\Omega_b\omega_t}\Omega_b E + \dot{H}_{\omega_t}\omega_t S_{43} + \frac{1}{2}\left(v_t^T\frac{\partial H^T_{V_b v_t}}{\partial\theta}V_b S_{13} + v_t^T\frac{\partial H^T_{v_t\Omega_b}}{\partial\theta}\Omega_b E + v_t^T\frac{\partial H^T_{v_t\omega_t}}{\partial\theta}\omega_t S_{43}\right)$$

$$HS\ddot{v} = \begin{bmatrix} \left(H_{V_b\Omega_b}S_{21} + H_{V_b q}E + H_{V_b\omega_t}S_{41}\right)\dot{\Omega}_b + \left(H_{V_b}S_{12} + H_{V_b q}E + H_{V_b v_t}S_{52}\right)\ddot{q} + \left(H_{V_b}S_{13} + H_{V_b\Omega_b}E + H_{V_b\omega_t}S_{43}\right)\dot{\omega}_t \\ \left(H_{\Omega_b}S_{21} + H_{\Omega_b q}E + H_{\Omega_b\omega_t}S_{41}\right)\dot{\Omega}_b + \left(H^T_{V_b\Omega_b}S_{12} + H_{\Omega_b q}E + H_{\Omega_b v_t}S_{52}\right)\ddot{q} + \left(H^T_{V_b\Omega_b}S_{13} + H_{\Omega_b}E + H_{\Omega_b v_t}S_{43}\right)\dot{\omega}_t \\ \left(H^T_{\Omega_b q}S_{21} + H_q E + H_{q\omega_t}S_{41}\right)\dot{\Omega}_b + \left(H^T_{V_b q}S_{12} + H_q E + H_{qv_t}S_{52}\right)\ddot{q} + \left(H^T_{V_b q}S_{13} + H^T_{\Omega_b q}E + H_{qv_t}S_{43}\right)\dot{\omega}_t \\ \left(H^T_{\Omega_b\omega_t}S_{21} + H^T_{q\omega_t}E + H_{\omega_t}S_{41}\right)\dot{\Omega}_b + \left(H^T_{V_b\omega_t}S_{12} + H^T_{q\omega_t}E + H_{\omega_T v_t}S_{52}\right)\ddot{q} + \left(H^T_{V_b\omega_t}S_{13} + H^T_{\Omega_b\omega_t}E + H_{\omega_T v_t}S_{43}\right)\dot{\omega}_t \\ \left(H^T_{\Omega_b v_t}S_{21} + H^T_{qv_t}E + H^T_{\omega_t v_t}S_{41}\right)\dot{\Omega}_b + \left(H^T_{V_b v_t}S_{12} + H^T_{qv_t}E + H_{v_t}S_{52}\right)\ddot{q} + \left(H^T_{V_b v_t}S_{13} + H^T_{\Omega_b v_t}E + H_{v_t}S_{43}\right)\dot{\omega}_t \end{bmatrix}$$

$$HS\dot{v} = \begin{bmatrix} \left(H_{V_b\Omega_b}\dot{S}_{21} + H_{V_b\omega_t}\dot{S}_{41}\right)\Omega_b + \left(H_{V_b}\dot{S}_{12} + H_{V_b v_t}\dot{S}_{52}\right)\dot{q} + \left(H_{V_b}\dot{S}_{13} + H_{V_b\omega_t}\dot{S}_{43}\right)\omega_t \\ \left(H_{\Omega_b}\dot{S}_{21} + H_{\Omega_b\omega_t}\dot{S}_{41}\right)\Omega_b + \left(H^T_{V_b\Omega_b}\dot{S}_{12} + H_{\Omega_b v_t}\dot{S}_{52}\right)\dot{q} + \left(H^T_{V_b\Omega_b}\dot{S}_{13} + H_{\Omega_b v_t}\dot{S}_{43}\right)\omega_t \\ \left(H^T_{\Omega_b q}\dot{S}_{21} + H_{q\omega_t}\dot{S}_{41}\right)\Omega_b + \left(H^T_{V_b q}\dot{S}_{12} + H_{qv_t}\dot{S}_{52}\right)\dot{q} + \left(H^T_{V_b q}\dot{S}_{13} + H_{qv_t}\dot{S}_{43}\right)\omega_t \\ \left(H^T_{\Omega_b\omega_t}\dot{S}_{21} + H_{\omega_t}\dot{S}_{41}\right)\Omega_b + \left(H^T_{V_b\omega_t}\dot{S}_{12} + H_{\omega_T v_t}\dot{S}_{52}\right)\dot{q} + \left(H^T_{V_b\omega_t}\dot{S}_{13} + H_{\omega_T v_t}\dot{S}_{43}\right)\omega_t \\ \left(H^T_{\Omega_b v_t}\dot{S}_{21} + H^T_{\omega_t v_t}\dot{S}_{41}\right)\Omega_b + \left(H^T_{V_b v_t}\dot{S}_{12} + H_{v_t}\dot{S}_{52}\right)\dot{q} + \left(H^T_{V_b v_t}\dot{S}_{13} + H_{v_t}\dot{S}_{43}\right)\omega_t \end{bmatrix}$$

$$\dddot{C} = \ddot{C}\dot{v} = CS\dot{v}$$

$$\ddot{C}_1 = \dot{H}_{V_b\Omega_b}\Omega_b S_{21}\Omega_b + \dot{H}_{V_bq}\dot{q}E\Omega_b + \dot{H}_{V_b\omega_t}\omega_t S_{41}\Omega_b +$$

$$\frac{1}{2}\left(V_b^T\frac{\partial H_{V_b\Omega_b}}{\partial\theta}\Omega_b S_{21} + V_b^T\frac{\partial H_{V_bq}}{\partial\theta}\dot{q}E + V_b^T\frac{\partial H_{V_b\omega_t}}{\partial\theta}\omega_t S_{41}\right)\Omega_b$$

$$+\dot{H}_{V_b}V_b S_{12}\dot{q} + \dot{H}_{V_bq}\dot{q}E\dot{q} + \dot{H}_{V_bv_t}v_t S_{52}\dot{q} +$$

$$\frac{1}{2}\left(V_b^T\frac{\partial H_{V_b}}{\partial\theta}V_b S_{12} + V_b^T\frac{\partial H_{V_bq}}{\partial\theta}\dot{q}E + V_b^T\frac{\partial H_{V_bV_R}}{\partial\theta}v_t S_{52}\right)\dot{q}$$

$$+\dot{H}_{V_b}V_b S_{13}\omega_t + \dot{H}_{V_b\Omega_b}\Omega_b E\omega_t + \dot{H}_{V_b\omega_t}\omega_t S_{43}\omega_t +$$

$$\frac{1}{2}\left(V_b^T\frac{\partial H_{V_b}}{\partial\theta}V_b S_{13} + V_b^T\frac{\partial H_{V_b\Omega_b}}{\partial\theta}\Omega_b + V_b^T\frac{\partial H_{V_b\omega_t}}{\partial\theta}\omega_t S_{43}\right)\omega_t$$

$$\ddot{C}_2 = \dot{H}_{\Omega_b}\Omega_b S_{21}\Omega_b + \dot{H}_{\Omega_bq}\dot{q}E\Omega_b + \dot{H}_{\Omega_b\omega_t}\omega_t S_{41}\Omega_b$$

$$+\frac{1}{2}\left(\Omega_b^T\frac{\partial H_{\Omega_b}}{\partial\theta}\Omega_b S_{21} + \Omega_b^T\frac{\partial H_{\Omega_bq}}{\partial\theta}\dot{q}E + \Omega_b^T\frac{\partial H_{\Omega_b\omega_t}}{\partial\theta}\omega_t S_{41}\right)\Omega_b$$

$$+\dot{H}^T_{V_b\Omega_b}V_b S_{12}\dot{q} + \dot{H}_{\Omega_bq}\dot{q}E\dot{q} + \dot{H}_{\Omega_bv_t}v_t S_{52}\dot{q} +$$

$$+\frac{1}{2}\left(\Omega_b^T\frac{\partial H^T_{V_b\Omega_b}}{\partial\theta}V_b S_{12} + \Omega_b^T\frac{\partial H_{\Omega_bq}}{\partial\theta}\dot{q}E + \Omega_b^T\frac{\partial H_{\Omega_bV_R}}{\partial\theta}v_t S_{52}\right)\dot{q}$$

$$+\dot{H}^T_{V_b\Omega_b}V_b S_{13}\omega_t + \dot{H}_{\Omega_b}\Omega_b E\omega_t + \dot{H}_{\Omega_b\omega_t}\omega_t S_{43}\omega_t +$$

$$\frac{1}{2}\left(\Omega_b^T\frac{\partial H^T_{V_b\Omega_b}}{\partial\theta}V_b S_{13} + \Omega_b^T\frac{\partial H_{\Omega_b}}{\partial\theta}\Omega_b E + \Omega_b^T\frac{\partial H_{\Omega_b\omega_t}}{\partial\theta}\omega_t S_{43}\right)\omega_t$$

$$\overline{\overline{C}}_3 = \dot{H}^T_{\Omega_b q}\Omega_b S_{21}\Omega_b + \dot{H}_q \dot{q}E + \dot{H}_{q\omega_t}\omega_t S_{41}\Omega_b$$
$$+\frac{1}{2}\left(\dot{q}^T\frac{\partial H^T_{\Omega_b q}}{\partial\theta}\Omega_b S_{21} + \dot{q}^T\frac{\partial H_q}{\partial\theta}\dot{q}E + \dot{q}^T\frac{\partial H_{q\omega_t}}{\partial\theta}\omega_t S_{41}\right)\Omega_b$$
$$+\dot{H}^T_{V_b q}V_b S_{12}\dot{q} + \dot{H}_q\dot{q}E\dot{q} + \dot{H}_{qv_t}v_t S_{52}\dot{q}$$
$$+\frac{1}{2}\left(\dot{q}^T\frac{\partial H^T_{V_b q}}{\partial\theta}V_b S_{12} + \dot{q}^T\frac{\partial H_q}{\partial\theta}\dot{q}E + \dot{q}^T\frac{\partial H_{qv_t}}{\partial\theta}v_t S_{52}\right)\dot{q}$$
$$+\dot{H}^T_{V_b q}V_b S_{13}\omega_t + \dot{H}^T_{\Omega_b q}\Omega_b E\omega_t + \dot{H}_{\omega_t}\omega_t S_{43}\omega_t +$$
$$\frac{1}{2}\left(\dot{q}^T\frac{\partial H^T_{V_b q}}{\partial\theta}V_b S_{13} + \dot{q}^T\frac{\partial H^T_{\Omega_b q}}{\partial\theta}\Omega E + \dot{q}^T\frac{\partial H_{q\omega_t}}{\partial\theta}\omega_t S_{43}\right)\omega_t$$

$$\overline{\overline{C}}_4 = \dot{H}^T_{\Omega_b\omega_t}\Omega_b S_{21}\Omega_b + \dot{H}^T_{q\omega_t}\dot{q}E\Omega_b + \dot{H}_{\omega_t}\omega_t S_{41}\Omega_b$$
$$+\frac{1}{2}\left(\omega_T^T\frac{\partial H^T_{\Omega_b\omega_t}}{\partial\theta}\Omega_b S_{21} + \omega_t^T\frac{\partial H^T_{q\omega_t}}{\partial\theta}\dot{q}E + \omega_t^T\frac{\partial H_{\omega_t}}{\partial\theta}\omega_t S_{41}\right)\Omega_b$$
$$+\dot{H}^T_{V_b\omega_t}VS_{12}\dot{q} + \dot{H}^T_{q\omega_t}\dot{q}E\dot{q} + \dot{H}_{\omega_T v_t}v_t S_{52}\dot{q}$$
$$+\frac{1}{2}\left(\omega_t^T\frac{\partial H^T_{V_b\omega_t}}{\partial\theta}V_b S_{12} + \omega_t^T\frac{\partial H^T_{q\omega_t}}{\partial\theta}\dot{q}E + \omega_t^T\frac{\partial H_{v_t\omega_t}}{\partial\theta}v_t S_{52}\right)\dot{q}$$
$$+\dot{H}^T_{V_b v_t}V_b S_{13}\omega_t + \dot{H}^T_{\Omega_b\omega_t}\Omega_b E\omega_t + \dot{H}_{\omega_t}\omega_t S_{43}\omega_t +$$
$$\frac{1}{2}\left(\omega_t^T\frac{\partial H^T_{V_b\omega_t}}{\partial\theta}V_b S_{13} + \omega_T^T\frac{\partial H^T_{\Omega_b\omega_t}}{\partial\theta}\Omega_b E + \omega_t^T\frac{\partial H_{\omega_t}}{\partial\theta}\omega_t S_{43}\right)\omega_t$$

$$\overline{\overline{C}}_5 = \dot{H}^T_{\Omega_b v_t}\Omega_b S_{21}\Omega_b + \dot{H}^T_{qv_t}\dot{q}E\Omega_b + \dot{H}^T_{\omega_t v_t}\omega_t S_{41}\Omega_b$$

$$+\frac{1}{2}\left(v_t^T\frac{\partial H^T_{v_t\Omega_b}}{\partial\theta}\Omega_b S_{21} + v_t^T\frac{\partial H^T_{v_t q}}{\partial\theta}\dot{q}E + v_t^T\frac{\partial H^T_{v_t\omega_t}}{\partial\theta}\omega_t S_{41}\right)\Omega_b$$

$$+\dot{H}^T_{V_b v_t}V_b S_{12}\dot{q} + \dot{H}^T_{qv_t}\dot{q}E\dot{q} + \dot{H}_{v_t}v_t S_{52}\dot{q}$$

$$+\frac{1}{2}\left(v_t^T\frac{\partial H^T_{V_b v_t}}{\partial\theta}V_b S_{12} + v_t^T\frac{\partial H^T_{v_t q}}{\partial\theta}\dot{q}E + v_t^T\frac{\partial H_{v_t}}{\partial\theta}v_t S_{52}\right)\dot{q}$$

$$+\dot{H}^T_{V_b v_t}V_b S_{13}\omega_t + \dot{H}^T_{\Omega_b\omega_t}\Omega_b E\omega_t + \dot{H}_{\omega_t}\omega_t S_{43}\omega_t +$$

$$\frac{1}{2}\left(v_t^T\frac{\partial H^T_{V_b v_t}}{\partial\theta}V_b S_{13} + v_t^T\frac{\partial H^T_{v_t\Omega_b}}{\partial\theta}\Omega_b E + v_t^T\frac{\partial H^T_{v_t\omega_t}}{\partial\theta}\omega_t S_{43}\right)\omega_t$$

Appendix K

Derivation of the Regressor Y and the Parameter Vector α of a Based-Satellite 6-DOF Space Robot in Contact with a Target Satellite

$$Y_{1,1} = \left(- \sum_{i=0,i\neq b}^{n+1} \left[r_{i/b} \times \right] S_{21} + \sum_{i=0,i\neq b}^{n+1} J_{L_i} E, \alpha_1 \right) \dot{\Omega}_b,$$

$$Y_{1,2} = \left(E_3 \sum_{i=0}^{n+1} S_{12} + \sum_{i=0,i\neq b}^{n+1} J_{L_i} E \right) \ddot{q},$$

$$Y_{1,3} = -\left[r_{t/EE} \times \right] S_{41} \dot{\Omega}_b + E_3 S_{52} \ddot{q},$$

$$Y_{1,4} = \left(E_3 \sum_{i=0,i\neq b}^{n+1} S_{13} - \sum_{i=0,i\neq b}^{n+1} \left[r_{i/b} \times \right] E \right) \dot{\omega}_t,$$

$$Y_{1,5} = \left(- \sum_{i=0,i\neq b}^{n+1} \left[r_{i/b} \times \right] \dot{S}_{21} \right) \Omega_b,$$

$$Y_{1,6} = -\left[r_{t/EE} \times \right] S_{43} \dot{\omega}_t - \left[r_{t/EE} \times \right] \dot{S}_{41} \Omega_b,$$

$$Y_{1,7} = E_3 \sum_{i=0}^{n+1} \dot{S}_{12} \dot{q},$$

$$Y_{1,8} = \left(E_3 \sum_{i=0}^{n+1} \dot{S}_{13} \right) \omega_t,$$

$$Y_{1,9} = E_3 \dot{S}_{52} \dot{q} - \left[r_{t/EE} \times \right] \dot{S}_{43} \omega_t,$$

$$Y_{1,10} = \sum_{i=0,i\neq b}^{n+1} \dot{J}_{A_i} \Omega_b S_{21} \Omega_b,$$

$$Y_{1,11} = \sum_{i=0,i\neq b}^{n+1} m_i \left[\dot{r}_{i/b} \times \right] J_{L_i} \Omega_b S_{21} \Omega_b,$$

$$Y_{1,12} = 2 \sum_{i=0,i\neq b}^{n+1} \left\{ m_i J_{L_i}^T \cdot \dot{J}_{L_i} \right\} \dot{q} E \Omega_b,$$

$$Y_{1,13} = 2 \sum_{i=0,i\neq b}^{n+1} \left\{ J_{A_i}^T \dot{J}_{A_i} \right\} \dot{q} E \Omega_b,$$

$$Y_{1,14} = \dot{J}_{A_t}{}^T \omega_t S_{41} \Omega_b,$$

$$Y_{1,15} = \dot{J}_{L_t}{}^T \left[r_{t/EE}^T \times \right] \omega_t S_{41} \Omega_b + J_{L_t}{}^T \left[\dot{r}_{t/EE}^T \times \right] \omega_t S_{41} \Omega_b,$$

$$Y_{1,16} = \dot{q}^T \frac{\partial \sum_{i=0,i\neq b}^{n+1} \left\{ {}^B I_i J_{A_i}^T \right\}}{\partial \theta} \Omega_b S_{21} \Omega_b,$$

$$Y_{1,17} = \dot{q}^T \frac{\partial \sum_{i=0,i\neq b}^{n+1} \left\{ \left[r_{i/b} \times \right]^T J_{L_i}^T \right\}}{\partial \theta} \Omega_b S_{21} \Omega_b,$$

$$Y_{1,18} = \dot{q}^T \frac{\partial \sum_{i=0,i\neq b}^{n+1} \left\{ J_{L_i}^T \cdot J_{L_i} \right\}}{\partial \theta} \dot{q} E \Omega_b,$$

$$Y_{1,19} = \dot{q}^T \frac{\partial \sum_{i=0,i\neq b}^{n+1} \left\{ J_{A_i}^T J_{A_i} \right\}}{\partial \theta} \dot{q} E \Omega_b,$$

$$Y_{1,20} = \dot{q}^T \frac{\partial \left\{ J_{A_{n+1}}{}^T \right\}}{\partial \theta} \omega_t S_{41} \Omega_b,$$

$$Y_{1,21} = \dot{q}^T \frac{\partial \left\{ J_{L_{n+1}}{}^T \left[r_{t/EE}^T \times \right] \right\}}{\partial \theta} \omega_t S_{41} \Omega_b,$$

$$Y_{1,22} = \sum_{i=0,i\neq b}^{n+1} \dot{J}_{L_i} V_b S_{12} \dot{q},$$

$$Y_{1,23} = 2 \sum_{i=0,i\neq b}^{n+1} \left\{ J_{L_i}^T \cdot \dot{J}_{L_i} \right\} \dot{q} E \dot{q},$$

$$Y_{1,24} = 2 \sum_{i=0,i\neq b}^{n+1} \left\{ J_{A_i}^T \dot{J}_{A_i} \right\} \dot{q} E \dot{q},$$

$$Y_{1,25} = J_{L_{n+1}}{}^T E_3 v_t S_{52} \dot{q},$$

$$Y_{1,26} = \dot{q}^T \frac{\partial \sum_{i=0,i\neq b}^{n+1} \dot{J}_{L_i}^T}{\partial \theta} V_b S_{12} \dot{q},$$

$$Y_{1,27} = \dot{q}^T \frac{\partial \sum_{i=0,i\neq b}^{n+1} \left\{ J_{L_i}^T \cdot J_{L_i} \right\}}{\partial \theta} \dot{q} E \dot{q},$$

$$Y_{1,28} = \dot{q}^T \frac{\partial \sum_{i=0,i\neq b}^{n+1} \left\{ J_{A_i}^T J_{A_i} \right\}}{\partial \theta} \dot{q} E \dot{q},$$

$$Y_{1,29} = \dot{q}^T \frac{\partial \left\{ m_{n+1} J_{L_{n+1}}{}^T E_3 \right\}}{\partial \theta} v_t S_{52} \dot{q},$$

$$Y_{1,30} = \dot{q} \sum_{i=0,i\neq b}^{n+1} \dot{J}_{L_i} V_b S_{13} \omega_t,$$

$$Y_{1,31} = \sum_{i=0,i\neq b}^{n+1} \left\{ \dot{J}_{A_i} \right\} \Omega_b E \omega_t,$$

$$Y_{1,32} = \sum_{i=0,i\neq b}^{n+1} \left\{ m_i \left[r_{i/b} \times \right] \dot{J}_{L_i} + m_i \left[\dot{r}_{i/b} \times \right] J_{L_i} \right\} \Omega_b E \omega_t,$$

$$Y_{1,33} = \dot{D}(r_{t/EE}) \omega_t S_{43} \omega_t,$$

$$Y_{1,34} = \dot{q}^T \frac{\partial \sum_{i=0,i\neq b}^{n+1} \dot{J}^T_{L_i}}{\partial \theta} V_b S_{13},$$

$$Y_{1,35} = \dot{q}^T \frac{\partial \sum_{i=0,i\neq b}^{n+1} \left\{ J^T_{A_i} \right\}}{\partial \theta} \Omega E,$$

$$Y_{1,36} = \dot{q}^T \frac{\partial \sum_{i=0,i\neq b}^{n+1} \left\{ \left[r_{i/b} \times \right]^T J^T_{L_i} \right\}}{\partial \theta} \Omega E,$$

$$Y_{1,37} = \dot{q}^T \frac{\partial \left\{ J_{A_{n+1}}{}^T \right\}}{\partial \theta} \omega_t S_{43},$$

$$Y_{1,38} = \dot{q}^T \frac{\partial \left\{ J_{L_{n+1}}{}^T \left[r^T_{t/EE} \times \right] \right\}}{\partial \theta} \omega_t S_{43},$$

$$Y_{2,1} = \left(- \sum_{i=0, i\neq b}^{n+1} D(r_{i/b}) S_{21} + \sum_{i=0, i\neq b}^{n+1} \left[r_{i/b} \times \right] J_{L_i} E, \right) \dot{\Omega}_b,$$

$$Y_{2,2} = \left(E_3 \sum_{i=0}^{n+1} \left[r_{i/b} \times \right] S_{12} + \sum_{i=0, i\neq b}^{n+1} \left[r_{i/b} \times \right] J_{L_i} E \right) \ddot{q},$$

$$Y_{2,3} = D(r_{t/EE}) \; S_{41} \dot{\Omega}_b + E_3 \left[r_{n+1} \times \right] \; S_{52} \ddot{q},$$

$$Y_{2,4} = \left(E_3 \sum_{i=0, i\neq b}^{n+1} \left[r_{i/b} \times \right] S_{13} - \sum_{i=0, i\neq b}^{n+1} D(r_{i/b}) E \right) \dot{\omega}_t,$$

$$Y_{2,5} = \left(- \sum_{i=0, i\neq b}^{n+1} m_i D(r_{i/b}) \dot{S}_{21} \right) \Omega_b,$$

$$Y_{2,6} = -\left[r_{n+1} \times \right] \; S_{43} \dot{\omega}_t - D(r_{t/EE}) \; \dot{S}_{41} \Omega_b,$$

$$Y_{2,7} = E_3 \sum_{i=0}^{n+1} \left[r_{i/b} \times \right] \dot{S}_{12} \dot{q},$$

$$Y_{2,8} = \left(E_3 \sum_{i=0}^{n+1} \left[r_{i/b} \times \right] \dot{S}_{13} \right) \omega_t,$$

$$Y_{2,9} = E_3 \left[r_{n+1} \times \right] \dot{S}_{52} \dot{q} - \left[r_{n+1} \times \right] \; \dot{S}_{43} \omega_t,$$

$$Y_{2,10} = \sum_{i=0, i\neq b}^{n+1} \dot{D}(r_{i/b}) \Omega_b S_{21} \Omega_b,$$

$$Y_{2,11} = O,$$

$$Y_{2,12} = \sum_{i=0, i\neq b}^{n+1} \left\{ \left[r_{i/b} \times \right] \cdot \dot{J}_{L_i} + \left[\dot{r}_{i/b} \times \right] J_{L_i} \right\} \dot{q} E \Omega_b,$$

$$Y_{2,13} = \sum_{i=0, i\neq b}^{n+1} \left\{ \dot{J}_{A_i} \right\} \dot{q} E \Omega_b,$$

$$Y_{2,14} = \dot{D}(r_{t/EE}) \omega_t S_{41} \Omega_b,$$

$$Y_{2,15} = O,$$

$$Y_{2,16} = \dot{q}^T \frac{\partial \sum_{i=0, i\neq b}^{n+1} D(r_{i/b})}{\partial \theta} \Omega_b S_{21} \Omega_b,$$

$$Y_{2,17} = O,$$

$$Y_{2,18} = \dot{q}^T \frac{\partial \sum_{i=0,i\neq b}^{n+1} \left\{ \left[r_{i/b} \times \right] J_{L_i} \right\}}{\partial \theta} \dot{q} E \Omega_b,$$

$$Y_{2,19} = \dot{q}^T \frac{\partial \sum_{i=0,i\neq b}^{n+1} \left\{ J_{A_i} \right\}}{\partial \theta} \dot{q} E \Omega_b,$$

$$Y_{2,20} = \dot{q}^T \frac{\partial \left\{ D(r_{t/EE}) \right\}}{\partial \theta} \omega_t S_{41} \Omega_b,$$

$$Y_{2,21} = O,$$

$$Y_{2,22} = \sum_{i=0,i\neq b}^{n+1} \left[\dot{r}_{i/b} \times \right] V_b S_{12} \dot{q},$$

$$Y_{2,23} = \sum_{i=0,i\neq b}^{n+1} \left\{ \left[\dot{r}_{i/b} \times \right] J_{L_i} + \left[r_{i/b} \times \right] \dot{J}_{L_i} \right\} \dot{q} E \dot{q},$$

$$Y_{2,24} = \sum_{i=0,i\neq b}^{n+1} \left\{ \dot{J}_{A_i} \right\} \dot{q} E \dot{q},$$

$$Y_{2,25} = \left[\dot{r}_{n+1} \times \right] E_3 v_t S_{52} \dot{q},$$

$$Y_{2,26} = \dot{q}^T \frac{\partial \sum_{i=0,i\neq b}^{n+1} \left[r_{i/b} \times \right]}{\partial \theta} V_b S_{12} \dot{q},$$

$$Y_{2,27} = \dot{q}^T \frac{\partial \sum_{i=0,i\neq b}^{n+1} \left\{ \left[r_{i/b} \times \right] J_{L_i} \right\}}{\partial \theta} \dot{q} E \dot{q},$$

$$Y_{2,28} = \dot{q}^T \frac{\partial \sum_{i=0,i\neq b}^{n+1} \left\{ {}^B I_i J_{A_i} \right\}}{\partial \theta} \dot{q} E \dot{q},$$

$$Y_{2,29} = \dot{q}^T \frac{\partial \left\{ \left[r_{n+1} \times \right] \right\}}{\partial \theta} v_t S_{52} \dot{q},$$

$$Y_{2,30} = \sum_{i=0,i\neq b}^{n+1} \left[\dot{r}_{i/b} \times \right] V_b S_{13} \omega_t,$$

$$Y_{2,31} = \sum_{i=0,i\neq b}^{n+1} \left\{ \dot{D}(r_{i/b}) \right\} \Omega_b E \omega_t,$$

$$Y_{2,32} = O,$$

$$Y_{2,33} = \dot{D}(r_{t/EE})\omega_t S_{43}\omega_t,$$

$$Y_{2,34} = \dot{q}^T \frac{\partial \sum_{i=0, i\neq b}^{n+1}\left[r_{i/b}\times\right]}{\partial\theta} V_b S_{13}\omega_t,$$

$$Y_{2,35} = \dot{q}^T \frac{\partial \sum_{i=0, i\neq b}^{n+1}\left\{D(r_{i/b})\right\}}{\partial\theta} \Omega E\omega_t,$$

$$Y_{2,36} = O,$$

$$Y_{2,37} = E,$$

$$Y_{2,38} = \dot{q}^T \frac{\partial D(r_{t/EE})}{\partial\theta} \omega_t S_{43}\omega_t,$$

$$Y_{3,1} = \left(J_{L_i}^T \left[r_{i/b} \times \right]^T S_{21} + \sum_{i=0, i\neq b}^{n+1} J_{L_i} J_{L_i}^T E \right) \dot{\Omega}_b ,$$

$$Y_{3,2} = \left(E_3 \sum_{i=0}^{n+1} J_{L_i} S_{12} + \sum_{i=0, i\neq b}^{n+1} J_{L_i}^T J_{L_i} E \right) \ddot{q},$$

$$Y_{3,3} = J_{L_{n+1}}{}^T \left[r_{t/EE}^T \times \right] S_{41} \dot{\Omega}_b + J_{L_{n+1}}{}^T E_3 S_{52} \ddot{q},$$

$$Y_{3,4} = \left(\sum_{i=0, i\neq b}^{n+1} J_{L_i}^T S_{13} - \sum_{i=0, i\neq b}^{n+1} \left[r_{i/b} \times \right] J_{L_i} E \right) \dot{\omega}_t ,$$

$$Y_{3,5} = \left(- \sum_{i=0, i\neq b}^{n+1} J_{L_i}^T \left[r_{i/b} \times \right]^T \dot{S}_{21} \right) \Omega_b ,$$

$$Y_{3,6} = J_{L_{n+1}}{}^T S_{43} \dot{\omega}_t - J_{L_{n+1}}{}^T \left[r_{t/EE}^T \times \right] \dot{S}_{41} \Omega_b ,$$

$$Y_{3,7} = E_3 \sum_{i=0}^{n+1} J_{L_i} \dot{S}_{12} \dot{q},$$

$$Y_{3,8} = \left(E_3 \sum_{i=0}^{n+1} J_{L_i} \dot{S}_{13} \right) \omega_t ,$$

$$Y_{3,9} = E_3 J_{L_{n+1}}{}^T \dot{S}_{52} \dot{q} - J_{L_{n+1}}{}^T \dot{S}_{43} \omega_t ,$$

$$Y_{3,10} = \sum_{i=0, i\neq b}^{n+1} \dot{J}_{Ai} \Omega_b S_{21} \Omega_b ,$$

$$Y_{3,11} = \sum_{i=0, i\neq b}^{n+1} m_i \left[\dot{r}_{i/b} \times \right] J_{L_i} \Omega_b S_{21} \Omega_b ,$$

$$Y_{3,12} = 2 \sum_{i=0, i\neq b}^{n+1} \left\{ m_i J_{L_i}^T \cdot \dot{J}_{L_i} \right\} \dot{q} E \Omega_b ,$$

$$Y_{3,13} = 2 \sum_{i=0, i\neq b}^{n+1} \left\{ J_{A_i}^T \dot{J}_{A_i} \right\} \dot{q} E \Omega_b ,$$

$$Y_{3,14} = \dot{J}_{A_t}{}^T \omega_t S_{41} \Omega_b ,$$

$$Y_{3,15} = \dot{J}_{L_t}{}^T \left[r_{t/EE}^T \times \right] \omega_t S_{41} \Omega_b + J_{L_t}{}^T \left[\dot{r}_{t/EE}^T \times \right] \omega_t S_{41} \Omega_b ,$$

$$Y_{3,16} = \dot{q}^T \frac{\partial \sum_{i=0, i\neq b}^{n+1} \left\{ {}^B I_i J_{A_i}^T \right\}}{\partial \theta} \Omega_b S_{21} \Omega_b ,$$

$$Y_{3,17} = \dot{q}^T \frac{\partial \sum_{i=0, i\neq b}^{n+1} \left\{ \left[r_{i/b} \times \right]^T J_{L_i}^T \right\}}{\partial \theta} \Omega_b S_{21} \Omega_b ,$$

$$Y_{3,18} = \dot{q}^T \frac{\partial \sum_{i=0,i\neq b}^{n+1} \left\{ J_{L_i}^T \cdot J_{L_i} \right\}}{\partial \theta} \dot{q} E \Omega_b,$$

$$Y_{3,19} = \dot{q}^T \frac{\partial \sum_{i=0,i\neq b}^{n+1} \left\{ J_{A_i}^T J_{A_i} \right\}}{\partial \theta} \dot{q} E \Omega_b,$$

$$Y_{3,20} = \dot{q}^T \frac{\partial \left\{ J_{A_{n+1}}{}^T \right\}}{\partial \theta} \omega_t S_{41} \Omega_b,$$

$$Y_{3,21} = \dot{q}^T \frac{\partial \left\{ J_{L_{n+1}}{}^T \left[r_{t/EE}^T \times \right] \right\}}{\partial \theta} \omega_t S_{41} \Omega_b,$$

$$Y_{3,22} = \sum_{i=0,i\neq b}^{n+1} \dot{J}_{L_i} V_b S_{12} \dot{q},$$

$$Y_{3,23} = 2 \sum_{i=0,i\neq b}^{n+1} \left\{ J_{L_i}^T \cdot \dot{J}_{L_i} \right\} \dot{q} E \dot{q},$$

$$Y_{3,24} = 2 \sum_{i=0,i\neq b}^{n+1} \left\{ J_{A_i}^T \dot{J}_{A_i} \right\} \dot{q} E \dot{q},$$

$$Y_{3,25} = J_{L_{n+1}}{}^T E_3 v_t S_{52} \dot{q},$$

$$Y_{3,26} = \dot{q}^T \frac{\partial \sum_{i=0,i\neq b}^{n+1} \dot{J}_{L_i}^T}{\partial \theta} V_b S_{12} \dot{q},$$

$$Y_{3,27} = \dot{q}^T \frac{\partial \sum_{i=0,i\neq b}^{n+1} \left\{ J_{L_i}^T \cdot J_{L_i} \right\}}{\partial \theta} \dot{q} E \dot{q},$$

$$Y_{3,28} = \dot{q}^T \frac{\partial \sum_{i=0,i\neq b}^{n+1} \left\{ J_{A_i}^T J_{A_i} \right\}}{\partial \theta} \dot{q} E \dot{q},$$

$$Y_{3,29} = \dot{q}^T \frac{\partial \left\{ m_{n+1} J_{L_{n+1}}{}^T E_3 \right\}}{\partial \theta} v_t S_{52} \dot{q},$$

$$Y_{3,30} = \dot{q} \sum_{i=0,i\neq b}^{n+1} \dot{J}_{L_i} V_b S_{13} \omega_t,$$

$$Y_{3,31} = \sum_{i=0,i\neq b}^{n+1} \left\{ \dot{J}_{A_i} \right\} \Omega_b E \omega_t,$$

$$Y_{3,32} = \sum_{i=0,i\neq b}^{n+1} \left\{ m_i \left[r_{i/b} \times \right] \dot{J}_{L_i} + m_i \left[\dot{r}_{i/b} \times \right] J_{L_i} \right\} \Omega_b E \omega_t ,$$

$$Y_{3,33} = \dot{D}(r_{t/EE}) \omega_t S_{43} \omega_t ,$$

$$Y_{3,34} = \dot{q}^T \frac{\partial \sum_{i=0,i\neq b}^{n+1} \dot{J}^T_{L_i}}{\partial \theta} V_b S_{13} ,$$

$$Y_{3,35} = \dot{q}^T \frac{\partial \sum_{i=0,i\neq b}^{n+1} \left\{ J^T_{A_i} \right\}}{\partial \theta} \Omega E ,$$

$$Y_{3,36} = \dot{q}^T \frac{\partial \sum_{i=0,i\neq b}^{n+1} \left\{ \left[r_{i/b} \times \right]^T J^T_{L_i} \right\}}{\partial \theta} \Omega_b E ,$$

$$Y_{3,37} = \dot{q}^T \frac{\partial \left\{ J_{A_{n+1}}{}^T \right\}}{\partial \theta} \omega_t S_{43} ,$$

$$Y_{3,38} = \dot{q}^T \frac{\partial \left\{ J_{L_{n+1}}{}^T \left[r^T_{t/EE} \times \right] \right\}}{\partial \theta} \omega_t S_{43} ,$$

$$Y_{4,1} = \left(D(r_{t/EE})S_{21} + \sum_{i=0,i\neq b}^{n+1} J_{L_i} E,\alpha_1 \right)\dot{\Omega}_b,$$

$$Y_{4,2} = O,$$

$$Y_{4,3} = J_{L_{n+1}}{}^T \left[r_{t/EE}^T \times \right] \dot{\Omega}_b + D(r_{t/EE})\dot{\Omega}_b - \left[r_{t/EE} \times \right] S_{12}\ddot{q} + J_{L_{n+1}}{}^T \left[r_{t/EE}^T \times \right] E_3\ddot{q} + \left[r_{t/EE} \times \right] S_{52}\ddot{q},$$

$$Y_{4,4} = \left(E_3 \sum_{i=0,i\neq b}^{n+1} S_{13} - \sum_{i=0,i\neq b}^{n+1} \left[r_{i/b} \times \right] E \right)\dot{\omega}_t,$$

$$Y_{4,5} = O,$$

$$Y_{4,6} = -\left[r_{t/EE} \times \right] S_{43}\dot{\omega}_t + D(r_{t/EE})\dot{S}_{41}\Omega_b + \left(\sum_{i=0,i\neq b}^{n+1} D(r_{t/EE})\dot{S}_{21} \right)\Omega_b + m_{n+1}D(r_{t/EE})\dot{\omega}_t - \left[r_{t/EE} \times \right] \dot{S}_{12}\dot{q},$$

$$Y_{4,7} = O,$$

$$Y_{4,8} = O,$$

$$Y_{4,9} = -\left[r_{t/EE} \times \right] \dot{S}_{52}\dot{q} - \left(E_3 \sum_{i=0}^{n+1} \dot{S}_{13} \right)\omega_t - \left[r_{t/EE} \times \right] \dot{S}_{43}\omega_t + \dot{D}(r_{t/EE})\Omega_b S_{21}\Omega_b + {}^bI_{n+1} \sum_{i=0,i\neq b}^{n+1} \dot{J}_{Ai}\Omega_b S_{21}\Omega_b,$$

$$Y_{4,10} = O,$$

$$Y_{4,11} = O,$$

$$Y_{4,12} = O,$$

$$Y_{4,13} = O,$$

$$Y_{4,14} = \dot{J}_{A_{n+1}}{}^T \dot{q}E\Omega_b + J_{A_{n+1}}{}^T \ddot{q} + E\dot{\omega}_t + E\dot{S}_{21}\Omega_b,$$

$$Y_{4,15} = \sum_{i=0,i\neq b}^{n+1} \left\{ \dot{J}_{L_{n+1}}{}^T \left[r_{t/EE}^T \times \right] \right\}\dot{q}E\Omega_b + \sum_{i=0,i\neq b}^{n+1} \left\{ J_{L_{n+1}}{}^T \left[\dot{r}_{t/EE}^T \times \right] \right\}\dot{q}E\Omega_b + \dot{D}(r_{t/EE})\omega_t S_{41}\Omega_b,$$

$$Y_{4,16} = O,$$

$$Y_{4,17} = O,$$

$$Y_{4,18} = O,$$

$$Y_{4,19} = O,$$

$$Y_{4,20} = \frac{1}{2}\omega_t^T \frac{\partial\left\{J_{n+1}{}^T\right\}}{\partial\theta}\dot{q}E\Omega_b +,$$

$$Y_{4,21} = \frac{1}{2}\omega_T^T \frac{\partial D(r_{t/EE})}{\partial\theta}\Omega_b S_{21}\Omega_b + \frac{1}{2}\omega_t^T \frac{\partial\left\{J_{n+1}{}^T\left[r_{t/ee}{}^T\times\right]\right\}}{\partial\theta}\dot{q}E\Omega_b + \frac{1}{2}\omega_t^T \frac{\partial D(r_{t/EE})}{\partial\theta}\omega_t S_{41}\Omega_b,$$

$$Y_{4,22} = O,$$

$$Y_{4,23} = O,$$

$$Y_{4,24} = O,$$

$$Y_{4,25} = -\left[\dot{r}_{t/EE}\times\right]\ V_b S_{12}\dot{q} + \dot{J}_{n+1}{}^T\left[r_{t/ee}{}^T\times\right]\dot{q}E\dot{q} + J_{n+1}{}^T\left[\dot{r}_{t/ee}{}^T\times\right]\dot{q}E\dot{q},$$

$$Y_{4,26} = O,$$

$$Y_{4,27} = O,$$

$$Y_{4,28} = O,$$

$$Y_{4,29} = -\left[\dot{r}_{t/EE}\times\right]\ v_t S_{52}\dot{q} - \frac{1}{2}\omega_t^T \frac{\partial\left[r_{t/ee}{}^T\times\right]}{\partial\theta}V_b S_{12}\dot{q} + \frac{1}{2}\omega_t^T \frac{\partial\left\{J_{n+1}{}^T\left[r_{t/ee}{}^T\times\right]\right\}}{\partial\theta}\dot{q}E\dot{q} - \frac{1}{2}\omega_t^T \frac{\partial\left[r_{t/EE}\times\right]}{\partial\theta}v_t S_{52}\dot{q},$$

$$Y_{4,30} = O,$$

$$Y_{4,31} = O,$$

$$Y_{4,32} = O,$$

$$Y_{4,33} = O,$$

$$Y_{4,34} = O,$$

$$Y_{4,35} = O,$$

$$Y_{4,36} = O,$$

$$Y_{4,37} = \frac{1}{2}\omega_t^T \frac{\partial\left\{J_{An+1}{}^T\right\}}{\partial\theta}\dot{q}E\dot{q},$$

$$Y_{4,38} = -\left[\dot{r}_{t_{/EE}}\times\right]V_b S_{13}\omega_t + \dot{D}(r_{t/EE})\Omega_b E\omega_t + \dot{D}(r_{t/EE})\omega_t S_{43}\omega_t$$

$$-\frac{1}{2}\omega_t^T \frac{\partial\left[r_{t_{/EE}}\times\right]}{\partial\theta}V_b S_{13}\omega_t + \frac{1}{2}\omega_T^T \frac{\partial D(r_{t/EE})}{\partial\theta}\Omega_b E\omega_t + \frac{1}{2}\omega_t^T \frac{\partial D(r_{t/EE})}{\partial\theta}\omega_t S_{43}\omega_t,$$

$$Y_{5,1} = O,$$
$$Y_{5,2} = O,$$
$$Y_{5,3} = -\left[r_{n+1}\times\right]^T S_{21}\dot{\Omega}_b + E_3 J_{L_{n+1}} E\dot{\Omega}_b - \left[r_{t/EE}\times\right]^T S_{41}\dot{\Omega}_b,$$
$$Y_{5,4} = O,$$
$$Y_{5,5} = O,$$
$$Y_{5,6} = E_3 S_{12}\ddot{q} + E_3 J_{L_{n+1}} E\ddot{q} + E_3 S_{52}\ddot{q} + E_3 S_{13}\dot{\omega}_t - \left[r_{n+1}\times\right]^T E\dot{\omega}_t + E_3 S_{43}\dot{\omega}_t,$$
$$Y_{5,7} = O,$$
$$Y_{5,8} = O,$$
$$Y_{5,9} = -\left[r_{n+1}\times\right]^T \dot{S}_{21}\Omega_b - \left[r_{t/EE}\times\right]^T \dot{S}_{41}\Omega_b + E_3\dot{S}_{12}\dot{q} + E_3\dot{S}_{52}\dot{q} + E_3\dot{S}_{13}\omega_t + E_3\dot{S}_{43}\omega_t,$$
$$Y_{5,10} = O,$$
$$Y_{5,11} = O,$$
$$Y_{5,12} = O,$$
$$Y_{5,13} = O,$$
$$Y_{5,14} = O,$$
$$Y_{5,15} = -\left[\dot{r}_{n+1}\times\right]^T \Omega_b S_{21}\Omega_b + E\dot{J}_{L_{n+1}}\dot{q}E\Omega_b - \left[\dot{r}_{t/EE}\times\right]^T \omega_t S_{41}\Omega_b - \frac{1}{2}v_t^T \frac{\partial\left[r_{n+1}\times\right]}{\partial\theta}\Omega_b S_{21}\Omega_b +$$
$$\frac{1}{2}v_t^T \frac{\partial E_3 J_{L_{n+1}}}{\partial\theta}\dot{q}E\Omega_b - \frac{1}{2}v_t^T \frac{\partial\left[r_{t/EE}\times\right]^T}{\partial\theta}\omega_t S_{41}\Omega_b,$$
$$Y_{5,16} = O,$$
$$Y_{5,17} = O,$$

$$Y_{5,18} = O,$$
$$Y_{5,19} = O,$$
$$Y_{5,20} = O,$$
$$Y_{5,21} = E_3 \dot{J}_{L_{n+1}} \dot{q} E \dot{q},$$
$$Y_{5,22} = O,$$
$$Y_{5,23} = O,$$
$$Y_{5,24} = O,$$
$$Y_{5,25} = \frac{1}{2} v_t^T \frac{\partial E_3 J_{L_{n+1}}}{\partial \theta} \dot{q} E,$$
$$Y_{5,26} = O,$$
$$Y_{5,27} = O,$$
$$Y_{5,28} = O,$$
$$Y_{5,29} = \dot{D}^T (r_{t/EE}) \Omega_b E \omega_t,$$
$$Y_{5,30} = O,$$
$$Y_{5,31} = O,$$
$$Y_{5,32} = O,$$
$$Y_{5,33} = \dot{D}^T (r_{t/EE}) \omega_t S_{43} \omega_t,$$
$$Y_{5,34} = O,$$
$$Y_{5,35} = O,$$
$$Y_{5,36} = O,$$
$$Y_{5,37} = O,$$
$$Y_{5,38} = -\frac{1}{2} v_t^T \frac{\partial [r_{n+1} \times]^T}{\partial \theta} \Omega_b E \omega_t - \frac{1}{2} v_t^T \frac{\partial [r_{t/EE} \times]^T}{\partial \theta} \omega_t S_{43} \omega,$$

$$\alpha_1 = m_i, \alpha_2 = m_i, \alpha_3 = m_{n+1}, \alpha_4 = m_i, \alpha_5 = m_i, \alpha_6 = m_{n+1}, \alpha_7 = m_i, \alpha_8 = m_i, \alpha_9 = m_{n+1}, \alpha_{10} = {}^B I_i, \alpha_{11} = m_i,$$
$$\alpha_{12} = m_i, \alpha_{13} = {}^B I_i, \alpha_{14} = {}^B I_t, \alpha_{15} = m_t, \alpha_{16} = {}^B I_i, \alpha_{17} = m_i, \alpha_{18} = m_i, \alpha_{19} = {}^B I_i, \alpha_{20} = {}^B I_{n+1}, \alpha_{21} = m_{n+1}, \alpha_{22} = m_i,$$
$$\alpha_{23} = m_i, \alpha_{24} = {}^B I_i, \alpha_{25} = m_{n+1}, \alpha_{26} = m_i, \alpha_{27} = m_i, \alpha_{28} = {}^B I_i, \alpha_{29} = m_{n+1}, \alpha_{30} = m_i, \alpha_{31} = {}^B I_i, \alpha_{32} = m_i, \alpha_{33} = m_t,$$
$$\alpha_{34} = m_i, \alpha_{35} = {}^B I_i, \alpha_{36} = m_i, \alpha_{37} = I_{n+1}, \alpha_{38} = m_{n+1},$$